ЖУРНАЛ
ЭКСПЕРИМЕНТАЛЬНОЙ И ТЕОРЕТИЧЕСКОЙ
ФИЗИКИ
АКАДЕМИЯ НАУК СССР

SOVIET PHYSICS

JETP

VOLUME 3 **NUMBER 1**

A Translation

of the

Journal of Experimental and Theoretical Physics

of the

Academy of Sciences of the USSR

AUGUST, 1956

Published by the

AMERICAN INSTITUTE OF PHYSICS
INCORPORATED

SOVIET PHYSICS
JETP

A translation of the Journal of Experimental and Theoretical Physics of the USSR.

A publication of the

AMERICAN INSTITUTE OF PHYSICS

Governing Board

FREDERICK SEITZ, *Chairman*
ALLEN V. ASTIN
ROBERT F. BACHER
W. S. BAIRD
H. A. BETHE
R. T. BIRGE
FRANK D. DEZTER
I. C. GARDNER
S. A. GOUDSMIT
CHARLES KITTEL
HUGH S. KNOWLES
R. B. LINDSAY
WILLIAM F. MEGGERS
HARRY F. OLSON
R. R. PALMER
R. F. PATON
ERIC RODGERS
RALPH A. SAWYER
H. D. SMYTH
MARK W. ZEMANSKY

Administrative Staff

HENRY A. BARTON, *Director*
MARK W. ZEMANSKY, *Treasurer*
WALLACE WATERFALL, *Executive Secretary*
THEODORE VORBURGER, *Advertising Manager*
RUTH F. BRYANS, *Publication Manager*
EDITH I. NEFTEL, *Circulation Manager*
KATHRYN SETZE, *Assistant Treasurer*
EUGENE H. KONE, *Director of Public Relations*

American Institute of Physics Advisory Board on Russian Translations

ELMER HUTCHISSON, *Chairman*
DWIGHT GRAY, MORTON HAMERMESH, VLADIMIR ROJANSKY, VICTOR WEISSKOPF

Editor of SOVIET PHYSICS
ROBERT T. BEYER, DEPARTMENT OF PHYSICS, BROWN UNIVERSITY, PROVIDENCE, R.I.

SOVIET PHYSICS is a monthly journal published by the American Institute of Physics for the purpose of making available in English reports of current Soviet research in physics as contained in the Journal of Experimental and Theoretical Physics of the Academy of Sciences of the USSR. The page size of SOVIET PHYSICS will be 7⅞" x 10½", the same as other Institute journals.

Transliteration of the names of Russian authors follows the system employed by the Library of Congress.

This translating and publishing project was undertaken by the Institute in the conviction that dissemination of the results of researches everywhere in the world is invaluable to the advancement of science. The National Science Foundation of the United States encouraged the project initially and is supporting it in large part by a grant.

The American Institute of Physics and its translators propose to translate faithfully all the material in the Journal of EXPERIMENTAL AND THEORETICAL PHYSICS OF THE USSR appearing after January 1, 1955. The views expressed in the translated material, therefore, are intended to be those expressed by the original authors, and not those of the translators nor of the American Institute of Physics.

Two volumes are published annually, each of six issues. Each volume contains the translation of one volume of the Journal of EXPERIMENTAL AND THEORETICAL PHYSICS OF THE USSR. New volumes begin in February and August.

Subscription Prices:

Per year (12 issues)	
United States and Canada	$60.00
Elsewhere	64.00
Back Numbers	
Single copies	$ 6.00

Subscriptions should be addressed to the American Institute of Physics, 57 East 55 Street, New York 22, New York.

Copyright by American Institute of Physics 1956

SOVIET PHYSICS

JETP

SOVIET PHYSICS JETP VOLUME 3, NUMBER 1 AUGUST, 1956

Abram Fedorovich Ioffe

(On his seventy-fifth birthday)

J. Exper. Theoret. Phys. USSR 30, 3-6 (January, 1956)

OCTOBER 29, 1955 marked 75 years since the day of birth and 50 years of scientific activity of an outstanding Soviet physicist, Member of The Academy of Sciences, USSR, Abram Fedorovich Ioffe. All of the physicists and the learned world of the Soviet Union celebrate this famous jubilee and greet Abram Fedorovich Ioffe not only as an outstanding scientist, but also as one of the greatest organizers of science in the Soviet Union.

A. F. Ioffe was born in the cityof Romny (Poltav District) in 1880. After having completed the Real (Secondary) School in Romny, he entered the Petersburg Technological Institute.

Manifesting great interest in scientific investigation and experimental physics, Abram Fedorovich upon graduating from the Institute went to Munich to work with the great experimental physicist Roentgen. From 1902 to 1906 he worked with Roentgen, where he was occupied with the investigation of the electrical and elastic properties of quartz. He completed his studies at the Physics Institute of the University of Munich with great distinction and received the degree of Doctor of Philosophy.

In 1906, after having declined a proposal of Roentgen to remain and work in Munich, Ioffe returned to Petersburg and was appointed as a researcher to the chair of Physics in the Polytechnical Institute. Up to 1914 he still continued to collaborate with Roentgen. During this period, along with the investigation of the electrical and mechanical properties of crystals, Abram Fedorovich was studying the nature of light and the atomic structure of electricity. The investigations of the elementary photoeffect and of the magnetic field of cathode rays were the subject of his master's dissertation, which he defended in 1913. In the same year Ioffe was elected Professor of Physics of the Petersburg Polytechnical Institute. The continuing investigation of the electrical and elastic properties of quartz was the subject of his subsequent dissertation, for which the Petersburg University awarded him the degree of Doctor of Physics in 1915.

The real development of the scientific and organizational activity of A.F. Ioffe began after the great October Revolution. He was one of the great scientists who from the very first days of the establishment of Soviet rule fully supported it. In the difficult year of 1918 he was actively engaged in the organization of the State Roentgen (X-ray) and Radio Institute in Petrograd. Before long the Physics Department of this Institute, headed by Abram Fedorovich, was made into an independent State Physico-Technical Roentgen Institute.

From the very beginning of the foundation of the Physico-Technical Institute Ioffe considered that along with the investigation of the physical properties of matter, it is necessary to develop the trend of introducing the attainments of physics into industry. The name of the Institute itself emphasized that this course—the relationship between physics and technology—was the most important object of the Institute. The chief collaborators of the newly established Institute became the young physicists, students of Abram Fedorovich— participants in the physics seminar which he organized at the Polytechnical Institute in 1916. A great many of these first students of A. F. Ioffe became themselves great scientists: among them the Academicians N. N. Semenov, P. L. Kapitza, P. I. Lukirskii, associate member of the Academy of Sciences, USSR, Ia. I. Frenkel', and others. The new Institute became for a long time the main center of the development of physics in the Soviet Union.

In 1920 Abram Fedorovich was elected Member of the Academy of Sciences, USSR (in terms of the date of his election A. F. Ioffe is at present the oldest Academician).

Having foreseen that the development of socialist industry would require the intensive development of physics and the creation of new factory laboratories, A. F. Ioffe advanced the question of the training of new cadres. In 1919 he organized at the Polytechnical Institute a Physico-Mechanical Faculty for training cadres of new engineers and engineer-physicists. For more than ten years he was the Dean of this Faculty, which was closely associated with the Physico-Technical Institute, and students of this Faculty were drawn by him to do scientific work at the Institute. Among the graduates of the faculty we see now many of the great scientists—Academician A. I. Alikhanov, I. K. Kikoin, V. N. Kondrat'ev, G. V. Kurdiumov, Iu. B. Khariton, associate members of the Academy of Sciences, USSR, G. A. Grinberg, I. Ia. Pomeranchuk, A. I. Shal'nikov, and others. When speaking of the Physico-Mechanical Faculty and of the work of Ioffe at the Polytechnical Institute one should note especially that during all of his pedagogical activity his lectures were very popular and attracted large audiences.

During the first period of the existence of the Physico-Technical Institute the trend of the work there was closely connected with the investigations of Abram Fedorovich himself, the most important of which at that time were devoted to the studies of the mechanical and the electrical properties of crystals. The investigations of A. I. Ioffe on the mechanical properties, plastic deformation and elastic properties of crystals became the basis for contemporary ideas on the strength of materials. The studies of Abram Fedorovich on the electrical properties of dielectrics explained the mechanism of the processes occurring in insulating materials and made it possible to set up and solve a number of important practical problems.

In 1924 A. F. Ioffe jointly with N. N. Semenov organized a Physico-Technical Laboratory in order to improve the link with industry and to work out practically important problems in technical physics (electro-technical, radio-physical, acoustic, thermo-technical, and others). The activity of this laboratory was so closely interlinked with the activity of the Physico-Technical Institute that in fact it was a single institute (and soon these were amalgamated).

A significant role in the development of Soviet Physics was played by the Allunion meetings and conferences of physicists, the initiator and leader of which was A. F. Ioffe. Taking into account the rapid tempo of the industrialization of the country and the need of the most rapid development of physics in the Soviet Union, Abram Fedorovich entered upon the organization of a number of institutes in various regions of the Union. His initiative was greatly supported by the Soviet Government and in the beginning of the thirties he undertook with great energy the organization of a number of new physico-technical institutes. From the staff of the Leningrad Physico-Technical Institute (LPTI) Ioffe appointed talented physicists, who formed the main nucleus in the institutes established in Kharkov', Sverdlovsk, Tomsk and Dnepropetrovsk.

Not limiting himself to the organization of such institutes, Abram Fedorovich interested himself greatly in the application of physics not only to industry, but also to other fields and, in particular, to agronomy. He showed that physical methods may be effective for the solution of such problems as the heat and moisture condition of soils, improvement of the composition of soils, etc. In 1932 he organized in Leningrad a Physico-Agronomical Institute, of which he is the director up to the present.

In 1930 when a number of well-defined scientific trends crystallized out at the LPTI and quantitatively the Institute developed greatly, Ioffe proposed to subdivide it; it was separated into the Institutes of Chemical Physics and Electrophysics. In the remaining Physico-Technical Institute A. F. Ioffe developed energetically four main directions: nuclear physics, physics of polymers, studies of the mechanical properties of metals and physics of semiconductors. The latter trend was a result of the personal investigations of Abram Fedorovich and under his direct guidance.

It would be difficult to separate the scientific activity of A. F. Ioffe from the work of the LPTI. Regardless of the fact that, beginning with 1930, the personal investigations of Abram Fedorovich were concentrated on the studies of semiconductors, it can be stated with certainty that also the other investigations owed much to his initiative. At his suggestion a strong group was set up for the study of nuclear physics headed by I. V. Kurchatov, A. I. Alikhanov and A. A. Artsimovich, and during this period the LPTI became the main center of studies of nuclear physics in the Soviet Union. A. F. Ioffe influenced greatly the study of the physical properties of polymers. The investigation of the mechanical properties of metals was the direct result of his work on the mechanical properties of crystals. In a short article it would be impossible to enumerate all the investigations carried out at the LPTI. We will attempt only to describe briefly the studies of A. F. Ioffe and his coworkers in the field of semiconductors.

In the beginning of the thirties Abram Fedorovich stressed the importance of semiconductors and noted that for the practical use of semiconductors it will be necessary to have a profound knowledge of their physical properties and, in particular, to have the knowhow of effecting changes in these properties. The study of the electrical properties of semiconductors was started first. This permitted the understanding of the nature of impurity and specific conductivity, the electron and hole mechanism of conductivity and the effect of impurities and of deviations from stoichiometric composion. Detailed investigations were carried out on the internal photoeffect of cuprous oxide. The behavior of semiconductors in strong electric fields was studied. Great interest was aroused by the hypothesis on the mechanism of rectification on a contact with two semiconductors having a different type of conductivity (electron and hole). The studies on semiconductors which were carried out at the PTI in the prewar years beginning with 1930 were devoted not only to physical investigations, but also to a number of important industrial applications. New photoelements of high sensitivity were produced from thallium sulfide; new rectifiers using cuprous oxide with magnesium for high current densities were produced. By analyzing the thermoelectric and thermal properties of semiconductors, Ioffe pointed out a practical use of semiconductive thermoelements for the direct transformation of heat into electric energy.

At the beginning of World War II, the LPTI was evacuated from Leningrad to Kazan'. During this period the work of the institute was reorganized and directed towards the solution of problems important for defense. Some of these problems were already studied theoretically at the institute, and now individual groups of workers took an active part in their practical solution. Some problems produced by the war were successfully solved by the workers and students of A. F. Ioffe under his direct leadership. A group of workers of the institute, headed by P. P. Kobeko, one of the closest students of Ioffe, carried out, under the difficult conditions of the siege, the important work connected with the "ice road" over Lake Ladoga, and others.

At the end of the war the LPTI returned to Leningrad and under the leadership of A. F. Ioffe and owing to the untiring efforts of the whole staff it was reinstalled. After the war, the same as before the war, the work of the institute continued along the same lines, that is, nuclear physics, the physics of polymers, semiconductors, and metals. The personal interests of Abram Fedorovich were again concentrated on the studies of semiconductors and under his leadership the workers of the institute extended greatly the work in this field.

In 1951 A. F. Ioffe left the position of the director of LPTI and organized a separate laboratory of Semiconductors at the Academy of Sciences, USSR, and Abram Fedorovich was appointed director.

In the last decade, as was foreseen by A. F. Ioffe, semiconductors have become exceptionally important technically and the interest in the theory of semiconductors increased greatly. Simultaneously with essential improvements in the known industrial semiconductive devices, new, industrially valuable devices were also produced; it suffices to mention only semiconductive amplifiers as an example.

In the post war period Abram Fedorovich conducted thorough investigations of the physical properties of semiconductors. As a result of the work of Ioffe and his students, a number of problems connected with the actual control of the properties of semiconductors has been largely solved. These problems are of primary importance for industrial applications. As an example we may point out the solution of the problem of the actual control of the thermoelectromotive force and the thermal conductivity of semiconductors, which made it possible to construct batteries of high efficiency and thermoelectrocoolers. In order to coordinate all of the scientific investigations on semiconductors in the Union, a commission on semiconductors under the chairmanship of Ioffe was set up at the Academy of Sciences, USSR.

The achievements of A. F. Ioffe as a reknowned scientist are well known and highly valued not only in our country, but also abroad. A. F. Ioffe has been elected as honorary member of a number of foreign Academies.

The untiring, long, passionate scientific work of Abram Fedorovich, his service to the motherland, have long been acclaimed. On the day of his seventy-fifth birthday A. F. Ioffe received the title of Hero of Socialist Labor.

The importance of the role of A. F. Ioffe as an organizer of Soviet Physics is expressed best of all by the fact that he had established a whole network of physical and physico-technical institutes (16 institutes), by the organization of the first Physico-Mechanical Faculty— a forge for specialists of a new type: engineer physicists, by his long and brilliant pedagogical and scientific activity. Abram Fedorovich is the teacher of several generations of Soviet physicists. He succeeded in instilling in his students a love for science and a desire to apply the results of their studies for the good of their country, that is, those features which are characteristic of all of his activity.

Now, in the days of his seventy-fifth anniversary Abram Fedorovich Ioffe is full of creative powers, full of ideas for new work and plans for wide practical applications of semiconductors.

All the physicists of the Soviet Union warmly congratulate Abram Fedorovich on his seventyfifth birthday and wish him great success in his future activity and many years of fruitfull work.

Translated by E. Rabkin
1

SOVIET PHYSICS JETP VOLUME 3, NUMBER 1 AUGUST, 1956

Photoelectric Quantum Yield in Silver Bromide Crystals

M. S. EGOROVA AND P. V. MEIKLIAR
Molotov State Pedagogical Institute

(Submitted to JETP editor November 9, 1954)
J. Exper. Theoret. Phys. USSR 30, 60-67 (January 1956)

The quantum yield of the photoelectric effect in silver bromide was determined. It was shown that as one increases the concentration of electron emitting centers, one decreases the magnitude of the quantum yield.

A GREAT deal of work has been devoted to the study of the photoelectric effect in silver halides.[1] Only Lehfeld[2] and Hecht[3], however, actually measured the quantum yield of the reaction. The difficulty of determining this quantity, even in terms of the energy absorbed, is due to the fact that it depends on the quantum yield as well as on the "displacement" of the electrons. For this reason Lehfeld performed his experiments under saturation conditions when all electrons freed by the light quanta reach the anode. Measurements at such great field strengths (3000 v/cm) are hard to perform at room temperature, because of the presence of large and unsteady background (dark room) currents. For this reason Lehfeld and Hecht performed their experiments at liquid air temperatures. They found the quantum yield to be between 0.1 and 0.6 and the electron displacement per unit field strength was of the order of 4×10^{-4}cm / (volt/cm).

The literature contains no data on the above quantities at room temperature. It was this lack that inspired the present work.

EXPERIMENTAL METHOD

Silver bromide crystals were prepared by allowing the fused salt to flow between two glass discs, as was previously described by one of the authors.[4]

In order to measure the photoelectric current we built a special ac amplifier that was calibrated by means of an audio oscillator with a vacuum tube voltmeter as well as with a 50 cycle alternating current. In the latter case a known voltage was attenuated by means of a voltage divider. The silver bromide crystals were placed in a metal box in which the electrodes rested on insulated discs. The box was connected to the amplifier by means of a coaxial cable. The inner conductor applied the voltage from one of the electrodes to the input grid of the amplifier through a coupling condenser. The input impedance was 47.5 megohms. The second electrode and the metal box were grounded. The photoelectric current was amplified, rectified with a diode and then measured on a moving pointer type galvanometer. When relaxation times were to be observed, the electrodes were connected directly to an oscillograph of type FO-4. Windows in front and back of the metallic box allowed light to shine through the crystal. This permitted us to measure both the photoeffect and the absorption without disturbing the position of the crystal. An oven was mounted in such a way that when needed it could be lowered so that the crystal was inside it. The oven was equipped with windows that allowed the crystal to be illuminated. It was thus possible to measure the photoeffect and the absorption at higher temperatures. The crystal was illuminated by means of a monochromator of type UM-2. The monochromator lamp was fed from a stabilized 12 volt, 30 watt source. The light was modulated by means of a slotted disc driven by a constant current motor. The needed current for a given speed of rotation was predetermined by means of a stroboscope and kept constant throughout the experiment. The angular rotation of the disc was such as to modulate the light at 50 cycles per second. The coefficient of absorption was measured with the help of a selenium photocell attached to a high sensitivity mirror galvanometer. A special apparatus was used to measure the coefficient of reflection. Monochromatic light was made to pass through a half mirrored surface, reflected from the crystal and again made to fall on the semitransparent surface, 45° to the path of the beam, from which it was reflected to the photocell. One compared the galvanometer deflection in this case with the deflection when the crystal was replaced by a mirror of known coefficient of reflection (close to unity). The energy distribution in the monochromator was determined by means of a thermocouple previously calibrated against a standard light of known color temperature and known intensity.

---

[1] E. A. Kirillov and A. S. Fomenko, Trudy Odessa Inst. 3, Odessa, 1951, p. 7.

[2] W. Lehfeldt, Nachr. Akad. Wiss. Göttingen Math.-physik. Kl I, 171 (1933).

[3] K. Hecht, Z. Physik 77, 235 (1932).

[4] P. V. Meikliar, J. Exper. Theoret. Phys. USSR 21, 42 (1951).

In the region of wavelength between 400 and 450 mμ the galvanometer deflection was very small. In this region we made use of a photomultiplier, a specially designed tube that gave a galvanometer deflection of 45 mm when the output slit of the monochromator was set at 1.0 mm.

The low temperature measurements were made in a cylindrical container with the crystal placed in it in a horizontal position. The container was in a wooden box packed with solid carbon dioxide. Light from the monochromator was deflected down on the crystal by means of a mirror. After passing through the crystal the light fell on the selenium cell underneath the crystal. This allowed the determination of the photoelectric current and the coefficient of absorption at low temperatures. The temperature in all cases was measured with a thermocouple.

In some of our experiments the crystal was illuminated with light of wavelength 365 mμ. This was obtained from a mercury lamp of type SVDSh-250 passed through a type FS-2 filter. In this case the light was modulated by the alternating current through the mercury lamp.

RESULTS OF THE EXPERIMENT

Figure 1 shows the conductivity of silver bromide as a function of wavelength expressed in coulombs per erg, i.e., per unit energy absorbed at room temperature. Figure 2 shows a similar curve for silver

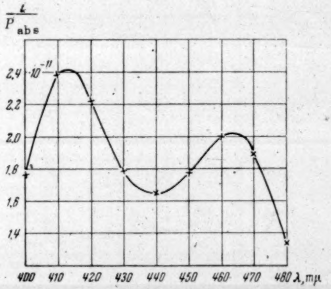

FIG. 1. Photoelectric current in AgBr expressed per unit of energy absorbed.

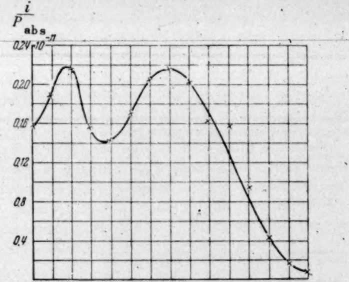

FIG. 2. Photoelectric current in AgBr with 10 mole percent of AgI (per unit energy absorbed.)

bromide crystals that contain 10 mole per cent silver iodide as an impurity. We see that in the blue portion of the spectrum the curve has two maxima, one at $\lambda = 410$ to 420 mμ and one at $\lambda = 460$ mμ. This agrees with the results of Kirilov and Fomenko[1] and those obtained by Zaidman[5].

Changes in the temperature of the crystal greatly effect the magnitude of the photoelectric effect. Figure 3 shows graphs of the photoelectric sensitivity at various temperatures. It is seen that as the temperature goes up there is a drastic change in the photoelectric sensitivity. This agrees with the qualitative observations of Putseiko and Meikliar[6]. One could suspect that the decrease in the photoelectric sensitivity with increase in temperature was due to a higher relaxation time. We therefore performed special measurements of the relaxation time at temperatures that were used in our experiments. These showed that always during the time that the crystals were illuminated, the relaxation curves showed saturation.

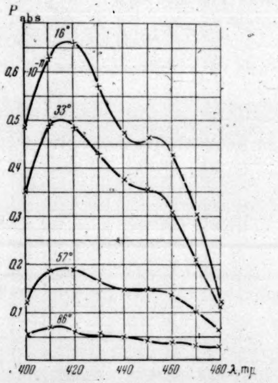

FIG. 3. Curves of photoelectric current in AgBr at different temperatures.

In order to clarify the reason for the decrease in photoelectric sensitivity with increase in temperature, we determined the quantum yield of the photoeffect as well as the electron displacement, both per unit field strength. For uniform illumination of the entire crystal one may use Hecht's equation[7]

$$\psi = \frac{w}{l}\left[1 - \frac{w}{l}\left(1 - e^{-l/w}\right)\right],$$

where ψ is the ratio of the total charge Ne released by the light to the charge $Ne(\bar{x}/l)$, which passes through the measuring apparatus. Here e is the charge on the electron, l is the distance between electrodes, $\bar{x}$ the mean free path of the electrons and w is the electron "displacement", i.e., the distance in which the number of free electrons released by the light and traveling towards the anode is diminished by e.

Hecht and Lehfield found that the electron displacement w is proportional to the field strength E. One may therefore introduce the constant $c = w/E$. Furthermore $N = P_{abs}\,\eta/h\nu$ where P_{abs} is the ammount of monochromatic energy absorbed by the crystal, $h\nu$ the energy of the quantum, and η the quantum yield of the photoeffect. One can therefore rewrite Hecht's equation in the form

$$i = \frac{P_{abs}}{h\nu}\, e\eta\, \frac{cE}{l}\left[1 - \frac{cE}{l}\left(1 - e^{-l/cE}\right)\right]$$

The above equation expresses the photoelectric current i as a function of field strength E. Figure 4 shows the experimental curve of $i = f(E)$. The independent determination of η and c was performed as follows: We determined the value of $\tan\alpha = (di/dE)_{E=0}$. Letting $l/cE = a$ we obtained

$$\left(1 - \frac{1}{\tan\alpha}\,\frac{i}{E}\right)a = 1 - e^{-a}.$$

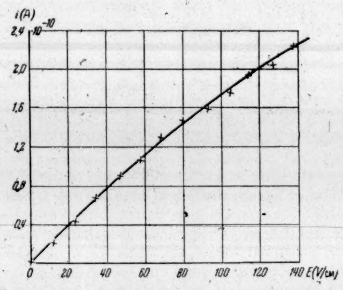

FIG. 4. Photoelectric current as a function of field strength.

---

[5] H. M. Zaidman, Zh. Fiz. Khim 26, 1791 (1952).

[6] E. K. Putseiko and P. B. Meikliar, J. Exper. Theoret. Phys. USSR 21, 341 (1951).

[7] R. Gerni and N. Mott, *Electronic Processes in Ionic Crystals*, p145.

From this we obtain a graphically as the abscissa of the point of intersection of the curves

$$y=\left(1-\frac{1}{\tan\alpha}\frac{i}{E}\right)a, \qquad y=1-e^{-a}.$$

The magnitude of E was varied from 0 to 100 volts at each wavelength; η and c were measured for a variety of values of E and i; l was measured independently. In addition, the resistance of the crystal was always measured for each trial. This was necessary because the applied voltage was divided between the crystal and the input resistance of the amplifier. η and c were both fairly constant with different values of E. This gives experimental justification to Hecht's equation.

In addition to the above method η and c were also determined by considering two points on the $i=f(E)$ curve, i.e., by using two pairs of values of i and E. Both methods gave approximately the same results.

Figures 5 and 6 show the dependence of the quantum yield η on wavelength at various temperatures. Figure 7 shows η and c as a function of temperature at a fixed wavelength. These curves show that the quantum yield decreases as the temperature goes up.

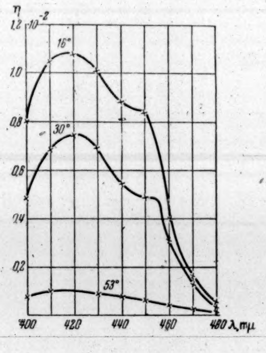

FIG. 5. Graphs showing the dependence of the quantum yield upon wavelength at different temperatures.

Although changes in temperature have a very great effect on the quantum yield of a given crystal, one must realize that from crystal to crystal the yield may differ by as much as ten fold. In order to find out what it is that determines the quantum yield, we measured the concentration of the centers from which the electrons are freed in a silver bromide crystal. We consider those to be identical with the so called F-centers in the alkali halides. Our results, by the way, apply to any kind of photoelectrically active centers.

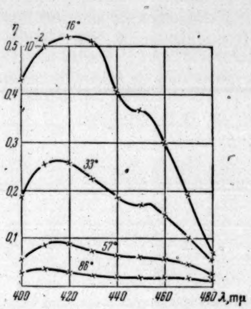

FIG. 6. Graphs showing the effect of wavelength upon the quantum yield at different temperatures.

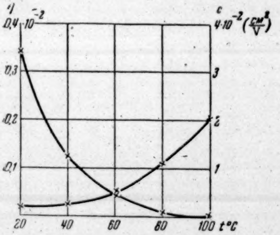

FIG. 7. Graphs showing η and c as a function of temperature.

The concentration of F-centers was determined as follows: The optical density of the crystal was measured at a number of temperatures (see Fig. 8). From the area under the curve one determined the increase in the number of F-centers, ΔN_F, from room temperature to the given temperature[8]. Considering that

$$N_F=N_0e^{-W/kT},$$

we can write $N_0=\Delta N_F/(e^{-W/kT_1}-e^{-W/kT_2}),$

---

[8] P. V. Meikliar and R. S. Shimanski, J. Exper. Theoret. Phys. USSR 27, 156 (1954).

Where w is the activation energy (0.15 ev), T_2 = room temperature and T_1 = the crystal temperature after it was heated. Having once established N_0 from known ΔN_F for several temperatures, it was possible to determine the concentration of F-centers at any temperature.

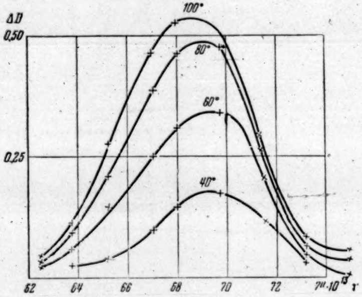

FIG. 8. Increase in the optical density of AgBr crystals as a function of frequency at different temperatures.

The concentration of F-centers was also varied by means other than temperature; such as by illumination of the crystals, cooling, and the addition of impurities. In each case the concentration of F-centers was measured.

It was determined that as the crystal was illuminated the concentration of F-centers went up while the quantum yield went down. Similar results were obtained when the crystals were quickly cooled from a temperature of 200 to 250°C. In each case, regardless of the method used to increase the concentration of F-centers, the quantum yield went down as the concentration of F-centers went up. The relation is shown in Fig. 9 (for λ = 430 mμ) where a linear relation is seen to obtain between log η and N_F, that is a relation of the form $\eta = A \exp(-BN_F)$, (where A = 0.04 and B = 0.65). The table shows the complete data.

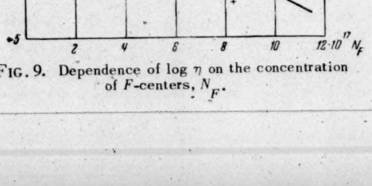

FIG. 9. Dependence of log η on the concentration of F-centers, N_F.

The decrease in photoelectric sensitivity with increase in temperature takes place also at λ = 365 mμ, that is in the region of absorption of crystalline silver bromide. The dependence of the quantum yield η on the temperature at λ = 365 mμ is shown in Fig. 10. Figure 11 shows log η as a function of N_F, the concentration of F-centers.

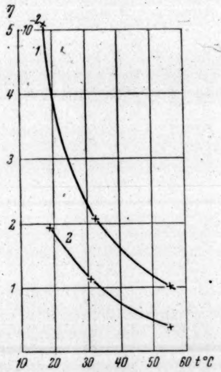

FIG. 10. η as a function of temperature for λ = 365 mμ; 1 – No. 18, 2 – No. 32.

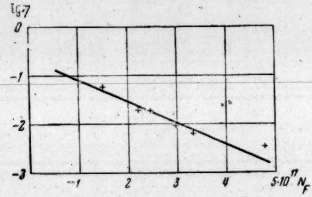

FIG. 11. log η as a function of F-centers for λ = 365 mμ.

DISCUSSION

It is hard to establish definitely the reason for the dependence of the quantum yield upon the concentration of F-centers. One might venture the following hypothesis: In the case of the lumines-

Test No.	3					12		22			31		33	25	28		21	
Temperature in °C.	20	40	60	80	100	20	30	16	30	53	-20	20	20	20	20 before cooling	20 after cooling	20 before illumination	20 after illumination
Concentration of F-centers $\times 10^{-17}$	2.75	4.34	5.98	7.60	8.35	5.48	6.44	2.43	3.58	4.9	0.58	1.45	2.28	1.82	1.63	2.21	0.55	3.86
Quantum yield $\times 10^2$	0.34	0.12	0.047	0.011	0.005	0.097	0.05	1.01	0.68	0.087	3.57	2.78	0.99	1.36	1.42	0.39	1.29	0.64

cence of dyes one recognizes the phenomenon of concentration quenching. It consists of the fact that as the concentration of the luminescent dye goes up, the luminescent yield decreases. There is a transfer of energy absorbed by one molecule to another similar molecule, as a result of which there is an increase in the probability of energy degradation into heat or some photochemical reaction. Vavilov[9] obtained the following equation for the probability of nontransfer of energy as a function of molecular concentration $C: q(C) = e^{-aC}$ where a is a linear function of time.

The presence of a dependence of photoconduction upon the concentration of F-centers gives reason to believe that we are dealing here with a concentration quenching of photoconductivity.

Experiments show that the concentration effects for dye solutions occur at concentrations of 10^{-3} mol per liter, where the mean distance between the molecules in solution is about 50 A, although, according to the quantum theory, the phenomenon should begin to be apparent at mean molecular separation of about 200 A. The phenomenon that is observed in silver bromide occurs when the concentration of F-centers is 10^{17} to 10^{18} cm^{-3}, i.e., when the distance between neighboring centers is about 100A.

The energy flowing through the crystal may be degraded into heat or it may bring about a photochemical reaction yielding sensitized silver bromide. Favoring the latter assumption is the fact that the lesser photoconductive crystals are usually more active photochemically. Similarly it is known that the photoelectric sensitivity of photographic emulsions is negligible. It is of course possible that production of photoactivated silver may be due to the migration of electrons as is suggested by the experiments of Haynes and Shockley[10].

The intrinsic photoelectric activity of crystals also seems to be related to the concentration of F-centers. From this we might deduce the active nature of absorption in the region of self absorption and release of F-centers.

---

[9] A. N. Terenin, *Problems in Physical Optics*, Papers presented in memory of S. I. Vavilov, GTTI, Moscow, 1951, p20

[10] J. R. Haynes and W. Shockley, Report on Conference on Strength of Solids, London, 1948 p151.

Translated by M. M. Kessler
9

SOVIET PHYSICS JETP VOLUME 3, NUMBER 1 AUGUST, 1956

Total Cross Sections of Positive π-Mesons on Hydrogen

A. E. IGNATENKO, A. I. MUKHIN, E. B. OZEROV, AND B. M. PONTECORVO
Institute for Nuclear Problems, Academy of Sciences, USSR

(Submitted to JETP editor July 15, 1955)
J. Exper. Theoret. Phys. USSR 30, 7-11 (January, 1956)

Total cross sections of positive π-mesons on hydrogen were determined by the attenuation method, the beam of mesons passing through a scatterer of liquid hydrogen. From the set of measured total cross sections of π^+ mesons on hydrogen and deuterium, carried out by the authors, the contributions to the scattering of the different isotopic spin states at energies between 140 and 400 mev is derived.

EXISTING data on the total cross sections of positive π-mesons on hydrogen obtained by the attenuation method can be divided into two groups. In the first group, precise data with good energy resolution have been obtained recently by Ashkin et al.[1] Their measurements appear continuous with others at higher energy (up to ~200 mev) carried out earlier by Anderson, Fermi et al.[2] The second group of data,[3,4] of a preliminary character, covers the interval of energy from 150 mev to 450 mev. These measurements make it possible to decide whether there exists a maximum of the total cross section $\sigma_t(\pi^+, p)$ in its dependence on the energy, but because of insufficient energy resolution it is not possible to say anything definite about the position of the maximum or the magnitude of the cross section in its neighborhood.

We have made measurements of the total cross sections of π^+ mesons on hydrogen in the energy interval 140 to 230 mev. Positive mesons, produced in a copper target placed inside the vacuum chamber of the synchrocyclotron, passed through a channel made in the vertical mounting of the yoke of the accelerator's electromagnet. Consequently, special shielding against the direct radiation of the synchrocyclotron was not required. The total cross section was determined from the attenuation of the beam of mesons in passing through a hydrogen scatterer. The geometry of the experiment is shown in Figure 1. The target used in the experiment held about 12 liters of liquid hydrogen. The length of the scatterer was 28 cm, which corresponds to 1.97 gm/cm^2 of hydrogen.

As in the experiment on the scattering of negative π-mesons,[5] the beam of π^+ mesons falling on the target was detected by a system of three counters (1,2,3). However, in view of the fact that the beam of positive mesons contains a very great number of protons having the same momentum as the mesons, one of the scintillation counters in the defining telescope (1,2,3) was replaced by a Cerenkov detector. This lowered the effectiveness for registering protons to approximately one hundredth of one per cent, but even this does not exclude the possibility of their being registered completely because the plexiglass used as Cerenkov radiator scintillates slightly. In order to avoid all errors in the measurement of attenuation due to the admixture of protons of low energy, a filter (4.6 gm/cm^2 of polyethylene) capable of stopping protons contained in the meson beam was placed in front of the third scintillator.

Mesons which passed through the last scintillator (4) were registered by a coincidence counting arrangement. In the measurements, to exclude the possibility of error arising from the drift of electronic apparatus, the hydrogen dewar was replaced by a blank at intervals of 5-10 minutes. The identity of the path of the beam through the walls of the dewar and the blank was checked by a special experiment with an intense beam of negative π-mesons. On account of the low current of π^+-mesons, the determination of their energy during the measurement runs was extremely difficult. We used another method of measuring the energy, the method of the flexible current bearing conductor immersed in the magnetic field.[6] As a control, the range of the mesons in copper was measured at an energy of 145 mev. This measurement coincided with that obtained by the method of the current bearing filament. The maximum possible inhomogeneity in the energy of the beam of mesons which fell on the target was also determined with the help of the current bearing conductor in the magnetic field. This maximum dispersion in energy was determined by the aperture of the collimating system; it was approximately ± 1.5 % of the nominal beam energy. The total uncertainty in the energy (taking into account the slowing down of the mesons in hydrogen, the errors in the measurement, and the initial maximum possible inhomogeneity of the beam in energy) was about ± 6 mev.

---

[1] J. Ashkin, J. P. Blaser, F. Feiner, J.G. Gorman, and M. O. Stern, Phys. Rev. 96, 1104 (1954).

[2] H. L. Anderson, E. Fermi, E. A. Long, and D. E. Nagle, Phys. Rev. 85, 936 (1952).

[3] L. C. L. Yuan and S. J. Lindenbaum, Bull. Amer. Phys. Soc. 28, 13 (1953); Phys. Rev. 92, 1578 (1953).

[4] L. C. Yuan et al, cited in F. de Hoffman et al, Phys. Rev. 95, 1586 (1954).

[5] A. E. Ignatenko, A. E. Mukhin, E. B. Ozerov, and B. M. Pontecorvo, Dokl. Akad. Nauk SSSR 103, 45(1955).

[6] J. J. Thomson, Phil. Mag. 13, 561 (1907); M. C. Kazodaev and A. A. Tyapkin, Report for 1952 of Institute of Nuclear Problems, Academy of Sciences.

It is well known, that in a beam of positive π-mesons of energy from 130 to 200 mev, the admixture of μ^+-mesons remains practically constant.[1] From experiments with beams of negative π-mesons[5] it is seen that in a very wide band of energies above 180 mev, the admixture of μ^--mesons also changes insignificantly. On the basis of the experimental facts presented above, the admixture of μ^+-mesons was measured by absorption only for one energy, 145 mev, and assumed constant for all energies which are of interest for the following. The admixture was (7.0 ± 1.5) %.

Under the geometrical conditions of the experiments, (average angle registered by the last detector, $\theta = 8^\circ$) the last scintillator was registering an appreciable part of the recoil protons and scattered mesons. The correction taking this effect into account was determined from the known angular distribution at three energies [7-9]. At an energy of 144 mev, where the filter in front of the last scintillator was sufficient to stop all recoil protons, the experimentally measured correction for recoil protons practically coincided with the calculated correction (Table 1).

TABLE I.

	$\sigma_t(\pi^+, p)$ (10^{-27}cm^2) measured	Correction		$\sigma_t(\pi^+, p)$ (10^{-27}cm^2) corrected
		Recoil Protons	Mesons	
Without filter	$135{,}9 \pm 4{,}0$	9,7	3,8	$149{,}4 \pm 4{,}7$
With filter	$147{,}4 \pm 3{,}8$	—	3,8	$151{,}2 \pm 3{,}9$

The results of the measurements, with the corresponding corrections inserted, are displayed in Table 2. The errors indicated in the second column are statistical and include uncertainties arising from the insertion of corrections. The first number was obtained with the help of the method of (CH_2-C) differences (with a geometry described earlier in Reference 5); the remaining data were obtained with liquid hydrogen.

TABLE II.

Energy of meson (mev)	Total cross section (10^{-27}cm^2)
140 ± 7	133 ± 8
144 ± 6	151 ± 4
164 ± 6	169 ± 5
174 ± 6	193 ± 6
184 ± 6	196 ± 6
194 ± 6	200 ± 6
209 ± 6	179 ± 6
219 ± 6	156 ± 7
229 ± 6	132 ± 7

The numbers indicated in Table 2 for the total cross section in the neighborhood of 195 mev are in good agreement with the data of Ashkin et al.[1] The continuation of the measurements in the direction of higher energy where, up to the present, no direct measurement of the total cross section existed, shows that it reaches its maximum value ($200 \times 10^{-27}\text{cm}^2$) at approximately 190 mev. After achieving the maximum, the cross section falls relatively rapidly with further increase in energy. Earlier the position of the maximum of $\sigma_t(\pi^+, p)$ could be judged only from the results of indirect measurements, which were discussed in Reference 10.

---

[7] W. B. Fowler et al., Phys. Rev. 92, 832 (1953).

[8] M. Glicksman and H. L. Anderson, Bull. Amer. Phys. Soc. 29, 24 (1954).

[9] U. Kruse, H. L. Anderson, W. C. Davidon, and M. Glicksman, Bull. Amer. Phys. Soc. 30, 49 (1955).

[10] A. E. Ignatenko, A. E. Mukhin, E. B. Ozerov, and B. M. Pontecorvo, Dokl. Akad. Nauk SSSR 103, 209(1955).

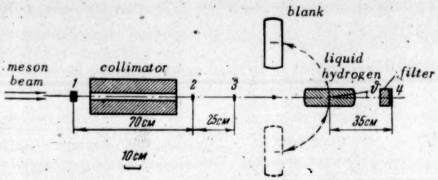

FIG. 1. Scheme of the experiment. 1--Cerenkov detector; 2,3,4--scintillation counters.

It is worth noting that the position of the maximum for π^+ mesons coincides with the position of the maximum in $\sigma_t(\pi^-, p)$.

In the neighborhood of the maximum, the magnitude of the total cross section $\sigma_t(\pi^+ p)$ reaches the value $8\pi\lambda\!\!\!^{-2}$ (where $\lambda\!\!\!^{-}$ is the wavelength in the center of mass system) i.e., it reaches the maximum value of the cross section for elastic scattering in P-states with total angular momentum equal to 3/2. As is well known [1,5] for π^--mesons, the magnitude of the cross section in the region of the maximum is also equal to the maximum possible value for the cross section in a $P_{3/2}$ state with isotopic spin T=3/2, i.e., it is (8/3) $\lambda\!\!\!^{-2}$.

From the requirement of charge independence, there follows the relation $\sigma_{1/2}=(3\sigma_t(\pi^-, p)-\sigma_{3/2})/2$ which connects the total cross section of the states with isotopic spin T=3/2 ($\sigma_{3/2}$) and T=1/2($\sigma_{1/2}$). It determines the contribution to the scattering of the state with isotopic spin T=1/2. Our measurements of $\sigma_t(\pi^+, p)=\sigma_{3/2}$ up to the energy 230 mev are plotted in Figure 2. At higher energies, the quantity $[\sigma_t(\pi^-, d)-\sigma_t(\pi^-, p)] \approx \sigma_t(\pi^+, p)$ is plotted[10].

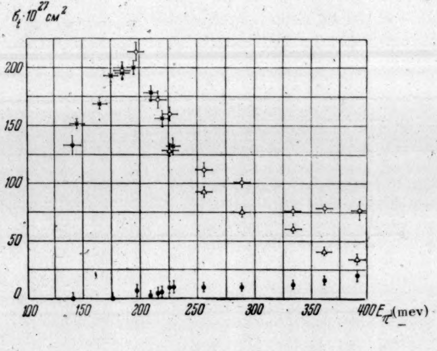

FIG. 2 Total cross sections $\sigma_{1/2}$ and $\sigma_{3/2}$ for π-mesons on nucleons in the states of isotopic spin T=1/2 and T=3/2
× — $\sigma_t(\pi^+, p) = \sigma_{3/2}$;
Δ — $[\sigma_t(\pi^-, d) - \sigma_t(\pi^-, p)] \approx \sigma_{3/2}$; ○ — $3\sigma_t(\pi^-, p)$;
● — $[3\sigma_t(\pi^-, p) - \sigma_t(\pi^+, p)]/2 = \sigma_{1/2}$

For the purpose of comparison, both $\sigma_t(\pi^+, p)$

and $[\sigma_t(\pi^-, d) - \sigma_t(\pi^-, p)]$ are plotted at an energy of 226 mev. As one can see, these quantities agree sufficiently well. In the figure, the energy dependence of $3\sigma_t(\pi^-, p)$ is also shown, as well as the value of $\sigma_{1/2}$ obtained with the help of the relation written down above.

Although the entire set of measurements is consistent with the idea that the interaction of π-mesons with hydrogen in the energy interval 140 to 300 mev takes place principally in a single state with T=3/2, it should be remarked that already at an energy of 250 mev, as one can see from Figure 2, the contribution to the scattering of the state with T=1/2 becomes noticeable.

In Fig. 3, our experimental data are plotted together with the curve of the energy dependence of the total cross section of positive mesons in hydrogen calculated by Bethe et al.[11] This curve corresponds to their "resonance" solution (resonance refers to the phase shift α_{33}, corresponding to the state $P_{3/2}$ with isotopic spin T=3/2). The experimental points are in very good agreement with this solution. It should be noted that the entire set of results of our measurements of the total cross sections of π-mesons in hydrogen and deuterium in the energy interval 140 to 400 mev are well described by the semi-phenomenological "isobar" theory of Tamm et al.[12]

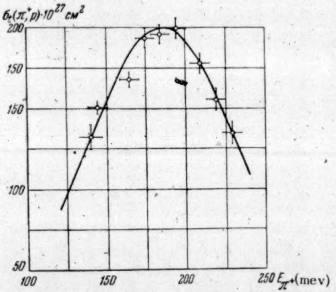

FIG. 3. Total cross section of π^+ mesons on hydrogen $\sigma_t(\pi+, p)$. The solid curve is the "resonance" solution of Bethe et al.[11]

It is of definite interest to compare our measurements of the cross section $\sigma_t(\pi^-, d)$ with the sum of the total cross sections for free particles $\sigma_t(\pi^-, p) + \sigma_t(\pi^+, p)$, which is equal, according to the principle of charge symmetry, to $\sigma_t(\pi^-, p) + \sigma_t(\pi^-, n)$. In Fig. 4 the values of $\sigma_t(\pi^-, d)$[10] are plotted, and also the area of possible values of the sum $\sigma_t(\pi^-, p) + \sigma_t(\pi^+, p)$, indicated by the striped area (values taken from the present work and Ref. 5). It is clear that in the neighborhood of the maximum there is a noticeable decrease of $\sigma_t(\pi^-, d)$ in comparison with the sum $\sigma_t(\pi^-, p) + \sigma_t(\pi^+, p)$.

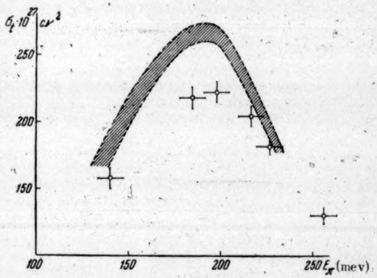

FIG. 4. Comparison of $\sigma_t(\pi^-, d)$ and the sum $\sigma_t(\pi^-, p) + \sigma_t(\pi^+, p)$. ○ – $\sigma_t(\pi^-, d)$, striped area-- $\sigma_t(\pi^+, p) + \sigma_t(\pi^-, p)$

Such behavior of the cross section of the deuteron is in agreement with theoretical predictions of Tamm[12] and Brueckner.[13] From their calculations in impulse approximation with the inclusion of the effects of multiple scattering one can derive that in the case of interaction in the state of isotopic spin 3/2 there will be observed a noticeable decrease of the total cross section of the deuteron in comparison with the sum of the cross sections of the free nucleons at a phase shift greater than 45°.

The authors are deeply grateful to Academician I. E. Tamm for numerous discussions.

---

[11] F. de Hoffman, N. Metropolis, E. F. Alei, and H. A. Bethe, Phys. Rev. 95, 1586 (1954).

[12] I. E. Tamm, Iu. A. Gol'fand, G. F. Zharkov, L. V. Pariskaia, and V. Ia. Feinberg, Report of the All Union Conference on Quantum Electrodynamics and the Theory of Elementary Particles (31 March-7 April 1955).

Added in proof. After the present paper was written, the use of beams of π^+ mesons, produced by external protonbeams, made possible measurements of the total (and differential) cross section of hydrogen at meson energies above 300 mev. The results of that work as well as the recently appeared work of Lindenbaum and Yuan[14] will be discussed in a communication which will appear soon.

[13] K. A. Brueckner, Phys. Rev. 89, 834 (1953).

[14] S. J. Lindenbaum and L. C. L. Yuan, Phys. Rev. 100, 306 (1955).

Translated by A. S. Wightman
2

SOVIET PHYSICS JETP VOLUME 3, NUMBER 1 AUGUST, 1956

An Investigation of High-Frequency Discharge

G. M. PATEIUK

Moscow State University

(Submitted to JETP editor, September 4, 1954)

J. Exper. Theoret. Phys. USSR 30, 12-17 (January, 1956)

The striking and maintaining voltages have been investigated in argon, neon and hydrogen as a function of gas pressure and geometry of discharge space in the frequency range from 57 to 500 mc. It has been established that boundary conditions at the electrodes and walls of the discharge tube have a substantial influence on the striking and maintaining voltages. As the frequency of the a-c field is increased from 57 to 500 mc, the curves showing striking and maintaining voltages vs. pressure in hydrogen, argon and neon are displaced into the high voltage region, and the minima of these curves are displaced into the high gas pressure region. A region of critical frequencies has been found for hydrogen within which the dependence of striking voltage on gas pressure remains practically constant with changes in field frequency. Results of the present investigation are in accord with conclusions of the diffusion theory of high-frequency discharge[1,2].

INTRODUCTION

It is known that when pressure in a high-frequency discharge is reduced, the striking and maintaining voltages diminish as the frequency of the electrical field is increased from the order of 10^5 to the order of 10^6 cycles[3-6]. At the same time the minima of $V_s(p)$ and $V_m(p)$ curves (showing striking and maintaining voltages vs. gas pressure) are displaced into the low pressure region.

Study of high-frequency discharge in hydrogen has shown that minimum striking voltage occurs at a frequency of 4×10^7 cycles, above which striking voltage again increases with increased frequency. This frequency will be referred to as the critical frequency. Aside from the frequency of the electrical field, the striking and maintaining voltages in high-frequency discharges are significantly affected by the geometry of the discharge space[5,7].

In the literature there is a dearth of data on research in high-frequency discharge at frequencies above the critical. The present study comprises an experimental investigation of striking and maintaining voltages as a function of gas pressure under conditions of several different discharge space geometries and boundary conditions in a frequency region above the critical frequency.

APPARATUS AND METHODS OF MEASUREMENT

High-frequency fields were obtained with the use of tuned-grid tuned-cathode push-pull oscillators over a frequency range from 54 to 750 mc.

A diode voltmeter was used for high-frequency voltage measurements. Calibration and checking of diode voltmeter for resonances were conducted with the aid of a dielectric voltmeter developed in the laboratory. The diode voltmeter permitted high-frequency voltage measurements with a relative error not over 10-12 percent at 750 mc. Field frequency was measured with a two-conductor line as well as with a resonant wave-meter.

In conducting the experiments special attention was paid to shielding all elements of electrical circuits, to cleanness of electrodes and discharge tubes, and to oscillator stability.

For the basic measurements, four types of tubes (A,B,C,D) were used, as shown in Fig. 1. In the type A tube, plane electrodes of electrolytic nickel, 30 mm in diameter, were used. The operating surfaces of the electrodes were thoroughly polished. The edges of the electrodes were rounded off to eliminate edge effects. In order that the discharge not extend outside the discharge space, the leads and the back areas of electrodes were covered with glass insulation. One of the electrodes in the tube was movable. The internal diameter of the tube was 40 mm, and its length was 80 mm.

In the type B tube the electrodes were similar to those of type A but were covered with a thin layer of glass (0.2 to 0.3 mm). The internal diameter of

---

[1] M. A. Herlin and S. C. Brown, Phys. Rev. 74, 291, 910, 1650 (1948).

[2] A. D. MacDonald and S. C. Brown, Phys. Rev. 75, 411, 1324 (1949), 76, 1634(1949).

[3] F. Kirchner, Ann. der Physik 77, 287(1925).

[4] L. Rohde, Ann. der Physik 12, 569 (1932).

[5] J. Thomson, Phil. Mag. 23, 1(1937).

[6] M. Chenot, Ann. der Physik 3, 277(1948).

[7] S. Githens Jr., Phys. Rev. 57, 822(1940).

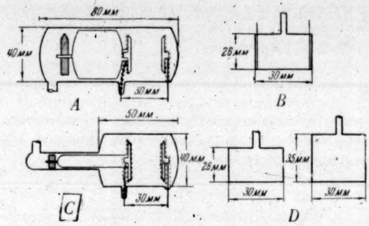

FIG. 1. Types of experimental discharge tubes.

the tube *B* was 40 mm, its length 50 mm.

Type C tube was a cylindrical glass tube with parallel plane ends. Electrodes consisting of thin sheet nickel discs were tightly soldered to the inside of these tube ends. The diameter of these electrodes was equal to the inside diameter of the tube. The high-frequency voltage could be applied to this type of tube either through these internal nickel electrodes or through external electrodes consisting of round discs tightly bound to the parallel plane tube ends.

Type D tubes (26 and 35 mm in diameter and 30 mm long) were cylindrical tubes with parallel plane ends. The external electrodes were round discs of copper sheet tightly bound to the plane tube ends from the outside. The voltage indicated just prior to striking was taken as the striking voltage of the high-frequency discharge. The maintaining voltage of the high-frequency discharge was considered the minimum voltage indicated just prior to extinguishing of the discharge.

RESULTS OF EXPERIMENTS

To determine the effect of the size as well as the boundary conditions of the discharge space, and, in particular, to find the effect of electrode material on striking and maintaining of a high-frequency discharge, the striking and maintaining voltages were studied in neon in type *A* and *B* tubes, at a frequency of 158 mc, and with different electrode spacings (L=20 and 5 mm).

Figures 2 and 3 curves show striking voltages (solid lines) and maintaining voltages (dotted lines for L=20 and 5 mm) vs. gas pressure for clean metal electrodes (Fig. 2), and for glass-covered electrodes (Fig. 3). On these curves the abscissa shows the gas pressure in mm of mercury, and the ordinate shows striking and maintaining voltages. In all curves the voltages shown are peak values.

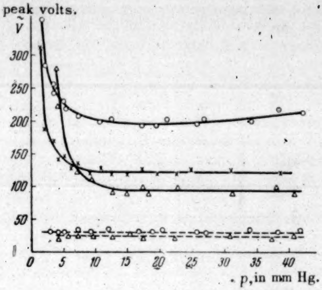

FIG. 2. Striking and maintaining voltages vs. pressure in neon with different electrode spacings using clean nickel electrodes. ν=158 mc.
O L=20mm
x L=10 mm
Δ L=5mm

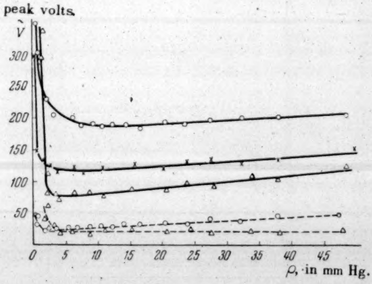

FIG. 3. Striking and maintaining voltages vs. pressure in neon for glass-covered nickel electrodes. O–L=20mm, X–L=10mm, Δ-L=5 mm, ν=158mc

The curves of Figs. 2 and 3 show that an increase in electrode spacing is accompanied by an increase in striking and maintaining voltages, and that curve shape is similar to the striking characteristic for a d-c discharge. However, the curves show that under the present conditions Paschen's law is not obeyed, a conclusion also reached on the basis of theoretical considerations.[8]

The left ends of the curves showing the relation between striking voltage and pressure, $V_s(p)$, for electrode spacing L=5 mm pass through a pressure region considerably higher than the left ends of $V_s(p)$ curves for L=20 and 10 mm. In the low pressure region the shape of $V_s(p)$ curves differs for nickel electrodes and for glass-covered electrodes. The left ends of curves for glass-covered electrodes are steeper and pass through considerably lower pressure regions than those for nickel electrodes.

---

[8] H. Margenau, Phys. Rev. 73, 297, 326(1948), 74, 706(1948). H. Margenau and L. M. Hartman, Phys. Rev. 73, 309(1948). L. M. Hartman, Phys. Rev. 73, 316(1948).

To ascertain the effect of discharge tube diameter on striking and maintaining of high-frequency discharge, measurements were conducted in neon at 158 mc field frequency in type D tubes (Fig. 1) 26 and 35 mm in diameter. Figure 4 shows curves of striking and maintaining voltages vs. gas pressures, $V_s(\rho)$ and $V_m(p)$, for these two tubes. Experimental points for the smaller discharge tube are indicated by circles and for the larger tube by x's. Dotted lines indicate maintaining voltages.

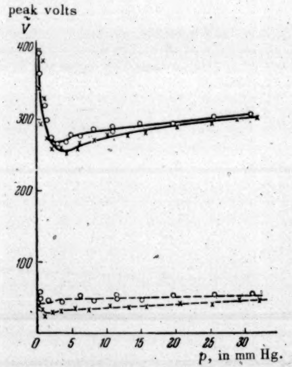

FIG. 4. Striking and maintaining voltages vs. pressure in neon for tubes of different diameters. O--d = 26mm; X --d=35mm; ν=158mc.

Curves of Fig. 4 show that for equal gas pressures, the striking and maintaining voltages in the smaller tube are higher than in the larger tube.

A certain modification of striking and maintaining conditions was obtained as a result of simultaneous application of a d-c field and a high-frequency field to the discharge space. Measurements were made of striking and maintaining voltages of high-frequency discharge in argon with a field frequency of 500 mc in type C discharge tube (Fig.1). High-frequency voltage was applied to the external electrodes, which consisted of round discs tightly pressed to the plane ends of the discharge tube, and the d-c voltage was appled to the internal electrodes.

Figure 5 shows the results of measuring striking and maintaining voltages of high-frequency discharge as a function of gas pressure, with a d-c field of 0, 50 and 100 volts applied simultaneously to the discharge space. The $V_s(p)$ curves are shown as solid lines and the $V_m(p)$ are dotted.

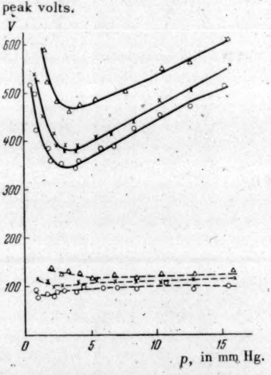

FIG. 5. Striking and maintaining voltages of high-frequency discharge vs. pressure in argon with simultaneous application of a d-c field. o-v=0, x-v=50v, Δ-v=100v; ν=500mc

Figure 5 curves show that with a simultaneous application of a d-c field to the discharge space, $V_s(p)$ and $V_m(p)$ curves display considerably higher voltages than in the absence of the d-c field (curves when v=0). The effect of more difficult striking of high-frequency discharge in the presence of simultaneously applied d-c field is clearly evident. This effect, as the curves show, considerably increases the striking and maintaining voltages, and the higher the d-c voltage, the higher the striking and maintaining voltages of the high-frequency discharge.

To clarify the character of $V_s(\rho)$ and $V_m(\rho)$ curves as functions of field frequency, investigation of striking and maintaining voltages was carried out in hydrogen and argon with field frequencies of 57.7, 78.9, 136, 167, and 500 mc in a type D discharge tube (Fig. 1), 30 mm long and 35 mm in diameter. Figure 6 shows the relation between striking and maintaining voltages (the latter dotted) and pressure in hydrogen for the above field frequencies. In order not to make the drawing too complicated, curves for $V_m(p)$ are shown only for the extreme frequencies of 57.7 and 500 mc. For intermediate frequencies, the $V_m(p)$ curves lie between the 57.7 and 500 mc curves. These curves show that in raising the field frequency from 57.7 to 500 mc the striking and maintaining voltages increase. The minima of the $V_s(p)$ curves are displaced into the high-pressure region as the frequency increases. For hydrogen, the $V_s(p)$ curves are practically identical for frequencies of 57.7 and 79.9 mc, i.e., in changing the field frequency from 57.7 to 79.9 mc, the striking voltages undergo practically no change.

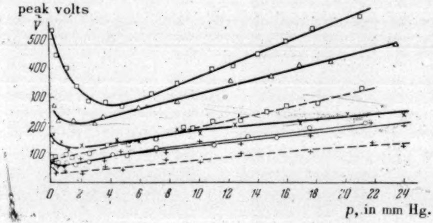

FIG. 6. Striking and maintaining voltages vs. pressure in hydrogen for several field frequencies. +-v=57.7 mc; o-v=78.9 mc; x-v=136 mc Δ-v=167 mc; □ -v=500 mc.

Thus, in investigating striking and maintaining voltages in hydrogen a region of critical frequencies has been determined (57.7 to 79.9) mc). For argon a similar critical frequency region must obtain at lower frequencies.

DISCUSSION OF EXPERIMENTAL RESULTS

The experimental results obtained can be explained in the following fashion on the basis of the initial assumptions of the diffusion theory of high-frequency discharge.[1,2] In the high pressure region the cause of the increase in striking and maintaining voltages with increase in gas pressure is the same as for d-c discharge. As the pressure is increased, the mean free path of the electron, as well as the energy of the electron on this path, are decreased. In order that the electron receive from the field the energy required for ionizing a gas molecule, higher and higher voltages must be applied to the electrodes as the pressure is increased At high pressures, diffusion of electrons to the electrodes and to the walls of the tube is insignificant.

At low pressures the main factor which determines the striking and maintaining voltages is the departure of electrons from the discharge space, to the electrodes and tube walls as a result of diffusion, and not the increase in electron energy along the free path. Therefore, at low pressures it is necessary to increase the voltage on the electrodes to replace the increasing depletion of electrons due to diffusion. The minima of $V_s(p)$ curves correspond to optimum conditions for starting the high-frequency discharge.

With decreased spacing between electrodes, on the one hand the high-frequency field intensity is increased, and therefore the energy which electrons acquire along the free path is increased, which in turn leads to increased gas ionization; on the other hand, with decreased spacing between electrodes loss of electrons takes place due to diffusion to the electrodes. With large electrode spacing and high gas pressure the fundamental part in striking and maintaining voltages is played by the first factor--the high-frequency field intensity; with small spacing and low pressure the other factor begins to play the fundamental role, i. e., loss of electrons by diffusion.

The curves in Figs. 2 and 3 show that striking voltages at 20 mm spacing are considerably higher than at 10 and 5 mm. These curves also show that for 5 mm electrode spacing the left ends of $V_s(p)$ curves pass through a region of considerably higher pressures than the left ends of curves for 20 and 10 mm spacing. The displacement of left ends of $V_s(p)$ curves at 5 mm into the region of higher pressures is caused by high electron losses due to diffusion to the electrodes.

With glass-covered electrodes (Fig. 3) the left ends of V_s (p) and V_m(p) curves are considerably displaced in the direction of low pressures as compared to similar curves for nickel electrodes shown in Fig. 2. This displacement of V_s (p) and V_m (p) curves in the direction of low pressures is due to the lower electron losses with glass-covered electrodes. Accordingly, the balance of charged particles resulting from ionization and diffusion in the case of glass-covered electrodes takes place at lower pressures than in the case of nickel electrodes.

In a d-c discharge, because of secondary processes affecting the electrode material, the latter plays an important part in the very mechanism of the starting and development of the discharge. The role of electrodes in high-frequency discharge fundamentally comes down to the conditions of maintaining a balance of charged particles in the discharge space.

The curves in Fig. 4 show that striking and maintaining voltages are affected not only by boundary conditions near the electrodes, but also by conditions at the walls of the discharge tube. In the small tube, under otherwise identical conditions, more electrons leave the discharge space due to bi-polar diffusion to the walls of the discharge tube. Therefore, for initiating and maintaining high-frequency discharge in a narrow tube, under otherwise identical conditions, considerably higher electrode voltage is required than for a wide tube.

In the presence of only an a-c field, loss of electrons in the discharge space is fundamentally determined by diffusion to the electrodes as well as by bi-polar diffusion to the walls of the discharge tube. In the simultaneous presence of high-frequency and d-c fields, electron loss from the discharge space also increases as a result of withdrawal of electrons to the electrodes caused by the d-c field. Accordingly, in the presence of a d-c field considerably higher electrode voltage is required for initiating and maintaining high-frequency discharge, as has already been shown in reference 10. Thus, the boundary conditions of the discharge space substantially affect the striking and maintaining voltages of high-frequency discharge.

The increase of striking and maintaining voltages with an increase in frequency (at frequencies higher than critical) is explained fundamentally by the decrease of average energy received by electrons from the field at high frequencies.[9]

In conclusion, the author takes this opportunity to express his gratitude to Prof. N. A. Kaptsov for suggesting the subject matter and for his constant interest in the work.

---

[9] H. Margenau, Phys. Rev. 69, 508(1946).

[10] A. Varela, Phys. Rev. 71, 124(1947).

Translated by K. Amatneek
3

SOVIET PHYSICS JETP VOLUME 3, NUMBER 1 AUGUST, 1956

An Investigation of Magnetic Spectra of Solid Solutions of Some NiZn-Ferrites in the Radiofrequency Range

L. A. FOMENKO

Central Industrial Radio Interference Laboratory of the Ministry of Electrotechnical Industry of the USSR

(Submitted to JETP editor July 30, 1954).

J. Exper. Theoret. Phys. USSR 30, 18-29, (January, 1956).

Results are presented of the investigations of magnetic spectra of NiZn ferrites with initial permeabilities $\mu_a \approx 200$, 400, and 2000 gauss/oersted in the range of 0.2-60 megacycles/sec. An examination is made of the method of measuring the spectra and of eliminating possible inaccuracies in the results. Samples have been studied in the state of complete demagnetization, in a state of residual magnetization, and at various values of a constant magnetizing field. It is shown that the spectra of ferrites have a resonance or a relaxation character, are practically independent of core dimensions, and can be interpreted in terms of the dispersion of the ferromagnetic substance which, for ferrites with $\mu_a \approx 2000$ gauss/oersted, is apparently due principally to the inertia of the effective mass of the boundaries, and for ferrites with $\mu_a \approx 200$ gauss/oersted is due to the precessional motion of the magnetization vector in the effective field of the anisotropy of the substance of the ferrite.

---

1. IN magnetic spectra* of continuous polycrystalline ferrites, at least five regions of dispersion have been recognized: a) the low-frequency region, characterized by an insignificant decrease in the permeability μ in the range 0-0.2 mc.[2]. b) the "infraradiofrequency" range characterized by a sharp resonance peak in μ_1 at $f \sim 0.1$ mc due to magnetomechanical effects[2-4]; c) the radiofrequency range, characterized by a rapid falling off of the real component of the complex magnetic permeability of the ferrites, and by a clearly pronounced absorption peak in the range ~ 1-200 megacycles [2,5-12]; d) the ultrahigh-frequency range, characterized by the phenomenon of natural ferromagnetic resonance, usually observed at frequencies of 10^3-10^4 mc, which is due to the precession of the electron spin in the effective field of the anisotropy of the substance of the ferrite[13,14]; e) the "infrared" region. According to calculations, since the "natural exchange resonance" in the field of exchange interaction has not yet been experimentally observed by anyone, this region should be characterized by a small resonance change of the curves of dispersion and absorption at frequencies $\sim 10^7$ mc[15]. The main decrease in the permeabilities μ and μ_1 of ferrites is observed in the radiofrequency range, as a result of which the investigation of dispersion at radiofrequencies has the greatest practical significance.

For a bicomplex medium, i.e., (according to Arkad'ev) for a medium with complex magnetic permeability and dielectric permittivity $\epsilon' = \epsilon - j\sigma'$ the phenomena of radio-frequency dispersion and absorption are ascribed in the literature to the following three causes: a) the dispersion of the ferrite substance, which may be due, in accordance with the theories of Landau and Lifshitz[16], and of Döring[17] to the inertia of the effective mass of the boundaries, and according to Landau and Lifshitz[16] and Snoek[18] may be due to the precession of the magnetization vector in the effective field of the anisotropy of the substance of the ferrite; b) to the dispersion caused, in accordance with Ref. 12, by the specific structural peculiarities of the material; c) to the dispersion of the permeabilities of the body of the ferromagnetic, which is due to dimensional effects: a surface effect and a volume resonance*, and which was first discovered in MnZn-ferrites by Brockman, Dowling, and Steneck[19].

---

* According to Arkad'ev[1] the name magnetic spectrum is given in the general case to dispersion curves $\mu_1(f)$ and absorption curves $\mu_2(f)$ or dispersion curves $\mu(f)$ and absorption curves $\rho'(f)$ where μ_1 and μ_2 are the real and imaginary parts of the complex magnetic permeability of a ferromagnetic body ($\bar{\mu} = \mu_1 - j\mu_2$), while μ and ρ' are the elastic and the viscous components of the complex magnetic permeability of a ferromagnetic substance $\mu' = \mu - j\rho'$; here f is the frequency.

[1] V.K.Arkad'ev. Collection of articles entitled *Problems of ferromagnetism and magnetodynamics*. Published by the Academy of Sciences of the USSR Moscow-Leningrad, 1946.

[2] R. Feldtkeller and O. Kolb, Z. angew. Physik. 4,448, (1952).

[3] A. Weis, Electrotechnik 5, (1951).

[4] A.A.Shvarts, Jour .Tech. Phys. (USSR) 3, 413(1953).

[5] D. Polder, Proc. Inst. Elec. Engrs. 2, 97, 246(1950).

[6] A. L. Fomenko, J. Exper. Theoret. Phys. USSR 21, 1201(1951); 24, 365(1953); 25, 107(1953).

[7] D. Vent and E. Gorter, Collection of Articles entitled *Problems in the technology of radiolocation* IIL, Moscow 1, (1953) (Russian translation).

[8] H.P.J.Wijn, M.Gevers and C.M.van der Burgt, Revs. Mod. Phys. 25, 91, (1953).

[9] R.E.Alley and F.J.Schnether, J. Appl. Phys. 24, 1524(1953).

[10] J.P.Blewett, M.H.Blewett and M.Plotkin, Rev. Sci. Instr. 24, 800(1953).

[11] I. Lucas, Z. angew. Physik 6, 127,(1954).

[12] N.G.Katkov, Thesis summary. MEI, Moscow(1954).

[13] A. Welch, P.Nicks, A.Fairweather and F.Roberts, Collection of articles entitled *Ferromagnetic Resonance*, IIL, Moscow(1952), p. 154.(Russian translation).

[14] G.T.Rado, Rev. Mod. Phys. 25, 81(1953).

[15] J. Kaplan and C. Kittel, Collection of articles entitled *Problems of modern physics* 6, 50(1954)(Russian translation).

[16] L.D.Landau and E.M.Lifshitz, Z. Physik Sovjetunion 8, 157(1935).

[17] V. Döring, Collection of articles entitled *Ferromagnetic Resonance* IIL, Moscow(1952) p.312(Russian translation).

As has been noted by Polivanov[20] the phenomena indicated above can, as a result of superposition, lead to quite complicated dispersion curves which differ in their appearance from the simplest types of magnetic spectra dealt with in Arkadiev's theory of magnetic viscous spectra.

Investigations (which have been largely carried out by Rado and collaborators[14]) using certain ferrites have shown that in the general case, under the condition that dimensional effects have been eliminated, magnetic spectra of the ferrite substance in the ranges of radiofrequencies and ultra high frequencies have two pronounced dispersion regions, one of which, the radio frequency one, is interpreted in terms of the inertia of the effective mass of the boundaries, and the other one, the ultra high frequency one, in terms of gyromagnetic resonance. Moreover, as a result of investigations by a number of authors[8,14] the existence of another, more numerous group of ferrites has been discovered, to which in particular, the NiZn-ferrites are found to belong, the magnetic spectra of which show a single pronounced dispersion region within the range of radio and ultra high frequencies. This region has been interpreted by the majority of investigators[5,7,8,11,18] from the point of view of rotational processes.

The study of radio frequency magnetic spectra of ferrites (with one exception[21]) has been carried out for the state of complete demagnetization of the material. The object of the present work is the investigation of magnetic spectra of several types of NiZn ferrites in the demagnetized state, as well as in a state of residual magnetization, and also at various values of the intensity of the constant magnetizing field.

2. Investigations were carried out using toroidal samples of Ni-Zn ferrite of the oxyfer types 0-2000-I, 0-400 and 0-200[22] with an ambient temperature of 25°. The values of saturation intensity of magnetization I_s, of the coercive force H_c, and of the initial permeability μ_a are given in the table. By definition, μ_a was taken to be the high-frequency permeability of samples measured in very weak fields at a frequency of f=0.25 mc.

By means of a high-frequency bridge, and also by means of Q-meters of types KV-1 and UK-1 the dependence of ϵ (f) and σ' (f) on f was measured for the various samples. For measurements made with the aid of the high-frequency bridge, the quantities ϵ and σ' were calculated from the data on effective series impedances X_c and R_c of an experimental condenser:

$$\varepsilon - j\sigma' = \frac{1{,}8\cdot 10^{12} b}{f S_\kappa}\left(\frac{X_c}{R_c^2 + X_c^2} - j\frac{R_c}{R_c^2 + X_c^2}\right), \quad (1)$$

where S_k is the area of the ring of the side surface of the toroid which was coated with soft graphite and then metallized; f is the frequency in cycles/sec, and b is the axial thickness of the toroid in centimeters.

For samples 0-200 and 0-400 in the frequency range 0.15-60 mc, the permittivity ϵ showed little dependence on the frequency (Fig. 1), while the permittivity σ' was, as a rule, much smaller than ϵ. For samples of 0-2000-I, the frequency dependence of ϵ and σ' is shown in Figure 2.

The magnitudes of the permeabilities of ferrites at different frequencies were determined from the results of investigating the frequency dependence of the values of the effective inductance L_x and the effective resistance R_x of toroidal coils wound on the core being investigated. The measurements of the coil parameters were carried out by means of a high-frequency bridge.

3. A simplified circuit diagram of the bridge is given in Fig. 3. The main idea of the method of measurement consisted of the following: For each frequency used, the bridge circuit was first

---

* The volume resonance arises when the wavelength penetrating into the core is close to twice the dimensions of its cross section; standing waves are set up in the core, as a result of which the values of the magnetic flux and of the scattered power increase[20].

[18] J. Snoek, *Investigations in the field of new ferromagnetic materials* IIL, Moscow(1949)p.162(Russian translation).

[19] F.G. Brockman, P.H.Dowling, and W.G.Steneck, Phys. Rev. 77, 85 (1950).

[20] K.M.Polivanov, Proceedings of M.E.I., 14, G.E.I., Moscow- Leningrad(1953).

[21] D. Rado, R. Wright, and V. Emerson. Collection of articles *Ferromagnetic Resonance, IIL*, Moscow, 1952, p. 284, (Russian translation).

[22] N.N.Shol'ts and K.A.Piskarev, Izv. Akad. Nauk SSSR, Ser. Fiz. 16. 6 (1952).

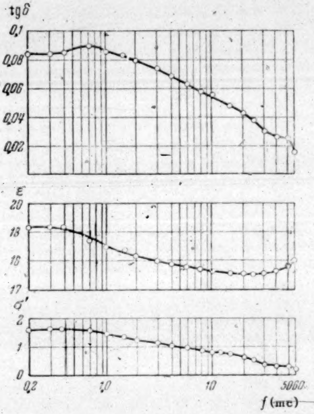

FIG. 1. Frequency dependence of the dielectric permittivities ε and σ' and of the tangent of the phase angle due to dielectric losses tan δ=σ'/ε for sample 6 of 0-400.

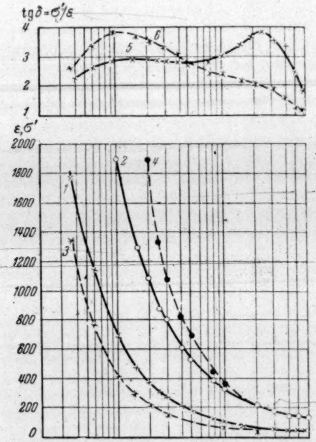

FIG. 2. Frequency dependence of ε,σ' and tan δ for 0-200-I: 1,2 and 5—sample 8; 3,4 and 6—sample 9(curve 6 corresponds to tan δ/2).

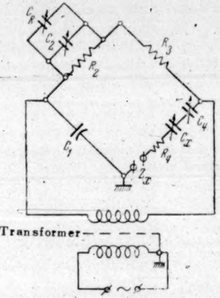

FIG. 3. Simplified circuit diagram of the high-frequency bridge.

balanced by means of C_2 and C_4, with Z_x shorted out. After the coil to be measured had been connected to the terminals Z_x the circuit was balanced again, but this time by means of condensers C_R and C_x. The equations for the preliminary (2) and final (3) balance are given below:

$$C_2 = \frac{R_4}{R_3} C_1 - C_{R\,\min}; \tag{2}$$

$$C_4 = \frac{R_2 C_1 C_{x\,\max}}{C_{x\,\max} R_3 + C_{x\,\max}\omega^2 C_1 L_4 R_2 - R_2 C_1};$$

$$R_x = R_3 (\Delta C_R / C_1); \tag{3}$$

$$X_x = \omega L_x = \frac{1}{\omega} \frac{\Delta C_x}{C_{x\,\max}(C_{x\,\max} - \Delta C_x)}.$$

Consequently, the increment in the capacitance C_R is proportional to the value of R_x and does not depend on the frequency; the increment in the capacitance C_x is a function of the quantity L_x and of $\omega^2 = (2\pi f)^2$.

A block diagram of the measuring apparatus in which the high-frequency bridge was utilized is given in Fig. 4. The use of sensitive null indicators allowed the reduction, without a loss in the precision of measurement, of the high-frequency voltage supplying the bridge down to a value of 0.1-0.5 v, which insured the possibility of measuring cores at very weak variable magnetic fields $H < 1$ milli-oersted. The possibility of using sensitive null indicators was in turn insured by suitable screening of the apparatus and by filtering its supply circuits. For the measurement of the inductance L_x the error in the measurement, as follows from equation (3), depends on the accuracy of determining the frequency; therefore the frequencies of the generators supplying the bridge were controlled by means of a heterodyne wavemeter, which in turn was checked against a quartz calibrator. Results of measurements of special selected points of the curves $\mu(f)$ and $\rho'(f)$ were in addition checked by a comparison method.

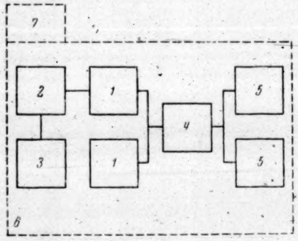

FIG. 4. Skeleton diagram of the measuring apparatus: *1*-high-frequency generators; *2*-heterodyne wavemeter; *3*-quartz calibrator; *4*-high-frequency bridge; *5*-null indicators which consist of superheterodyne receivers provided with input voltage dividers and output vacuum tube voltmeters with a maximum sensitivity with respect to the input high-frequency voltage of the order of $1\mu V$; *6*-shielding chamber; *7*-high-frequency interference-suppressing filter connected into the 50 cycle mains supplying power to the installation.

The total experimental error in the main part of the frequency range investigated is estimated to be less than ±6%. The influence of accidental error in the course of measurement was excluded by taking each measurement at least three times. With the same end in view, a large number (50-100) of experimental points were taken within the frequency range, and only a part of them is shown on the graphs.

When spectra of ferrite samples in a magnetized state were being obtained, the direct current which magnetized the core was introduced into the toroidal winding through special separating chokes characterized by low self-capacitance. Moreover, the choice of the number of turns of the toroidal winding, and the choice of the type of the separating choke, was made in such a way that, in control experiments without the magnetizing current, the influence of the introduction of the separating chokes on the results of measurement was quite negligible. In addition to the method described above, measurements were made in which the separating choke was replaced by a second ferrite toroid which carried a winding identical with the winding of the first toroid. The toroids were chosen in such a way that their magnetic spectra in the demagnetized state would be the same. In this case the magnetic spectrum of the samples was determined as a certain mean spectrum--from the results of measuring the effective inductances and resistance of the toroid windings connected in parallel (through a 1 mfd. blocking condenser).

4. During the investigation of magnetic spectra, the toroidal cores of Ni-Zn ferrites were placed inside electrical (open-circuited) screens made from soft aluminum foil of 0.08 mm thickness, which were then covered by winding them with insulating tape made of styroflex, the total thickness of the insulating layer being 1-1.5mm. The cores which had been screened and insulated in this manner were then wound with a single layer of windings which had small thicknesses, and which, insofar as it was possible, were uniformly distributed along the whole length of the core. In order to compare results, additional measurements were made with identical windings wound without the preliminary introduction of a screen either directly on the core, or on the core with an insulating layer.

The main idea in using electric screening consisted first of all in the simplicity of determining in this case the distributed capacity** C_0 of the windings, and second, in eliminating the uncertainty in that part of the losses which must be ascribed to the capacitative branch of the coil in the case of an unscreened core, when the influence of dielectric losses in the latter is unavoidable (but which, however, turned out to be insignificant).

In the case of an unscreened core and with a small number of turns in the winding, the estimate of the value of C_0 was carried out in an indirect way; for this purpose X_x and R_x were measured over the frequency range for coils wound on the same ferrite core both with and without screens. The thicknesses of the insulating layers between the winding and the screen were so chosen, that measurements of X_x and R_x of coils with unscreened and screened cores would give, in the frequency range in question, approximately the same results,

---

** C_0 was determined by a graphical method by means of plotting the experimental points, obtained with the aid of Q-meters, for the dependence of $C=\phi(1/f^2$ with a subsequent extrapolation of the straight lines so obtained until they intersect the capacitance axis. During measurements, the ferrite toroid was replaced by a polystyrol one with identical screening, insulation, and winding.

which allowed one to consider the values of C_0 for both types of coil to be the same. For coils with a large number of turns, the values of C were measured in the region μ=const, and in this case, therefore, the cores were not replaced by polystyrol ones.

Windings with different numbers of turns were used. Each of the experimental points obtained for one winding was duplicated by a measurement on the other winding. The number of turns on the windings was so chosen that their resonance frequencies would be considerably higher than the frequency at which measurements were made, but that the reading of condenser C_x would not lie at the beginning of its scale. Moreover, at high frequencies, measurements were made with the aid of a shorted section of coaxial line into which the toroid under investigation was placed.

5. The values of L_x and R_x obtained as a result of such measurements were recalculated to the true values ++ of L and R by means of the following formulas which take into account the influence of the capacitance C_0 and the parasitic capacitance C' of the measuring circuit, with $C' = C_0 + C_0'$:

$$L = q_L L_x, \quad R = q_R R_x, \tag{4}$$

where

$$q_L = \frac{1 + \beta^2 + \xi^2}{(1 + \beta^2)^2 + (\beta\xi)^2}; \quad q_R = \frac{1}{(1 + \beta^2)^2 + (\beta\xi)^2}; \tag{4a}$$

$$\beta = \omega / p; \ \xi = R / K; \ p = (L_x C')^{-1/2};$$

$$K = (L_x / C')^{1/2}.$$

In order to reduce the recalculation to the true values of L and R according to Eq (4) the graph shown in Fig. 5 was constructed.

The values of R_c and L_c were obtained from L and R. These new values depend only on the properties of the cores used. The quantity R_c was found by measuring the actual resistance R_w of windings wound on a polystyrol toroid of dimensions identical with the ferrite core, and then taking the difference $R_c = R - R_w$. The value of L_c was determined by taking into account the corrections for leakage flux, which were estimated by means of measurements (these being significant only for low values of $\mu < 100$ gauss/oersted. The permeabilities μ_1 and μ_2 of the body of the core were computed with the aid of typical formulas (cf., for example, Eqs. (1) and (2) of Ref. 6 or page 183 of Ref. 23).

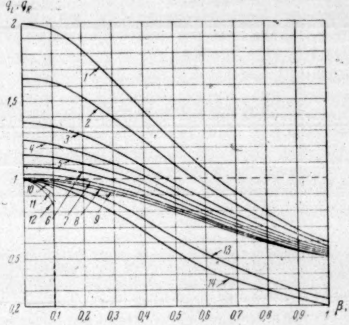

FIG. 5. dependence of the coefficients q_L and q_R on the quantities β and ξ : q_L =curves 1—9; q_R = curves 10-14; ξ has the values : 1=1.0; 2=0.8; 3=0.6; 4=0.5; 5=0.4; 6=0.3; 7=0.2; 8=0.1; 9=0; 10=2.0; 11=3.0; 12=4.0; 13=0. 14=1.0.

6. The subsequent transition from the quantities μ_1 and μ_2 to the values directly of interest to us of the elastic (non-dissipative) permeability μ and the viscous (dissipative) permeability ρ' of the substance of the ferrite can be carried out for a given ϵ and σ' by means of eliminating (by calculation) the effect on the permeability of the surface effect and of the volume resonance in the ferromagnetic substance. In particular, the solution of this problem makes possible the method of two experiments which was suggested by Polivanov[24].

According to Polivanov[20], the condition for the ocurrence of volume resonance in a bicomplex medium can be written in the following form:

$$\operatorname{Re}(j\omega\mu'\mu_0\gamma - \omega^2\varepsilon'\varepsilon_0\mu'\mu_0) \tag{4b}$$

$$= -(m^2 / a^2 + n^2 / b^2)\pi^2,$$

where m, n are odd integers which determine the order of the resonance; a, b are the sides of the cross section of the core; $\epsilon_0 \mu_0 = c^{-2} = (3.10^{10})^{-2}$ (cm/sec)$^{-1}$; γ is the conductivity of the material of the core.

++ The equivalent circuit of the coil is referred to here in which R has been ascribed to the inductive branch.

[23] L.I.Rabkin and N.N.Shol'ts, *Magnetodielectrics and ferro-coils*, GEI, Moscow-Leningrad, (1948).

[24] K.M.Polivanov, Elektrichestvo 3, 19(1954).

Assuming that the dielectric losses in ferrites at high frequencies considerably exceed losses due to conductivity currents, we shall rewrite the given expression for the resonance of the first order ($m=n=1$) in the case of a core of square cross section $a=b$ in the form $\mathrm{Re}\,(-\omega^2 \; \epsilon' \mu' \; /c^2) = -2\pi^2/a^2$ or, taking the real part of the left hand term, we get

$$a = \lambda_B / \sqrt{2(\varepsilon\mu - \sigma'\rho')}, \tag{5}$$

where λ_B is the wavelength of electromagnetic waves in vacuo. Consequently, if

$$\lambda_B \gg a\sqrt{2(\varepsilon\mu + \sigma'\rho')} \approx a\sqrt{2\varepsilon\mu}, \tag{6}$$

then volume resonance cannot occur in the ferrite core.

The influence of the surface effect is described by the expression for the equivalent penetration depth δ_E for the electromagnetic field into a bicomplex medium (cf. Eqs. (89)-(93) of Ref. 1)

$$\delta_E = (\lambda_B / \pi)\,[2(|\mu'|\,|\varepsilon'| - \mu\varepsilon + \rho'\sigma')]^{-1/2}. \tag{7}$$

Under the condition that $\delta_E \gg a$, i.e.,

$$\lambda_B \gg a\pi\,[2(|\mu'|\,|\varepsilon'| - \mu\varepsilon + \rho'\sigma')]^{1/2} \tag{8}$$

$$\approx a\pi\,(2|\mu'|\,|\varepsilon'|)^{1/2},$$

the surface effect will not be present in the ferrite core.

Calculations show that inequalities (6) and (8) are fully satisfied for ferrites 0-200 and 0-400, and are approximately satisfied for 0-2000-I. Therefore, for the whole frequency range we assume that approximately*

$$\mu_1 = \mu, \; \mu_2 = \rho' \tag{9}$$

7. Results of the investigation of frequency dependence of the permeabilities μ and ρ' of samples of NiZn-ferrites are shown in the graphs of Figs. 6-11. An examination of curves 1 of Figs. 6-11 of the completely demagnetized state of the ferrite samples shows that the dependence $\mu\,(f)$ of 0-200 and 0-2000-I has a relaxation character, while that of 0-400 has a resonance character, which does not depend on any accidental factors such as: choice of the number of turns of the winding (Fig. 12a, b,c), or volume resonance whose frequency (according to Ref. 20) should have become displaced when the sides of the toroidal core are metallized, an event which was not observed (Fig. 12d) in our case. From a comparison of the curves 1 of the above graphs it follows, moreover, that for samples of NiZn-ferrite of the same composition and of the same technology of manufacture, the magnetic spectra differ but little from sample to sample. In particular, this conclusion is supported also by the investigation of spectra of samples 4 and 5 of 0-400, whose dimensions are significantly larger than those of samples 3 and 7 (Figs. 9 and 11), and of sample 8 of 0-2000-I whose $\mu\,(f)$ and $\rho'\,(f)$

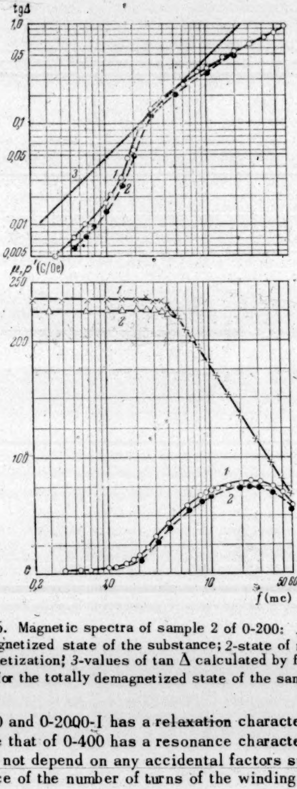

FIG. 6. Magnetic spectra of sample 2 of 0-200: *1*-totally demagnetized state of the substance; *2*-state of residual magnetization; *3*-values of tan Δ calculated by formula (13) for the totally demagnetized state of the sample.

---

* A certain indeterminacy is introduced into this conclusion only by the possible dependence of ϵ and σ' on the intensity of the electric field, which will be different when electric and when magnetic measurements are made. However, measurements of ϵ and σ' at various electric field intensities did not demonstrate any noticeable change in them.

curves are close to curves 1 of Figs. 7 and 10 in spite of a noticeable difference in their dielectric permittivities (Fig. 2); apparently these data once again point to the independence from dimensional (volume resonance and surface effect) effects of the dispersion μ and absorption ρ' observed by us.

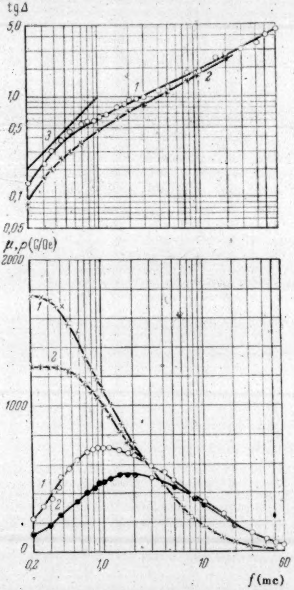

FIG. 7. Magnetic spectra of sample 9 of 0-2000-I(the labels are the same as in Fig. 6.)

The independence of the observed dispersion of the permeability of the material of the ferrite from the surface effect follows, moreover, from the measurements on the spectra of sample 7 of Fig.11, which was hand ground with abrasives in order to avoid any appreciable heating in the course of grinding. The ground sample had, in comparison with the whole sample of lower μ_a, a higher f_u (in contrast to the data of Ref. 9), whose shift is approximately given by Eq. 10, a flatter maximum in the curve $\rho'(f)$, a larger slope of the curve $\mu(f)$, and also a smaller value ρ' max $=0.39\,\mu_a$, as against ρ' max $= 0.43\,\mu_a$ for the whole sample, which points to the broadening of the band of frequencies of relaxation and of resonance for samples of smaller axial thickness. The observed character of dependence of f_u on the thickness of the sample most likely is a consequence of its macroscopic inhomogeneity, as the character of the shape of the curves $\rho'(f)$ of the ground and of the whole samples in the region of high frequencies excludes the possibility of explaining the appearance of the dispersion curves through a surface effect. However, the possibility is not excluded that the effective anisotropy constant is altered in the course of grinding, because of the increase in the demagnetizing factor of the body of the toroid, and also because of the change in the dimensions d of ferromagnetic regions [25] (page 257) which may lead to a change in the frequency f_u.

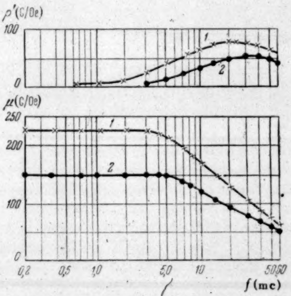

FIG. 8. Magnetic spectra of sample 1 of 0-200 for different values of the intensity of the constant magnetizing field: *1-H*=0; *2-H*=4 oersteds.

8. The values of the frequencies of absorption maxima f_u of the ferrites investigated, which are approximately (up to a factor of the order of two, since in the case of relaxation spectra the damping is apparently close to critical) equal to the average resonance frequencies of their material, are given by the espression

$$f_u \approx CI_s/(\mu_a - 1), \qquad (10)$$

where C is a certain constant of the material of the ferrite (see table), which is approximately equal to the gyromagnetic ratio of the electron spin, $C \approx ge/2mc \approx e/mc = 17.6$ mc/oersted.

The theoretical basis for Eq. (10) may be found:

---

[25] S.V.Vonsovskii, *Modern theory of magnetism* GITTL, Moscow-Leningrad, 1952.

a) in the case of the predominance of the process of rotation in the theory of Landau and Lifshitz[16] and of Snoek[18] with Eq. (11) arising from it;
b) in the case of the predominance of displacement processes in the theory of Landau and Lifshitz[16] and of Döring [17] with Eq. (12) arising from it for 90° boundaries; c) in the case of the approximate equality of the weighting factors for the processes of displacement and of rotation, in the approximate equality of the resonance frequencies of the material of the ferrite due to both types of processes of magnetization

$$f_{0\,\mathrm{rot}} = \frac{ge}{4\pi mc} H_i \approx \frac{1}{\pi} \frac{ge}{2mc} \frac{k}{I_s} \approx \frac{4}{3} \frac{ge}{2mc} \frac{I_s}{\mu_{a\,\mathrm{rot}} - 1}; \tag{11}$$

$$f_{0\,\mathrm{dis}} = (ge/2mc)\sqrt{\delta/d}\,[I_s/(\mu_{a\,\mathrm{dis}} - 1)]. \tag{12}$$

Here H_i is the internal effective magnetic field due to the anisotropy of the material of the ferrite, $H_i \approx 2k/I_s$; k is the anisotropy constant; μ_{rot} is the initial permeability due to rotation; $\mu_{a\,\mathrm{rot}} \approx 4I^2/k$; δ/d is the ratio of the effective thickness of the boundary layer to the size of the ferromagnetic domain; phenomenologically, based on the experimental data of Ref. 14 one can assume that $\delta/d \sim 1/(\mu_{a\,\mathrm{dis}}-1)$; $\mu_{a\,\mathrm{dis}}$ is the inital permeability due to displacement; g is the Landé spectroscopic splitting factor which, at room temperature and depending on the composition of the NiZn-ferrite, may vary[26-28] within a range not greater than from 1.93 (Zn-ferrite) to 2.36(Ni-ferrite) and which consequently can be approximated by $g=2$.***

9. Examination of graphs 6 and 7 shows that the nature of the curves of $\mu(f)$ and $\rho'(f)$ is also preserved in the state of residual magnetization.

It is known both from theory[30] and from experiment[21] that in ferrites for which $I_R/I_S \approx 0.5$, if the complex permeability $\mu' = \mu - j\rho'$ is determined exclusively by processes of rotation of the magnetization vector, then the value $\mu'_R = \mu_{R'} - j\rho'_R$ in a state of residual magnetization must be equal to the value of μ' in the demagnetized state; however, if μ' is determined primarily by the displacement of boundaries, then μ'_R must be considerably lower than μ' in the demagnetized state.

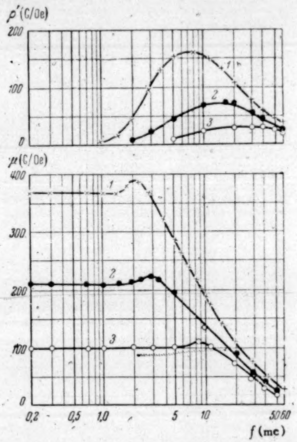

FIG. 9. Magnetic spectra of sample 3 of 0-400 for various values of the constant magnetizing field: 1-H=0; 2-H=1.8; 3-H=4.5 oersteds.

In the case of 0-2000-I the value of the ratio $\mu_{aR}/\mu_a = 0.72$, and $(\rho'_R/\rho')_{\mu=\mu_a} = 0.5$. As the frequency is increased, the curves of $\mu(f)$ for both states of the substance of the ferromagnetic approach one another rapidly and coalesce at the frequency $f=3$ mc. At frequencies of 10 to 30 mc, a certain increase of μ_R above μ is observed which would not be shown on the scale of our graph. The curves for $\rho'(f)$ coalesce at $f=15$ mc and beyond that are practically identical. In the case of 0-200, $\mu_{aR}/\mu_a = 0.96$, $(\rho'_R/\rho')_{\mu=\mu_a} = 0.85$ and the spectra of both states of the ferrite substance differ little from one another.

If the coming together of the curves of μ' and μ'_R is taken as evidence of the gradual growth with frequency of the relative importance of rotation

---

*** In particular, taking into account the data of Ref. 29 and the fact that in the determination of the g-factor the influence of H_i was not taken into account in Refs. 26-28.

[26] H.G.Beljers and D.Polder, Nature 165, 800 (1950).

[27] T.Okamura and Y.Torizuka, Collection of articles entitled *Problems of Modern Physics* 5, 182 IIL, Moscow (1952).

[28] E.I.Kondorskii and N.A.Smolkov, Doklady Akad. Nauk USSR 93, 237 (1953).

[29] T. Okamura, Y. Torizuka and Y. Kojima, Phys. Rev. 88, 1425 (1952).

[30] S.V.Vonsovskii and Ia. S.Shur, *Ferromagnetism*, State Technical Publishing House, Moscow-Leningrad, 1948.

processes, then one may suppose that in 0-200-I, in very weak fields, magnetization by means of rotation processes takes place only starting at a frequency $f \sim 10$ mc and that consequently the radiofrequency dispersion at lower frequencies must be described, according to Döring, by Eq. (12)

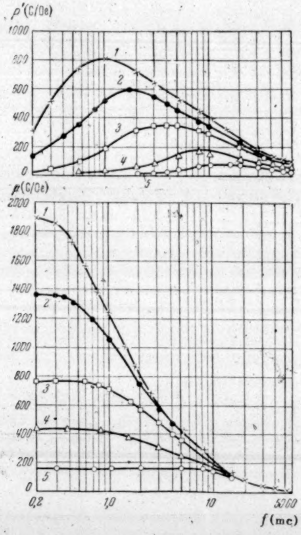

FIG. 10. Magnetic spectra of sample 10 of 0-2000-I for various values of the constant magnetizing field: 1-H=0; 2-H=0.1; 3-H=0.2; 4-H=0.5: 5-H=1.5 oersteds.

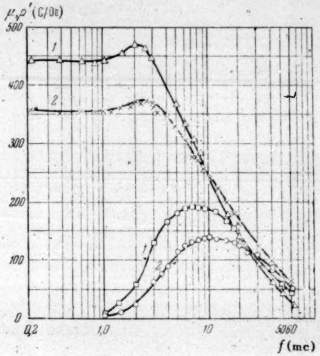

FIG. 11. Magnetic spectra of sample 7 for various axial thicknesses obtained by means of grinding it down; 1-6.98 mm (weight of sample 21.889 gm); 2-2.84 mm (weight of sample 9.155 gm).

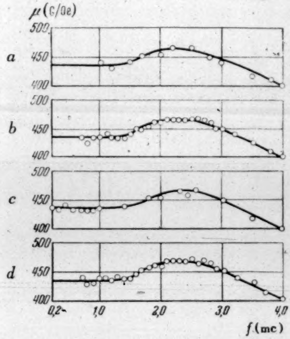

FIG. 12. Dispersion curves of sample 6 of 0-400 in the range 0.2 to 0.4 mc for various windings: a-3 turns of ribbon; b-7 turns of wire; c-14 turns of wire; d-7 turns of wire; sides of core metallized.

In 0-200, rotation processes are possibly the dominant factor which determines the character of the whole radiofrequency dispersion, which will be described, according to Snoek, by Eq. 11. Taking into account the fact that samples 0-2000-I and 0-200 have approximately the same composition and differ from each other only in that the sintering temperature t_s is appreciably higher for the sample with the higher permeability, one may suppose[++] that the relative importance of the processes of displacement in the ferrite increases with increasing temperature t_s. The theoretical basis for this hypothesis is the decrease in the porosity of the sample and in the values of internal strains which is observed as the sintering temperature is raised.

The values of the tangents of the phase angles due to the losses tan $\Delta = \rho'/\mu$ for ferrite samples

---

[++] This assumption needs testing on a large number of samples of ferrite of the same composition sintered at different t_s.

TABLE

Data for toroidal cores which have been studied.

No. of sample	μ_a in gauss/oersted	I_s, gauss	H_c, oersteds	I_R, gauss	ε	f_u, mc	C, mc/oersted	Toroid dimesnsions in mm. external diameter	internal diameter	axial thickness
1	225	145	1,45	80	19	25	39	37,3	23,8	7,08
2	234	140	1,4	80	20	25	41	37,2	23,7	7,05
3	365	220	0,8	96	17	8	13	38,05	24	6,96
4	370	220	—	96	16	7,5	13	67,75	42,3	14,03
5	434	210	—	100	19	8	16	57,15	34	11,34
6	438	220	0,79	97	16	8	16	38,2	24	6,82
7	443	220	0,8	98	18	8	16	38,2	24,2	6,98
8	1680	200	0,1	98	—	1,2	9	37,9	24,15	7,11
9	1750	195	0,1	96	—	1,0	9	37,9	24,05	6,96
10	1880	200	0,1	98	—	1,0	9,3	37,9	24,1	7,05

are shown in Figs. 6 and 7, from which it may be seen that the nature of the dependence of tan $\Delta(f)$ on the frequency apparently varies but little with a variation in the value of the ratio $(\mu_{a\,\mathrm{rot}}-1)/(\mu_{a\,\mathrm{dis}}-1)$ for the ferrite. For a rough estimate of the value of tan Δ in the frequency range 0.01 0.01 $f_u \lesssim f \lesssim f_u$ one can use[6] the expression

$$\mathrm{tg}\,\Delta \sim f/f_u \sim (f/C)(\mu_a - 1)/I_s, \qquad (13)$$

which establishes the practically important connection between tan Δ and the fundamental parameters of the ferrites.

10. Examination of the graphs of Figs. 8,9 and 10 shows that the nature of the spectrum is preserved independent of the influence of the constant magnetizing field. The frequency f_u, according to data[31] on spectra of metallic ferromagnetics, is displaced into the region of higher frequencies as the intensity of this magnetizing field is increased, with the law given by expression (10) being approximately preserved. The preservation of this law has an essential practical significance since this makes it possible to estimate with the aid of formula (13) the order of magnitude of the values of tan Δ for the core in the frequency range 0.01 $f_u \leqq f \leqq f_u$ for various values of the intensity of the magnetizing field.

---

[31] I.M.Kirko, B.O.Grosskaufman and L.D.Daube, Trudy Inst. Phys. Math. Acad. Sci. Latvian SSR 2, 9(1950).

Translated by G. M. Volkoff
4

SOVIET PHYSICS JETP VOLUME 3, NUMBER 1 AUGUST, 1956

The Change of the Absorption Spectrum of Copper Chloride Containing an Excess of Copper Under the Action of Water Vapor

P. N. KOKHANENKO
Siberian Physico-Technical Institute

(Submitted to JETP editor, July 8, 1954)
J. Exper. Theoret. Phys. USSR 30, 30-32(January, 1956)

When water vapor acts on copper chloride films sublimed in vacuum and containing an excess of copper their color vanishes. In the absorption spectrum the sharp maxima due to the excess copper at 3725 A° and 3780 A° are replaced by a broad maximum at 3900 A°. Near 2800 A° a new maximum appears and disappears with time. It is shown that the absorption of the excess copper particles in the surface layers differs from the absorption of the copper particles in the interior layers of the crystal.

COLOR of a yellow or brown tint of copper chloride films sublimed in vacuum quickly fades when the films contact moist air. Carefully dried air in no way affects the color of the films. In the present work the influence of water vapor on the absorption spectrum of copper chloride films sublimed in vacuum and containing an excess of copper has been investigated. Use is made of the gradual change of the absorption spectrum upon the adsorption of water vapor by the films to obtain a separation of the absorption spectrum of the excess copper in the surface layers and the absorption spectrum of the excess copper in the inner layers of the crystal.

The films of copper chloride containing an excess of copper were obtained by sublimation in a vacuum. The compounds used were either cuprous chloride or anhydrous cupric chloride. All experiments were carried out at constant temperature. In Fig. 1 the change in the spectrum of one of the samples is shown in the region of the absorption band due to a stoichiometric excess of copper. Curve 1 is the absorption of the film before the admission of water vapor. In the curve are the sharp maxima characteristic of the excess copper 3720 A (unresolved doublet) and 3810 A . The film is yellow. Curve 2 is the absorption 10 minutes after the admission of the water vapor. The film has faded. Curve 3 was obtained after the water vapor had acted 3 hours on the film, while curve 4 was obtained after the water vapor had acted 50 hours on the film. From the figure we see that the sharp maxima due to the excess copper gradually disappear and are replaced by a broad diffuse maximum from 3880 to 3900 A . Upon removing the adsorbed water, by heating and pumping, the film again becomes yellow (dotted Curve 5). However the original absorption spectrum of the film is not reestablished. Upon proceeding still further, the broad maximum increases and is shifted toward the short wavelength side. The appearance of this broad maximum indicates a transition of the particles of excess copper to new energy states. This transition does not correspond to the transition of excess copper in the colloidal state because the absorption maximum of colloidal particles of copper is found in the visible region.

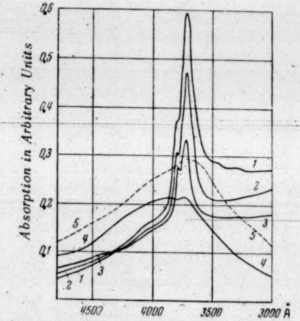

FIG. 1

The time for the complete disappearance of the characteristic absorption band of the excess copper particles under the action of water vapor on the film of copper chloride depends upon the structure and thickness of the film.

In addition to the change of the characteristic band in the absorption spectrum of the film which is acted upon by water vapor, a new strong absorption maximum appears from 2750 to 2800 A . In Fig. 2 is shown the absorption of one of the samples before the admission of water vapor (Curve 1) and 10 minutes after the admission of water vapor into the reaction chamber (Curve 2). Upon the admission of water vapor the sharp intense maximum at 3730 A weakens, and there is a new maximum at 2800A. Curve 3 is the absorption spectrum 5 hours after the admission of the water vapor. Not only has the

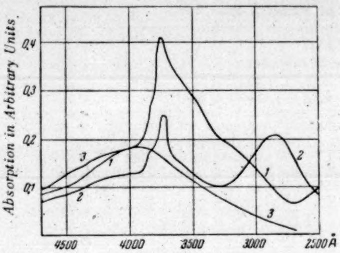

FIG.2

absorption band of the excess copper disappeared but also the new maximum. The final absorption spectrum, as has already been noted above, consists of one diffuse band with a maximum at 3900 Å. The water adsorbed by the surface layers is bound very loosely. A film whitened by the adsorption of water vapor becomes yellow again upon heating it up to 36 to 40°C. If the water which was separated by heating is not withdrawn upon cooling the film to room temperature, the film again whitens as a result of the interaction with water vapor. The experiment can be repeated many times with similar changes in color of the film.

Under the action of water vapor on the film of copper chloride the first change in the absorption spectrum is the disappearance of the absorption of the excess copper particles found in the surface layers and not in the interior of the crystal. In the first stages of this process the absorption band of the excess copper is observed merely to decrease in absorption. The newly formed maximum near 3900 Å appears only after the water vaporhas acted upon the film for a long time. The disappearance of the absorbing light centers in the surface layers of the salt crystals is caused by the penetration of the water molecules into the crystal and is not accompanied by the formation of new surfaces, since the copper particles distributed within the crystal do not occupy levels characteristic of the surface layers. By making use of this situationit is possible to obtain separately spectra of the absorbing particles of excess copper (atoms or ions) located in the surface layers and the spectrum of the absorbing particles found in the interior of the crystal. If the absorption curve obtained a short time after water vapor is admitted to the apparatus is subtracted from the initial absorption curve of a given sample, the resulting difference will give the absorption spectrum of the copper particles of the surfaces. If differences between the absorption curves obtained after more or less extended times of action of the water vapor on the film are taken they will be characteristic of the absorption spectrum of the particles of excess copper within the crystal. In Fig. 3 is an example of two difference curves pertaining to the sample whose absorption was given in Fig. 1. Curve 1 in Fig. 3 is the difference between Curve 1 in Fig. 1 corresponding to the initial absorption of the sample and Curve 2 of the same sample which was obtained 10 minutes after the admission of the water vapor. The curve is a wide band with a diffuse shape on the short wavelength side and a maximum at 3620 to 3630 Å. On the long wavelenth side of this band is an adjoining weak band at 3720 Å. In the case of other samples the difference curves have a similar form. In the difference curves of certain samples the band at 3725 Å is even less apparent than in Fig. 3. The position of the maximum of the wide band varies for different samples and lies between 3580 and 3630 Å. The dotted Curve 2 of Fig. 3 was obtained by subtracting Curve 3 in Fig. 1, which corresponds to the absorption after the water vapor has acted on the film for 3 hours, from Curve 2 in this same figure. This curve is due to the absorption of the particles of excess copper found in the interior of the salt crystal and has the form of a narrow symmetric band. Judging by the form of similar difference bands we can conclude that the particles of excess copper (atoms or ions) located inside the crystal give a sharp narrow band in the absorption spectrum and particles located in the surface layers of the crystal give a wide band which is diffuse on the short wavelength side. It is interesting that in general the absorption spectra of vacuum sublimed films of the halogen series of salts with a stoichiometric excess of metal often have the form of either a

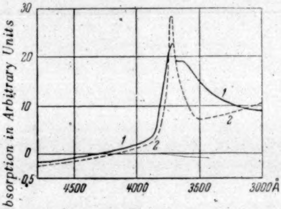

FIG.3

single band that is diffuse on the short wavelength side or the form of a continuous absorption with a sharp long wavelength cutoff, the position of the long wave length band depends upon the excess metal.[1] This indicates that the surface layers play a significant role in the total absorption of sublimed films of salt.

With regard to the strong absorption maximum at 2800 A upon the adsorption of water, we can definitely say only that is is connected with the presence of particles of excess copper in the surface layers of the salt crystal. This maximum is usually as intense as the intensity of the diffuse absorption on the short wavelength of the band of the excess copper at 3725 A in the original spectrum of the sample as is due to the copper particles located in the surface layers of the crystal. The disappearane of the maximum at 2800 A after a lengthy action of water vapor is connected with a general change in the structure of the film which also brings about the replacement of the clear maximum of the excess copper at 3790 and 3725 A by a diffuse maximum at 3900 A . If a small amount of water vapor is admitted to the reaction apparatus and the vapor inlet then closed, a maximum at 2800 A which appears remains longer. It is possible to believe that this maximum is connected with complex bonds of the copper. The tendency of the cations of heavymetals to associate with different anions is known.

Because of the incomplete thermal dissociation upon heating, the sublimed films of copper chloride contain the impurity cupric chloride. Upon the adsorption of water vapor on these films the transformation to chlorine ions from hhe solution of cuprous chloride impurity is possible. The chlorine can transform to polyhalide complexes of various compounds with CuCl, $CuCl_2$ or ions of excess copper.

---

[1] P. N. Kokhanenko, J. Exper. Theoret. Phys. USSR 26, 120(1954).

Translated by F. P. Dickey
5

SOVIET PHYSICS JETP VOLUME 3, NUMBER 1 AUGUST, 1956

The Absolute Luminescence Yield for γ-Scintillations in a Naphthalene Crystal with Anthracene

M.D. GALANIN AND A.P. GRISHIN

P.N. Lebedev Physical Institute, Academy of Sciences, USSR

(Submitted to JETP editor, September 4, 1954)
J. Exper. Theoret. Phys. USSR 30, 33-41 (January, 1956)

By means of apparatus calibrated in absolute units, the absolute energy yield of luminescence for γ-scintillations induced in a naphthalene-anthracene crystal by Compton electrons was found to be 0.7 ±0.2%.

1. INTRODUCTION

THE question of the magnitude of the energy yield of luminescence under excitation by particles has essential theoretical and practical significance. Nevertheless, experimental data on the fraction of the energy of a particle which is transformed into light energy of a scintillation are not yet sufficiently reliable. This question was a topic of discussion even at the time when scintillations under the action of α-particles were observed visually. Ril', in a series of works (see, for example, Reference 1) indicated very high values of energy yield (of the order of 80%) for scintillations in zinc sulphide. Timofeeva, in work carried out under the suggestion of S. I. Vavilov[2], obtained very much lower values (1-2.5%). In the more recent works of Kallmann and co-workers[3], carried out with the use of photo multipliers, a value of 25% was obtained.*

Equally contradictory are the data on the energy yield of luminescence of organic crystals under the action of fast electrons. For anthracene, values of 10%[4]; 3.7%[5] and 1-2%[6] are indicated. The first two values refer to integral measurements, i.e., to measurements of the mean intensity under continuous excitation. The last refers to pulse measurements, i.e., of light energy realized in a short scintillation. The reason for the discrepancies between these values, however, apparently can not be ascribed to the difference in method, since it has been shown[7] that the afterglow of anthracene for hard excitation is small.

In a majority of the works, data on the energy yield are obtained under various more or less reliable assumptions about the spectral distribution of the luminescence energy and of the sensitivity of the photo multiplier (efficiency of the photocathode) and spectral distribution of sensitivity). In the present work, the task was set insofar as possible to avoid such arbitrary assumptions, and to find all the necessary quantities experimentally.

2. METHODS OF THE MEASUREMENTS

For the determination of the value of the absolute energy yield for scintillations induced by γ-rays, it is necessary to: 1) measure the luminous energy of a scintillation by means of an apparatus which was calibrated in absolute units, 2) compare the measured scintillation with the amount of energy lost in the crystal by the fast electron which resulted upon absorption of the γ-quantum.

The apparatus which served to determine the energy of a scintillation, consisted of 1) a photometric sphere for utilization of all of the light which leaves the crystal, 2) a photomultiplier, 3) a linear amplifier and 4) a discriminator, which analyzes the amplitude of the amplified pulses.

In order that the reading of the discriminator (the amplitude of the output pulse) be proportional to the integral of the input pulse, the time constant of the input circuit of the amplifier was chosen of sufficient length in comparison with the duration of a scintillation. The amplifier was calibrated by means of short light pulses of known energies, expressed in terms of photocurrent of the phototube for steady illumination × the duration of a pulse.

---

[1] G. I. Born, H. Ril' and K. G. Tsimmer, Dokl. Akad. Nauk SSSR 59, 1269 (1948).

[2] T. V. Timofeeva, Izv. Akad. Nauk SSSR, Ser. Fiz. 13, 135 (1949).

[3] I. Broser, H. Kallmann and U. M. Martius, Z. Naturforsch, 4a, 204 (1949).

[4] M. Furst, H. Kallmann and B. Kramer, Phys. Rev. 89, 416 (1953).

[5] J. B. Birks and M. E. Szendrei, Phys. Rev. 91, 197 (1953).

[6] J. I. Hopkins, Rev. Sci. Instr. 22, 29, (1951).

* Note in proof: This question has been treated in an observation by Ril' (N. Ril' and G. Ortman, Zh. Obshch. Khim) 25, 1697 (1955).

[7] J. A. Jackson, and F. B. Harrison, Phys. Rev. 89, 322, 1953.

The sensitivity of the photomultiplier was determined separately in microamperes per watt of light incident on the photocathode. For this purpose, the photomultiplier was illuminated by a lamp with a known light intensity through a blue filter, selected in order that this source approximately reproduced the energy distribution in the luminescence spectrum. The identical nature of the conditions of light-utilization was assured in that the light from the lamp-standard was passed through an aperture into the photometric sphere and fell on its wall (which was covered with magnesium oxide). Under these very conditions, i.e., with the sphere, the curve of spectral sensitivity of the photomultiplier, needed for the introduction of a correction for the difference in spectra of the crystal radiation and of the standard source, was measured.

The conversion from photo-technological units to energy (units) can be accomplished, if one knows the energy distribution in the spectrum of the lamp, which is specified to sufficient accuracy by its color temperature, and the transmission of the filter.

An exact comparison of the size of a γ-scintillation with the energy lost by an electron presents certain difficulties. On absorption of γ-rays in an organic crystal with relatively small density, the Compton effect plays the basic role. The energy distribution of the Compton electrons, which falls off on the side of large energies, can serve for a crude comparison of the magnitude of a scintillation with the specific energy lost by a particle. For this, one must determine the maximum momentum in the integral distribution curve. However, the measurement of the magnitude of the maximum momentum is connected with some uncertainty, since the limit of the Compton distribution can be washed out by statistical fluctuations in the number of electrons ejected from the photocathode for a single scintillation.

In the present work a coincidence method, borrowed from γ-spectroscopy,[8] was used. The method consists in the observation of coincidences between pulses originated by Compton electrons and pulses from the scattered γ-quanta. If an electron has energy close to the maximum, its momentum is directed approximately in the direction of the primary quantum, and the scattered quantum flies back at some angle θ with respect to the direction of the primary quantum. For angles θ in the interval 135-180°, the energy of the scattered quantum is close to $\frac{1}{2}m_0c^2$ and depends weakly on θ. Therefore, if a collimated beam of γ-rays is directed on the investigated crystal I (Fig.1) and an auxiliary crystal II with a photomultiplier is set in the path of the quanta scattered through large angles, and only those scintillations are recorded in the measured crystal which coincide with scintillations in the auxiliary crystal, then the differential distribution of pulse sizes must give a narrow maximum (in the case of monochromatic rays), which corresponds to the distinct energy of the electrons.

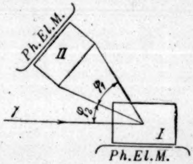

FIG. 1. Scheme of observation of the scattered γ-quanta.

Even for angles $\phi_1 = \pi - \theta$ of the order of 60-80°, the width of the maximum, which is dependent upon the finite dimensions of the second crystal (for example, for $\phi_1 - \phi_2 = 40\text{-}50°$) does not exceed 8-10%, i.e., is of the same order as the width due to fluctuations. The determination of the position of the maximum can thus be made to an accuracy fully sufficient for our purposes.

The integral curve of the distribution obtained by the method described, with excitation by γ-rays from Co^{60} (1.17 and 1.33 mev), (and the differential curve calculated from it) is shown in Fig.2.

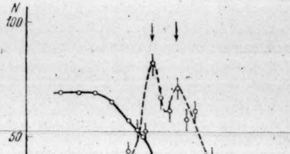

FIG. 2. Integral curve (solid) and differential curve (dashed) obtained by the method of coincidences. (Co^{60} radiation)

3. MEASURING APPARATUS

The crystal for the measurements was placed in a photometric sphere (Fig. 3), covered from within with powdered magnesium oxide. The half of the sphere exposed to the source of γ-rays was spun from aluminum and had a wall thickness of 0.2 mm in order to minimize the scattering of γ-rays in the wall of the sphere. The sphere had an opening (2 cm diameter) against the window of the photomultiplier, and a small aperture for admission of the light from the standard lamp. A small internal shield screened the photocathode from direct incidence of light from the crystal.

---

[8] R. Hofstadter and J. A. McIntyre, Phys. Rev. 78, 619(1950).

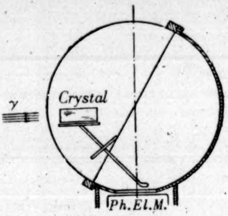

FIG. 3. Diagram of the photometric sphere.

The electronic part of the apparatus is schematically shown in Fig. 4. A cathode follower was built within the housing of the phhotomultiplier. The parameters of the amplifier are: amplification factor-from 3 to 200 (for most measurements~30), pulse rise time (time constant of the input circuit)–of the order of a few microseconds.

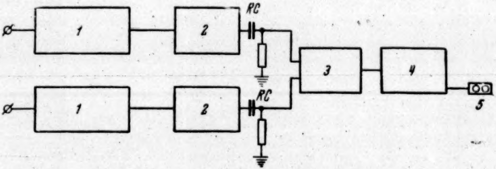

FIG. 4. Block diagram of the electronic apparatus. *1*-Amplifier; *2*-Discriminator; *3*-Coincidence circuit; *4*-PS-64; *5*-Mechanical counter; RC=0.5 μ-sec.

The amplitude of the pulses was measured with a simple integral discriminator. The pulses given by the discriminator (rectangular), were further differentiated and, together with the primary pulses formed in the second channel, were fed to the circuit which selects the coincidences.

A drawback to the system is the large number of accidental coincidences due to the dark noises of the second multiplier, which must register relatively small impulses from γ-quanta with energy ~0.25 mev. At the same time, it is not possible to reduce the duration of the pulses, since the rise time of the amplifier must be sufficiently great for the integration of all of the studied pulses. A more ideal system would be to have a coincidence circuit before the amplifier which would operate with the passing through to the amplifier of previously delayed pulses.

The Co^{60} compound (~150mC) was placed in a lead shield with a 4 mm bore collimator in a lead block 20 cm long. The detector of the scattered γ-quanta was a crystal of NaI-Tl mounted near the photocathode of the photomultiplier.

4. CALIBRATION OF THE AMPLIFIER AND OF THE PHOTOMULTIPLIER

The calibration of the amplifier was accomplished by means of a mechanical generator of short light pulses.[9] The entrance slit S_1 (Fig.5), illuminated by a projection lamp fed through a stabilizer, is imaged on the plane of the exit slit S_2 by a long focal-length objective (f=50cm.). The slits were arranged parallel to one another. A rotating plane mirror was set in the path of the beam so that the photomultiplier, located behind S_2, registers the light pulse. The time of passage of each point of the image past the exit slit equals

$$\tau = S_2/4\pi\nu L, \qquad (1)$$

where S_2 is the breadth of the exit slit, L-the length of the rotating arm (L=746mm) and ν the number of revolutions per second of the motor, which could reach 120. The energy contained in each impulse is determined by the product of τ and the magnitude of the total light flux in the image. This light flux is proportional to the strength of the current from the anode of the photomultiplier and can be measured when the entire flux is steadily incident on the cathode (with the mirror still).

---

[9] S. M. Raiskii, J. Exper. Theoret. Phys. USSR 22. 780 (1952).

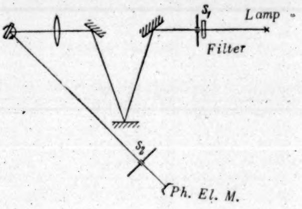

FIG. 5. Plan of the mechanical generator of light pulses.

It should be noted that, owing to statistical fluctuations in the photocurrent of the photomultiplier (on account of the small number of electrons from the photocathode for a single impulse) the pulses in the output of the photomultiplier have some scatter in amplitude. For calibration, a reading of the discriminator was taken which corresponds to the mean of this dispersion, i.e., to the point where the integral curve of displacements has the largest slope.

In order to allow for the effect of the duration of the pulses, the dependence of A/τ (A is the reading of the discriminator) on τ was measured. The result is described in Fig. 6. Had the pulses been fully "integrated," then A/τ would have to be constant.

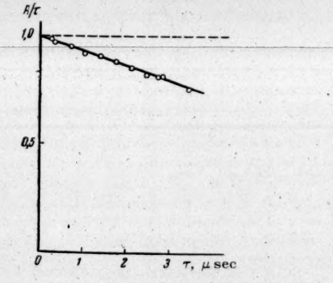

FIG. 6. Dependence of A/τ on the duration of the pulse τ.

The calibrating pulses had a duration of 2.80 μsec. For them, A/τ amounts to 0.82 of the value of this ratio for infinitessimal τ. This was accounted for in the calibration. As a result of the measurements it was found that for very short pulses a pulse size of $0.33 \times 10^{-6} \mu A$ sec corresponds to one scale division.

For the determination of the energy sensitivity of the photomultiplier, it was illuminated through the 1.68 mm diameter aperture in the photometric sphere by a standard light source-an incandescent lamp with a BG-12 filter. The light intensity of the lamp was determined by an AEI (All-Union Electrical Engineering Institute) colorimeter and was found equal to 13.2 candles. The color temperature of the lamp (2600°K) was measured on the same colorimeter by the method of the red-blue ratio. The tungsten filament in the lamp can be considered a gray body to an accuracy of 1%. The curve given in Fig. 7 represents the product of the energy distribution in the radiation of the lamp and the transmission of the filter, i.e., the spectrum of the radiation of the standard source.

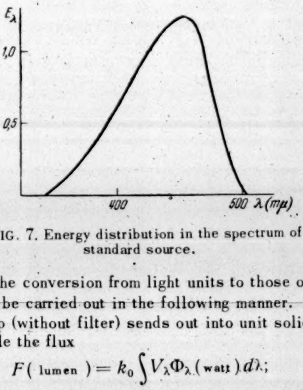

FIG. 7. Energy distribution in the spectrum of the standard source.

The conversion from light units to those of energy can be carried out in the following manner. The lamp (without filter) sends out into unit solid angle the flux

$$F(\text{lumen}) = k_0 \int V_\lambda \Phi_{\lambda}(\text{watt})\, d\lambda; \tag{2}$$

here V_λ is the factor of relative visibility for the average eye, k_0 is the reciprocal of the mechanical equivalent of light, k_0=683 lum/W. Considering (2), we obtain that the flux in watts, emitted in unit solid angle by the standard source, is equal to 2.05×10^{-3} W/sterad.

The light from the standard source, set at 5.605 m. from the hole in the photometric sphere, excited a current of 0.48 μA in the photomultiplier. Under these conditions the flux into the aperture amounted to 1.44×10^{-10} W, so that a current of 1 μA is excited by a flux of 3.00×10^{-10}W, distributed in the spectrum of the source.

The curve of the relative spectral sensitivity of the photomultiplier (with the photometric sphere) f_λ, necessary for the calculation of the difference in the spectra of the standard and of the crystal, was measured on a Hilger double monochromator by means of comparison with a thermal column. A PRK-4 lamp and an incandescent lamp were used as the source. The curve f_λ of the photomultiplier with the sphere (Fig.8, solid line) differs from the sensitivity of the photomultiplier under direct incidence of light on the photocathode in the region 300-400 mμ (dashed curve), because of some rise in the absorption of MgO in this range of the spectrum.

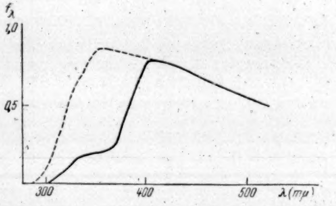

FIG. 8. Spectral sensitivity of the photomultiplier (solid curve-with the photometric sphere, dashed-without the sphere).

Proceeding on the assumption, corroborated by measurements published in the literature[10], that the luminescence spectrum of the crystal for γ-excitation is identical to the photoluminescence spectrum, the luminescence spectrum of the crystal was measured with excitation by the 365 mμ line of a mercury lamp (Fig.9), to get the correction for the difference in spectra of the crystal and of the standard source. Multiplying the distribution of energy in the spectra of the crystal and of the standard by f_λ, and comparing the areas under the curves obtained, one can find the difference in utilization of energy by the photomultiplier. It was found that light of luminescence with the same energy as the standard must give a 9% larger photocurrent. Introducing the appropriate correction, we find that 1μA of photomultiplier current corresponds to a luminescence output of the crystal in the sphere equal to 2.76×10^{-10}W.

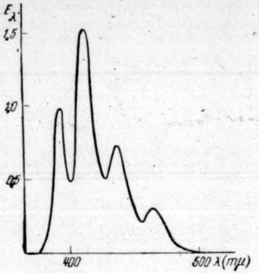

FIG. 9. Energy distribution in the photoluminescence spectrum of a naphthalene-anthracene crystal.

5. RESULTS OF THE MEASUREMENTS

During the measurements of the energy of scintillation according to the method described in section 2, the angle $\phi=\pi-\theta$, corresponding to the direction through the middle of the auxiliary crystal, was approximately equal to 70°. With this, the mean energy of the Compton electrons, corresponding to γ-rays from Co^{60} (1.17 and 1.33 mev), came to approximately 0.95 mev.

The crystal of naphthalene +1% anthracene was placed inside the sphere with the long side along the beam of γ-rays. The range of electrons with 0.95 mev energy in the crystal, which has near unit density, amounts to about 2.5 mm. which is substantially less than the dimension of the crystal in the direction of the trajectories of the electrons.

The measured pulse height which was determined by the method described in section 2, was found equal to A=11.7 divisions on the discriminator*, for the same voltage on the photomultiplier as used during the calibration. Converting the value of a division into energy gives: 1 division=$2.76 \times 10^{-10} \times 0.33 \times 10^{-6}$ Wsec.=0.57×10^{-3}mev. The energy of the scintillation is hence equal to $11.7 \times 0.57 \times 10^{-3}=0.67 \times 10^{-2}$ mev and the value of the absolute energy yield is 0.70%.

The mean square error of this result, due to the accidental errors in all phases of the measurement, does not exceed 10%. But systematic errors are possible on account of insufficiently close maintenance of the conditions identical to those during calibration: a certain difference is probable, for example, in the utilization of the light from the crystal and from the external source. To all appearances, owing to the precautions taken, the systematic error should not exceed 20-30%. Such accuracy must also be ascribed to the result derived above. It is necessary to stress likewise, that the measured value pertains to the energy which escapes from the crystal. Here there are not taken into account losses on reabsorption and on ''capture'' of luminescence due to total internal reflection. The latter, however, could hardly be effective, since the crystal had a rough surface.

---

[10] J. C. D. Milton and R. Hofstadter, Phys. Rev. 75, 1289 (1949); F. B. Harrison and C. T. Reynolds, Phys. Rev. 79, 732(1950).

*This value pertains to the final series of tests, for which the entire distribution curve was not taken down, but only the inflexion point, and therefore does not correspond to the curve in Fig. 2.

If we use the measured ratio of the scintillation intensities in anthracene, and in naphthalene with anthracene* (1:0.41), and disregard the small shift of the luminescence spectrum of the anthracene crystal in comparison with the spectrum of anthracene and naphthalene, then for the absolute energy yield of the anthracene crystal under excitation by electrons with energy ~ 1 mev, we obtain 1.7%. This value fits in with the results of the work of Reference 6, and is lower than the other values quoted in the literature.

6. DISCUSSION OF THE RESULTS

The theoretical interpretation of the size of the energy yield of luminescence on excitation by charged particles must be based on the theory of ionization losses. The problem of excitation of luminescence by charged particles reduces to the question of the division of ionization losses over losses strictly for ionization and losses for excitation. The next stage must end in a clarification of the efficiency of excitation of luminescence by ionization and by excitation of atoms and molecules.

This problem is very complex, on account of the necessity of taking into account secondary particles of low energy, and is not completely solved even as concerns the older question of the number of ions formed by a moving charged particle (see, for example, Reference 12). The empirical result consists in a proportionality between the number of ions formed and the particle energy loss. It is natural to assume that a similar proportionality likewise exists for the number of effectively excited molecules. Birks[13] makes such an assumption in his works, in which, for explanation of the experimentally observed dependence of the intensity of scintillations on the energy and type of particle, an additional assumption on quenching has to be introduced. Birks assumes that, together with the transition of molecules into excited states (''exciton'' formation), a charged particle gives rise to the formation of "damaged" molecules, the number of which is likewise proportional to the specific energy loss. These ''damaged'' molecules are able to trap excitons, which thus leads to quenching. Birks' theory is in good agreement with the experimental data on the dependence of the intensity of scintillations on the energy of the different particles, which justifies its initial assumptions. Thus it is possible to regard the energy given up to excitation of luminescence as amounting to a definite portion of the general loss of energy per given element of path of the particle, independent of its energy.

The other side of the question concerning the theoretical computation of the ratio of losses for excitation of luminescence to the overall energy losses of a particle, i.e., the question of the size of the energy output of luminescence, presents no less interest. There is not yet sufficient data, apparently, for an exhaustive answer to this question. An analysis of the possible contribution of the various processes in excitation of luminescence, however, seems desirable.

For organic crystals it is natural to make the assumption that the ionization and subsequent recombination of molecules is not very effective with regard to the excitation of luminescence. Recombination processes, if also able to give light in organic materials (experimental data on such luminescence seems to be lacking), then must have a duration considerably in excess of the lifetime of an excited state. Consequently, the contribution of these processes to the intensity of scintillation is slight. Ionization processes are essential in this case insofar as they provide secondary particles which are able to excite luminescence.

Excitation processes can be more or less definitely separated into two types: "long range" excitation, when a molecule is excited as a whole (in the case of most organic molecules, excitation of the system of π-electrons occurs), and excitation with "local" emphasis, when to a first approximation one can concentrate on a single atom of the molecule, disregarding its bonds with the other atoms. The question, with what probability does the excitation energy of atoms go over into excitation of a molecule, is not clear at the present time and requires further investigation

It is essential to note that the energy lost by a particle for excitation with long range effect can be comparatively large in some cases. For the estimation of these losses, one can use Fermi's theory[14] of ionization losses, where the medium is considered continuous and is characterized by macroscopic parameters.

---

*Note that our comparative measurements for anthracene, stilbene and phenanthrene (100:45:25) conform nicely with the data of Ref. 11, (100:45:30).

[11] H. Kallmann, M. Furst and M. Sidran, Nucleonics 10,No.9, 15, (1952).

[12] E. Fermi, *Nuclear Physics*, (Univ. of Chicago notes, 1952).

[13] J. B. Birks, Proc. Phys. Soc. (London), A64, 874(1951); Phys. Rev. 86, 569(1952).

Let a particle (for example, an electron) be moving with velocity v in the direction of the x axis. The energy flux per unit length through the surface of a cylinder of radius ρ, the axis of which is the trajectory of the electron, is given by the expression[15,16] (for the condition $s\rho \ll 1$)

$$-\frac{dE}{dx} = \frac{ie^2}{2v^2} \times \int_{-\infty}^{\infty} \left(\frac{1}{\varepsilon(\omega)} - \beta^2\right)\left(-i + \frac{2}{\pi} \ln \frac{2}{\gamma s \rho}\right) \omega d\omega, \tag{3}$$

where $\epsilon(\omega)$ is the dielectric permeability of the medium (generally speaking, complex), $\beta=v/c$, $\gamma=1.78$ and $s=(|\omega|/v)(\beta^2\epsilon-1)^{1/2}$ If $\beta^2\epsilon<1$, then a factor $-i$ comes out of the parentheses and $s=(|\omega|/v)(1-\beta^2\epsilon)^{1/2}$

In order to be able to make a simple estimate, we consider that case (which is found, really, in the limit of the experimental conditions) where the absorption over a wavelength in the frequency range considered is small. Then the dielectric permeability can be approximately expressed through the index of refraction n and the coefficient of absorption α in the following way:

$$\varepsilon(\pm\omega) \approx n^2(1 \pm i\alpha\lambda\!\!\!^{-}), \tag{4}$$

where $\lambda\!\!\!^{-}$ is the wavelength in the medium, divided by 2π. For the condition

$$|\alpha\lambda\!\!\!^{-}(\beta^2 n^2)/(\beta^2 n^2 - 1)| \ll 1$$

the expression (3) gives (see, for example, reference 17)

$$-\frac{dE}{dx} = \frac{e^2}{v^2}\int_0^{\infty}\left[\frac{\beta^2 n^2 - 1}{n^2} + \frac{\alpha\lambda\!\!\!^{-}}{\pi n^2}\left(\ln\frac{4\beta^2}{3.17\,(\rho/\lambda\!\!\!^{-}_0)^2(\beta^2 n^2 - 1)} - \beta^2 n^2\right)\right]\omega d\omega \tag{5}$$

($\lambda\!\!\!^{-}_0=\lambda_0/2\pi$, λ_0 is the wavelength in vacuum). For particles of low energy, when $\beta^2\epsilon<1$, the first term in (5) (losses on absorption of Cherenkov radiation) is absent.

In order to obtain the energy converted into luminescence, it is necessary to take into account the depencence of the luminescence yield on the exciting frequency. According to Vavilov's principle[18], this dependence can be expressed in the following manner: $\eta=\eta_0\omega_1/\omega$ for $\omega>\omega_1$, $\eta=0$ for $\omega<\omega_1$. Having substituted these values in (5), we get for the energy of luminescence per unit length (for $\beta^2\epsilon<1$)

$$\frac{dF}{dx} = \frac{e^2}{v^2}\eta_0\omega_1 \times \int_{\omega_1}^{\omega_2}\frac{\alpha\lambda\!\!\!^{-}}{\pi n^2}\left(\ln\frac{4\beta^2}{3.17\,(\rho/\lambda\!\!\!^{-}_0)^2(\beta^2 n^2 - 1)} - \beta^2 n^2\right) d\omega \tag{6}$$

Here ω_1 is the frequency which approximately corresponds to the maximum of the fluorescence, ω_2 is the frequency of ionization of a molecule (assuming that $\eta(\omega)=0$ for $\omega>\omega_2$).

For computation of the value of dF/dx we do not have sufficiently complete data on the value of the coefficient of absorption and its dependence on frequency, and likewise on the quantity ω_2 and on the output $\eta(\omega)$ for $\omega>\omega_2$. The following data can be used for a rough estimate. Let the electron have an energy of ~0.01 mev ($\beta^2=0.04$). The coefficient of absorption for organic crystals (for instance, anthracene) has the order of $10^5\,\mathrm{cm}^{-1}$, i.e., $\alpha\lambda\!\!\!^{-}\approx 1$. For the index of refraction we assume $n^2\approx 3$. The frequencies are $\omega_1\approx 5\times 10^{15}\,\mathrm{sec}^{-1}$ (~4000 Å) and $\omega_2\approx 20\times 10^{15}\,\mathrm{sec}^{-1}$ (~1 000 Å). The quantum yield $\eta_0\approx 1$, $\rho\approx 10^{-7}$cm. Then $dF/dx\approx 0.2$ mev / cm. The general ionization losses for an electron of such energy in a substance the type of anthracene amount to $(dE/dx)_{\text{ion}}\approx 25$ mev / cm. Thus the ratio

$$a = (dF/dx)/(dE/dx)_{\text{ion}} \approx 1\%.$$

In order to compare this estimate with the value of the yield, one must take into account the corresponding losses of the secondary particles. Here one can be guided by that fact, known from experiments on gases, that only about half of the energy of a particle is expended in ionization. If one assumes that the same sort of relation is maintained for crystals, then the total energy of the secondary particles, which originate per element of path Δx, is equal approximately to $\frac{1}{2}(dE/dx)\Delta x$. If for all of the secondary particles, the quantity a is the same, then the portion of the losses to long range excitation can amount to $\sim 3a/2$.

---

[14] E. Fermi, Phys. Rev. 57, 485(1940); see also the reference collection (Problems in Modern Physics)(USSR) 7, (1935).

[15] I. E. Tamm, Phys. USSR 1, 439(1939).

[16] P. E. Kunin, Collected Work *Meson* (1947) (in Russian).

[17] P. Budini, Nuovo Cim., 10, 236 (1953).

[18] S. I. Vavilov, Z. Physik 42, 311 (1927).

This estimate gives only the lower limit of the losses to excitation. Actually, for secondary particles of low energy in the neighborhood of the binding energy of the electrons in the molecule, the portion a of the losses for excitation of luminescence must increase. This can be concluded by analogy from the form of the functions of excitation and ionization of atoms by electrons. The estimate made here, however, shows that possibly a significant part of the excitation of luminescence is explained by the mechanism indicated. The question as to how, along with this, a linear dependence between the number of excited molecules and the energy of a particle comes about, requires a special analysis. Together with that, the occurrence of the above-mentioned processes of intramolecular conversion of excitation energy is not excluded*.

From these deliberations it is clear that a comparison of the optical properties of luminescent materials (coefficient of absorption and luminescence output for various frequencies of excitation) with their ability to luminesce under the influence of charged particles has essential value for the further clarification of the question.

---

*We note that we have neglected here processes of extinction, which must be taken into account especially for a high density of ionization.

Translated by R. L. Eisner
6

SOVIET PHYSICS JETP VOLUME 3, NUMBER 1 AUGUST, 1956

Electrical Explosion of Metal Wires

I. F. KVARKHTSAVA, A. A. PLIUTTO, A. A. CHERNOV AND V. V. BONDARENKO

(Submitted to JETP editor Sept. 8, 1954)
J. Exper. Theoret. Phys. USSR 30, 42-53 (January 1956)

Shadow photography and oscillograms of the current and voltage are used to investigate wires exploded by electric current. It is shown that the energy liberated in the wire at the instant of the first current pulse is sometimes less than the energy needed to evaporate the wire fully, and sometimes considerably more. Shadow photographs of the successive stages of wire explosion show a strong dispersion of the wire material after the flow of the first current pulse. A qualitative explanation is given for the basic features of the wire explosion phenomenon, taking into account the high mechanical stresses produced by heating and the radial pressures due to the magnetic field produced by the current.

1. INTRODUCTION

THE flow of a large current pulse through a thin wire results in its explosion, owing to its almost instantaneous evaporation. This phenomenon, called electric explosion, is of interest in many respects. Experiments with pulsed currents show that Ohm's law holds at current densities up to approximately 10^8 a/cm^2 [1-6]. Electric explosion of a wire is accompanied by a flash of light of high brightness and very rich in ultraviolet. In many investigations this was used to study the spectra of various metals and to produce pulsed sources of light[7-11]. Within a time interval of the order of a microsecond, enough energy is received to melt and completely evaporate the wire; in view of the short duration of the process, deviations from the ordinary course of melting and evaporation are to be expected[12,13].

Owing to the almost instantaneous heating and corresponding thermal expansion, the wire is subject to very high mechanical stresses during the explosion process. This makes it possible to investigate the properties of the wire under shock compression conditions[14].

Rupture in water or other liquids causes intense dispersion of the wire material. High degrees of dispersion can be obtained, depending on the power of the explosion. Powerful ruptures are accompanied by shock waves, which lead to strong cavitation in the liquid (see below).

Explosion of a wire in vacuum produces supersonic hydrodynamic streams with which it is probably possible to produce molecular beams denser than usual. Such beams can be used to study how one beam interacts with another, or how the beams interact with surfaces of bodies, with beams of charged particles, with electric and magnetic fields, etc. Electric explosion of wire can be used to produce films of certain metals without the use of crucibles or other means of liquefying the metal.

Wire explosion can be used in the laboratory to produce high temperatures at relatively high densities of matter. Ruptures in air and in vacuum do not make it possible to attain a temperature higher than 30,000 °K[7-8], owing to the so-called discharge-pause phenomenon and to the possible formation of shunting discharges. However, it is possible to obtain a temperature of 100,000 °K and higher if the wire is exploded in a liquid or solid medium (see below).

This phenomenon can also be used to investigate certain properties of explosion under conditions of infinite detonation velocity. The explosion starts simultaneously at all points of the wire. In this case the quantity of exploded matter, explosion time, total explosion energy etc. can all be readily controlled.

---

[1] L. A. Ignat'eva and S. G. Kalashnikov, J. Exper. Theoret. Phys. USSR 22, 385 (1952).

[2] H. R. Traubenberg, Physik. Z. **18**, 74 (1917).

[3] S. E. Khaikin and S. V. Lebedev, J. Exper. Theoret. Phys. USSR **26**, 629 (1954).

[4] E. S. Borovik, Dolk. Akad. Nauk SSSR **91**, 771 (1953).

[5] H, Margenau, Z. Physik **4**, 254 (1924).

[6] V. V. Bondarenko, I. F. Kvartskhava, A. A. Pliutto, and A. A. Chernov, J. Exper. Theoret. Phys. USSR **28**, 191, 1955; Soviet Phys. JETP **1**, 221 (1955).

[7] J. A. Anderson, Astrophys. J. **51**, 37 (1920); J. A. Anderson and S. Smith, Astrophys. J. **64**, 295 (1926).

[8] N. N. Sobolev, J. Exper. Theoret. Phys. USSR **17**, 986 (1947).

[9] G. Vaudet Ann. Phys. **9**, 645 (1938).

[10] W. M. Conn, J. Opt. Soc. Am. **41**, 445 (1951).

[11] L. Eckstein and J. M. Freeman, Z. Physik **64**, 547 (1930).

[12] I. S. Abramson and I. S. Marshak, Zh. Tekhn. Fiz. **12**, 632 (1942).

[13] F. Braun, Ann. Physik **17**, 359 (1905).

[14] O. Bethge, Ann. Physik **8**, 475 (1931).

The electric explosion phenomenon is thus related to many interesting problems. Nevertheless, the phenomenon has not yet been thoroughly studied. We approach the investigation of the electric explosion of wires from two points of view; one involving a study of the energy balance of explosions in various surrounding media (air, water, solid insulator) and the other involving a study of the external appearance of the wire at various stages of the explosion. The former uses oscillographs of the explosion made with a two-beam driven-sweep oscillograph capable of recording voltage and current simultaneously. The latter employs shadow photographs made with a spark synchronized with various stages of the explosion.

2. MEASUREMENT PROCEDURE

The principal diagram of the setup for simultaneous oscillography of the explosion and shadow photography of the exploding wire is shown in Fig. 1. The setup consists of three interconnected parts: explosion circuit, spark circuit for shadow photography, and a circuit to trigger the discharges in the first and second circuits. The explosion circuit consists of capacitor C_1, discharge gap P_1 with starting electrode, noninductive current-measuring resistor R, and wire W; B_i is an electroacoustic voltmeter and D a voltage divider. The spark circuit contains capacitor C_2, resistor R_7, and spark gap P_2 with starting electrode; B_3 is an electrostatic voltmeter. The trigger circuit consists of capacitors C_3 and C_4, resistors R_2, R_3, R_4, and R_5, choke L and switch K; B_2 is an electrostatic voltmeter.

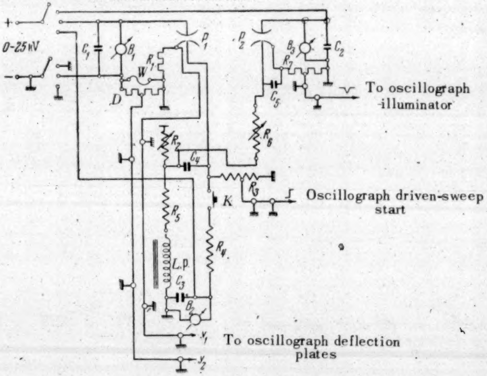

FIG. 1. Principal diagram of installation.

The operation of the setup is clear from the drawing. The trigger circuit is coupled through the resistor R_3 with the starting circuit of the oscillograph driven sweep that is common to both beams. The trigger circuit is also coupled through R_2, R_4, and C_4 with the starting electrode of gap P_2. Capacitances C_7, C_2, and C_3 are voltages sources for the respective circuits. They are charged in sequence by a common rectifier. When all capacitors are charged to the proper voltages, closing switch key K starts the oscillograph driven sweep. After a certain time interval, gap P_1 is operated and a discharge is produced in the explosion circuit. After still another time interval, operation of the gap P_2 energizes the spark circuit and a shadow photograph of the wire is taken through the open camera shutter. Depending on the value of R_6, the time interval between the start of the discharge in the explosion circuit and the flash of the spark can be varied from several microseconds to several hundred microseconds. The parameters of the spark circuit were chosen to produce a discharge with a single pulse of light lasting 2 - 3 microseconds. This established the shadow-photography exposure. The in the wire itself. The pause is longer in water and in organic glass than in air, particularly at low voltages and for long wires. In the case of short wires and high voltages, there is no pause, and the current decreases after passing through the maximum but does not reach zero. The same occurs with tungsten, molybdenum, and potassium wires under all conditions, i.e., the current never stops in the case of these wires.

From the oscillograms obtained, it is possible to calculate the energy delivered to the wire during any time interval elapsed since the start of the discharge. We are interested here only in the total energy W of the first pulse. This can be calculated from the well-known relationship

$$W = {}^1/_2 C(V_0^2 - V_1^2), \qquad (1)$$

where C is the capacitance in the rupture circuit, V_0 the initial voltage across the capacitor, V_1 the voltage at the instant of the pause. V_0 is measured with an electrostatic voltmeter and V_1 is taken from the voltage oscillogram. It is assumed here that all energy delivered by the capacitor during the first pulse is liberated by the wire. The correctness of this assumption was checked by plotting a current-voltage curve for the process to permit direct comparison of the energy liberated by the wire with the energy delivered by the capacitors.

Equation (1) was used to determine from the oscillograms the energy of the first pulse as functions of the amplitude of the initial voltage for copper, silver, and steel wires. The corresponding curves are shown in Figs. 4-6. The abscissas represent initial volts, and the ordinates first-pulse energy in watt-seconds. The dotted parabolas show the dependence of the total capacitor energy on the initial voltage (to the same scale). The wire material and the explosion-circuit parameters are given in the figure captions. Heavy lines A and B, drawn parallel to the abscissa in Figs. 4 and 5, indicate the values of energy required for complete evaporation of the corresponding wire, as calculated from tabular data. Line B on Fig. 4 corresponds to a wire 120mm long. From the positions of these lines it is evident that, depending on conditions, the energy of the first pulse can be several times higher or several times lower than the energy required for complete evaporation of the wire. It can be seen that the energy of the first pulse increases rapidly with the initial voltage. This is caused principally by the increase in the overvoltage produced across the wire at the end of the first surge. An especially large amount of energy can be absorbed by the wire at high voltages and when exploded in a dense medium. For example, a silver wire 0.15 mm in diameter and 3 cm in length, embedded in organic glass, absorbs during a first pulse lasting 1.5-2 microseconds enough energy from a 10-microfarad capacitor at 7 kilovolts to heat the wire to 150,000° Kelvin. The temperature is calculated by determining the average energy available for each atom of wire material and subtracting the energy required for complete evaporation of the wire. Here we neglected the radiation losses and disregarded the energy losses involved in ionizing and exciting the atoms

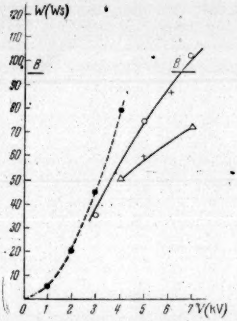

FIG. 4 Curves of $W = f(V_0)$ for copper wire of 0.15 mm cross section diameter. Δ — l = 120 mm, C_1 = 10 μF, inductance $L = 2.8 \times 10^{-6}$ H; x — l = 240 mm, C = 10 μF, $L = 2.8 \times 10^{-6}$ H; o — l = 120 mm, C_1 = 10 μF, $L = 3.5 \times 10^{-6}$ H.

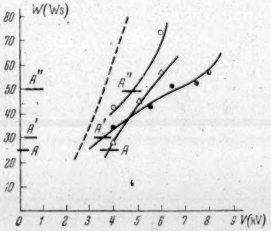

FIG. 5. Curves of $W=f(V_0)$ for silver wire. ○ — d=0.15 mm, l=120 mm C_1 = 10 μF, inductance $L = 3.5\text{x}10^{-6}$H; Δ — d = 0.25 mm, l = 160 mm, C_1 = 10 μF, $L = 3.5\text{x}10^{-6}$H; ● — d = 0.13 mm, l = 100 mm, C_1 = 10 μF, $L = 1.5\text{x}10^{-6}$H

one-microfarad capacitor C_2 was charged to 30 kv in all experiments. The shadow-photography optical system is shown in Fig. 2. In many cases, the shadow photographs were paralleled by oscillograms of the wire explosion. The oscillograph recorded simultaneously the voltage across the wire and the voltage across current-measuring resistor R_1, proportional to the current in the wire. All of the latter voltage and a fraction of the former (from the voltage divider) were applied through a coaxial cable to the oscillograph deflection plates owing to the special construction of the resistor R_1, the resultant oscillograms of the current were quite free of inductive distortion and induced noise. The inductive distortion of the voltage oscillograms was controlled in a special manner*.

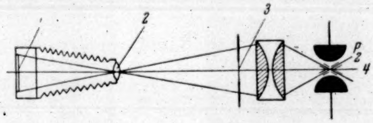

FIG. 2. Shadow photography diagram
1 - photographic plate, *2* - objective, *3* - wire
4 - spark.

Applying suitable corrections, oscillograms obtained in this manner permit calculation of the explosion energy at any instant of time with an accuracy to 5-7%. Shadow photographs were taken of explosions in air and water. A container made of organic glass and having plane parallel walls was used for the latter.

3. EXPERIMENTAL RESULTS

a) WIRE EXPLOSION OSCILLOGRAMS. EXPLOSION ENERGY

Figure 3 shows oscillograms obtained with different wires under varying experimental conditions. The upper and lower curves show respectively current and voltage vs. time. Oscillograms obtained with copper, silver and platinum wires were described by us in Ref. 6 and are not repeated here.

Oscillogram I was taken with a potassium wire in a glass capillary tube. Oscillograms II (copper wire) and III (tungsten wire) are given as examples to illustrate the entire wire-explosion process, starting with the first pulse and ending with the complete discharge of the capacitor in the second pulse. The oscillograms were made at high voltages. Oscillogram III shows only the current curve.

The oscillograms show that during the initial stage of the discharge, lasting from a few up to several dozens of microseconds the wire first receives a fraction of the energy in the form of a pulse. This first pulse is followed in most cases by the so-called current pause, when the current drops to zero[8,12,15,16].

The voltage across the wire first rises and reaches at the point of maximum current a value that is somewhat less than the initial voltage across the capacitor.** Next, in view of the fact that the current starts decreasing, $\partial I/\partial T < 0$, and an overvoltage occurs across the wire. At the end of the first pulse both current and $\partial I/\partial T$ approach zero, and the voltage, which passes through its maximum at the instant $I = 0$, assumes a constant value, which nevertheless represents a considerable fraction of the initial voltage. Once the pause starts, no more energy is liberated in the wire. The duration of the pause, depending on experimental conditions may usually range from zero to several hundred microseconds. The pause is followed by a second discharge pulse, characterized by higher currents and lower voltages than the first pulse. This means that in the second pulse an arc strikes across the gap formerly short circuited by the wire and the following full capacitor discharge is accompanied in this case by the usual damped oscillations. The length of the pause depends both on the processes occurring during the wire explosion and on the de-ionization time of the discharge gap. If the pause is longer than the gap de-ionization time, the second pulse cannot occur at all.

The oscillograms of aluminum, silver, and gold wires are similar to the copper-wire oscillogram. The oscillograms of tungsten, molybdenum, iron, nickel, and nichrome wires are similar to that of platinum wire, and are characterized by a first-pulse region in which the current and voltage vary little with time. A similar region, although less clearly pronounced, occurs in the case of long copper, silver, and aluminum wires.

Oscillograms were also taken of exploding wires placed in water or embedded in organic glass. These oscillograms showed that the waveform and amplitude of the first pulse depend little on the character of the surrounding medium, and are consequently determined by the processes occurring

---

* A detailed description of the oscillography, an evaluation of the fidelity of the oscillograms, and the construction of current-measuring resistor R_1 are given in Ref. 6.

** Because only a small fraction of the energy can be liberated by the wire in the form of heat and in the form of magnetic energy of the current within that time. Furthermore, the voltage drops across the resistances in the explosion circuit are low.

[15] J. Wrana, Archiv. Elektrotech 33, 656 (1938).

[16] B. Eiselt, Z. Physik 132, 54 (1952).

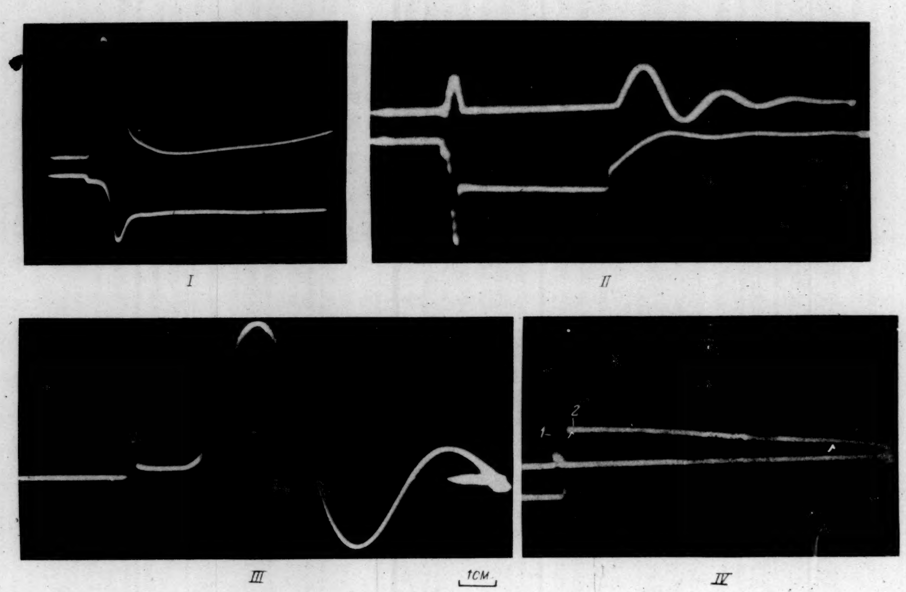

FIG. 3. Samples of current and voltage oscillograms (current--upper curves, voltage--lower curves, horizontal axis--time axis). I -- K, $d = 0.14$ mm, $l = 140$ mm, $V_0 = 7$ kv, $C_1 = 8\ \mu F$, current scale $m = 100$ A/mm, voltage scale $n = 550$ V/mm, time scale $\tau = 2 \times 10^{-7}$ sec/mm. II--Cu, $d = 0.05$ mm, $l = 60$ mm, $V_0 = 5$ kv, $C_1 = 8\mu F$, $m = 150$ A/mm, $n = 600$ V/mm, $\tau = 2.5 \times 10^{-7}$ sec/mm. III--W, $d = 0.08$ mm, $l = 100$ mm, $V_0 = 10$ kv, $C_1 = 0.5\ \mu F$, $m = 60$ A/mm, $\tau = 8 \times 10^{-8}$ sec/mm. IV -- Cu, $d = 0.05$ mm, $l = 150$ mm, $V_0 = 3.5$ kv, $C_1 = 8\mu F$, $m = 120$ A/mm, $\tau = 1.1 \times 10^{-6}$ sec/mm.

of the wire material.

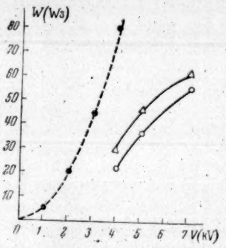

FIG. 6. Curves of $W = f(V_0)$ for steel wire of 0.15 mm cross-section diameter. Δ – l = 60 mm, $C_1 = 8.4$ μF, inductance $L = 3.5 \times 10^{-6}$ H; O – l = 120 mm, $C_1 = 8.4$ μF, inductance $L = 3.5 \times 10^{-6}$ H.

b) SHADOW PHOTOGRAPHY

Many wire-explosion oscillograms were paralleled by shadow photographs showing various stages of explosion in air and water. To prevent doubly exposing the film by the light of the second pulse, most photographs were made of copper wires at conditions under which no second pulse occurs. The photographs were taken at time intervals ranging from several microseconds to several hundreds of microseconds after the start of the discharge. The state of the wire at a given instant was established for each explosion with an exposure of 2-3 microseconds. To obtain shadow photographs of successive states of the wire, the explosions were repeated under identical conditions and the photography was carried out at various time intervals measured from the start of the process. The reproducibility of the shadow photographs was quite satisfactory in these experiments.

Figure 7 shows shadow photographs of an enamel-insulated copper wire of diameter $d = 0.10$ mm and length $l = 15$ cm taken at an initial voltage $V_0 = 3.5$ kv. Photographs V, VI, VII, and VIII, correspond to an elapsed time of 5, 10, 15, and 50 microseconds from the start of the discharge. The magnification of the photographs is approximately 15 diameters. It is evident from these photographs that during the first five microseconds after the start of the discharge (photograph V) there is no external change in the wire, except for a few short incandescent wire segments still seen in photograph VI that follows. After 10 microseconds (photograph VI) the layer of enamel peels off the wire noticeably and continues to peel off the wire, as shown in the subsequent photographs. Noticeable evaporation of the wire, becoming progressively stronger, begins at 15 microseconds (photograph VII). At 50 microseconds (photograph VIII) a considerable portion of the wire is still unevaporated, and the wire splits into individual longitudinally-elongated "beads". A photograph taken at 150 microseconds after the start of the discharge (not reproduced here) shows that the evaporation is almost complete by that time, and the unevaporated remnants of the wire, in the form of small particles, are scattered in space in disorderly manner. What calls attention in these photographs is the uneven explosion of the wire.

The oscillogram belonging to the above series of shadow photographs shows that the first discharge pulse lasts not more than 3-5 microseconds. The energy of this pulse is sufficient to evaporate completely 60% of the entire mass of the wire. It must therefore be assumed that the wire is in a superheated liquid state for some time after the first pulse. In view of the high surface tension of metals, the formation of incipient gas state is difficult, and therefore there is a short period of time (on the order of microseconds) when evaporation cannot begin over the entire volume. The evaporation occurs only on the surface of the wire. Since the wire liberates energy very rapidly (the power is 10^8 watts) it should become considerably superheated. Our shadow photographs confirm such an assumption. To obtain a more convincing proof of a superheated state, simultaneous oscillograms were taken of the current in the explosion circuit and of the photoelectric current excited in a photocell multiplier by a strongly collimated beam of light coming from a narrow portion of the surface of the wire. The corresponding curves are shown in Fig. 3 (oscillogram IV). A much longer sweep time was used to cover the entire evaporation process. The current curve (upper beam) shows the presence of the very narrow first pulse (arrow 1) in the initial portion of the oscillogram. This is followed by a current pause. The photocell-current curve (lower beam) has a maximum (arrow 2) at the start of the oscillogram, followed by a gradual decrease. This indicates that the wire, having its maximum temperature at the end of the first pulse, is consequently in a superheated state. Later on, the temperature of the wire should decrease as the energy of the superheated state is consumed by the evaporation. However, the shadow

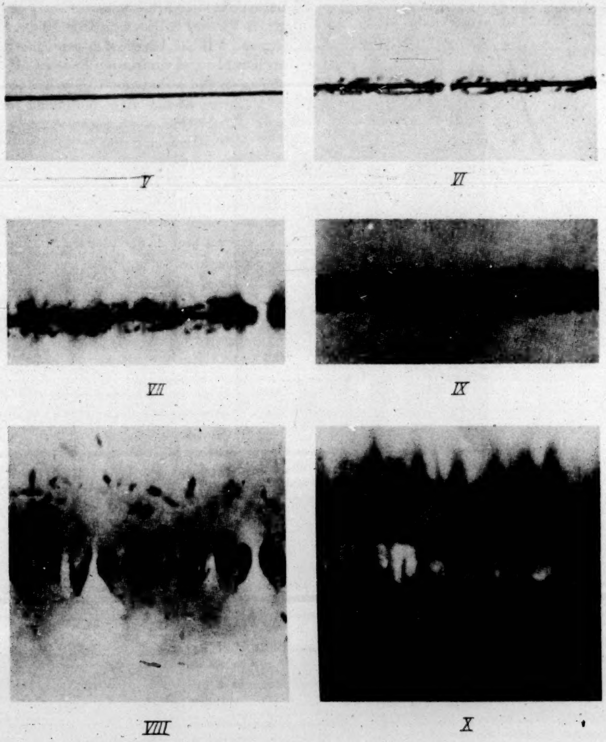

FIG. 7. Shadow photographs of wire explosion. Photos V, VI, VII, and VIII show successive explosion stages for enameled copper wire 0.1 mm dia. and 15 cm long (weak explosion); IX and X show the scattering of explosion products at relatively high voltages (strong explosion).

photographs show that the evaporation gains intensity with time. This must be explained by the fact that the wire becomes gradually broken up into individual "beads" and the evaporation surface increases greatly.

Photograph IX (Fig. 7) shows the condition of an uninsulated wire with $l = 15$ cm, $d = 0.05$ mm, exploding in air at $V_0 = 5.2$ kv. There is no second pulse. The photograph was taken 28 microseconds after the start of the discharge, and the magnification is 1.5-2 diameters. It is evident from this photograph that the evaporation proceeds in layers that run perpendicular to the axis of the wire. The stratified nature of the evaporation is shown even more clearly in photograph X, taken 28 microseconds after the start of the discharge with l=15 cm, d=0.15 mm, and V_0=5kv.

$V_0 = 5$ kv. One sees clearly here two streams of explosion products, one with a small quantity of matter, low velocity, and deeper penetration into the air; the other with a larger quantity of matter lower velocity, and shallower penetration in the air. Both streams are radially stratified.

The accompanying shadow photographs thus disclose certain interesting details of the explosion process. However, the corresponding experiments were carried out at relatively low initial voltages (3.5 kv) to slow down the process and to make it possible to distinguish the individual explosion stages. At higher voltages the explosion is much faster and the pictures all merge. To obtain a better understanding of the explosion phenomenon in general and of the mechanism of current interuption in particular, it is necessary to investigate the behavior of the wire at higher values of V_0, i.e., at higher rates of energy influx in the first pulse. The method employed for this purpose was to shunt a segment of the wire with a discharge gap[8] connected in series with a resistor. Since considerable overvoltage occurs across the wire before the end of the first pulse (see rupture oscillograms), it is possible to produce breakdown of the shunt at the required instant of time by adjusting the length of the gap. If the resistance of the shunt is nearly zero, almost all of the current flows through the shunt once the gap breaks down and no more energy is liberated by the wire. If the shunt resistance is not zero, the voltage drop across this resistance continues to feed energy to the wire. By varying the breakdown voltage of the shunt and its resistance it is possible to change the energy of the first pulse and its delivery rate over a wide range. The results obtained in this manner are not sufficiently quantitative, for we know that the starting time and development of a discharge in a gap has a certain statistical dispersion. However, the results are well founded qualitatively. Figure 8 shows three photographs of a copper wire having $d = 0.05$ mm. Photograph XI was taken 28 microseconds after the start of the discharge at $V_0 = 4$ kv and $l = 65$ cm. The breakdown voltage of the shunt was 2.5 kv. Photographs XII and XIII were taken 15 microseconds after the start of the discharge at $l = 12$ cm and at 5 and 6 kv respectively. The approximate breakdown voltage of the shunt was 5 kv and its resistance was approximately 0.2 ohm. The magnification of the photographs is 10 diameters. It is evident from these photographs that the current interruption is preceeded by states characterized by an intense movement of the matter in the wire. At low pulse energies (photograph XI) the wire remains solid and after several tens of microseconds it manages to assume a well-developed wave-like shape. At higher energies (photograph XII) individual highly-superheated sections evaporated completely. The remaining portions did not have a chance to curve noticeably and enter into a dispersed-state with a large number of breaks along the entire wire, probably under the influence of shock wave occuring when the material is ejected at the superheated locations. It can be seen from photograph XIII that the distribution of the superheated sections becomes almost periodic in the more uniform sections of the wire and at larger pulse energies. Careful examination of photograph VII, corresponding to a low-energy first pulse also discloses the beginning of dispersion.

The next photograph (XIV) illustrates the explosion of copper wire in water at $l = 12$ cm, $d = 0.05$ mm, and $V_0 = 1.5$ kv. The photograph was taken 150 microseconds after the start of the discharge and the magnification is 3-4x. The shadow spots on these photographs indicate the formation of gas bubbles around short glowing sections of the wire. Some of these bubbles have a regular spherical shape, indicating that individual overheated sections are small in size. Where several superheated sections have accumulated, the bubbles are drawn out in the direction of the wire axis. The presence of illuminated sections in the middle regions of the spots is due to the radiation of the overheated sections of the wire.

The last photograph XV shows the explosion of a copper wire with $l = 12$ cm, $d = 0.05$ mm, and $V_0 = 6$ kv. The photograph was taken 50 microseconds after the start of the discharge. The pause is less than 15 microseconds. What is remarkable in this photograph is the water cavitation resulting from the wire explosion. The bubbles formed are illuminated by light from the arc of the second discharge pulse. It is probable that the cavitation of the water is related to the shock waves propagated in the water as the result of the second current pulse.

Several experiments were performed to clarify the role of the superheated short sections, appearing in the wire at the initial stage of the discharge. They are assumed to be very short arcs produced where the wire has slight inhomogeneities due to rapid evaporation or occurring where the wire breaks. Shallow and very narrow equidistant transverse notches were made in a uniform copper wire with a knife. Shadow photographs of the explosion of such wires showed that short arcs actually occur at such notches and that these arcs were further developed than the short arcs on homogeneous

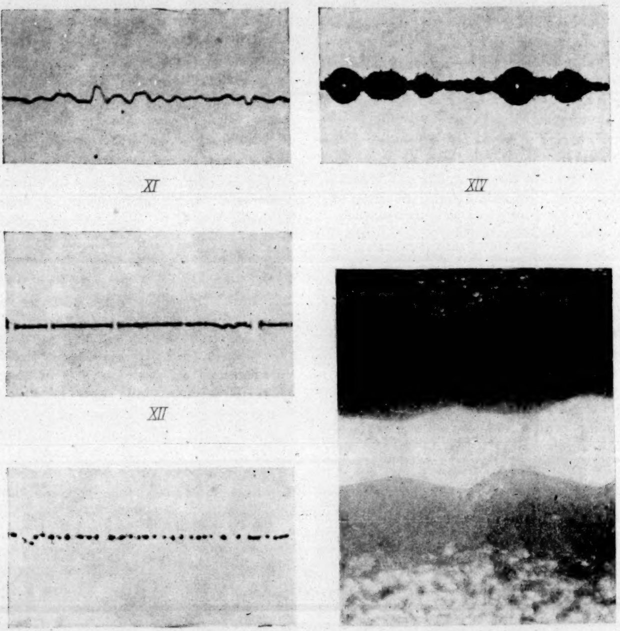
XI XIV XII XV XIII

FIG. 8. Shadow photographs of wire explosion. Photos XI, XII, and XIII show explosion of shunted wire; XIV and XV show explosion of wire in water.

wires. This is probably related to the magnitude of the inhomogeneity. Comparison of current oscillograms of a notches and a homogeneous wire shows that in the former current diminishes faster after the maximum of the first pulse is steeper. This indicates a faster rise in the resistance of the wire due to the presence of stronger short arcs. From this it follows that in the case of a strong explosion, when the evaporation has a clearly pronounced stratified character, the simultaneous occurrence of a large number of short arcs over the entire length of the wire may contribute to the interruption of the current.

4. EVALUATION OF RESULTS

The now prevalent ideas concerning the mechanism of electric wire explosion cannot explain the basic features of the phenomenon. For example, the almost-instantaneous interruption (within several tenths of a microsecond) of such large currents (several thousands of amperes) has been attributed to the transformation of the wire from metal into non-conducting--very dense--gas[12,15,16]. This hypothesis, on first glance quite natural, is contradicted by experimental data. Actually, the oscillographic data above show that, depending on experimental conditions, the energy of the first pulse of the discharge can be several times greater or smaller than the energy needed for total evaporation of the wire. Consequently, not all the wire need evaporate before the current is interrupted. Furthermore, the shadow photographs show that if the explosion is delayed, the current is interrupted even before the wire starts evaporating noticeably. In cases where the energy of the first pulse exceeds by many times the energy required for total evaporation of the wire, there is every reason for assuming that this wire is fully evaporated even within the first pulse . Nevertheless, in those cases the current is frequently not fully interrupted.

There is no explanation, particularly in the case of strong explosion, for the clearly pronounced stratified character of the evaporation and for the tendency of the wire to break up into minute "beads" when the explosion is delayed. Attempts to explain the stratified nature of the evaporation by attributing it only to the action of the surface-tension forces in the molten metal[17] must be considered groundless because these forces are too small. In fact, as was already noted, the wire in the explosion process may even reach critical temperature, and therefore the surface tension tends to zero.

It is equally incorrect to attribute the discharge pause to the reaction of the metal vapors with the oxygen in the air and to the accompanying further heating of the vapor (thermal breakdown). Such a point of view is disproved by wire-explosion experiments in inert gases (nitrogen, argon) and dense insulators (water, organic glass, glass, etc.) in which a reaction with the vapors of the metal is impossible, and the character of the pause remains unchanged. References 8, 12, and 16 correctly relate the appearance of the pause with the radial expansion of the vapor during the explosion. However, they do not take into account the cylindrical symmetry of the explosion,[18] and cannot give a convincing explanation of the phenomenon.

Nor are explanations given for the large dispersion of the energy of the first pulse, for the dependence of the waveform of the first pulse on the wire material, for the role of superheated short segments produced in the wire in the initial stage of the discharge, etc.

Analysis of the experimental material given above permits forming a definite concept of the mechanism of electric wire explosion, giving at least a qualitative explanation for the basic features of the phenomenon. We start with the fact that in the first pulse, even before noticeable evaporation begins, the wire material is already in state of intense motion. For correct understanding of the explosion mechanism, it is first necessary to evaluate the forces causing this motion and their action, taking into account the gradual transition of the wire from solid into liquid and from liquid into gas. In the initial stage of the explosion the wire heats rapidly, while still in a solid state; not having enough time to expand in an axial direction (owing to inertia), it becomes subject to a strong axial compression. The magnitude of the compression can be approximately calculated from the following equation:

$$f = \alpha TES, \tag{2}$$

where α is the average coefficient of linear expansion, E the modulus of elasticity of the wire material, T the temperature rise, and S the transverse cross section area of the wire. Since the volume of the wire does not have time to change noticeably while it is being heated in a solid state, we can roughly assume E to be constant. Then Eq. (2) for copper wire, say, at temperature $T = 1{,}000\,^\circ$ gives an axial stress of approximately 20,000 atmospheres.

According to Euler, an axially-stressed homogeneous wire should assume a sinusoidal form. The connection between the wave length λ of the deformation and the critical axial compression stress f_n is given by the following expression

$$(\lambda/2)^2 = \pi^2 EM/f_n, \tag{3}$$

where E has the same meaning as before, and M is the moment of inertia of the transverse cross section of the wire ($M = \pi d^4/64$, where d is the diameter of the wire). Since an actual wire has a certain inhomogeniety, one cannot expect a strict periodicity . A detailed theoretical study of this problem and an experimental check on the results of the theory in the case of a platinum wire is found in Ref. 14. That such a phenomenon actually occurs in the initial stage of wire explosion is confirmed by the shadow photograph (Figure 7). Even though the wire remains only briefly in the solid state (less than 1 microsecond) it manages during that time to assume the shape of a wave of certain small amplitude. As a result, the compression along the wire distributes itself with the same periodicity. Since the melting point depends on the pressure, and the compression is periodic, the distribution of the regions where the melting begins will also have a periodical character. Where the compression is high, the mass should immediately begin to shift so as to reduce the compression. Thus there are dynamic reasons for a periodic variation in the transverse cross section along the wire as the wire changes to the liquid state. It is also necessary to take into account the action of the forces due to the magnetic field of the current, tending to compress the wire in a radial direction (the so-called "pinch effect"). This compression can be characterized by a force F acting on a unit of wire perimeter surface and directed toward its center. The magnitude of this force is given by the equation

---

[17] W. Kleen, Ann. Physik 11, 579 (1931).

[18] L. I. Sedov, Metody podobiia i razmernosti v mekhanike (Analogue and Scale-Model Methods in Mechanics), Moscow-Leningrad, 1952.

$$F = \sigma j^2, \tag{4}$$

where σ is the perimeter of the wire and j is the current density.*** [20] Under the conditions of our experiments, with a wire of approximately 0.1 mm the current density reaches values of $10^6 - 10^7$ electromagnetic current units. According to Eq.(4) the corresponding forces will be on the order of $10^{10} - 10^{12}$ dynes. These forces reach a maximum in the region of the current maximum, where according to oscillographic data the wire begins its transformation to the liquid state. Under the influence of these forces, the masses begin to shift where the liquid wire becomes narrower, the shift being in a direction perpendicular to the axis of the wire. Conversely the masses are pushed out in the opposite direction where the liquid wire becomes wider. The acceleration of the motion will increase with the difference in the radii in the compression and expansion locations (F is inversely proportional to the third power of the radius). Under the influence of the large currents flowing through them, the compressed sections will start to evaporate much sooner than the neighboring sections, and this will accelerate the compression. The compression accelerates both because of the evaporation of the material, and also because of the forces produced in this evaporation.

Since the transverse periodicity along the entire wire occurs simultaneously, the compression of the narrow portions begins simultaneously everywhere. Consequently a set of short superheated sections is produced simultaneously over the entire wire and for a very short time (considerably shorter than the duration of the first pulse) the matter appears to be expelled from this set beyond the limits of the charge. It is evident that intense shock waves will propagate along the wire from the superheated sections, and these shock waves are capable of causing a considerable disturbance and result in the dispersion of the remaining sections of the wire (a phenomenon similar to the initial stage of cavitation in liquid without vapor bubbles developing). As a result of such dispersion, these sections apparently lose their conductivity, and this in turn also contributes to the interruption of the current. According to Eq. (4), the compression forces of the magnetic field of the current rise very rapidly with the current density, and it is therefore possible that this generally limits the maximum current density that can be reached in metals. The picture drawn here for the processes occurring in the first pulse makes it also possible to explain other facts that characterize the electric wire explosion. For example, it follows naturally from this picture that the evaporation of the wire should be characterized by strata perpendicular to the axis of the wire.

Taking into account the uneven rate at which energy is liberated along the wire and the possibility that in short wires the isolating sections can be broken down by the large initial voltages, the high limit of energy absorbed by the wire during the first pulse becomes now understandable.

Also understandable now is the tendency of the wire to break down into individual "beads" if the explosion is slowed down. In fact, while processes contributing to the dispersion of the wire predominate before the current is interrupted, once the current is interrupted, the reverse processes start predominating and lead at least to a partial rejoining of the small liquid particles into larger droplets. In view of the intense evaporation, these droplets which interact with each other flatten out in an axial direction and stretch out in a radial direction. The random character of the rejoining of the particle leads to a certain statistical distribution of the droplet dimensions along the wire.

The role played by the compression forces of the magnetic field due to the current is further corroborated in the fact that in wires having a high specific resistivity, and consequently carrying low current, such as tungsten, molybdenum, platinum, iron, nichrome, nickel, and the like, the first pulse is characterized by a slight step in which the current in the voltage changes little in time, i.e., the wires have a negligible thermal coefficient of resistivity within the confines of this step. The reason is that in view of the low current the compression effect is weakly pronounced and the liquid wire maintains its cylindrical shape for a certain time. In the liquid state

---

***We neglect the skin effect[19] and the inverse skin effect as being too small.

[19] Z. Lubin, Zhur. Prikl Fiz 4, 2, 45 (1927).

[20] E. Fr. Russ, Z. techn. Phys. 11, 529, (1930).

the metals, as is well known, have a low coefficient of resistivity. An analogous phenomenon occurs also for copper, silver, and aluminum in the case of long wires and relatively low voltages. Under these conditions the currents in these materials during the first pulse are also low.

As was shown above, potassium, tungsten, and molybdenum cannot produce a complete interruption of the current under any condition. This is explained by the thermal ionization of the vapors and by the intense thermal electron emission of tungsten and molybdenum. Not one of the materials can lead to a complete interruption of the current regardless of the vapor pressure and meet the conditions required for sufficient thermal ionization of the vapor. This holds for all materials in the case of short wires and high voltages.

The duration of the pause is determined principally by the energy of the first pulse, which in the final analysis determines the radial velocity of the vapor. The higher the energy of the first pulse, the higher the velocity of the vapor. In particular, it was shown in Ref. 18 that, depending on the initial energy, the pressure on the axis and near the axis can drop to any value down to a vacuum in the case of a radial scattering of particles in the explosion of a wire with cylindrical symmetry. Under this condition, and in the presence of a certain residual voltage, it is quite natural for a finite pause to exist, that is, for a second pulse to form as a result of the breakdown that occurs within a finite time after the beginning of the pause. As to the possibility of the existence of an infinite pause, this can be basically explained by two causes.

An infinite pause is characteristic of a delayed explosion with low energy in the first pulse. In view of this, the radial velocity of the vapor is insufficient to reduce the pressure enough to permit a breakdown to occur. Furthermore, under those conditions when the duration of the pause exceeds the de-ionization time of the gas in the discharge gap of the rupture, the pause becomes practically infinite, since the residual voltage is insufficient to produce breakdown.

It thus becomes possible to explain qualitatively the principal outlines of the phenomenon of electric explosion of wires.

Translated by J. G. Adashko
7

SOVIET PHYSICS JETP VOLUME 3, NUMBER 1 AUGUST, 1956

The Investigation of Cathode Sputtering in the Near Threshold Region. I

N. D. MORGULIS AND V. D. TISHCHENKO
Kiev State University

(Submitted to JETP editor June 18, 1954)
J. Exper. Theoret. Phys. USSR 30, 54-59 (January, 1956)

It is proposed to make use of the method of tracer atoms for the investigation of cathode sputtering in the near threshold region, and for the determination of the magnitude of the threshold energy of sputtering. Results are presented of such an experimental investigation of the sputtering of cobalt by the ions of mercury and argon, traced with its radioactive isotope Co^{60}.

THE investigation of cathode sputtering in the near threshold region, i. e., at small energies V_p of the sputtering ions, bordering on threshold, has always been associated with great experimental difficulties. The problem consists in the determination of both the threshold of sputtering, i. e., the mimimum energy V_0 which the bombarding ion must have for the actual occurence of this process, as well as the dependence of the coefficient of sputtering μ on V_p, for $V_p \geq V_0$[1]. Only a very small part of this problem, consisting in the determination of the quantity V_0 for thermoelectric cathodes covered with active adsorbed films (for example, thoriated tungsten), could be in some measure resolved, thanks to the fact that for a fixed origin of sputtering of this film, the precise method of thermoelectric emission could be used. The determination of the relation $\mu = f(V_p)$ for this case could be realized by an approximate, indirect, and rather unwieldy method[2]. But as regards the vast majority of all other important and interesting materials, and in the first place metals, the straightforward solution of the indicated questions would be practically hopeless in view of the fact that for $V_p \geq V_0$, the magnitude of μ is so small that its immediate determination, for instance by weighing the sputtered deposit, by measuring its transparency, etc., is unrealizable practically. Therefore, in the past, the following method has generally been used: the determination of the relation $\mu = f(V_p)$ was performed in the region of medium and large energies. Then, using the fact that in these regions this relation, according to the experimental data, is generally more or less linear, i. e., $\mu = B(V_p - V_0)$, a linear extrapolation was performed to $\mu = 0$. By such means, untrustworthy in principle, it is of course possible to obtain rough, inaccurate values of the quantity V_0. This deprives us of the opportunity to seek for a correlation between this quantity and other physical characteristics of the metals investigated, i. e., to clarify the nature of the phenomenon of cathode sputtering. Recently, a communication [3] appeared, in which it is suggested that the above mentioned investigations be performed by using the change in the contact potential of a probe in the gaseous discharge, i. e., the shift of the probe characteristics under the influence of a layer of sputtered material deposited on it. This method is essentially a variation of another, already used in the past for this same purpose, in an application to oxidized cathodes[4]. It is readily seen, however, that the probe method is far from universal, because its sensitivity will depend on the difference in the work functions of the electrons in the material being sputtered and in the probe. For the majority of metals, this difference of work functions among them is not great, and therefore there is no basis to expect great success in applying this method. Even the values presented in reference 3 for the quantity V_0 appear so improbably large ($\sim$50-70 v.) that one does not feel obliged generally to take them into account.

Thus we see that although a large number of works have been devoted to the investigation of the cathode sputtering of solid bodies[1], still, at the present time, the laws governing this phenomenon inthe near threshold region remain an open question. Meanwhile, at the present time we already have at our disposal a powerful method not previously accessible in the near threshold region – the method of radioactive tracer atoms. We have made use of this method for the solution of the above-stated problem. Some preliminary results obtained by us in this direction are presented below.

---

[1] N. Morgulis, Usp. fiz nauk 28, 202 (1946)

[2] N. Morgulis, "Rozporoshuvannia metalichnoi poverkhni pri udarakh pozitivnikh ioniv", Izd-vo AN Ukrainian SSR, 1936, p. 46.

[3] G. Wehner and G. Medicus, Phys. Rev. 89, 339 (1953); G. Wehner, Phys. Rev. 93, 633, 653 (1954); J. Appl. Phys. 25, 270 (1954).

[4] N. Morgulis and Ia. Liubarskii, Fiz. zap. Akad. Nauk USSR 9, 233 (1941); Sb. statei potekhn. fizike, 1947, P. 261.

The appartus used consisted of a tube with the usual gasotron discharge by an incandescent tungsten cathode in the following atmospheres: 1) mercury vapor, and 2) argon. A small (diam. ~ 3 mm) flat target-probe made of the investigated metal mixed with a radioactive isotope, with a suitable protective ring of common nickel, was introduced into the plasma of the discharge. All leads to the probe and its rear surface were carefully insulated. Placing the corresponding negative potential V_p on the probe with respect to the potential at that point in the plasma, we bombarded it with ions with the current I_p and energy V_p (neglecting the extremely small magnitude of the initial energy of the ions). For the accurate determination of the quantity V_p, the probe characteristic was obtained at each measured point of the curve $\mu = f(V_p)$ (see below). In this way, we determined the potential of the plasma at the point where the target-probe was located. An example of such a probe characteristic in mercury vapor for the important case of a small value of $V_p = (V_z - V_\pi) = (25\text{-}14) = 11\text{v}$, is given in Fig. 1, in which is seen its normal character. The correction to the quantity I_p, associated with the secondary emission of mercury ions (in the first case) from the target, is insignificant.

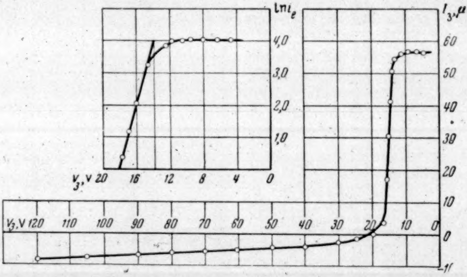

FIG. 1

At a small distance $d \sim 2$ mm in front of the probe, a collector was placed, on which atoms of the metal under investigation, sputtered from the target-probe, were deposited. In order to reduce the reflection of the atoms under investigation[5] from the collector to a minimum, the collector was fabricated either from the same metal, or from a metal with very similar properties (Ni), carefully purified and degreased. Moreover, immediately before the actual experiment, the surface of the collector was cleaned additionally with bombarding ions, i. e., by some sputtering. While the experiment was being carried out, the collector was maintained at a "floating" potential, i. e., was disconnected from the circuit. However, sputtering from the collector of the deposit from the target being studied could be completely ignored because its negative potential with respect to the plasma $V_{\pi\lambda} = (kT_e/e)\ln(u_p/u_e)$ was extremely small since in our experiments the electronic temperature was only ~ 14000°K and did not vary essentially from point to point (Fig. 1). The distance d was generally markedly less than the free path of an atom in the discharge in order to avoid scattering of the latter during their flight from the probe to the collector. However, the use of a discharge in mercury vapor in one of the variations of our investigations might appear not completely successfulfor the following reason; the surfaces of all cold parts of the apparatus, among them being the probe under investigation, might be partially covered with a thin film of mercury which could to some extent lower the effectiveness of the impact of the bombarding ion, i. e., its sputtering effect[6], and consequently could increase somewhat the value obtained for the quantity V_0. Moreover, this influence might be somewhat different at various energies of the bombarding ions, etc. Since it would be very difficult in our experiments to heat the probe to a high temperature and thereby preclude the presence of mercury films[6,7], similar measurements were also performed (second case) in the atmosphere of an inert gas-argon. However, a comparative investigation of the sputtering of a cold cathode of thoriated tungsten, carried out with mercury vapor as well as with inert gases Ne and A at not too great values of the quantity V_p[8], showed that the error associated with the possible role of the mercury film did not require undue consideration in this case.

---

[5] M. Devienne, J. phys. radium, **13**, 53 (1952); **14**, 257 (1953). N. Morgulis, V. Gavriliuk, and A. Kulik, Dokl. Akad Nauk SSSR **101**, 479 (1955).

[6] L. Koller, Physics **7**, 225 (1936). A. Patiokha, Usp. fiz. nauk **28**, 208 (1946).

Measurements were performed in the following manner. After the discharge was started, the probe characteristic was obtained, the required value of the quantity V_p was established, and the value of Ip was measured. After the target-probe was bombarded for the time t, the tube was opened, the collector with its deposit of active sputtered material was removed, and the number of counts N given by it during the time τ was determined (using an apparatus of type B). The thickness of the layer on the collector was so small that its self-absorption of the radiation could be neglected. The quantity thus obtained, $\nu = N/I_p t\tau = A\mu$, is proportional to the coefficient of sputtering μ atoms/ion, where the coefficient of proportionality A depends on 1) the relative (constant) location of the target and collector, in connection with the flight of the sputtered atoms in the different directions; 2) the specific activity of the initial material of the target; 3) the relative (constant) locations and shapes of the collector with the radioactive deposit and the radiation detector; 4) the counting efficiency. All that was required for the determination of this quantity A was the assumption that the flight of the sputtered particles in the various directions obeyed a cosine law, as is done at the present time[1].

As sputtering targets we used an alloy of nickel with 1% radioactive cobalt^{60} of one activity, and pure nickel, electrolytically coated with a layer of radioactive cobalt^{60} of another activity. The latter emits β-rays of energy 0.32 mev and γ-rays of energies 1.17 and 1.32 mev, has a large specific activity and a long half-life (5.3 years), i.e., is extremely convenient to work with. Its activity is determined in the usual way by γ-radiation.

A typical example of the results obtained by such means for the relation $\mu = f(V_p)$ is shown in Fig. 2 for the case of the alloy Ni + 1% Co^{60}. Here the coefficient of sputtering μ by ions of mercury refers to the common sputtering of Co as well as Ni. Since the physical properties of these two metals are very similar (in particular they have almost the same heat of evaporation, $Q = 4.0$ ev for Ni and 4.1 ev for Co) it is reasonable to expect that the ratio of these components in the sputtered deposit on the collector will be the same as in the sputtered target. A curve of $\nu = f(V_p)$ is shown in Fig. 3 for the case of the sputtering of a layer of pure Co^{60} by ions of mercury. This curve has precisely the same character as the curve in Fig. 2. Finally, Fig. 4 shows the results in the form of the curve of $\mu = f(V_p)$ of the sputtering by ions of argon of the same target made of the alloy Ni + 1% Co^{60}; the method used for these measurements was essentially the same as that used with ions of mercury, described above. On all of the curves in Figs. 2-4, the vertical "antennae" indicate the limits of the statistical error in the measurements of each point; moreover, the points representing very small values of the quantity V_p were redetermined as a control (with the same results).

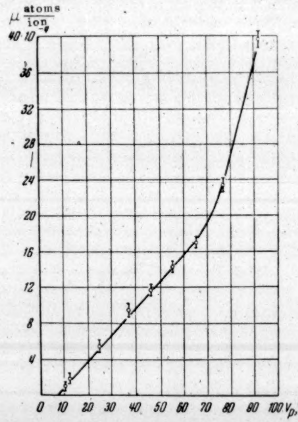

FIG. 2

---

[7] S. Sonkin, Phys. Rev. **43**, 788 (1933).

[8] L. Koller, Phys. Rev. **47**, 806 (1935).

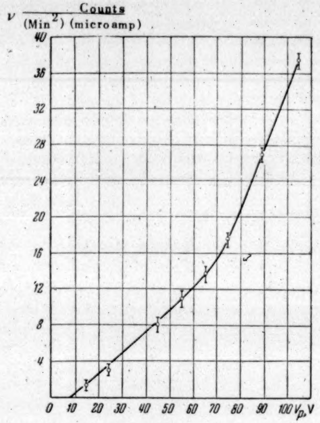

FIG. 3

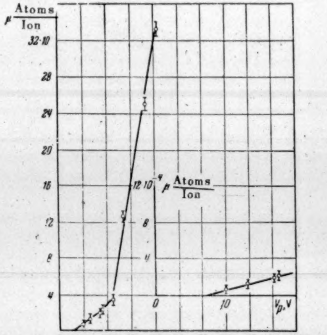

FIG. 4

An examination of the results obtained, presented in Figs. 2-4, leads us to the following conclusions:

1) As the energy of the sputtering ion is diminished and approaches the threshold of sputtering, the basic relation $\mu = f(V_p)$ does not preserve its linear form, but acquires a more concave character, somewhat similar to that obtained by us in reference 2 for the sputtering of thoriated tungsten (see above) Therefore, the method used in the past for the determination of the threshold energy of sputtering V_0, involving a linear extrapolation from the region of large and medium values of V_p to small values is inadmissible, because it may lead to incorrect (too large) values of the quantity V_0. Such an extrapolation to the axis $\mu = 0$, for the determination of the quantity V_0, may be made only in our case, where, by using the method of radioactive tracer atoms, we were able to carry out measurements of sputtering down to energies V_p almost equal to V_0. Our concrete case of the sputtering of metalic cobalt indicates that $V_0 \simeq 8$ ev.

2) For a preliminary examination of certain peculiarities of sputtering by mercury ions in the near threshold region, we compared the results obtained herein for cobalt with the results obtained in the past for the case of an activated thermocathode made of a coating of thorium on tungsten[8,9], and also, an activated film of an oxidized cathode[4]. The results of such a comparison are presented in the table below. We see here the presence of indications of some regular correlation between the characteristic quantities V_0 and μ of sputtering, and such an important parameter of the sputtered target as the heat of evaporation Q^1.

Sputtered Material	V_0 ev	$\mu \frac{\text{Atoms}}{\text{Ion}}$ for $V_p = 40$ V	Q, eV
Co (Ni)	8	$10 \cdot 10^{-4}$	4.1
Th — W	13	$1 \cdot 10^{-4}$	7.8
Oxidized Cathode	$\leqslant 5.6$	—	3.3

3) A comparison of Fig. 4 for sputtering by ions of argon with the corresponding Fig. 2 for ions of mercury indicates that: 1) the threshold of sputtering has approximately the same value $V_0 \approx 7$-8 ev and 2) the coefficient of sputtering μ in the case of A^+ is considerably larger than in the case of Hg^+; for example, for $V_p = 40$ v we obtain the values $\mu = 30 \times 10^{-4}$, and 10×10^{-4}, respectively. The last relation does not correspond to that which might be expected in this case from the relation between the masses of the sputtering ions and the value of the coefficient of accomodation implied herein; however, owing to the possibility here of a partially masking in-

---

[9] N. Morgulis and M. Bernadiner, Z. tekhn. fiz. 5, 1231 (1935).

fluence of a mercury film on the target(see above), to insist on this at the present time is still premature.

4) Also of great interest is the question of the degree of condensation on the surface of the collector under the conditions of a gaseous discharge of comparatively rapid sputtered atoms[10]. Our preliminary experiments indicate that such condensation on the collector of particles of metal might be incomplete, because during the coating of the collector by a layer of lamp-black, the quantity of sputtered atoms condensed on it could become somewhat larger.

Thus the results of the present work show the possiblity of obtaining reliable and interesting data concerning the question of the sputtering of various solid bodies in the previously inaccessible near threshold region by using radioactive tracer methods. Therefore, similar investigations are being expanded by us at present to a whole range of other objects, with the aim of establishing the general laws governing this phenomenon.

Translated by D. Lieberman and M. Mestchersky
8

---

[10] R. Ditchburn, Proc. Cambr. Phil. Soc. 29, 131 (1933); *Proc. Roy. Soc.* (London) A 141, 169 (1933). R. Tr. fiz. otd. Kharkov State University 2, 65, 73 (1950). Zaichik, Tr. fiz. otd. Kharkov State University 2, 65 73 (1950).

SOVIET PHYSICS JETP VOLUME 3, NUMBER 1 AUGUST, 1956

The Multiplicative Renormalization Group in the Quantum Theory of Fields

N.N.BOGOLIUBOV AND D.V.SHIRKOV
V.A.Steklov Mathematical Institute, Academy of Sciences, USSR

(Submitted to JETP editor, May 20, 1955)
J. Exper. Theoret. Phys. USSR 30, 77-86

We have derived Lee's differential equations for the multiplicative normalization group in the quantum theory of fields. As an example of the application of these equations, the Green's function of spinor electrodynamics has been derived in the regions of the infrared and ultraviolet catastrophes.

1. ONE of the basic problems of present day quantum theory of fields, and, in particular, of quantum electrodynamics, is the question of the behavior of the Green's function when large momenta are involved. It is well known that, in quantum electrodynamics, the expansions of the usual renormalized perturbation theory contain terms of the type $(e^2 \ln|k^2/m^2|)^n$. Due to these terms, the expansions can give the asymptotic behavior only in the region where $e^2 \ln|k^2/m^2| \ll 1$. There arises, therefore, the apparently complicated problem of summing the series of perturbation theories, in order to combine the important terms so as to put the results into the form

$$f(e^2 \ln|k^2/m^2|) + e^2 f_1(e^2 \ln|k^2/m^2|) + \dots, \tag{1}$$

In this, each of the coefficients $f, f_1, \dots f_n \dots$ represents the sum of an infinite number of Feynman diagrams of various orders.

The main term f of a series of the type (1) was found, for the basic Green's function of quantum electrodynamics, by Landau, Abrikosov and Khalatnikov[1] using asymptotic solutions of complicated integral equations which can be obtained by summing a definite class of "main" Feynman diagrams. However, it appears as if the problem of the transformation of the usual expansions of perturbation theory into the form (1), as well as a number of other problems (for example, that of understanding the singularity of the electronic Green's function in the "infrared region" $k^2 \sim m^2$) can be solved directly, without any summations of infinite series, using the renormalizing group of quantum electrodynamics. Attention was first called to the existence of such a group and to its general role in quantum field theory by Stückelberg and Petermann[2]. They also pointed out the possibility of introducing the corresponding infinitesimal operators, and of constructing the differential equations of Lee.

Starting with a different viewpoint, but in essence using the same renormalization group, Gell-Mann and Low[3] obtained concrete results on the behavior of Green's function in the asymptotic region of large momenta.

The purpose of this work is the extension of these ideas, and, in part, the derivation of general formulae for making use of the results of ordinary perturbation theory not only in the case of large momenta, but also in the region of the "infrared catastrophe."

2. In order to formulate clearly the equations describing the renormalization group of quantum electrodynamics, we recall briefly the main points of the procedure[4] for the removal of divergences from the scattering matrix, since the Green's functions can always be represented by this matrix with the help of variational derivatives. As usual, we will start by expanding the scattering matrix in powers of the interaction parameter. The coefficients in such an expansion are the chronological T-products of various numbers of Lagrangians of the interactions. Taking advantage of the arbitrariness implied in the T-products when all the arguments are equal, we can evaluate these products in such a way that taking into account the requirements of unitarity, causality, and covariance, the resulting operator functions are integrable. In order that intermediate steps should not involve actual infinities, we can introduce at this stage a formal regularization, for example, of the Pauli-

---

[1] L.D.Landau, A.A.Abrikosov, and I.M.Khalatnikov, Dokl. Akad. Nauk. SSSR. 95, 497,773, 1177 (1954); 96, 261 (1954).

[2] E.C.Stückelberg and A. Petermann, Helv. Phys. Acta. 26, 499 (1953).

[3] M.Gell-Mann and F.E.Low, Phys. Rev. 95, 1300 (1954).

[4] N.N.Bogoliubov and D.V.Shirkov, Usp. Fiz. Nauk 55, 149 (1955); 57, 3 (1955).

Villars type, which can be removed after the evaluation of the singularities. The recipe obtained for the evaluation of the T-products turns out to be equivalent to the usual subtraction formalism, which, in turn, is equivalent to the introduction into the original interaction Lagrangian of divergent counter terms. As a result of this procedure we get an expansion of the scattering matrix, no term of which contains divergencies. If it is assumed that an expansion of this type is summable, we now have to do with a finite scattering matrix and a finite Green's function. The finite expressions obtained in this way still contain an arbitrariness corresponding to the possibility of introducing (into the Lagrangian) finite counter terms of the same operator structure as the basic diverging counter terms. This arbitrariness, however, can likewise be removed if it be required that the theory describe particles with masses and charges equal to the experimentally known values of m_0 and e_0.

As has already been noticed by Dyson, the transition from the divergent scattering matrix to a finite one by use of subtraction techniques is equivalent (except for the counter term corresponding to intrinsic mass of the electron) to the multiplicative renormalization of the elementary Green's function and of the charge of the electron. A more detailed analysis of Dyson's discussions and their application to the general theory of Green's functions shows that, because of the presence of the counter term

$$^1/_2(Z_3 - 1)(\partial A_n/\partial x_n)^2$$

(which doesn't affect the scattering matrix elements because of the Lorentz conditions on acceptable states, and which is therefore usually thrown away), the subtraction procedure is equivalent to a multiplicative renormalization only when the unperturbed photon source function is chosen to be

$$D^{\mathrm{tr}}_{mn}(k) = \frac{i}{k^2}\left(g^{mn} - \frac{k_m k_n}{k^2}\right), \tag{2}$$

thus satisfying conditions of transversality.

This requirement was not noticed by Gell-Mann and Low, who tried to study the group equations for the Green's function of an electron by using the expression for the Green's function of a photon which is not transverse. As a result they arrived at a contradiction which we will discuss later.

As has already been mentioned, after removal of the infinities of the theory, there still remains a finite arbitrariness. We will now analyze in more detail this arbitrariness, paying special attention to its relation to the multiplicative renormalization of the Green's function and of the charge on the electron.

We will thus consider that, having removed the infinities by using some definite subtraction method, we have obtained finite Green's functions G and D, and the vertex part of Γ. In this case, due to the identity of the mass of the electron with its experimentally observed mass, the counterterm δm is uniquely determined, irrespective of any new multiplicative renormalization. The counterterm Z_3 is completely determined by the requirement that the electronic charge be the same as the experimentally measured e_0. At the same time, the multiplication of the diverging constant Z_3 by the finite factor z_3 leads to a finite renormalization of the charge

$$Z_3 \to Z_3 z_3; \quad e \to z_3^{-1/2} e. \tag{3}$$

Finally, the counterterms Z_1 and Z_2 are found to be determined to within finite constants z_1 and z_2, subject only to the Ward identity

$$Z_1 \to Z_1 z_1; \quad Z_2 \to Z_2 z_2; \quad z_1 = z_2. \tag{4}$$

In view of the fact that changing the counterterm in the investigated situation(2) leads to a new normalization of the Green's function, we arrive at the following set of finite transformation of finite quantities.

$$G_1 \to G_2 = z_2 G_1; \quad \Gamma_1 \to \Gamma_2 = z_1^{-1}\Gamma_1; \quad z_1 = z_2; \tag{5}$$

$$D_1 \to D_2 = z_3 D_1; \quad e_1 \to e_2 = z_3^{-1/2} e_1.$$

The sense of the tranformations (5) is that the use of the quantities Γ_1, G_1, D_1 and e_1, in the theory, leads to the same results as the use of Γ_2, G_2, D_2 and e_2—that is, to a description of particles involving masses and charges equal to their experimental ones. The transformation group (5) represents the "renormalization group" of Stückelberg and Petermann[2], and makes it possible to get simple functional equations for the Green's functions that are similar to those of Gell-Mann and Low.[3]

3. Bearing in mind that such equations can be obtained, let us represent G and D in the form (the vertex part of Γ will be examined separately):

$$G(k) = i\,\frac{a(k^2)\,\hat{k} + b(k^2)\,m}{k^2 - m^2}; \tag{6}$$

$$D_{mn}(k) = \frac{i}{k^2}\left(g^{mn} - \frac{k_m k_n}{k^2}\right) d(k^2). \tag{7}$$

It should be noted that the determination of G

and D involved two arbitrary constants z_2 and z_3 which can be determined by using the following relations:

$$d = 1, \quad a = 1 \quad \text{where } k^2 = \lambda^2, \tag{8}$$

when $\lambda^2 < 0$. The discussion that follows is easily generalized to the case of $\lambda^2 > 0$ where it suffices (due to the complex nature of the functions being studied when $k^2 > 0$) to study only their real parts separately. From considerations of single valuedness in momentum space it follows that a, b, and d have the form $f(k^2/\lambda^2, m^2/\lambda^2, e^2)$, wherefore, upon fixing the momentum λ,

$$a(1, m^2/\lambda^2, e^2) = d(1, m^2/\lambda^2, e^2) = 1. \tag{9}$$

It should be pointed out that the second of the conditions (8) does not appear to be necessary, since, if, for example, $k^2=\lambda^2$, $a=a_0$, then an unimportant multiplying factor will be involved in the following discussions of a_0.

The square of the momentum λ^2 can be directly related to the charge e. Insertion of (7) into the second equation of (5), and using the third equation of (5), we get

$$d(k^2/\lambda_2^2, m^2/\lambda_2^2, e_2^2) = z_3\, d(k^2/\lambda_1^2, m^2/\lambda_1^2, e_1^2), \tag{10}$$

where $e_2^2 = z_3^{-1} e_1^2$.

If we assume that $k^3=\lambda^2$, in (10), we get, from (9)

$$z_3 = d(\lambda_1^2/\lambda_2^2, m^2/\lambda_2^2, e_2^2) \tag{11}$$

from which there follows the functional equation for d

$$d\left(\frac{k^2}{\lambda_1^2}, \frac{m^2}{\lambda_1^2}, e_1^2\right) = \frac{d(k^2/\lambda_2^2, m^2/\lambda_2^2, e_2^2)}{d(\lambda_1^2/\lambda_2^2, m^2/\lambda_2^2, e_2^2)}, \tag{12}$$

in which

$$e_1^2 = e_2^2\, d(\lambda_1^2/\lambda_2^2, m^2/\lambda_2^2, e_2^2). \tag{13}$$

Let us now identify the charge e^2 occurring in Eqs. (12) and (13) with the observed values of the charge e_0^2. In this case the true photon function is normalized at the point $k^2=0$, and so has the form

$$d = d^0(k^2/m^2, e_0^2). \tag{14}$$

We have, consequently,

$$e^2 = e_0^2 d^0(\lambda^2/m^2, e_0^2). \tag{15}$$

Let us now treat the fermion Green's function. We will treat simultaneously the functions a and b, giving them for this purpose a general designation s. Having written down equations for s analogous to (10), and having determined the constant z_2, we get, after eliminating of z_2, the functional equation for s

$$s\left(\frac{k^2}{\lambda_2^2}, \frac{m^2}{\lambda_2^2}, e_2^2\right) = s\left(1, \frac{m^2}{\lambda_2^2}, e_2^2\right) \frac{s(k^2/\lambda_1^2, m^2/\lambda_1^2, e_1^2)}{s(\lambda_2^2/\lambda_1^2, m^2/\lambda_1^2, e_1^2)} \tag{16}$$

4. We now proceed to the solution of the differential equations for d and s. If we make the substitutions $k^2/\lambda_2^2=x$, $m^2/\lambda_2^2=y$, $\lambda_1^2/\lambda_2^2=t$, we can write (12) and (16) in the form

$$e^2 d(x, y, e^2) = e^2 d(t, y, e^2)\, d(x/t, y/t, e^2 d(t, y, e^2)) \tag{17}$$

and

$$\ln s(x, y, e^2) = \ln s(x/t, y/t, e^2 d(t, y, e^2)) + \ln s(t, y, e^2) - \ln s(1, y/t, e^2 d(t, y, e^2)). \tag{18}$$

If we differentiate (17) and (18) with respect to x and then let $t=x$, we get the sought-for Lee equations in the form

$$\frac{\partial e^2 d(x, y, e^2)}{\partial x} = \frac{e^2 d(x, y, e^2)}{x} \times \left[\frac{\partial}{\partial \xi} d\left(\xi, \frac{y}{x}, e^2 d(x, y, e^2)\right)\right]_{\xi=1}; \tag{19}$$

$$\frac{\partial \ln s(x, y, e^2)}{\partial x} = \frac{1}{x} \times \left[\frac{\partial}{\partial \xi} \ln s\left(\xi, \frac{y}{x}, e^2 d(x, y, e^2)\right)\right]_{\xi=}. \tag{20}$$

We now see that to get the functions d and s for all values of their arguments it is sufficient to determine $d(k^2/\lambda^2, y, e^2)$ and $s(k^2/\lambda^2, y, e^2)$ only in the neighborhood of $k^2/\lambda^2 \sim 1$ for which one can use usual perturbation theory.

The equations obtained illustrate the fact that due to the renormalization group it is possible to vary the scale of momenta, at the same time changing the charge.

We now notice that actually we have only to solve equation (19), since, for a given d, the expression for s can be obtained from (20) by simple quadrature:

$$\frac{s(x, y, e^2)}{s(x_0, y, e^2)} = \int_{x_0}^{x} \frac{dz}{z}\left[\frac{\partial}{\partial \xi} \ln s\left(\xi, \frac{y}{z} e^2 d(z, y, e^2)\right)\right]_{\xi=1}. \tag{21}$$

The charge e^2 appearing here is related to the experimental charge e_0^2 by the expression

$$e^2 d(k^2/\lambda^2, m^2/\lambda^2, e^2) = e_0^2 d^0(k^2/m^2, e_0^2),$$

which makes it possible to consider e^2 as a function of λ.

We now make use of the general group equations that we have obtained, for the region of large impulses: $|m^2/k^2| \ll 1$. When we set $\lambda^2 \sim k^2$, we see that in the given region the expression

$$e_\lambda^2 d(k^2/\lambda^2, e_\lambda^2) \equiv e_\lambda^2 d(k^2/\lambda^2, 0, e_\lambda^2) \tag{22}$$

when $k^2 < 0$ asymptotically approaches $e_0^2 d^0(k^2/m^2, e_0^2)$. From the other side (22) is identically equal to $e_m^2 d(k^2/m^2, e_m^2)$. For this reason, letting d_{as}^0 indicate the asymptotic part of the function d^0, we have everywhere:

$$e_0^2 d_{\text{ac}}^0(k^2/m^2, e_0^2) = e^2 d(k^2/m^2, e^2),$$

where $e^2 = e_m^2 = e_0^2 d_{as}^0(1, e_0^2)$. In exactly the same way, we can convince ourselves that the expression $s(k^2/m^2, e^2)$ is the asymptotic form of the functions to within an unimportant constant multiplier.

Thus, to get the asymptotic form of the functions in question we can insert into our equations (19), (21) $x = |k^2/m^2|$ and eliminate y. We then obtain:

$$\frac{\partial e^2 d(x, e^2)}{\partial x} = \frac{e^2 d(x, e^2)}{x} \varphi\{e^2 d(x, e^2)\}, \tag{23}$$

where

$$\varphi(e^2) = \left[\frac{\partial}{\partial \xi} d(\xi, e^2)\right]_{\xi=1} \tag{24}$$

and, moreover

$$\ln \frac{s(x, e^2)}{s(x_0, e^2)} = \int_{x_0}^{x} \frac{dz}{z}\left[\frac{\partial}{\partial \xi} \ln s(\xi, e^2 d)\right]_{\xi=1}. \tag{25}$$

Integrating the differential equation (23) by the usual method of separation of variables, we come to the equation obtained by Gell-Mann and Low.[3]

$$\int_{e^2}^{e^2 d} \frac{dz}{z\varphi(z)} = \ln x. \tag{26}$$

Furthermore, introducing into the integral (25) a new variable $e^2 d$ for z, we find on the basis of (23) an equation for the determination of s in the form

$$\ln \frac{s(x, e^2)}{s(x_0, e^2)} = \int_{e^2 d(x_0)}^{e^2 d(x)} \frac{dz}{z\varphi(z)}\left[\frac{\partial}{\partial \xi} \ln s(\xi, z)\right]_{\xi=1}. \tag{27}$$

We now make a series of observations about the Gell-Mann-Low equation in the form (26). First, it is obvious that in order to use this equation for the actual determination of d, it is necessary to have an expression for the function $\varphi(z)$. It is not hard to get such an expression with the help of perturbation theory.

We have, in fact

$$d^{-1}(\xi, e^2) = 1 - \frac{e^2}{3\pi} \ln \xi - \frac{e^4}{4\pi^2} \ln \xi + \ldots$$

and, therefore, on the basis of (24)

$$\frac{1}{\varphi(z)} = \frac{3\pi}{z}\left\{1 - \frac{3z}{4\pi} + a_1 z^2 + \ldots\right\}. \tag{28}$$

Next, it is not hard to conclude, from equation (26) that the magnitude of $e^2 d(x)$ cannot remain small for all values of x. Actually, for small z

$$1/\varphi(z) < (3\pi/z)(1 + c),$$

where c is a constant. For this reason, as long as $e^2 d$ is small, we will have:

$$\ln x < 3\pi(1 + c)\int_{e^2}^{e^2 d} \frac{dz}{z^2} < 3\pi(1 + c)\int_{e^2}^{\infty} \frac{dz}{z^2} = \frac{3\pi(1 + c)}{e^2}$$

and then the corresponding possible values of $|k^2|$ are bounded.

It should be pointed out that the argument of the function φ is the square of the charge. Because of this, in order to understand the behavior of the Green's function at extremely high momenta, when $e^2 d$ becomes of the order of unity and larger, it is necessary to examine the region of large charges (strong forces). In this connection it should be emphasized that the structure of $\varphi(z)$ here cannot be established on the basis of an analysis of a finite number of terms of an expansion of the type of (28). It would appear as if the region of such momenta is unimportant practically, since it is hardly to be expected that electrodynamics, as we know it, ignoring as it does heavy particles, is any good at energies of the order of $me^{137/2}$.

However, as is correctly pointed out by Gell-Mann and Low, the study of this region is an interesting mathematical problem, which might be useful in the construction of future theories. For example, if, as a result of more detailed investigations, it should turn out that

$$\int\limits_{e^2}^{\infty} \frac{dz}{z\varphi(z)} < \infty,$$

then the hypothesis of Landau and Pomeranchuk concerning the essential incompleteness of present day electrodynamics would be confirmed. This follows since

$$\ln\left|\frac{k^2}{m^2}\right| < \int\limits_{e^2}^{\infty} \frac{dz}{z\varphi(z)},$$

and the possible values of $|k^2|$ are therefore bounded, which is contrary to the assumption that the theory is local.

Since at present we do not have any other information about the behavior of the function $\varphi(z)$ than the expansion (28), it is necessary to restrict ourselves to momenta for which

$$(e^2/3\pi)\ln|k^2/m^2| < 1. \tag{29}$$

In this region a very simple expression for d can be obtained* from relations (26) and (28).

We emphasize that even the general problem of the construction of the renormalized usual expansion for d in the form (1) in the case where (29) holds can be solved directly. In fact, setting (28) into (26) we find

$$1 - d^{\ 1} + \frac{3}{4\pi}e^2\ln d^{-1} + a_1e^4(d-1) + \ldots = \frac{e^2}{3\pi}\ln x,$$

from which we immediately get the sought-for expansion:

$$d^{-1}(x, e^2) = 1 - \frac{e^2}{3\pi}\ln x + \frac{3}{4\pi}e^2\ln\left(1 - \frac{e^2}{3\pi}\ln x\right) + e^4\ldots \tag{30}$$

Completely analogously we can get an expansion of the type (1) for the asymptotic form of the function $s=a,b$ which determines the electronic Green's function. For this it is only necessary to make use of our equation (27) and usual perturbation theory formulae:

$$a(x, e^2) = 1 + ce^4\ln x + \cdots \tag{31}$$

$$b(x, e^2) = b_1\left\{1 - \frac{3e^2}{4\pi}\ln x + \frac{e^4}{\pi^2}(\alpha_1\ln^2 x + \alpha_2\ln x) + \cdots\right\},$$

where c, b_1, α_1, α_2 are numerical coefficients.

We have:

$$\left[\frac{\partial}{\partial\xi}\ln a(\xi, z)\right]_{\xi=1} = cz^2 + \cdots, \left[\frac{\partial}{\partial\xi}\ln b(\xi, z)\right]_{\xi=1} = -\frac{3z}{4\pi} + \alpha_2\frac{z^2}{\pi^2} + \cdots$$

Inserting these expansions, together with (28) into equation (27), we will find that

$$\ln a(x, e^2) = e^2 3\pi c(d-1) + \cdots; \tag{32}$$

$$\ln\frac{b(x, e^2)}{b(1, e^2)} = \frac{9}{4}\ln d^{-1} + e^2\frac{3}{\pi}\left(\alpha_2 + \frac{9}{16}\right)(d-1) + \cdots$$

In order to get expressions of the type (1) for the functions a,b, it remains only to use d from equation (30).

If we restrict ourselves to the main terms, we get the formulae of Landau et al[1].

We emphasize that the formulae (31) have been obtained from perturbation theory using only the transverse source function of the photon (2). It is easy to see that if we use, instead of (2), the usual coupling

$$D^c_{mn} = ig^{mn}/k^2,$$

we arrive, in (32) at relations not agreeing with the true asymptotic behavior (1) for this situation. As we have mentioned, this contradiction was reached by Gell-Mann and Low who worked with the usual photon couplings.

As we see, the method used here does not require summation over infinite systems of Feynman diagrams. In order to determine the series (1) through members of order e^{2n} it is sufficient to have for the functions d,a,b, being investigated, only formulae of the usual renormalized perturbation theory to an accuracy of order e^{2n+2}. Their conversion into form (1) is merely an algebraic operation.

---

* Comment in proof: Landau[5] has used this case to obtain corrections to the formula for d derived in Ref. 1.

[5] L. D. Landau, Nils Bohr and the Development of Physics, London, 1955, p. 52.

All these remarks have been on the use of the general Lee equations of renormalized groups that we have obtained for the purpose of constructing the asymptotic parts of the Green's function for large impulses. We emphasize that the meaning of these equations is not at all limited by such a use.

For example, let us examine the region $k^2 \sim m^2$ in which the electronic Green's function has a singularity. Since d here is regular, we are interested only in the functions $s=a,b$. It will be convenient to express them in the form

$$s\left(\frac{k^2}{\lambda^2}, \frac{m^2}{\lambda^2}, e^2\right) = S\left(\frac{k^2-m^2}{\lambda^2-m^2}, \frac{\lambda^2-m^2}{m^2}, e^2\right). \tag{33}$$

Let us now return to equation (21) and set $y=1$. Then, using the representation (33) we will get:

$$\ln\frac{s(k^2/m^2, e^2)}{s(k_0^2/m^2, e^2)} = \int\limits_{k_0^2/m^2}^{k^2/m^2} \frac{dx}{x-1}\left[\frac{\partial}{\partial\xi}\ln S(\xi, x-1, e^2 d(x, 1, e^2))\right]_{\xi=1}. \tag{34}$$

The interval of integration has to be taken as indicated in order not to fall into the pole x-1=0. For this reason we set $k^2/m^2>1$, $k_0^2/m^2>1$ or $k^2/m^2<1$, $k_0^2/m^2<1$. In order to use in practice, the relation (34) for the determination of s, we see that it is necessary to know the function $S(\xi,x\text{-}1,e^2)$ only in the infinitesimally small region of the point $\xi \equiv (k^2\text{-}m^2)/(\lambda^2\text{-}m^2)=1$, which is its "point of normalization". For this reason, in order to obtain the part of (34) in square brackets, we again use perterbation theory formulae.

Taking the second approximation:

$$A(\xi, y, e^2) = 1 - \frac{3e^2}{2\pi}\left(\frac{\ln \xi y}{1+\xi y} - \frac{\ln y}{1+y}\right) + \ldots;$$

$$B(\xi, y, e^2) = 1 - \frac{3e^2}{2\pi}\left(\frac{2+\xi y}{1+2\xi y}\ln \xi y - \frac{\ln y}{1+y}\right) + \ldots;$$

$$e^2 d(x, 1, e^2) = e^2 + \ldots,$$

we find

$$\left[\frac{\partial}{\partial\xi}\ln A(\xi, x-1, e^2 d)\right]_{\xi=1} = \frac{3e^2}{2\pi}\left[\frac{(x-1)\ln|x-1|}{x^2} - \frac{1}{x}\right] + \ldots;$$

$$\left[\frac{\partial}{\partial\xi}\ln B(\xi, x-1, e^2 d)\right]_{\xi=1} = \frac{3e^2}{4\pi}\left[\frac{(x-1)\ln|x-1|}{x^2} - \frac{x+1}{x}\right] + \ldots,$$

and from (34) we get

$$\frac{a(x, 1, e^2)}{a(x_0, 1, e^2)} \sim (|x-1|)^{-3e^2/2\pi x}(|x_0-1|)^{-3e^2/2\pi x_0};$$

$$\frac{b(x, 1, e^2)}{b(x_0, 1, e^2)} \sim (|x-1|)^{-(3e^2/4\pi)(1+x)/x} \times (|x_0-1|)^{(3e^2/4\pi)(1+x_0)/x_0}.$$

From this we see that the functions a,b, near $k^2 \sim m^2$ have the well known "infrared singularity."

$$a \sim a_0\left(\left|1-\frac{k^2}{m^2}\right|\right)^{-3e^2/2\pi}; \qquad b \sim b_0\left(\left|1-\frac{k^2}{m^2}\right|\right)^{-3e^2/2\pi}. \tag{35}$$

Such a behavior for these functions actually follows directly from (34). Indeed the main part of the integral on the right side of this equation in the region of interest will be:

$$\alpha(e^2)\ln\left|1-\frac{k^2}{m^2}\right|$$

and, for this reason, the main part of the function s will be

$$C\left|1-\frac{k^2}{m^2}\right|^{\alpha(e^2)}; C = \text{const.} \tag{36}$$

We have seen that second order perturbation theory gives for the exponent $\alpha(e^2)$ the value $-3e^2/2\pi$.

We now make some remarks on vertex parts. Let us take for example, the vertex value of Γ with two electron lines and one photon line. The transformation law for Γ in the multiplicative renormalization group, as is well known, will be

$$\Gamma \to \Gamma' = z_2^{-1}\Gamma, \tag{37}$$

whereupon

$$a' = z_2 a. \tag{38}$$

From the other side, under our "λ-normalization", the Γ function, from considerations of single valuedness in momentum space must have the form

$$\Gamma_\lambda = \Gamma\left(\frac{k}{\lambda}, \frac{k-q}{\lambda}, \frac{m}{\lambda}, e_\lambda^2\right).$$

We find, then, from (37) and (38)

$$\Gamma\left(\frac{k}{\lambda_2}, \frac{k-q}{\lambda_2}, \frac{m}{\lambda_2}, e_{\lambda_2}^2\right) \tag{39}$$

$$= \frac{a\,(1, m^2/\lambda_1^2, e_{\lambda_1}^2)}{a\,(\lambda_1^2/\lambda_2^2, m^2/\lambda_2^2, e_{\lambda_2}^2)}\,\Gamma\left(\frac{k}{\lambda_1}, \frac{k-q}{\lambda_1}, \frac{m}{\lambda_1}, e_{\lambda_1}^2\right),$$

in which

$$e_{\lambda_1}^2 = e_{\lambda_2}^2\, d\,(\lambda_1^2/\lambda_2^2,\ m^2/\lambda_2^2,\ e_{\lambda_2}^2).$$

If here we take λ_1^2, to be of the order of the larger of the quantities $|k^2|$, $|(k-q)^2|$, $|q^2|$, we can, using these formulae, study the behavior of Γ for arbitrary values of $k, k-q, q$ as the largest of the quantities $|k^2/m^2|$, $|(k-q)^2/m^2|$, $|q^2/m^2|$ gets to be of the order of unity.

We note, in conclusion, that the method of renormalization groups that we have presented can be carried over likewise into meson theories also. For example, let us consider the neutral pseudoscalar theory.

We set:

$$G = \frac{a\hat{p} + bm}{p^2 - m^2},\quad D = \frac{d}{p^2 - \mu^2},\quad \Gamma^5(p, p) = \gamma^5\Gamma,$$

where m, μ are the experimental masses of the nucleon and meson. With these designations the renormalization group will be (if we neglect some difficulties connected with the introduction of a direct meson-meson interaction, arising from the presence of the known four vertex part):**

$$a \to a' = z_2 a,\quad b \to b' = z_2 b, \tag{40}$$

$$\Gamma \to \Gamma' = z_2^{-1}\Gamma,$$

$$d \to d' = z_3 d,\quad g^2 \to g'^2 = g^2 (z_1 z_2^{-1})^2 z_3^{-1}.$$

It is convenient, further, to introduce the function

$$\delta = d \cdot a^2 \cdot \Gamma^2, \tag{41}$$

for which

$$g'^2 \delta' = g^2 \delta. \tag{42}$$

We now make use of λ-normalization, and set $d=1, \delta=1$ for $p^2=\lambda^2$. Then, drawing on considerations of single valuedness in momentum space, we note that all functions being studied will depend only on the arguments

$$p^2/\lambda^2,\quad m^2/\lambda^2,\quad \mu^2/\lambda^2,\quad g^2.$$

For this reason, we get from (40) and (41):

$$\delta\left(\frac{k^2}{\lambda_1^2}, \frac{m^2}{\lambda_1^2}, \frac{\mu^2}{\lambda_1^2}, g_1^2\right) = \frac{\delta\,(k^2/\lambda_2^2, m^2/\lambda_2^2, \mu^2/\lambda_2^2, g_2^2)}{\delta\,(\lambda_1^2/\lambda_2^2, m^2/\lambda_2^2, \mu^2/\lambda_2^2, g_2^2)}; \tag{43}$$

$$g_1^2 = g_2^2\,\delta\,(\lambda_1^2/\lambda_2^2,\ m^2/\lambda_2^2,\ \mu^2/\lambda_2^2,\ g_2^2);$$

$$s\left(\frac{k^2}{\lambda_2^2}, \frac{m^2}{\lambda_2^2}, \frac{\mu^2}{\lambda_2^2}, g_2^2\right) = s\left(1, \frac{m^2}{\lambda_2^2}, \frac{\mu^2}{\lambda_2^2}, g_2^2\right) \frac{s\,(k^2/\lambda_1^2, m^2/\lambda_1^2, \mu^2/\lambda_1^2, g_1^2)}{s\,(\lambda_2^2/\lambda_1^2, m^2/\lambda_1^2, \mu^2/\lambda_1^2, g_1^2)},$$

where $s = a, b, \Gamma, d$.

Hence, arguing as before, we get the general Lee equations in the form

---

** Remark in Proof. An investigation of the renormalization group in meson theory taking into account direct meson-meson interactions has recently been carried out by one of the authors.[6]

[6] D.V.Shirkov, Dokl. Akad. Nauk. SSSR, 105, 972 (1955).

$$\frac{\partial}{\partial x}\left(g^2\delta(x, y, z, g^2)\right) = \frac{g^2\delta(x, y, z, e^2)}{x}\left[\frac{\partial}{\partial\xi}\delta\left(\xi, \frac{y}{x}, \frac{z}{x}, g^2\delta\right)\right]_{\xi=1}, \tag{44}$$

$$\frac{\partial}{\partial x}\left[\ln s(x, y, z, g^2)\right] = \frac{1}{x}\left[\frac{\partial}{\partial\xi}\ln s\left(\xi, \frac{y}{x}, \frac{z}{x}, g^2\delta\right)\right]_{\xi=1}.$$

In the region of high momenta, when $|k^2/m^2| \gg 1$, $|k^2/\mu^2| \gg 1$, equations (44) can be simplified, just as in the case of electrodynamics, by setting $x = |k^2/m^2|$ and discarding y and z.

We then obtain:

$$\int_{g^2}^{g^2\delta}\frac{dt}{t\varphi(t)} = \ln x; \quad \varphi(t) = \left[\frac{\partial}{\partial\xi}\delta(\xi, t)\right]_{\xi=1};$$

$$\ln\frac{s(x, g^2)}{s(x_0, g^2)} = \int_{e^2 d(x_0, g^2)}^{e^2 d(x, g^2)}\frac{dt}{t\varphi(t)}\left[\frac{\partial}{\partial\xi}\ln s(\xi, t)\right]_{\xi=1},$$

into which we can introduce perturbation theory formulae. Completely analogous equations can be written for charge symmetrical theories.

Translated by A. Turkevich
11

SOVIET PHYSICS JETP VOLUME 3, NUMBER 1 AUGUST, 1956

Vertex Parts at Very High Energies in Quantum Electrodynamics

V. V. SUDAKOV

(Submitted to JETP editor Nov. 4, 1954)
J. Exper. Theoret. Phys. USSR 30, 87-95 (January 1956)

A method is developed for calculating Feynman integrals with logarithmic accuracy, working to any order of perturbation theory. The method is applied to calculate the vertex part in quantum electrodynamics for a certain range of values of the momenta. The result is displayed as the sum of a perturbation series.

THE technique of Feynman[1] for calculating matrix elements in quantum electrodynamics is only suitable for the lowest-order approximations, since the algebraic complexities increase extremely rapidly when we consider contributions to the matrix element from higher-order perturbations. When perturbation theory is not applicable and it is necessary to consider the sum of the entire perturbation series[*], another technique must be developed. For example, one elegent method[3] of calculating integrals with logarithmic accuracy depends on changing k_0 into ik_0. This method is, however, not applicable to all cases. In particular, it is inapplicable to the calculation of the vertex part $\Gamma_\sigma(p, q; l)$ in the case when the absolute value of the square of one of the vectors p, q, l is much larger than the absolute squares of the other two vectors. This case is especially important for concrete physical applications. There appear in this case terms with the structure $e^2L_1L_2$, a product of two big logarithms entering with each power of e^2 (we call these doubly-logarithmic terms). But the earlier method[3] can give only terms with the structure e^2L (singly-logarithmic terms), in which one large logarithm enters with each power of e^2.

1. To explain the method[+] of obtaining the doubly-logarithmic terms, we shall consider as an example the integral[*]

$$I = \lim_{\varepsilon \to +0} \frac{d^4k}{[(p-k)^2 - m^2 + i\varepsilon]\,[(q-k)^2 - m^2 + i\varepsilon]\,(k^2 + i\varepsilon)}. \tag{1}$$

In what follows we shall everywhere omit the limiting process, simply choosing ϵ to be a positive number so small that it does not make any contribution in the final result. We shall evaluate (1) supposing that

$$|l^2| \gg |p^2|,\ |q^2|, \tag{2}$$

where $l = p - q$. For simplicity we assume

$$|p^2|,\ |q^2| \gg m^2, \tag{3}$$

which allows us to omit m^2 in the first two factors of the denominator in (1).

From (2) it follows that to a close approximation $l^2 = -2pq$, which allows us to rewrite (2) in the form

$$|pq| \gg |p^2|,\ |q^2|. \tag{2a}$$

Hence it is clear that the squares of the vectors p, q are very small compared with the squares of their components; the squares of the vectors p, q are almost null.

---

[*] We do not need to worry about the divergence of the perturbation series,[2] which occurs at much higher energies than those which we consider.

[1] R. P. Feynman, Phys. Rev. 76, 769 (1949)

[2] F. J. Dyson, Phys. Rev. 85, 631 (1952).

[3] L. D. Landau, A. A. Abrikosov and I. M. Khalatnikov, Dokl. Akad. Nauk. SSSR 95, 497, 773, 1177 and 96, 261 (1954).

[+] In this paper the Feynman notations are used:

$$pq = p_0q_0 - PQ = p_0q_0 - p_1q_1 - p_2q_2 - p_3q_3,$$

$$d^4k = (2\pi)^{-2}\, dk_0\, dk_1\, dk_2\, dk_3.$$

[*] The integral (1) is singular. To define it precisely we have to specify the Feynman rules for integrating round the poles. This is done by adding infinitesimal imaginary terms to the factors in the denominator.

It is very useful, and appropriate to the nature of the problem, to introduce variables u, v, x, in terms of which the vector k takes the form

$$k = k_{\parallel} + k_{\perp} = up + vq + k_{\perp}; \quad k_{\perp}^2 = -x. \tag{4}$$

The vector $k_{\perp}$ is perpendicular to p and q, while $k_{\parallel}$ lies in the plane of p and q. When the inequality (2) holds, the time-axis can be chosen to lie in the plane of p and q. Therefore the vector $k_{\perp}$ is spacelike, and the variable x takes only positive values $x > 0$.

A rigorous argument (see Appendix 1) shows that the region in which doubly-logarithmic terms appear is limited by the inequalities

$$|q^2/l^2| \ll |u| \ll 1, \quad |p^2/l^2| \ll |v| \ll 1, \tag{5}$$

$$x \ll \min[\,|l^2u|,\ |l^2v|\,].$$

In this region the integrand, written in terms of the new variables, simplifies considerably, and the integral (1) takes the form

$$I = -\frac{1}{8\pi\,|l^2|}\int \frac{du}{u}\,\frac{dv}{v}\,\frac{dx}{x + l^2uv - i\varepsilon}. \tag{6}$$

In (6) we carry out the integration with respect to x,

$$\int\limits_0^{\min[|l^2u|\ |l^2v|]} \frac{dx}{x + l^2uv - i\varepsilon} = \ln\min\left[\frac{1}{|v|},\ \frac{1}{|u|}\right] + \frac{i\pi}{2}\,[1 - \operatorname{sign}(l^2uv)].$$

The first term vanishes after integration with respect to u or v, and the second gives

$$I = (i/4l^2)\ln|l^2/p^2|\ln|l^2/q^2|. \tag{7}$$

It is to be noted that only the imaginary part of the result of the x-integration is significant, and this imaginary part is different from zero and equal to $i\pi$ only when

$$l^2uv < 0. \tag{8}$$

In the more complicated problem considered below, we carry out the integrations in the same order; after the x- integration we obtain an imaginary result, with the range of the subsequent u and v integrations limited by the same inequality (8).

We may define the region determined by the inequalities (5) as the region in which the integrand is logarithmically maximal. As we see from (6), the integrand is in fact triply-logarithmic in this region. But various parts of the range of integration almost compensate each other. One of the logarithmic integrations gives an imaginary result of the order of unity instead of a large logarithm.

2. We calculate the vertex part $\Gamma_{\sigma}(p,\ q;\ l)$ in the region of values of the momenta defined by the inequalities (2), (3). In second-order perturbation theory it is given by the integral

$$\Gamma_{\sigma}^{(2)}(p,q;l) = \frac{e^2}{\pi i} \times \int \frac{\gamma_{\mu}(\hat{p}-\hat{k})\gamma_{\sigma}(\hat{q}-\hat{k})\gamma_{\mu}\,d^4k}{[(p-k)^2+i\varepsilon]\,[(q-k)^2+i\varepsilon]\,[k^2+i\varepsilon]}. \tag{9}$$

The numerator may be expressed in terms of the new variables in the form

$$\gamma_{\mu}(\hat{p}-\hat{k})\gamma_{\sigma}(\hat{q}-\hat{k})\gamma_{\mu} = \gamma_{\mu}[\hat{p}(1-u) - v\hat{q} - \hat{k}_{\perp}] \times \gamma_{\sigma}[\hat{q}(1-v) - u\hat{p} - \hat{k}_{\perp}]\gamma_{\mu}. \tag{10}$$

We average over the direction of the vector $k_{\perp}$. Terms linear in $k_{\perp}$ then vanish, while the quadratic term becomes

$$\hat{k}_{\perp}\gamma_{\sigma}\hat{k}_{\perp} = {}^1/{}_2\,k_{\perp}^2\,\delta_{\perp\lambda\rho}\gamma_{\lambda}\gamma_{\sigma}\gamma_{\rho} = -{}^1/{}_2\,x\delta_{\perp\lambda\rho}\gamma_{\lambda}\gamma_{\sigma}\gamma_{\rho}. \tag{11}$$

Here $\delta_{\perp\lambda\rho}$ is a symmetric matrix defined by

$$\delta_{\perp\lambda\rho}\,p_{\rho} = \delta_{\perp\lambda\rho}\,q_{\rho} = 0, \quad \delta_{\perp\lambda\rho}\,k_{\perp\rho} = k_{\perp\lambda}. \tag{12}$$

We are not interested in obtaining an explicit representation of $\delta_{\perp\lambda\rho}$. It will be enough for our purposes to know that the eigenvalues of the matrix $\delta_{\perp\lambda\rho}$ are 0 and 1 according to (12), so that the matrix is of the order of magnitude unity. Substituting (11) into (10) we obtain

$$\gamma_{\mu}[\hat{p}(1-u) - v\hat{q}]\gamma_{\sigma}[\hat{q}(1-v) - u\hat{p}]\gamma_{\mu} - {}^1/{}_2\,x\delta_{\perp\lambda\rho}\gamma_{\mu}\gamma_{\lambda}\gamma_{\sigma}\gamma_{\rho}\gamma_{\mu}. \tag{13}$$

In the region of momenta defined by the inequalities (5), all terms other than the term $\gamma_\mu p \gamma_\sigma \bar{q} \gamma_\mu$ are negligible, since the presence of the small factors u, v, (x/l^2) converts one of the integrations from logarithmic to non-logarithmic. Consequently all such terms are singly-logarithmic and represent small corrections to the main term. As is well-known, the term with k^2 in the numerator contains a logarithmic divergence which is removed by renormalization, the remainder after renormalization being singly-logarithmic. Since we are neglecting such terms, the process of renormalization can for our purposes be reduced to the following simple rules: (1) all singly-logarithmic terms are dropped, whether they are convergent or divergent; (2) the symbol e denotes the renormalized experimental charge.

We consider the only surviving term in (13), namely

$$\gamma_\mu \hat{p} \gamma_\sigma \hat{q} \gamma_\mu. \tag{14}$$

The operator $\Gamma_\sigma(p, q; l)$ always appears in diagrams with an electron Green's function on either side,

$$G(p)\,\Gamma_\sigma(p, q; l)\,G(q). \tag{15}$$

Now for $p^2 >> m^2$, $G(p)$ takes the form $(\hat{p}/p^2)$. The operator (14), with the numerators of the Green's functions on each side, becomes

$$\hat{p} \gamma_\mu \hat{p} \gamma_\sigma \hat{q} \gamma_\mu \hat{q}. \tag{16}$$

When the operators are commuted by the usual rules, (16) may be written in the form

$$-p^2 \gamma_\mu \gamma_\sigma \hat{q} \gamma_\mu \hat{q} - 2q^2 \hat{p} \gamma_\sigma \hat{p} + 4pq\,\hat{p} \gamma_\sigma \hat{q}. \tag{17}$$

We mentioned earlier that p and q are vectors with large components but with small lengths. Therefore the terms containing p^2 and q^2 explicitly are negligible, and (17) can be replaced to a good approximation by its last term

$$\hat{p} \gamma_\mu \hat{p} \gamma_\sigma \hat{q} \gamma_\mu \hat{q} \rightarrow 4pq\,\hat{p} \gamma_\sigma \hat{q} = -2l^2 \hat{p} \gamma_\sigma \hat{q}. \tag{18}$$

The original operator (14) thus becomes

$$\gamma_\mu \hat{p} \gamma_\sigma \hat{q} \gamma_\mu = 4pq\gamma_\sigma = -2l^2 \gamma_\sigma. \tag{19}$$

Therefore

$$\Gamma_\sigma^{(2)}(p, q; l) = -\frac{2e^2 l^2}{\pi i} \gamma_\sigma \times \int \frac{d^4 k}{[(p-k)^2 + i\varepsilon]\,[(q-k)^2 + i\varepsilon]\,[k^2 + i\varepsilon]}, \tag{20}$$

and so Eq. (7) gives

$$\Gamma_\sigma^{(2)}(p, q; l) = -(e^2/2\pi) \times \ln|l^2/p^2| \ln|l^2/q^2| \gamma_\sigma. \tag{21}$$

We now carry out the calculation of $\Gamma_\sigma(p, q; l)$ in the (2n)'th order of perturbation theory. Using the method described in Appendix 2, one can verify that the terms with the greatest number of large logarithmic factors, i. e. terms of the type $e^2 L_1 L_2$, are precisely those in which all the virtual photon lines overlap the point of emission of the external photon l. The general term of this type in the (2n)'th order contribution to $\Gamma_\sigma(p, q; l)$ is

$$\begin{aligned}
&\left(\frac{e^2}{\pi i}\right)^n \int \frac{\gamma_{\mu_1}(\hat{p}-\hat{k}_1)\gamma_{\mu_2}(\hat{p}-\hat{k}_1-\hat{k}_2)\ldots\gamma_{\mu_n}\left(\hat{p}-\sum_1^n \hat{k}_i\right)\gamma_\sigma}{[(p-k_1)^2+i\varepsilon]\,[(p-k_1-k_2)^2+i\varepsilon]\ldots\left[\left(p-\sum_1^n k_i\right)^2+i\varepsilon\right]} \\
&\times \frac{\left(\hat{q}-\sum_1^n \hat{k}_i\right)\gamma_{\mu_{i_n}}\left(\hat{q}-\sum_1^n \hat{k}_i+\hat{k}_{i_n}\right)\gamma_{\mu_{i_{n-1}}}}{\left[\left(q-\sum_1^n k_i\right)^2+i\varepsilon\right]\left[\left(q-\sum_1^n k_i+k_{i_n}\right)^2+i\varepsilon\right]} \\
&\times \frac{\left(\hat{q}-\sum_1^n \hat{k}_i+\hat{k}_{i_n}+\hat{k}_{i_{n-1}}\right)\gamma_{\mu_{i_{n-2}}}\ldots(\hat{q}-\hat{k}_{i_1})\gamma_{\mu_{i_1}}}{\left[\left(q-\sum_1^n k_i+k_{i_n}+k_{i_{n-1}}\right)^2+i\varepsilon\right]\ldots[(q-k_{i_1})^2+i\varepsilon]} \\
&\times \frac{d^4 k_1}{k_1^2+i\varepsilon}\,\frac{d^4 k_2}{k_2^2+i\varepsilon}\ldots\frac{d^4 k_n}{k_n^2+i\varepsilon}.
\end{aligned} \tag{22}$$

Here $i_1, i_2, \ldots, i_n$ is a permutation of the integers 1, 2, ..., n. When $i_1, i_2, \ldots, i_n = 1, 2, \ldots, n$, we have the so-called "ladder diagram" in which the virtual photon lines do not intersect. For all other permutations $i_1, \ldots, i_n$, some of the photon lines will intersect.

Just as in the calculation of the second-order contribution, all the $\hat{k}_i$ may be dropped from the numerator of the integrand. Any term containing even a single $\hat{k}_1$ gives rise to a lower power of the large logarithm and is therefore a small correction to the main term. After dropping the $\hat{k}_i$, the operator remaining in the numerator is

$$\gamma_{\mu_1}\hat{p}\gamma_{\mu_2}\hat{p}\ldots\gamma_{\mu_n}\hat{p}\gamma_\sigma\hat{q}\gamma_{\mu_{i_n}}\hat{q}\gamma_{\mu_{i_{n-1}}}\hat{q}\ldots\hat{q}\gamma_{\mu_{i_1}}. \tag{23}$$

As in the step from (14) to (16), we multiply (23) on each side by operators arising from electron Green's functions, and we commute the operators $\hat{p}$ with γ_{μ_i} and $\hat{q}$ with $\gamma_{\mu_{ik}}$, dropping the small terms in which p^2 or q^2 appears explicitely. After removing the $\hat{p}$ and $\hat{q}$ which belong to the electron Green's functions, we obtain the approximate equation

$$\gamma_{\mu_1}\hat{p}\gamma_{\mu_2}\hat{p}\ldots\gamma_{\mu_n}\hat{p}\gamma_\sigma\hat{q}\gamma_{\mu_{i_n}}\hat{q}\gamma_{\mu_{i_{n-1}}}\hat{q}\ldots\hat{q}\gamma_{\mu_{i_1}} = (4pq)^n\gamma_\sigma = (-2l^2)^n\gamma_\sigma. \tag{24}$$

Equation (22) then takes the form

$$\gamma_\sigma\left(-\frac{2e^2l^2}{\pi i}\right)^n \times \int[(p-k_1)^2+i\varepsilon]^{-1}[(p-k_1-k_2)^2+i\varepsilon]^{-1} \ldots \left[\left(p-\sum_1^n k_i\right)^2+i\varepsilon\right]^{-1} \times \left[\left(q-\sum_1^n k_i\right)^2+i\varepsilon\right]^{-1} \times\left[\left(q-\sum_1^n k_1+k_{i_n}\right)^2+i\varepsilon\right]^{-1}\ldots[(q-k_{i_1})^2+i\varepsilon]^{-1} \times\frac{d^4k_1}{k_1^2+i\varepsilon}\frac{d^4k_2}{k_2^2+i\varepsilon}\cdots\frac{d^4k_n}{k_n^2+i\varepsilon}. \tag{25}$$

To evaluate (25), we introduce the variables u_i, v_i, x_i, which we used in the derivation of Eq. (7). As we remarked in connection with the integral (1), the region which gives doubly-logarithmic terms is limited by the inequalities (5) for each triad of variables u_i, v_i, x_i. The important region is in fact even smaller, and its true limits will be determined below.

By analogy with the derivation of (7), we shall suppose that $k_{\perp i}$ may be neglected in every factor of the denominator except k_i^2. This can be justified by an exact argument. In fact all our estimates reduce to the determination of the region in which the integral is logarithmically maximal.

We first integrate with respect to x_i, keeping only the imaginary part of the result. This gives

$$\int\frac{dx_i}{k_i^2+i\varepsilon}\rightarrow\begin{cases}-\pi i & l^2u_iv_i<0\\ 0 & l^2u_iv_i>0.\end{cases} \tag{26}$$

It remains to integrate with respect to u_i and v_i the integral

$$\gamma_\sigma\left[\frac{e^2}{4\pi}\operatorname{sign}(l^2)\right]\int\frac{du_1}{u_1}\frac{du_2}{u_1+u_2}\cdots\frac{du_n}{u_1+u_2+\cdots+u_n} \times\frac{dv_{i_n}}{v_{i_n}+v_{i_{n-1}}+\cdots+v_{i_1}} \times\frac{dv_{i_{n-1}}}{v_{i_{n-1}}+\cdots+v_{i_1}}\cdots\frac{dv_{i_1}}{v_{i_1}}. \tag{27}$$

All the integrations give a logarithm only in the ranges

$$|u_1|\ll|u_2|\ll\cdots\ll|u_n|, \qquad |v_{i_1}|\ll|v_{i_2}|\ll\cdots\ll|v_{i_n}|. \tag{28}$$

Taking (28) together with (5) for each variable, we obtain

$$\begin{aligned}|q^2/l^2|&\ll|u_1|\ll|u_2|\ll\ldots\ll|u_n|\ll 1,\\ |p^2/l^2|&\ll|v_{i_1}|\ll|v_{i_2}|\ll\ldots\ll|v_{i_n}|\ll 1.\end{aligned} \tag{29}$$

Using (29) with (26), we can write down immediately the value of (22),

$$\gamma_\sigma\frac{1}{(n!)^2}\left(-\frac{e^2}{2\pi}\ln\left|\frac{l^2}{p^2}\right|\ln\left|\frac{l^2}{q^2}\right|\right)^n. \tag{30}$$

The result is identical for all diagrams of the type under consideration. The existence of diagrams with intersecting virtual photon lines makes invalid the replacement of the summation of the perturbation series by an integral equation[3]. Therefore in our case the integral equation derived by Landau et al.[3] is incorrect.

The number of relevent diagrams in the (2n)'th order is equal to (n!) (the number of permutations $i_1, i_2, \ldots, i_n$). We can now sum the contributions from these diagrams over all values of n, and obtain

$$\begin{aligned}\Gamma_\sigma(p, q; l) &= \gamma_\sigma \sum_{n=1}^{\infty} \frac{1}{n!}\left(-\frac{e^2}{2\pi}\ln\left|\frac{l^2}{p^2}\right|\ln\left|\frac{l^2}{q^2}\right|\right)^n \\ &= \gamma_\sigma \exp\left\{-\frac{e^2}{2\pi}\ln\left|\frac{l^2}{p^2}\right|\ln\left|\frac{l^2}{q^2}\right|\right\}.\end{aligned} \tag{31}$$

This expression for $\Gamma_\sigma(p, q; l)$ may be regarded as the scattering matrix element of a bound electron by an external field or by a virtual photon. Equation (31) shows that the probability of such a scattering tends to zero as $|l^2|$ tends to infinity. Processes in which a large number of real photons are simultaneously emitted[4] will occur with much greater probability. The method developed in the present paper is in no way limited to the problem here considered.

In conclusion I express my thanks to Academician L. D. Landau and Professor I. Ia. Pomeranchuk for suggesting the problem and for their constant attention, and to A. A. Abrikosov for many valuable comments.

APPENDIX

1. For the purpose of calculating integrals with logarithmic accuracy, it is advantageous to introduce instead of the vectors p, q the pair p', q' given by

$$p' = p - \alpha_2 q, \quad q' = q - \alpha_1 p, \tag{A1}$$

with α_1, α_2 chosen so that the squares of p' and q' are rigorously zero. Since the squares of p and q are "almost" zero, α_1 and α_2 are small quantities. With high accuracy we may write

$$\alpha_1 = q^2/2pq = -q^2/l^2, \tag{A2}$$

$$\alpha_2 = p^2/2pq = -p^2/l^2.$$

Since α_1, α_2 are small, the transformation (A1) can be inverted to give

$$p = p' + \alpha_2 q', \quad q = q' + \alpha_1 p'. \tag{A3}$$

We resolve the vector $k_{||}$ along p' and q' and obtain

$$k_{||} = u'p' + v'q'. \tag{A4}$$

In terms of the new variables, the integral (1) becomes

$$I = \frac{|l^2|}{8\pi}\int \frac{1}{[l^2(1-u')(v'-\alpha_2) - x + i\varepsilon]} \times \frac{du'dv'dx'}{[l^2(1-v')(u'-\alpha_1) - x + i\varepsilon][-l^2u'v' - x + i\varepsilon]}. \tag{A5}$$

The advantage of the variables u', v' lies in the fact that according to (A5) the factors of the denominator are linear in each of u' and v'. This considerably simplifies the investigation of the region in which u', v' take very small or large values. It is especially easy to find the region in which the integrand is logarithmically maximal in terms of the variables u', v'; the upper bounds of the inequalities (5) are thus obtained immediately.

We calculate the integral (A5), integrating with respect to u' from $-\infty$ to $+\infty$, then with respect to x, and finally with respect to v'. The u' integration can be converted into a closed contour in the complex u' plane by the addition of a semi-circle of infinite radius either above or below the real axis; the integral then reduces to a sum of residues at the poles of the integrand. If the coefficients of u' in the three factors of the denominator have the same sign, then the closed contour encloses either all three poles or none at all. In either case the integral vanishes. To prove this we need only consider the second case. The sum of the three residues is proportional to the coefficient of u'^{-1} in the expansion of the integrand in negative powers of u', and this expansion obviously begins with a term in u'^{-3}.

Therefore the limits of the integration with respect to u' are given by

$$\min[0, \alpha_2] < v < 1. \tag{A6}$$

We can easily ascertain that the region $|v'| \sim |\alpha_2|$ does not give a doubly-logarithmic contribution. In the region $|\alpha_2| \ll v' \leq 1$, the expression obtained after the u'- integration takes the form

---

[4] A. A. Abrikosov, J. Exper. Theoret. Phys. USSR **30**, 96 (1956); Soviet Phys. JETP **3**, 71 (1956)

$$I = \frac{i}{4} \int\limits_{v' \gg |\alpha_2|}^{1} \frac{(1-v')\,dv'\,dx}{[l^2 v'(1-v') - x]\,[x + \alpha_1 l^2 v'(1-v')]}. \tag{A7}$$

The value of the elementary integral (A7) coincides with Eq, (7), as was to be expected. The important region in the integral (A7) is limited by the inequalities

$$|\alpha_1 l^2 v'| \ll x \ll |l^2 v'|, \quad |\alpha_2| \ll v' \ll 1. \tag{A8}$$

We can now simplify the expression (A5) by using the condition $|v'| \ll 1$ at an earlier stage. We may also limit u' by the condition $|u'| \ll 1$. Consequently we can now carry through the whole calculation with the simplified integral

$$\frac{i|l^2|}{8\pi} \int [l^2(v' - \alpha_2) - x + i\varepsilon]^{-1} \tag{A9}$$

$$\times\ [l^2(u' - \alpha_1) - x + i\varepsilon]^{-1} \frac{du'\,dv'\,dx}{[-l^2u'v' - x + i\varepsilon]}.$$

We retained the x in all terms of (A9); if the u'-integration is now performed first, the condition $x \ll |v'|$ follows automatically, and also the condition $v' > 0$. Because of the symmetry of the integral (A9), we could equally well begin with the v'-integration, thus obtaining another upper bound to the important range for x $(x \ll |u'|)$, and fixing the sign of u' $(u' > 0)$. Therefore, so far as doubly-logarithmic terms are concerned, the integral (A9) supplemented by the conditions

$$|u'|,\ |v'| \ll 1, \tag{A10}$$

is equivalent to the integral (A7). The most symmetrical way of evaluating (A9) is to integrate first with respect to x between the limits $0 < x \ll |l^2 u'|, |l^2 v'|$, which allow us to retain x only in the last factor of the denominator. The neglect of the other poles is equivalent to dropping a part of the integrand which vanishes after further integration.

The calculation has been carried out with the same accuracy as the derivation of Eq. (7), with this difference, that we have not excluded from the beginning the region $|u'| \sim |\alpha_1|$, $|v'| \sim |\alpha_2|$, but have verified that this region is unimportant. In this region the variables u, v, can differ greatly from u', v'; so even if the contribution from the region can be easily estimated in terms of the variables u', v', the same is by no means true of the variables u, v. For practical calculations, however, it is more convenient to use the variables u, v, limiting the range of the variables beforehand to the region (15).

2. The same method can be applied to calculate terms of order $e^2 L$, when they are the largest nonvanishing terms*. This situation arises in the calculation of $\Gamma_\sigma(p,\ q;\ l)$ by second-order perturbation theory, when $|p^2| \gg |q^2|$ and $|l^2| \gg m^2$.

As the simplest example which shows how to reformulate the method, we shall calculate an integral which differs from (A5) by an extra factor v'^m in the numerator, m being a positive integer. The integrations with respect to u' and x are completely unchanged; the integral with respect to v' ceases to be logarithmic and is to be taken between the precise limits $0 < v' < 1$. The integral which we shall calculate is

$$I[k_\mu,\ k_\mu k_\nu] \tag{A11}$$

$$= \int \frac{[k_\mu,\ k_\mu k_\nu]\,d^4k}{[(p-k)^2 + i\varepsilon]\,[(q-k)^2 + i\varepsilon]\,[k^2 + i\varepsilon]}$$

assuming the inequalities (2), (3) to hold. In the region $|k^2| \ll |l^2|$, the integral (A11) is equal to

$$\frac{i}{4l^2} \int\limits_{|q^2/l^2|}^{1} \frac{du}{u} \int\limits_{|p^2/l^2|}^{1} \frac{dv}{v}\, [k_{\parallel\mu},\ k_{\parallel\mu} k_{\parallel\nu}], \tag{A12}$$

where it is understood that the vector $k_\parallel$ is written in the form $up + vq$, and that after integration only the highest (first) power of the logarithm is to be retained. For the integral $I[k_\mu]$ this is the only important region. For $I[k_\mu k_\nu]$ the region $|k^2| \gg |l^2|$ is also important; the integral diverges logarithmically for large k and is made finite only by being cut off for $|k^2| > \lambda^2$. In the region $|l^2| \ll |k^2| \ll \lambda^2$ the integral (A11) takes the form

$$\int \frac{[0,\ k_\mu k_\nu]\,d^4k}{[k^2 + i\varepsilon]^3},$$

or, after averaging over the direction of k,

$$\int \frac{[0,\ {}^1\!/_4\,\delta_{\mu\nu}]\,d^4k}{[k^2 + i\varepsilon]^2}.$$

---

[*] The error in the evaluation of terms of order $e^2 L_1 L_2$, due to the uncertainty in the limits of the logarithmic integrals, is of the same order of magnitude as the terms of order $e^2 L$.

The last integral is evaluated[3] by changing k_0 into ik_0, and has the value

$$(i/16)\,[0, \delta_{\mu\nu}]\ln(\lambda^2/|l^2|). \tag{A13}$$

The results we have obtained can be immediately applied to the evaluation of the second-order contribution to $\Gamma_\sigma(p, q; l)$ in the case $|p^2| \gg |q^2|$, $|l^2| \gg m^2$. For this we need only introduce variables u, v, defined by

$$k = q(1-u) + lv + k_\perp. \tag{A14}$$

It is clearly advantageous to decompose $k_\parallel$ into vectors whose squares are small. The variables u, v are defined in such a way that the main part of the logarithmic integral comes from small u and v. After some elementary algebra, we obtain the result

$$\Gamma_\sigma(p, q; l) = \frac{e^2}{4\pi p}\left[\hat{l}\gamma_\sigma\hat{l}\ln\left|\frac{p^2}{l^2}\right|\right. \tag{A15}$$

$$\left. - \hat{q}\gamma_\sigma\hat{q}\ln\left|\frac{p^2}{q}\right| - \hat{q}\gamma_\sigma\hat{l}\ln\left|\frac{p^2}{q^2}\right|\right] + \frac{e^2}{4\pi}\gamma_\sigma\ln\frac{\lambda^2}{p^2}.$$

In this case no doubly-logarithmic terms appear.

Translated by F. J. Dyson
12

SOVIET PHYSICS JETP VOLUME 3, NUMBER 1 AUGUST, 1956

The Infrared Catastrophe in Quantum Electrodynamics

A. A. ABRIKOSOV
Institute for Physical Problems, Academy of Sciences, USSR

(Submitted to JETP editor, October 28, 1954)
J. Exper. Theoret. Phys. USSR 30, 96-108 (January, 1956)

The infrared catastrophe is investigated by summing over diagrams. Expressions are obtained for $G(p)$ when $e^2/\pi \ln m^2/(p^2 - m^2) \gtrsim 1$ and for $\Gamma_\mu(p, q; l)$ when $p \cdot q \gg p^2 - m^2$, $q^2 - m^2$. The problem of radiation of additional quanta during the scattering of an electron of arbitrary energy by an external field is considered.

IT is well known that the calculation of matrix elements of processes in quantum electrodynamics leads to infinities having various origins. Some of the infinities, which appear as a result of the divergence of integrals for large energies of virtual quanta and pairs, originate, as has already been pointed out[1], from an incorrect description of the interaction by means of the δ-function. In addition to these infinities (which are considered in references 1-4) there are also others, which result from integration over virtual quanta with k^2 close to zero, whenever the diagram under consideration includes a free electron with $p^2 = m^2$. This situation always occurs for matrix elements of real processes and has been named the infrared catastrophe. It is related to the fact that the very concept of a free line is a convention.

Actually, as shown by many authors[5], every process is accompanied by the radiation of a large number of low-energy quanta. For this reason, a properly formulated problem must take account of the possibility of such radiation with frequencies up to some maximum ω_{max}, corresponding to the fact that a real experimental apparatus always has a limited sensitivity to small changes in the energy of particles taking part in the process.

---

[1] L. D. Landau, A. A. Abrikosov and I. M. Khalatnikov, Dokl. Akad. Nauk SSSR 95, 497 (1954).

[2] L. D. Landau, A. A. Abrikosov and I. M. Khalatnikov, Dokl. Akad. Nauk SSSR 95, 773 (1954).

[3] L. D. Landau, A. A. Abrikosov and I. M. Khalatnikov, Dokl. Akad. Nauk SSSR 95, 1177 (1954)

[4] L. D. Landau, A. A. Abrikosov and I. M. Khalatnikov, Dokl. Akad. Nauk SSSR 96, 261 (1954).

[5] A. I. Akhiezer and V. B. Berestetskii, *Quantum Electrodynamics* GTTI (1953).

In practical calculations one usually uses the following device. One introduces a quantity $\lambda_{\min}$, which serves as a fictitious photon mass. Then when we integrate over the momentum of the virtual photon the divergent result is replaced by a value proportional to $\ln(m/\lambda_{\min})$. Next, one considers the same process, but replaces the virtual quantum by a real quantum (a process of the next higher order, in the preceeding approximation). It is not difficult to see that the cross section for the new process will be of the same order as the change in the first process which resulted from the introduction of the virtual quantum. We integrate over the momentum of the real quantum up to frequency $\omega_{\max}$, so that we again introduce the fictitious $\lambda_{\min}$. When we combine the new cross section with the correction to the old cross section, the terms in $\ln\lambda_{\min}$ cancel.

Such a procedure is completely valid for low energy processes and for large limiting frequencies $\omega_{\max}$. As we shall see later, the necessary conditions for applicability of this procedure are:

$$(e^2/\pi)\ln(m/\omega_{\max}) \ll 1 \quad \text{for} \quad E \lesssim m,$$

$$(e^2/\pi)\ln^2(E/m),$$

$$(e^2/\pi)\ln(m/\omega_{\max})\ln(E/m) \ll 1 \quad \text{for} \quad E \gg m,$$

where E is the order of magnitude of the energy of the process. When these conditions are violated, the procedure is invalid since, on the one hand, it becomes possible actually to radiate a large number of real quanta, and on the other hand virtual processes of arbitrary order begin to play an important role. The purpose of the present work is to investigate this question in general. In doing this, we shall here limit ourselves to considering the scattering of an electron by an external field. However, in principle, the results obtained are also applicable to other processes. In addition to the infrared catastrophe and the question of the radiation of soft quanta, we shall also consider the radiation of hard quanta during high energy scattering.

1. GREEN'S FUNCTION OF AN ELECTRON FOR $p^2 \approx m^2$

In reference 2 a calculation was made of the Green's function $G(p)$ and the vertex part $\Gamma_\mu(p, q; l)$ in the appropriate region. However, it is not hard to see that this calculation of $G(p)$ and Γ_μ applied only for $p^2 \gg m^2$. For the case where p^2 is so close to m^2 that $e^2/\pi \ln m^2/(p^2 - m^2) \gtrsim 1$, the calculation given in reference 2 is invalid. Since this region is directly related to the problem in which we are interested, we shall calculate $G(p)$ and the corresponding Γ_μ for this case.

The equations for Γ_μ and $G(p)$ are given in reference 1, Eq. (1.4). In solving them we can no longer (as was done in references 1,2) carry out a transition in the integrals to a four-dimensional Euclidean space by means of the substitution $k_0 \to ik_0$, since the vector p is essentially timelike. But for just this reason we can achieve this by the substitution $k_m \to -ik_m$ $(m = 1, 2, 3)$.

Let us consider the integral in the equation for $G(p)$. The region of integration where $k^2 \gg m^2$ gives a result already known from reference 2, and is of no special interest when $p^2 \approx m^2$. But now there is a new region which gives rise to a logarithmic integral. This is the region $p^2 - m^2 \ll (p-k)^2 - m^2 \ll m^2$.

For the case where $p^2 \approx m^2$, we shall try to find a $G(p)$ of the form

$$G(p) = \beta(m^2)\,\nu\left(\frac{m^2}{p^2 - m^2}\right)\frac{\hat{p} + m}{p^2 - m^2}, \tag{1}$$

where β was defined in reference 2, and ν is an unknown slowly varying function.

As for $\Gamma_\alpha(p, p-l; l)$, we make use of the fact that the Γ_μ always appears, in the cases which we need, with the factor $\hat{p} + m$ preceeding and following it (in the region of interest to us, $l^2 \ll m^2$, so that $\hat{p} \approx \hat{q}$), so we shall determine it up to terms which give a small contribution when bracketed in this way.

We shall show that $\Gamma_\sigma(p, p-l; l)$ should be of the form

$$(\hat{p} + m)\Gamma_\sigma(p, p-l, l)(\hat{p} + m) = \tag{2}$$
$$(\hat{p} + m)\gamma_\sigma(\hat{p} + m)\,\alpha(m^2)\,\mu\left(\frac{m^2}{(p-l)^2 - m^2}\right),$$

where μ is a slowly varying function. In fact, looking at the integral in the equation for Γ_σ, we see that the region of integration $k^2 \gg m$ together with the term γ_σ in the equation gives us the known result $\gamma_\sigma\alpha(m^2)$. In this way all the terms in the equation can be absorbed into $\alpha(m^2)$. But a logarithmic integral is obtained not only from this region but also from the region $q^2 - m^2 \ll (p-k)^2 - m^2 \ll m^2$. Here we can neglect k compared to m and, since $k^2 \ll m^2$, we can replace d_l and d_t by d_l^0 and $d_t^0 = 1$.

From the spinor factors appearing in the numerator of the integral we easily obtain

$$(\hat{p}+m)\gamma_\mu(\hat{p}-\hat{k}+m) \tag{3}$$

$$\times\ \gamma_\sigma(\hat{p}-\hat{l}-\hat{k}+m)\gamma_\nu(\hat{p}+m)$$

$$\approx 4\,p_\mu p_\nu(\hat{p}+m)\gamma_\sigma(\hat{p}+m).$$

The form of the spinor agrees with that assumed in (2). Furthermore it is easy to see that, except for the the rapidly varying part $D_{\mu\nu}$, the integrand depends only on the projection of k along the direction of p ($(p-k)^2 - m^2 \approx -2k \cdot p$). Because of this we can integrate over the other components of k.

Going over to a Euclidean space we obtain, as in reference 2, the relation (in our case $d^4k = (2\pi)^{-2}\, dk_0\, dk_1\, dk_2\, dk_3$),

$$d^4k \to (i/\pi)\, dk_p \mathrm{K}^2 d\,|\mathrm{K}|, \tag{4}$$

where the vector $\mathbf{K}$ is perpendicular to k_p.

Resolving the k which appears in $D_{\mu\nu}$ along k_p and $\mathbf{K}$, integrating over $\mathbf{K}$ and making a change of variables, we obtain for $\mu(\eta)$ the equation

$$\mu(\eta) = 1 - \frac{e^2}{2\pi}(3d_t^0 - d_l^0)\int_0^\eta \mu^3(z)\,\nu^2(z)\,dz, \tag{5}$$

where $\eta = \ln (m^2/[(p-l)^2 - m^2])$. In integrating over $\mathbf{K}$ we considered only those terms which give a logarithmic integral with respect to k_p. In addition we assumed that changing the sign of $q^2 - m^2$ in μ has no essential effect on its magnitude (as will be evident from the result). Equation (5) confirms the correctness of the form assumed for Γ_σ in Eq. (2).

We now look at the integral in the equation for $G(p)$[1,4] in the interesting region where $p^2 - m^2 \ll (p-k)^2 - m^2 \ll m^2$. It is not hard to show that the integral in this region is of order $\int k^{-3} d^4k$ so that, as in reference 2, we must include contributions to $G(p-k)$ and to Γ_μ in the integral of order $(p^2 - m^2)/[(p-k)^2 - m^2]$. The correction to $G(p)$ is obtained simply by expanding the denominator of formula (1) for $G(p-k)$. The correction to Γ_μ is gotten from the equation for Γ_μ, given in reference 1, Eq. (1). In the present case the important range in the integral in the equation for Γ_μ is $p^2 - m^2 \ll (p-k)^2 - m^2 \ll (p-l)^2 - m^2$. In this region the integral is of order $\int k^{-3}\, dk$, and therefore, as is easily seen, the main terms are those of order $(p^2 - m^2)/[(p-k)^2 - m^2]$ in the first $G(p-k)$ and the first $\Gamma_\mu(p, p-k; k)$. The corrections to the other terms in Γ and G are unimportant.

The correction to Γ_μ should be of the form

$$(\hat{p}+m)\,\Gamma\;(p, p-l; l)(\hat{p}+m) \tag{6}$$

$$= \alpha(m^2)(\hat{p}+m)\gamma_\mu(\hat{p}+m)$$

$$\times \frac{p^2 - m^2}{(p-l)^2 - m^2}\,\delta[p^2 - m^2,\ (p-l)^2 - m^2].$$

Substituting in the equation for Γ_μ, we get an equation for δ:

$$\delta(\xi, \eta) = -\frac{e^2}{2\pi}(3d_t^0 - d_l^0)\,\nu(\eta)\,\mu^2(\eta) \tag{7}$$

$$\times \int_\eta^\xi [-\mu(z) + \delta(\xi, z)]\,\nu(z)\,dz.$$

Now substituting the corrections to G and Γ_μ in the equation for G and using previous results[2,4], we obtain an equation for ν:

$$\frac{1}{\nu(\xi)} = 1 + \frac{e^2}{2\pi}(3d_t^0 - d_l^0) \tag{8}$$

$$\times \int_0^\xi [-\mu(z) + \delta(\xi, z)]\,\nu(z)\,dz.$$

Equations (5), (7), (8), enable us to determine μ and ν. However there is no need to solve them directly. Actually, according to Ward's theorem[6], the relation:

$$\mu(\eta)\,\nu(\eta) = 1 \tag{9}$$

must hold. But then Eq. (5) gives us the function $\mu(\eta)$ in the form:

$$\mu(\eta) = \exp[-(e^2/2\pi)(3d_t^0 - d_l^0)\,\eta]. \tag{10}$$

The solution of equation (7) also presents no difficulties, and leads to the following form for $\delta(\xi, \eta)$:

$$\delta(\xi, \eta)/\mu(\eta) \tag{11}$$

$$= 1 - \exp\{(e^2/2\pi)(3d_t^0 - d_l^0)(\eta - \xi)\}.$$

Substituting this in equation (8), which can be written in the form $1/\nu(\xi) = 1 - \delta(\xi, 0)$, we get

---

[6] J. Ward, Phys. Rev. 78, 182 (1950).

$$\nu(\xi) = \exp\left[(e^2/2\pi)(3d_t^0 - d_l^0)\xi\right]. \tag{12}$$

This formula satisfies (9), as required.*

2. THE VERTEX PART WHEN $p \cdot q \gg p^2 - m^2$, $q^2 - m^2$.

In the preceding section we have already calculated one of the vertex parts of the type of interest to us here, namely $\Gamma_\mu(p,q;l)$ for $p^2 \approx m^2$, $q^2 \approx m^2$, $l^2 \ll m^2$. The other type of vertex -- $\Gamma_\mu(p,q;l)$ for $l^2 \gg p^2$, q^2, $p^2 \gg m^2$, $q^2 \gg m^2$, was found in a paper by Sudakov.[7] Here we consider the general case, making no restrictions on the vectors other than $p \cdot q \gg p^2 - m^2$, $q^2 - m^2$. As before, we shall sum only over the principal terms, i.e., those containing the maximum logarithmic terms in e^2. In particular, we shall not include terms of order $e^2 \ln(l^2/m^2)$. For convenience of presentation, we shall use the symbols $p^2 - m^2 = 2m\Delta m_1$ and $q^2 - m^2 = 2m\Delta m_2$.

In the integrals representing the successive approximations to the vertex part, there are parts which include an integration over momenta of virtual quanta greater than the norms of the real momenta (in our case l^2 and m^2) which appear in the vertex part. If we separate this part in each of the integrals, it is not hard to see that together with the free term, the part containing only integrals over this region gives $\gamma_\mu \alpha(l^2)$ (just as in reference 2). In each of the remaining integrals, it turns out that the integration over $k \gg l$ (or m) must, if we neglect small terms, be carried out along a line lying closer to the principal vertex than that for the integrals with $k \ll l$ (or m). All this leads to the result that in the successive approximations for Γ_μ, we can integrate only over $k \ll l$ (or m), and take account of the integrals over the other region by a factor $\alpha(l)^2$ common to all terms, which determines the dependence of the integral on the "cutoff" limit. The dependence on l^2 given by this factor is unimportant in our case since, as we shall see later, there are terms in Γ_μ of order $[e^2 \ln^2(l^2/m^2)]^n$, which are much greater than the terms arising from $\alpha(l^2)$ which are of order $[e^2 \ln(l^2/m^2)]^n$. Because of this, we can always take $\alpha(l^2) \approx \alpha(m^2)$. In calculating the integrals for $k \ll l$, we use a method similar to that developed in the paper of Sudakov[7]. The principal part of the integral is gotten by resolving k along p, q, and in the plane perpendicular to these vectors. In integrating over the last component we must take the residue for $k^2 = 0$. Thus the additional vertex parts from the virtual quanta will be of the type considered in the preceding section, and each factor $\alpha(m^2)\mu$ from such a vertex will cancel against the factor $\beta(m^2)\nu$ from the factor G which is placed next to this Γ on the side toward the fundamental vertex. So, in calculating the vertex parts which we need, we can use the zeroth order result from neighboring Γ's and G's.

To make clear what the region of integration is, we shall first consider Γ_μ in first approximation. We begin with the part containing $d_t k^{-2} \delta_{\mu\nu}$. It has the the well-known form

$$\frac{e^2}{\pi i} \int \frac{\gamma_\mu (\hat{p} - \hat{k} + m)\gamma_\sigma(\hat{q} - \hat{k} + m)\gamma_\mu d_t(k^2)\, d^4k}{[(p-k)^2 - m^2][(q-k)^2 - m^2]\, k^2} \tag{13}$$

We introduce variables u, v, x:

$$k = p\left(\frac{a^2u - av}{a^2 - 1}\right) + q\left(\frac{a^2v - au}{a^2 - 1}\right) + k_\perp, \tag{14}$$
$$x = -k_\perp^2, \quad a = (pq)/m^2.$$

In terms of these variables, the volume element in k-space is

$$d^4k = (m^2/4\pi)\, a^2 (a^2 - 1)^{-1/2}\, dx\,du\,dv. \tag{15}$$

Expressed in terms of these variables, the important expressions which appear in the denominators are equal to

$$\begin{aligned} k^2 &= m^2a^2(a^2-1)^{-1}(2auv - u^2 - v^2) - x, \\ (p-k)^2 - m^2 &= 2m\Delta m_1 - 2(pq)v + k^2, \\ (q-k)^2 - m^2 &= 2m\Delta m_2 - 2(pq)u + k^2. \end{aligned} \tag{16}$$

Since x is positive (integration region $0 - \infty$), u and v must be chosen so that the point $k^2 = 0$ corresponds to $x > 0$. This requires that $2auv - u^2 - v^2 > 0$. We shall take $a > 0$, $a^2 - 1 > 0$. The contrary case is treated similarly, or even more simply by analytic continuation. Thus the integration must extend over the region between the two lines

$$\begin{aligned} u_1 &= v\left(a + \sqrt{a^2 - 1}\right), \\ u_2 &= v\left(a - \sqrt{a^2 - 1}\right) = v / \left(a + \sqrt{a^2 - 1}\right). \end{aligned} \tag{17}$$

---

* The product $\mu(\eta)\nu(\eta)$ does not depend on $p^2 - m^2$, so that at first glance it seems that the infrared catastrophe does not occur. Actually, the scattering matrix element contains terms in the exponent of order $\frac{e^2}{\pi}\frac{l^2}{m^2} \times \ln\frac{m^2}{p^2 - m^2}$ whose determination goes beyond the accuracy of this section. (cf. later sections).

[7] V. V. Sudakov, J. Exper. Theoret. Phys. USSR 30, 87, (1956). Soviet Phys. JETP 3, 65 (1956).

In addition it is clear from Eq. (16) that u and v are limited by the conditions

$$\Delta m_1/a \ll |v| \ll 1, \tag{18}$$

$$\Delta m_2/a \ll |u| \ll 1.$$

The limit from above corresponds to the condition $k \ll l$. It is not hard to see that integration over positive and negative regions of u and v which satisfy our conditions gives the same contribution, and can be replaced by twice the integral over $u > 0$, $v > 0$. In the numerator, because of the smallness of u, v, and x, we can drop the k. When we bracket Γ on the left and right with $(\hat{p} + m)$ and $(\hat{q} + m)$ we get the expression $4\, p\cdot q(\hat{p} + m)\gamma_\sigma \times (\hat{q} + m)$ in the numerator.

We introduce the variables $\lambda = -\ln v$, $\mu = -\ln u$. In terms of these variables, the region of integration will have a form like that shown in Fig.1 (the cross-hatched part). Of course, other relations between $\ln a$, $\ln(m/\Delta m_1)$ and $\ln(m/\Delta m_2)$ are possible. The integral will be proportional to the area cross-hatched in Fig. 1.

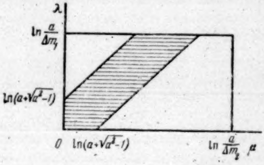

FIG. 1

We shall not yet give the corresponding expression, but will first consider the term in $(d_l - d_t)$ This term has the form

$$\frac{e^2}{\pi i}\int \frac{\hat{k}(\hat{p}-\hat{k}+m)\gamma_\sigma(\hat{q}-\hat{k}+m)\hat{k}[d_l(k^2)-d_t(k^2)]}{[(p-k)^2-m^2][(q-k)^2-m^2]k^4}\,d^4k\,. \tag{19}$$

If we introduce in this integral the same variables as in (13), then the conditions (18) still hold. Then we can once more neglect $\hat{k}$ compared with $\hat{p}$ and $\hat{q}$ in the numerator, and upon multiplying on the left and right by $(\hat{p} + m)$ and $(\hat{q} + m)$ the numerator takes the form $4\, p\cdot k q\cdot k\, (\hat{p} + m)\gamma_\sigma(\hat{q} + m)$. Since the principal terms in square brackets of the expression in the denominator give the product $4\; p\cdot k q\cdot k$, upon cancelling these factors in numerator and denominator, we get in place of (19) the much simpler integral $\int k^{-4}d^4k$.

If we express this integral in terms of u, v, and x, it turns out that once more the important region in the integral is that in which $k^2 = 0$, but unlike what we had before, now both $k^2_{||}$ and x go to zero. As a result, the integral becomes proportional to the sum of the integrals $\int u^{-1}du$ (or, what is the same thing $\int v^{-1}dv$) taken along the two lines bounding the cross-hatched region of the type shown in Fig. 1. The particular form of the integral depends on the relation between Δm_1, Δm_2, and a.

Finally we obtain for the first approximation $\Gamma_\mu^{(1)}(p,q;l)$ the following formula:

$$(\hat{p} + m)\Gamma_\mu^{(1)}(p, q; l)(\hat{q} + m)$$

$$= (\hat{p} + m)\gamma_\mu(\hat{q} + m)(-f),$$

where the function f has the form:

$$f = (e^2/2\pi)\{a(a^2-1)^{-1/2} \times ({}^3/_2\eta^2 + 2\zeta\xi_1) + (1 - d_l^0)\xi_1\} \tag{20a}$$

for $\xi_1 > 0, \quad \xi_2 > \xi_1 + \eta;$

$$f = (e^2/2\pi)\{a(a^2-1)^{-1/2}[\eta^2 + \zeta(\xi_1 + \xi_2) - {}^1/_2(\xi_1 - \xi_2)^2] + {}^1/_2(1 - d_l^0)(\xi_1 + \xi_2)\} \tag{20b}$$

for $\xi_1 > 0, \quad \xi_2 > 0, \quad \xi_1 + \eta > \xi_2 > \xi_1 - \eta;$

$$f = (e^2/2\pi)({}^3/_2\eta^2 + 2\eta\xi_1 + {}^1/_2\xi_1^2) \tag{20c}$$

for $-\eta < \xi_1 < 0, \quad \xi_2 > \xi_1 + \eta;$

$$f = (e^2/2\pi)[\eta^2 + \eta(\xi_1 + \xi_2) + \xi_1\xi_2 - {}^1/_2\xi_2^2] \tag{20d}$$

for $-\eta < \xi_1 < 0, \quad 0 < \xi_2 < \xi_1 + \eta;$

$$f = (e^2/2\pi)(\eta + \xi_1)(\eta + \xi_2) \tag{20e}$$

for $-\eta < \xi_1 < 0, \quad -\eta < \xi_2 < 0,$

where $\xi_1 = \ln(m/\Delta m_1), \quad \xi_2 = \ln(m/\Delta m_2),$

$\eta = \ln a, \ \zeta = \ln(a + \sqrt{a^2 - 1}).$

In all these terms, except those of the type $\zeta\xi$ in (20a) and (20b), we have taken $\zeta \approx \eta$, since taking account of their difference would go beyond our accuracy. For the same reason, the equations (20c), (20d) and (20e) should be taken for $a \gg 1$, and terms with one ξ or one η should be neglected.

We shall now assume that we are considering the n'th approximation for Γ_μ. In the corresponding diagram, n arbitrarily intersecting virtual lines can occur. We consider first the numerator of any diagram of this type. Upon multiplying on the left by $(\hat{p}+m)$ and on the right by $(\hat{q}+m)$ it will have the form

$$(\hat{p}+m)\gamma_\mu(\hat{p}+m)\gamma_\nu\ldots(\hat{p}+m)\gamma_\sigma(\hat{q}+m)\ldots\gamma_\xi(\hat{q}+m)\gamma_\eta(\hat{q}+m) \tag{21}$$
$$\approx 2^{2n}p_\mu p_\nu\ldots q_\xi q_\eta\ldots(\hat{p}+m)\gamma_\sigma(\hat{q}+m).$$

Throughout all of this we have neglected $\hat{k}$ compared to $\hat{p}$ and $\hat{q}$, and the quantities $p^2 - m^2$ and $q^2 - m^2$ compared to $p_\mu q_\nu$. From formula (21) it is clear that the numerators of all diagrams of the same order are equal to one another. Differences can occur only in the denominators.

First we consider diagrams with a pair of lines. There can only be two such: one with parallel and one with intersecting lines. The integrand in both diagrams will be proportional to

$$\{(pk_1)[(pk_1)+(pk_2)][(qk_1)+(qk_2)](qk_1)\}^{-1}$$
$$+\{(pk_1)[(pk_1)+(pk_2)][(qk_1)+(qk_2)](qk_2)\}^{-1}.$$

The integral with maximum degree of logarithmic divergence is obtained from the first term when $p\cdot k_2 \gg p\cdot k_1$, $q\cdot k_2 \gg q\cdot k_1$ and from the second if $p\cdot k_2 \gg p\cdot k_1$, $q\cdot k_1 \gg q\cdot k_2$ The expressions from both terms are the same, and so the integrations over $q\cdot k_1$ and $q\cdot k_2$ are independent. If we now make the change of variables $k_1 \rightleftarrows k_2$, and take half the sum of the expression thus obtained and the old expression, it turns out that $p\cdot k_1$ and $p\cdot k_2$ are also independent. Since the regions of integration are the same for both k's, we get the simple result

$$(\hat{p}+m)\Gamma_\mu^{(2)}(\hat{q}+m) \tag{22}$$
$$=(\hat{p}+m)\gamma_\mu(\hat{q}+m)(-f)^2/2.$$

Generalizing this to a diagram of n'th order, we have

$$(\hat{p}+m)\Gamma_\mu^{(n)}(\hat{q}+m) \tag{23}$$
$$=(\hat{p}+m)\gamma_\mu(\hat{q}+m)(-f)^n/n!$$

Summing all expressions of this type and noting, as pointed out at the beginning of this section, that the integrals over the momenta of virtual quanta in the region $k \gg l$ give a common factor $\alpha(m^2)$, we find the following result;

$$(\hat{p}+m)\Gamma_\mu(p,q;l)(\hat{q}+m) \tag{24}$$
$$=\alpha(m^2)(\hat{p}+m)\gamma_\mu(\hat{q}+m)e^{-f}$$

This formula coincides with formula (10), if we take f from (20a) or (20b) and set $a \to 1$ $(\eta \to 0)$. If, however, we take f in the form (20e) we arrive at the result obtained by Sudakov[7].

If we consider the process of scattering of an electron by an external field, then to get the matrix element we must multiply (24) by the expression corresponding to a free line. It is well known that to each free line there corresponds $\{G(p) \times (\hat{p}-m)\}^{1/2}$, which in our case is equal to

$$\sqrt{\beta(m^2)}\left(\frac{m}{\Delta m}\right)^{(e^2/4\pi)(3-d_l^0)}$$

Later we shall show that only the cases (20b), (20d) and (20e) have a direct physical interpretation. The results for these cases are:

$$M_0 = (\bar{u}_1\gamma_\sigma u_2)e^{-f_1}, \tag{25}$$

$$f_1 = (e^2/2\pi)\{a(a^2-1)^{-1/2}[\eta^2 \tag{26a}$$
$$+\zeta(\xi_1+\xi_2) - {}^1/_2(\xi_1-\xi_2)^2] - (\xi_1+\xi_2)\}$$

for $\quad \xi_1 > 0,\ \xi_2 > 0,\ \xi_1+\eta > \xi_2 > \xi_1-\eta;$

$$f_1 = (e^2/2\pi)[\eta^2 + \eta\xi_1 + \eta\xi_2 + \xi_1\xi_2 - {}^1/_2\xi_2^2] \tag{26b}$$

for $-\eta < \xi_1 < 0,\ 0 < \xi_2 < \xi_1+\eta;$

$$f_1 = (e^2/2\pi)(\eta+\xi_1)(\eta+\xi_2) \tag{26c}$$

for $\quad -\eta < \xi_1 < 0,\ -\eta < \xi_2 < 0.$

Generally speaking, when Γ_μ is an internal vertex, the relation between Δm_1 and Δm_2 is arbitrary. However, in this case we must consider lines which encompass several vertices, as we shall do for the case of one additional quantum.

3. GENERALIZATION OF THE FEYNMAN DIAGRAMS FOR OBTAINING PROBABILITIES OF MULTIPLE PROCESSES.

Before we consider the question of the radiation of additional quanta during the scattering of an electron, we shall present a method which considerably simplifies the calculation of processes involving a large number of real particles. In this section we shall consider the emission of real pairs as well as real quanta. In the literature, the rules for calculating matrix elements with virtual quanta are presented very well (cf., for example, reference 5). However the situation with regard to the rules for finding transition probabilities is not so satisfactory. We shall give a simple scheme which enables one to find such probabilities without difficulty.

First we consider processes in which the only real particles are photons. Aside from the appearance of their momenta in the propagation factors for virtual electrons, the presence of these photons manifests itself as follows. For each initial photon, there is a factor $2\pi/|\mathrm{K}|$ in the probability, where K is the photon wave vector. For all except one of the final photons there is a factor $(2\pi/|\mathrm{K}|) \times (2\pi)^{-3}\mathrm{K}^2 d|\mathrm{K}|\, d\Omega$ in the probability. The momentum of the remaining photon is determined by the conservation laws so that it gives only a factor $2\pi/|\mathrm{K}|$. In addition, each photon gives rise, in the appropriate place in the matrix element, to the factor $\hat{\epsilon}$ where ϵ is the polarization vector. The sum over polarizations is carried out by replacing $\hat{\epsilon}\cdot\cdot\cdot\hat{\epsilon}$ in the expression for the probability by $-\gamma_\mu\cdot\cdot\cdot\gamma_\mu$ ($\mu = 0, 1, 2, 3$). Finally there enters into the expression for the probability the quantity $2\pi\delta(E_{\text{in.}} - E_{\text{fin.}})$ where $E_{\text{in.}}$ and $E_{\text{fin.}}$ are the total energies of the initial and final states. The δ-function is eliminated by integrating over one of the $d|\mathrm{K}|$'s.

It is easy to see that the quantity $1/|\mathrm{K}|$ can be written in the form $2\int_{\omega>0} d\omega\,\delta(k^2)$, where $k^2 = \omega^2 - \mathrm{K}^2$. If we integrate with respect to the momentum of the corresponding photon, this replacement results in a great similarity between real and virtual photons. In fact, in place of $\int\cdots\gamma_\mu\cdots\gamma_\mu\cdots\delta_+(k^2) \times d^4k$ $(\delta_+(x) = \delta(x) - 1/i\pi x)$, which occurs for virtual photons, the expression

$$2\int_{\omega>0}\cdots\gamma_\mu\cdots\gamma_\mu\cdots\delta(k^2)\,d^4k$$

appears in the formula for the probability for real photons. The requirement $\omega > 0$ is relativistically invariant, and in particular signifies that the projection of the four-vector k on any time-like vector n with $n_0 > 0$ is positive. We note that in place of the factor $1/|\mathrm{K}|$ for the second photon, whose momentum is determined by the conservation laws and $\delta(E_{\text{in.}} - E_{\text{fin.}})$, we can simply put $2\,\delta_{\omega>0}(k^2)$. In doing this we still satisfy the energy conservation law and retain the correct factor, since $dE_{\text{fin}} = d\omega$.

We now go over to the case when the only real particles are electrons, and there are no photons or pairs. In this case each electron in the initial state contributes the expression $(1/2E)(\bar{u}\ldots u)$ to the probability, if we use the normalization $\bar{u}u = 2m$. Each of the electrons in the final state, except one whose momentum is determined by the conservation laws, gives the factor $(2E)^{-1}(\bar{u}\ldots u) \times (2\pi)^{-3}\mathbf{p}^2 d|\mathbf{p}|\, d\Omega$, where E is the energy of the electron. The last of the final state electrons gives simply $(2E)^{-1}(\bar{u}\ldots u)$. If we carry out the sum over electron spins, we replace $\bar{u}u \to \hat{p} + m$. In addition there is a factor $2\pi\delta(E_{\text{in.}} - E_{\text{fin.}})$ in the probability.

Just as in the case of photons, we can make the replacement

$$\frac{1}{E} = 2\int_{E>0}\delta(p^2 - m^2)\,dE.$$

If we are dealing with an electron for which we integrate over the momentum and sum over the spin, then we arrive at the result that each such electron gives a factor

$$\frac{\hat{p}+m}{2\pi}\int_{E>0}\delta(p^2 - m^2)\,d^4p.$$

As for the last of the final state electrons, after summing over its spin we can write for it $(\hat{p} + m)\,\delta_{E>0}(p^2 - m^2)$, which also includes $\delta(E_{\text{in.}} - E_{\text{fin}})$.

The similarity to virtual processes still does not appear explicitly in this form. In order to see the similarity, let us consider, for example, electron-electron scattering in zeroth approximation. From the conservation laws, it is clear that $d^4p = d^4q$, where q is the momentum of the virtual quantum which the electrons exchange with one another. If we make this substitution, then the expression for the probability suggests the matrix element for the interaction of a pair of electrons with exchange of a pair of identical virtual photons. A similar situation will occur in the more general case.

Now we consider the case when pairs are produced in a process. Since the momentum of one of the components of the pair is determined by the conservation laws if the momentum of the pair-producing photon is given, the integration need be taken over only one of the components, say the electron, and over the momentum of the photon producing the pair. In the integrand the factor $(\hat{p}+m)\delta_{E_p>0}(p^2-m^2)$ refers to the electron, and the factor $(\hat{p}-\hat{k}+m)\delta_{E_{p-k}>0}((p-k)^2-m^2)$ tothe positron. The generalization to the case where real quanta, electrons, and pairs are present, presents no difficulty.

The rules we have given can be presented in the form of generalized Feynman diagrams. In fact we shall draw a diagram which shows a sort of doubled diagram for the matrix element of our process--a diagram together with its mirror image (the latter corresponds to the Hermitian adjoint matrix element). We now join those photon and electron lines for which there is a summation over spin and integration over momentum, provided the latter is not excluded by the conservation laws. We shall put a dash through such connected lines in order to distinguish them from the usual ones. After this the diagram will be completely analogous to the usual Feynman diagram for a matrix element. In particular, real pairs will be described by a loop of dashed electron lines. We note that if the matrix element is a sum of diagrams, then in the generalized diagrams each of the initial ones is joined in turn to the mirror images of all the others as well as to its own image.

In addition to virtual and intermediate lines, the fundamental elements of the generalized diagram will be:

1. A real photon line. The factor for it is

$$2\delta_{\omega>0}(k^2).$$

2. A real electron line. Its factor is

$$\frac{\hat{p}+m}{2\pi}\delta_{E>0}(p^2-m^2).$$

3. Two identical photon lines between a pair of electrons, corresponding to the Coulomb interaction. The factor appearing for these lines is

$$(4\pi/q^2)^2.$$

The integration in the generalized diagram is taken over all closed photon lines, dashed as well as undashed, and over electron loops made up of ordinary and dashed lines. In the case of a loop, one also takes the spur. The factor $1/\pi i$ for photons and $-1/\pi i$ for a loop occurs only for virtual processes.

All of the rules given here refer to the case where the detailed characteristics of the emitted particles are not of interest (or are determined by conservation laws), i.e., we have closed lines. If this is not the case, then the usual factors for real particles occur. As examples, generalized diagrams are shown in Fig. 2 for: a – Compton effect, b – electron-electron scattering, c – materialization of a pair in the field of an electron. We show only one of the graphs for each effect.

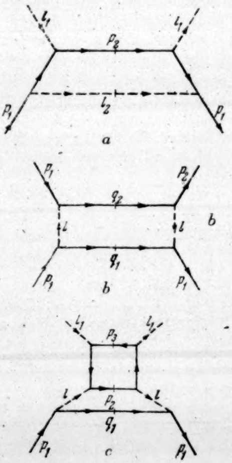

FIG. 2

4. SCATTERING ACCOMPANIED BY RADIATION OF ADDITIONAL QUANTA.

We now consider scattering with radiation of a single additional quantum $\varkappa$. We shall supose that the quantum is free ($\varkappa^2 = 0$) and that to the free line there corresponds certain Δm_1 and Δm_2, subject to the conditions $m\Delta m \ll q\varkappa \ll p\cdot q$. It is easy to see that the additional factor from the new vertex cancels against the factor from the internal electron line. There remain only lines which surround the fundamental vertex, or which circle both vertices. Since lines of these two types can be shifted arbitrarily, integrations over them are carried out independently, i.e., we must find the contribution from the lines surrounding both vertices, and then multiply by the already known factor for the fundamental vertex. As for lines surrounding both vertices, we see that, because of the appearance of a new denominator, we must impose the condition $|p\cdot qu| \ll q\cdot\varkappa$ in order to separate out the logarithmic part of the integral over u. We easily see that the new lines again give an exponential factor, while the sum of the exponents of the two exponentials does not depend on $q\cdot\varkappa$, but is determined only by the values of a, Δm_1, and Δm_2. Now considering an arbitrary number of additional quanta, we arrive at the conclusion that this same situation always occurs, i.e., the net effect of the virtual lines is a factor common to all the diagrams of scattering with radiation.

We now go on to consider the case of an arbitrary number of real quanta. We shall consider the probabilities of processes involving radiation of 1,2,...n quanta, making the following assumptions:

a). The total energy carried off by the quanta does not exceed ω_1 in the rest system of the initial electron, and does not exceed ω_2 in the rest frame of the final electron.

b). We associate with free electron lines, in all diagrams considered, certain values Δm_1 and Δm_2, such that $\Delta m_1 \ll m$, $\Delta m_2 \ll m$ and $a\Delta m_1 > \Delta m_2 > \Delta m_1/a$. In the present case the Δm are auxiliary quantities and can be chosen arbitrarily.

Let us consider the generalized diagrams corresponding to scattering with radiation. It is not hard to see that four groups of real lines occur (see Fig. 3): lines joining a--*the* q line on the left to the one on the right, b--the p line on the left to the one on the right, c--the left q line to the right p line, d--the left p line to the right q line. If we consider the possible transpositions of lines we see that each group can be treated independently. For the same reason as before, we can use zeroth order values for the new vertices and electron lines. Consider a line of type a. There corresponds to it the factor

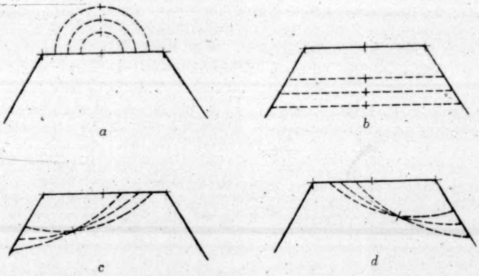

FIG. 3

$$-2e^2\int\frac{\gamma_\sigma(\hat q+\hat k+m)\gamma_\mu(\hat q+m)\gamma_\mu(\hat q+\hat k+m)\gamma_\tau\delta(k^2)\,d^4k}{[2m\Delta m_2+2(qk)+k^2]^2}. \qquad (27)$$

If we choose the time axis of the vector k along the direction of q and keep only the logarithmic part of the integral, we see at once that it is equal to

$$-(e^2/\pi)\ln(\omega_2/\Delta m_2)\,\gamma_\sigma(\hat q+m)\,\gamma_\tau, \qquad (28)$$

if $\omega_2 \ll m$. In the opposite case, ω_2 in (28) should be replaced by m.

If we consider successive lines of type a, it turns out that to get the maximum degree of logarithmic divergence in the integral, the lines must not intersect. Upon summing the integrals, we get the total result (for $\omega_2 \ll m$)

$$\gamma_\sigma(\hat q+m)\,\gamma_\tau\,(\omega_2/\Delta m_2)^{-e^2/\pi}. \qquad (29)$$

Similar expressions also occur for type b.

Now we go to lines of type c and d. Both types of lines give the same contribution. If we consider one of the lines, for example of type c, then we find that the integral obtained differs from the integral for the case where the photon is virtual only by the fact that in case c we have $\hat{q} + \hat{k}$ in the denominator, in place of $\hat{q} - \hat{k}$ for a virtual photon, i.e., the difference is merely a sign change. Actually, just as for the case of a real photon, the main term for the virtual photon case comes from taking the δ-function in the photon propagation factor. The change in the domain of integration also produces no difference, since the double integral over positive frequencies corresponds to a double integral over $u > 0$ and the corresponding v. But we know that the region $u < 0$ gives the same contribution.

Thus we obtain for a single line of type c an expression proportional to the area cross-hatched in Fig.1, from which the lower part is cut off by the lines $\lambda = \ln (am/\omega_1)$, $\mu = \ln (am/\omega_2)$. This expression appears as the exponent in the sum over all lines. Multiplying the common exponential factor from all the real lines by the common exponential for all the virtual lines, we find that we get in the exponent an expression of the type of (26), with ξ_1 and ξ_2 replaced by $\ln(m/\omega_1)$ and $\ln(m/\omega_2)$. Now it is no longer difficult to explain the physical meaning of (20), and also to give the reasons why the other cases of (20) have no physical interpretation.

Upon comparing the formulas with the ω's with formula (26) it is evident the latter determine the matrix element for scattering with radiation of additional quanta with energy not exceeding Δm_1 in the coordinate system of the initial electron and no greater than Δm_2 in the frame of the final electron. If we assign the quantum frequency in one coordinate system, say ω_1, then upon transforming to the other system, we find that ω_2 lies within the limits

$$(a + \sqrt{a^2 - 1})\,\omega_1 > \omega_2 > \omega_1/(a + \sqrt{a^2 - 1}). \tag{30}$$

We note that the sloping lines bounding the integration region in Fig. 1 correspond to just this condition. For this reason, if we impose the condition $\omega \ll \omega_1$ in one coordinate system, then the maximum frequency in the other system cannot exceed $\omega_1 (a + \sqrt{a^2 - 1})$, and conversely, i.e., it can actually be varied independently of ω_1 only within the interval given above. It is therefore clear that all the cases of (20) which are not contained in (26) have no physical meaning.

In a physical formulation of the problem, the frequency is limited in some one definite system. In general, such a bound would appear in Fig. 1. as some line bounding the cross-hatched region at its upper right corner. This line can be found by determining the maximum value of ω_2 for a given limiting frequency ω and a given ω_1. We shall not try to find the appropriate expressions for all cases which may arise, but merely point out that the resulting expression for the probability of a process with radiation of an arbitrary number of quanta with energy less than ω in the system of the initial electron, and of n additional quanta in the energy interval from ω to ω' is:

$$W = (W_0/n!)\, e^{-2f_1(\omega)} [f_1(\omega) - f_1(\omega)]^n, \tag{31}$$

where $f_1(\omega)$ is the f_1 of formula (26) with $\ln(m/\omega)$ substituted for ξ_1 and $\ln(m/\omega) + \eta$ in place of ξ_2.

Formula (31) is the familiar Poisson formula, and corresponds to the probability of n independent events. This is understandable, since we are dealing with quanta of such low energy that the radiation of these quanta essentially does not affect the electron's momentum, so that the radiation processes are actually independent. This result which we have obtained by a direct summation of diagrams was also demonstrated by Glauber[8] for the radiation of photons by an electron described by a given current.

We should point out that in order to get the correct result by such a method, we must impose restrictions on the domain of integration; these actually amount to a determination of the limits of energy and quantum frequency up to which the current can be regarded as classical. Strictly speaking, these limits can be obtained only through a quantum description of the current. This situation is not serious so long as one deals with quantum frequencies which are so small that $\ln(m/\omega) \gg \ln(E/m)$, but is very important for higher quantum energies.

In conclusion, I express my gratitude to Acad. L. D. Landau and V. V. Sudakov for many valuable comments.

---

[8] R. Glauber, Phys. Rev. **84**, 395 (1951).

Translated by M. Hamermesh
13

SOVIET PHYSICS JETP VOLUME 3, NUMBER 1 AUGUST, (1956)

A Theoretical Property of Relaxation Curves in Luminescence and Photoconductivity

N. A. TOLSTOI AND A. V. SHATILOV
The Lensoviet Technological Institute, Leningrad

(Submitted to JETP editor June 26, 1954)
J. Exper. Theoret. Phys. USSR **30**, 109-114 (January, 1956)

The universally accepted concepts concerning the recombination mechanism of phosphors and photoconductors are not suitable to describe the kinetics of concentration or temperature extinguished phosphorescence and of photoconductivity, although from a priori considerations, applicability of these concepts to extinction phenomena seems most natural.

1. INTRODUCTION

THE kinetic equations used to describe luminescence and conductivity in crystals excited by light are generally based on the assumption that the probability of the excited electron returning to its initial state is either proportional to n, i.e., the number of excited electrons (monomolecular or pseudomonomolecular reaction)* or proportional to n^2 (bimolecular reaction). Opinions of different writers concerning the degree of correspondence between equations of this type and the actual mechanism of the processes in semiconductors vary considerably and depend on the nature of the experiments, the results of which are being compared with the theory. In general, the simpler the experiments the closer are the results in agreement with the theory. It is customary to justify non-agreement of experimental results with the theory, especially where the shape of relaxation curves is concerned, by references to complications arising from the principles or methods employed in the experiment which were not reflected in the theoretical equations. Thus, the question as to whether or not the initial theoretical premises (for example, monomolecular or bimolecular nature of the reaction) are justified does not generally receive a final answer. At the same time a criterion of applicability can be established for the assumed theoretical solutions, a criterion that is not so sensitive to the secondary complications of the processes but which depends strongly on the type of the mechanism of excitation and recombination accepted by the theory. We are referring to the ratio L_p/L_3, the value of which can be different in different theories[1], and which will be designated by the letter s. L_p is the area above the curve of increasing light emission or conductivity, L_3 is the area under the quenching curve (Fig. 1). We shall present in this paper the computation of s for a very important general case and compare the result with experiment.

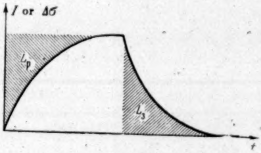

FIG. 1

2. FUNDAMENTAL EQUATION

Nail, Pearlman and Urbach[2] proposed the kinetic equation

$$dn/dt = E - \beta n^2 - \gamma n, \qquad (1)$$

where n is the number of excited electrons, E the intensity of exciting light, β and γ the probabilities of bimolecular and monomolecular recombinations. The brightness of illumination I, according to the assumption of the authors, is equal to

$$I = \varepsilon\beta n^2 + \eta\gamma n, \qquad (2)$$

where $0 \leqslant \varepsilon \leqslant 1$, and $0 \leqslant \eta \leqslant 1$. The quantity ϵ denotes the fraction of the total number of electrons, recombining according to the bimolecular law, that combine with emission of radiation. The quantity η is a similar quantity for the monomolecular process.

By means of Eqs. (1) and (2), the authors of reference 2 explained the various relationships between the background brightness I_{st} and the intensity of the exciting light E, especially the "greater-than-linear" dependence ($I_{st} \sim E^2$) observed at strong quenching, and also the experimentally observed weaker-than-linear relationships.

---

*We shall refer in this paper to both of these reactions as simply the monomolecular reaction.

[1] N. A. Tolstoi and I. A. Litvinenko, J. Exper. Theoret. Phys. USSR **29**, 507 (1955); Soviet Phys. JETP. **2**, 420 (1956)

[2] N. R. Nail, D. Pearlman and F. Urbach, *Solid Luminescent Materials*, Cornell Symposium, 1948, p. 190.

3. RISE OF LUMINESCENCE

We rewrite Eq. (1) in the form

$$\frac{dn}{dt} = \beta\left[\frac{E}{\beta} + \left(\frac{\gamma}{2\beta}\right)^2\right]\left[1 - \frac{(n + \gamma/2\beta)^2}{(E/\beta) + (\gamma/2\beta)^2}\right] \qquad (3)$$

and designate

$$(E/\beta) + (\gamma/2\beta)^2 = A. \qquad (4)$$

The solution of Eq. (3) for the luminescent rise process has the form

$$n = n_{st} - \sqrt{A}\,\frac{2ce^{-\tau}}{1 + ce^{-\tau}}, \qquad (5)$$

where

$$n_{st} = n_{t=\infty} = \sqrt{A} - \gamma/2\beta, \qquad (6)$$

$$\tau = 2\beta\sqrt{A}t, \quad c = \frac{\sqrt{A} - \gamma/2\beta}{\sqrt{A} + \gamma/2\beta}.$$

The quantity which interests us,

$$L_p = \int_0^\infty (I_{st} - I)\,dt$$

is computed by means of (2) and (5). By performing substitutions and integrating we obtain:

$$L_p = \left[\frac{\gamma}{\beta}(\varepsilon - \eta)\ln u + \frac{2\varepsilon\sqrt{A}}{u}\right]_{t=0}^{t=\infty}, \qquad (7)$$

where

$$u = 1 + ce^{-\tau}.$$

4. QUENCHING

Solving Eq. (1) with $E = 0$, we have

$$n = \frac{\gamma}{\beta}\,\frac{ce^{-\gamma t}}{1 - ce^{-\gamma t}}, \qquad (8)$$

where c again is obtained from (6). The quantity of interest, L_3, turns out to be equal to

$$L_3 = \int_0^\infty I\,dt = -\left[\frac{\gamma}{\beta}(\varepsilon - \eta)\ln v - \frac{\gamma\varepsilon}{\beta}\,\frac{1}{v}\right]_{t=0}^{t=\infty}, \qquad (9)$$

where

$$v = 1 - ce^{-\gamma\tau}.$$

5. THE QUANTITY $s = L_p/L_3$

By computing the limits in (7) and (9) and forming the ratio s we obtain, upon transformation,

$$s = \frac{\Delta\delta - 2\ln\left(\frac{1 + \Delta}{1 + (\Delta/2)}\right)}{\Delta\delta - 2\ln(1 + (\Delta/2))}, \qquad (10)$$

where there are introduced symbols

$$\Delta = \sqrt{1 + 4\beta\gamma^{-2}E} - 1, \quad \delta = \varepsilon/(\varepsilon - \eta). \qquad (11)$$

Thus

$$c = \Delta/(\Delta + 2) \quad (c \geqslant 0).$$

The variable Δ can vary within limits $0 \leqslant \Delta \leqslant \infty$. The limits of δ are determined by the fact that ϵ and η are both positive, and can have values from zero to unity. Therefore, either $-\infty \leqslant \delta \leqslant 0$, or $1 \leqslant \delta \leqslant \infty$, , i.e., δ cannot have values within the interval (0, 1).

6. VARIATION OF THE QUANTITY S

(a) Let $\Delta \to \infty$. Then, if $\delta \neq 0$, we have $s \to 1$. If, however, $\delta = 0$, $s \to 0$

(b) Let $\Delta \to 0$. Expanding the logarithmic terms into series up to terms of the order Δ^2, we find

$$s \approx \frac{(\delta - 1) + {}^3/_4\Delta}{(\delta - 1) + {}^1/_4\Delta}.$$

Then, if $\delta = 1$, we have*: $s \to 3$, and if $\delta \neq 1$, $s \to 1$

(c) Let us compute the partial derivative of s with respect to Δ for $\Delta \to 0$:

$$\frac{ds}{d\Delta} = \frac{(\delta - 1)\,\Delta^2}{[\Delta\delta - 2\ln(1 + \Delta/2)]^2} \qquad (12)$$

(the logarithmic terms in the numerator were expanded up to the order Δ^2).

When $\delta > 1$, $ds/d\Delta > 0$, and when $\delta \leq 0$, $ds/d\Delta < 0$, i.e., for the case of $\delta > 1$ s begins to increase with the increase of Δ (becomes > 1) and for the case of $\delta \leq 0$, s becomes < 1. When $\delta = 1$, as can be confirmed by a separate computation, $ds/d\Delta$ is negative in the region of small Δ, i.e., $s < 3$.

(d) Let us compute $ds/d\Delta$ for $\Delta \to \infty$:

$$\frac{ds}{d\Delta} \to \frac{2\delta\,[\ln(1 + \Delta) - \ln(1 + \Delta + \Delta^2/4)]}{[\Delta\delta - 2\ln(1 + \Delta/2)]^2}. \qquad (13)$$

It can be seen from (13) that $ds/d\Delta \to 0$ since the denominator approaches ∞ faster than the numerator.

---

* This special case was examined previously in the paper by Tolstoi[3].

[3] N. A. Tolstoi, Dokl. Akad. Nauk SSSR 95, 249 (1954).

The structure of the numerator in (13) shows that when $\delta \geq 1$, $ds/d\Delta \leq 0$, and when $\delta < 0$, $ds/d\Delta \geq 0$. When $\delta = 0$, as can be shown, $ds/d\Delta \leq 0$ for all values of Δ from 0 to ∞.

Thus the variations of s with Δ have a maximum (if $\delta > 1$) or a minimum (if $\delta < 0$). When $\delta = 1$ or $\delta = 0$, these variations are of the same kind: s decreases with the increase of Δ.

(3) Let us compute the derivative of s with respect to δ:

$$\frac{ds}{d\delta} = \frac{2\Delta \ln\left(\frac{1+\Delta}{1+\Delta+\Delta^2/4}\right)}{[\Delta\delta - 2\ln(1+\Delta/2)]^2}. \tag{14}$$

It is not difficult to see that $ds/d\delta$ is negative for all values of δ. Therefore, for any Δ, smaller values of s will correspond to larger δ. The curves $s(\Delta)$ will nowhere intersect and will coincide only at points $\Delta = 0$ and $\Delta = \infty$.

7. LIMITS OF VARIATION OF S

In order to evaluate the maximum possible values of s, let us rewrite (10) in the form:

$$\Delta\delta = 2\frac{s+1}{s-1}\ln(1+\Delta/2) - \frac{2}{s-1}\ln(1+\Delta), \tag{15}$$

and differentiate both sides with respect to Δ. Let us agree to differentiate only at those points where s (as a function of Δ) has a maximum or a minimum. It can then be considered that s and δ do not depend on Δ, and they can be treated as constants in the differentiation process:

$$\delta = \frac{s+1}{s-1}A - \frac{2}{s-1}B, \tag{16}$$

where $A = 1/(1+\Delta/2)$, $B = 1/(1+\Delta)$. Let $\delta = 0$. Then since $A > B$ and the right part must be negative, $s < 1$. Let $\delta > 1$ Then, by transformation of (16) we have:

$$(\delta - 1) = \frac{\Delta}{1+\Delta}\left[\frac{1}{(s-1)(1+\Delta)} - \frac{1}{2}\right]. \tag{17}$$

Since the expression inparentheses must be positive, $s < 3$. It is evident from this expression that $s \geq 1$.

For curves $s(\Delta)$ corresponding to the cases of $\delta = 0$ and $\delta = 1$ we know the values of $s(0)$ and $s(\infty)$. If these curves had maxima at $\Delta > 0$ the evaluations $s < 1$ (when $\delta = 0$) and $s < 3$ (when $\delta = 1$) would apply. If they have no maxima, i.e., s decreases uniformly with increase of Δ, then the following evaluations would apply: $s \leq 1$ (when $\delta = 0$) and $s \leq 3$ (when $\delta = 1$).

Summarizing, we have: for the case $1 \leq \delta \leq \infty$, $1 \leq s \leq 3$ and for the case $0 \geq \delta \geq -\infty$, $0 \leq s \leq 1$.

Figure 2 shows the general appearance of the family of curves $s(\Delta)$ for various values of δ. The table contains a summary of all results; the symbols 0-1, etc , indicate the limits of variations for the corresponding quantities.

TABLE

No.	Excitation	Quenching	β	γ	ε	η	$\Delta_{\varepsilon>0}$	δ	$s=L_p/L_3$	$s\|_{E\to 0}$	$s\|_{E\to\infty}$
1	Any	None	+	+	1	1	+	$\pm\infty$	1	1	1
2	Mono	Mono	0	+	—	0—1	0	—	1	1	1
3	”	Bi	+	+	0	1	+	0	0—1	1	0
4	”	Mono-Bi	+	+	0	0—1	+	0	0—1	1	0
5	Bi	Mono	+	+	1	0	+	1	1—3	3	1
6	”	Bi	+	0	0—1	0	∞	1	1	1	1
7	”	Moro-Bi	+	+	0—1	0	+	1	1—3	3	1
8	Mono-Bi	Mono	+	+	1	0—1	+	>1	1—3	1	1
9	” ”	Bi	+	+	0—1	1	+	<0	0—1	1	1
10	” ”	Mono-Bi	+	+	0—1	0—1	+	<0 >1	0—1 1—3	1 1	1 1

Mono - Monomolecular
Bi - Bimolecular

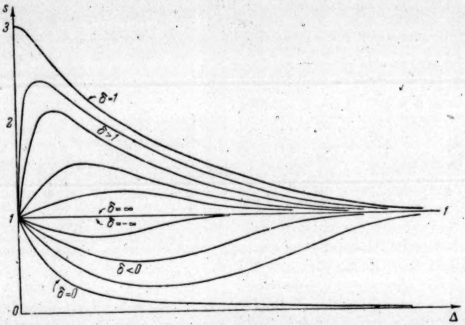

FIG. 2. General Shape of curves $s(\Delta)$ for different values of δ.

8. DISCUSSION

The most important result of the above computations is that in all cases the value of s remains less than 3. However, experiments indicate that under conditions of strong temperature and concentration quenching, the luminescence of sulphide type phosphors is characterized by values of s far in excess of 3 (for example, $s = 10$ – to 12, see reference 1). It is therefore necessary to conclude that even such a flexible and universal kinetic equation, which was assumed in reference 2 and which well describes the regular order of steady luminescence) cannot be adequate for the kinetics of luminescence of quenched phosphors of the sulphide type. It is natural to suppose that the reason why experimental results do not agree with the theory is that Eqs. (1) and (2) describe excited states singularly characterized by the number n of excited electrons.

In substance, this indicates that among the various energy levels of excitation (conduction band, levels of sticking) there exists also exchange equilibrium. Under ordinary conditions, the existence of such exchange equilibrium is more than doubtful. However, at a higher temperature under conditions of strong temperature quenching, for example i.e., exactly when values of $s > 3$ are observed, thermal exchange equilibrium becomes highly probable . Moreover, all other complications which are usually ascribed to kinetic processes in phosphors should, it seems, disappear at high temperatures^3 (for example, filling of local levels close to saturation, luminescent action of the exciting light, etc.). Such lack of agreement between experiment and theory, based on the application of the general criterion (value of s), must be considered as significant and compels a review of the widespread concepts concerning the mechanism of luminescence for sulphide phosphors.

The mechanism of photoconductivity is also generally described by type (1) equations with the difference that the value of photoconductivity $\Delta\sigma$, as distinguished from the brightness of luminescence I, is expressed as $\Delta\sigma = \alpha n$.

It is not difficult to see that it is possible to make use of the above results when one determines the value s for photoconductivity. Formally, the case of photoconductivity corresponds to monomolecular luminescence, and therefore, as seen from the table (Nos. 2, 3, 4) s for photoconductivity should be ≤ 1. Roughly speaking, this means that in the case of photoconductivity the curve of the current rise can only be "faster" than the decay curve; or, in the extreme case, equal to it. It follows that the appearance in photoconductivity experiments of values $s > 1$ also indicates sharp disagreement with accepted concepts. Nevertheless, such values are observed in experiments (for example, in CdS-Cu with high concentration of copper)

It is known that unequal excitation of the phosphor or the photoconductor in depth, connected with the absorption of light in the thickness of the sample, leads to additional complications in the case of non-linearly or non-exponentially relaxing substances. These complications, however, cannot influence the evaluated limits we have found for s, since any superposition of relaxation curves, for which these limits hold, cannot result in an integral curve for which s is outside the evaluated limits (above as well as below).

Translated by J. L. Herson

14

SOVIET PHYSICS JETP VOLUME 3, NUMBER 1 AUGUST, 1956

Diffraction Splitting of Fast Nonrelativistic Deuterons

A. I. ALIEV AND E. L. FEINBERG
P. N. Lebedev Physical Institute, Academy of Sciences, USSR

(Submitted to JETP editor October 5, 1954)
J. Exper. Theoret. Phys. 30, 115-125 (January, 1956)

A calculation of diffraction splitting is carried out for deuterons of energies of order 100 mev interacting with nuclei whose dimensions are large compared with those of the deuteron. It is shown that the total cross section for the process has the behavior of the stripping cross section. The angular distributions of the outgoing proton and neutron in correlated pairs and their energy distribution have the same behavior as in deuteron stripping when either a neutron or a proton is scattered out. Because of the indeterminacy of the structure of the nuclear surface (and its transparency for fast nucleons) and the lack of knowledge about the behavior of the deuteron wave function for small neutron-proton separations, the formulae obtained are good only for some of the processes; namely, the processes in which a small amount of momentum is transferred to the nucleus. The total cross section is only estimated. The angles and the energy spectrum for diffraction splitting are different from those of the electric (coulomb) splitting. The cross section of the diffraction splitting is independent of energy and increases with the atomic number as $A^{1/3}$.

1. INTRODUCTION

AS was shown by one of us previously[1], fast deuterons should undergo in collisions with nuclei a characteristic process of diffraction splitting due to the action of nuclear forces. This process would not, as a rule, be accompanied by a nuclear reaction and would take place outside the nucleus. In this work we calculate the cross section for diffraction splitting of deuterons of energies of the order 100 mev by sufficiently heavy nuclei. It will become evident that an exact calculation cannot be made for all conditions uniquely, because: a) the quantitative result is determined by the nature of the deuteron wave function that is known only for large separations between the particles; b) the result depends also on the transparency of the nucleus for a nucleon passing at various distances from its center. This dependence causes complications due to the lack of knowledge of the outer regions of the nucleus.

For the above reasons the differential cross section will be strictly obtained only for a group of the processes, namely, the cases in which the momentum q transferred to the nucleus is smaller than the reciprocal of the radius of nuclear forces $1/\mu$ (μ is the π-meson mass and we shall set $\hbar = c = 1$).

This range of processes is the most important one for the following reasons. From physical considerationsit is clear that for effective splitting the important q are those up to near the reciprocal dimensions of deuteron, i.e., $q \sim 2\sqrt{M\epsilon} \approx 0.6\,\mu$ (M is the mass of a nucleon and ϵ the binding energy of the deuteron). For $q \gtrsim 0.6\,\mu$ the cross section for the process should vanish rapidly (the corresponding matrix elements will contain rapidly oscillating multipliers; this conclusion follows also from purely optical wave analogies). Considering the boundary of the nucleus sharp we shall not make any error by limiting ourselves to that part of the effect due to small q, $q \ll \mu$. For the full effect we shall obtain an order of magnitude estimate by extrapolation to $q \sim \mu$. In accord with this incompleteness of the result we can allow other approximations in the calculations. However, the result seems to us to deserve attention even with such approximations. It turns out that the estimate results in a substantial value of the cross section – of the order of magnitude of the stripping cross section. The process has its peculiar characteristics which allow us to separate it from, for example, the process of electric splitting. Furthermore, even though the diffraction splitting of deuterons is only a small part of the total (for small q), it may be considered as a model for processes involving the diffraction splitting in other systems (for example, of other nuclei or, in particular, in cosmic rays). Therefore it has a methodological importance.

The cross section of the process in question, together with the process of electric splitting can be computed for sufficiently heavy nuclei from the Born approximation formula

$$d\sigma = 2\pi \left| < \chi_0^{(-)} \mid U + W \mid \psi_{0a} + \psi_d^{\text{диф}} > \right|^2 \delta(E_a - E_b). \tag{1.1}$$

Here U is the interaction potential of the proton-neutron system, which we shall consider dependent on the separation $r = r_p - \mathbf{r}_n$ between the proton and the neutron; $U = U(r)$; W is the electrostatic interaction potential of the proton with the nucleus: $W = Ze^2/r_p$; ψ_{0a} is the wave function of the incident deuteron which may be considered nonrelativistic for the region of the deuteron momenta of interest and Ω is the normalization volume:

---

[1] E. L. Feinberg, J. Exper. Theoret. Phys. USSR **29**, 115 (1955); Soviet Phys. JETP 2, 58 (1956).

$$\psi_{0a} = \Omega^{1/2} \exp\{ip_d(\mathbf{r}_p + \mathbf{r}_n)/2\}\, \varphi(|\mathbf{r}_p - \mathbf{r}_n|), \tag{1.2}$$

where φ is the wave function of a stationary deuteron written similarly for the potential $U(r)$. $\psi_d^{\text{dif.}}$ is the wave function for the deuteron scattered as a whole as a result of the diffraction on the nucleus; χ_0^- is the product of wave functions of mutually noninteracting outgoing neutron and proton, of momenta p_n and $\mathbf{p}_p$. It should be noted that χ_0^- takes into account the interaction of these particles with the field of the nuclear forces of the nucleus. The wave function of the deuteron φ is also needed for the calculations. Outside of the radius of action of the nuclear forces which is of the order $1/\mu$,

$$\varphi = Ne^{-\alpha r}/r, \quad \alpha = \sqrt{M\varepsilon}. \tag{1.3}$$

Since we shall consider only transferred momentum not exceeding μ, i.e., distances between deuteron and nucleus greater than $1/\mu$, then we may use just this function φ. As is well known[2], with the proper normalization we obtain

$$N = \sqrt{3\alpha/4\pi}. \tag{1.4}$$

Furthermore, we introduce the average radius of the deuteron

$$R_d = 1/2\alpha = 1/2\sqrt{M\varepsilon} \approx 1.6/\mu. \tag{1.5}$$

In the present we shall compute the cross section for pure diffraction splitting, neglecting the influence of the electrostatic field of the nucleus since, as we shall see, the diffraction process takes place mainly in a definite energy range. Therfeore we set $W = 0$ and in $\psi_d^{\text{dif.}}$ we shall include only diffraction by the nuclear forces of the nucleus. This latter approximation is possible only for deuterons of sufficiently high energies. $(Ze^2/\hbar v < 1)$. In particular, for medium heavy nuclei the deuteron energy should be greater than several tens of mev. In such a case the criterion of the external character of the process (cf. reference 1, Eq. (2.5)] is known to be satisfied.

Furthermore, the wavelength of all particles is much smaller than the radius of the nucleus. The wave functions of the particles diffracted by the field V of the nuclear forces will be found with the assumption that the nucleus is completely opaque to neutrons and protons. This assumption is not desirable, of course, for nucleon energies greater than 70 mev, i.e., for deuterons whose energy E_d exceeds ~ 150 mev. However, the generalization does not encourter any fundamental difficulties and we shall not yet discard it. Finally, in the range of energies E_d under consideration (40-150 mev), it is possible to neglect the exchange of the nucleons of the deuteron with the nucleons of the nucleus.

We shall see that under the described conditions diffraction splitting actually does take place and that the total cross section is of the order RR_d (R is the radius of the nucleus), and that the particles are scattered within angles of the order $\sqrt{M\epsilon}/p_d$, just as in deuteron stripping, and that the energies of the particles are equal to each other with accuracy of the order of $\sqrt{E_d\epsilon}$. The nucleus receives a small recoil (the recoil momentum is of the order $\sqrt{4M\epsilon}$. The energy transferred is smaller than the binding energy of the nucleon in the nucleus (even on recalculation for one nucleon); in reality, the momentum is absorbed by the surface layer of the nucleus – the "skin layer" – and the excitation energy is still smaller. Therefore, as a rule, the nucleus should remain undisturbed.

2. WAVE FUNCTIONS AND MATRIX ELEMENTS

The function χ_p^{-1} describes the noninteracting nucleons with momenta p_p and p_n, which leaves the interaction region of a nucleus R (which is considered to be absolutely opaque). In this case χ_b^{-1} has the form (cf, for example, reference 3).

$$\begin{aligned}\chi_b^{(-)} &= \Omega^{-1/2}\left(e^{i\mathbf{p}_n\mathbf{r}_n} + \frac{p_n}{2\pi i}\int \frac{\exp\{-ip_n|\mathbf{r}_n - \mathbf{s}_n|\}}{|\mathbf{r}_n - \mathbf{s}_n|}\,d\mathbf{s}_n\right) \\ &\times \Omega^{-1/2}\left(e^{i\mathbf{p}_p\mathbf{r}_p} + \frac{p_p}{2\pi i}\int \frac{\exp\{-ip_p|\mathbf{r}_p - \mathbf{s}_p|\}}{|\mathbf{r}_p - \mathbf{s}_p|}\,d\mathbf{s}_p\right) \\ &= \frac{1}{\Omega}(\psi_0^{(n)}(\mathbf{r}_n) + \psi_1^{(n)}(\mathbf{r}_n))(\psi_0^{(p)}(\mathbf{r}_p) + \psi_1^{(p)}(\mathbf{r}_p)),\end{aligned} \tag{2.1}$$

Here S_n, S_p are two-dimensional vectors in the plane passing through the cross section of the nucleus over which the integration is carried out. The section is chosen perpendicular to the vectors

---

[2] A. I. Akhiezer and I. Ia. Pomeranchuk, *Some Problems in Nuclear Theory*, 2nd ed., 1950, Sec. 2.

[3] L. L. Landau and I. Ia. Pomeranchuk, J. Exper. Theoret. Phys. USSR **24**, 505 (1953).

$\mathbf{p}_p$ and p_n (i.e., the region of integration is $s_n < R$, $\mathbf{s}_n \perp \mathbf{p}_n$; $\mathbf{s}_p < R$, $\mathbf{s}_p \perp \mathbf{p}_p$), and Ω is the normalizing volume.

The wave function of the deuteron turns out to be somewhat more complicated since it is necessary to take into account the final (larger) dimensions of the deuteron (it appears that they have a limiting value). Fundamentally, it is necessary to take into account the different effective radii of the nucleus in respect to the nucleon and to the deuteron. This can be done in the following manner. "Absorption" of the deuteron (i.e., its disappearance from the incident beam) will take place when the center of gravity of the deuteron passes outside of the nucleus ($S_d > R$) and if at the same time even only one nucleon of the deuteron falls within the limits of the section of the nucleus. As soon as $S_d - R >> R_d$ this effect can be neglected. In this way we obtain for the general case:

$$\psi_d = \Omega^{-1/2}\left(e^{i p_d \mathbf{r}_d} - \frac{p_t}{2\pi i}\int\limits_{\mathbf{s}_d \perp \mathbf{p}_d} f\left(\frac{s_t - R}{R_d}\right)\frac{\exp\{ip_t|\mathbf{r}_d - \mathbf{s}_t|\}}{|\mathbf{r}_d - \mathbf{s}_d|}\,d\mathbf{s}_d\right)\varphi(|\mathbf{r}_p - \mathbf{r}_n|), \tag{2.2}$$

where the "function of transparency" f is some function dependent on the structure of the deuteron and the opacity of the nucleus for nucleons at various distances from its center. For a completely opaque nucleus f is equal to unity for $S_d < R$ and it vanishes for $S_d - R >> R_d$.

Let us assume that the center of mass of the deuteron moves along the z axis and passes at distance S_d ($S_d > R$) from the center of the nucleus. Since the distance of one nucleon, say the neutron, from the center of mass is a half of its distance from the second nucleon (the proton) then the probability density that the nucleon is at a distance $\sqrt{\rho^2 + z^2}$ from the center of mass (ρ, χ are the cylindrical coordinates in a plane perpendicular to z) is . The total probability that one nucleon is absorbed by the nucleus when the center of mass of the deuteron is at a distance S_d (in the section plane of the nucleus) is

$$\int\limits_{-\infty}^{+\infty} dz \int\limits_{s_d - R}^{\infty} \rho\, d\rho \int\limits_{0}^{\arccos\frac{s_d - R}{\rho}} d\chi\, |\varphi(2\sqrt{\rho^2 + z^2})|^2. \tag{2.3}$$

(We consider the surface of the nucleus to be flat at $R >> R_d$. The probability of absorption of the second nucleon is the same. The function f is then equal to the square of Eq. (2.3) for $S_\alpha > R$. Inserting φ from Eq. (1.3) changing the variables $\rho = (s_d - R)\,x$, $\rho^2 + z^2 = \zeta^2\rho^2$, and Eq. (2.3) results in

$$\frac{1}{4} N^2 (s_d - R)\int\limits_1^{\infty} \arccos\frac{1}{x}\,dx \times \int\limits_1^{\infty}\frac{d\zeta}{\zeta}\,\frac{\exp\{-4\alpha(s_d - R)\,x\zeta\}}{(\zeta^2 - 1)^{1/2}}.$$

In this manner the characteristic parameter which determines the exponential vanishing of f for $S_d - R >> R_d$ is $a = 1/4\alpha \approx 0.8/\mu$.

The following calculations will be carried out with the assumption that all distances are large compared with $1/\mu$. Therefore we simply set

$$f\left(\frac{s_t - R}{R_d}\right) = \begin{cases} 1 & \text{for } s_d < R, \\ e^{-(s_d - R)/a} & \text{for } s_d > R, \end{cases} \tag{2.4}$$

$$a \approx R_d/2 \approx 0.8/\mu.$$

Now, omitting W in Eq. (1.1) and substituting Eq. (2.1) into Eq. (2.2), we obtain:

$$\begin{aligned} <\chi_0^{(-)}|U|\psi_d> = \Omega^{-3/2}\int d\mathbf{r}_p\,d\mathbf{r}_n\,(\psi_0^{(n)*}(\mathbf{r}_n) \\ + \psi_1^{(n)*}(\mathbf{r}_n))(\psi_0^{(p)*}(\mathbf{r}_p) \\ + \psi_1^{(p)*}(\mathbf{r}_p))\,U(|\mathbf{r}_p - \mathbf{r}_n|)\left(\psi_0^{(d)}\left(\frac{\mathbf{r}_p + \mathbf{r}_n}{2}\right)\right. \\ \left. - \psi_1^{(d)}\left(\frac{\mathbf{r}_p + \mathbf{r}_n}{2}\right)\right)\varphi(|\mathbf{r}_p - \mathbf{r}_n|), \end{aligned} \tag{2.5}$$

where

$$\psi_0^{(n)*}(\mathbf{r}_n) = \exp\{-i\mathbf{p}_n\mathbf{r}_n\};$$

$$\psi_0^{(p)*}(\mathbf{r}_p) = \exp\{-i\mathbf{p}_p\mathbf{r}_p\},$$

$$\psi_0^{(d)}\left(\frac{\mathbf{r}_p + \mathbf{r}_n}{2}\right) = \exp\{i\mathbf{p}_d(\mathbf{r}_p + \mathbf{r}_n)/2\},$$

$\psi_1^{(n)*}$, $\psi_1^{(p)*}$ are the complex conjugates of the second terms in the brackets of Eq. (2.2) taken with a plus sign. Multiplying out the quantities in parenthesis of Eq. (2.5) we obtain eight integrals, of which only some are different from zero.

We denote the integrals by symbols Y_{ijk}, $i, j, k = 0$ or 1, the indices 0 and 1 denoting which one of the terms is taken from the given parenthesis, the indices being written in the same order as the functions for n, p and d in Eq. (2.5). First of all Y_{000}, containing the product of plane waves, is different from zero only if the momentum of the center of mass is observed. This condition cannot be reconciled with the law of conservation of energy. Therefore Y_{000} vanishes. Furthermore, the diffraction cone of deuterons is distributed in the direction of the shadow formed by the nucleus, i.e., if deuterons are moving along the z axis from the region $z < 0$, then ψ_1^d is different from zero only for $z > 0$. Conversely, ψ_1^p and ψ_1^n are different from zero only for $z < 0$. Therefore, the integrals Y_{101}, Y_{011} and Y_{111} are vanishingly small. The remaining four integrals will be computed.

Introducing the coordinates of the center of mass: $\mathbf{r}_0 = (\mathbf{r}_p + \mathbf{r}_n)/2$, $\mathbf{r} = \mathbf{r}_p - \mathbf{r}_n$, we have:

$$Y_{100} = -\frac{1}{\Omega^{3/2}} \frac{p_n}{2\pi i} \int d\mathbf{r}_0 \int d\mathbf{r} \int d\mathbf{s}_n \exp\{i(\mathbf{p}_d - \mathbf{p}_p, \mathbf{r}_0 + p_n |\mathbf{r}_0 - \mathbf{r}/2 - \mathbf{s}_n|)\}$$

$$\times \exp\{i(\mathbf{p}_d - \mathbf{p}_p)(\mathbf{r}/2 + \mathbf{s}_n)\} \frac{U(r)\varphi(r)}{|\mathbf{r}_0 - (\mathbf{r}/2) - \mathbf{s}_n|}.$$

Integrating first over $\mathbf{r}_0$ (introducing the variables $\mathbf{r}_0 - \mathbf{r}/2 - \mathbf{s}_n$), and then over $\mathbf{s}_n$ (with limits $\mathbf{s}_n < R$, where R is the radius of the nucleus), we obtain

$$Y_{100} = \frac{4\pi i p_n}{(\mathbf{p}_d - \mathbf{p}_p)^2 - p_n^2} \frac{RJ_1(q_n R)}{q_n} \frac{1}{\Omega^{3/2}} \tag{2.6}$$

$$Y_{100} = \times \int \exp\left\{-\frac{i}{2}(\mathbf{p}_d - 2\mathbf{p}_p, \mathbf{r})\right\} U(r)\varphi(\mathbf{r})\, d\mathbf{r}. \quad (2.6)$$

Similarly

$$Y_{010} = \frac{4\pi i p_p}{(\mathbf{p}_d - \mathbf{p}_n)^2 - p_p^2} \frac{RJ_1(q_p R)}{q_p} \frac{1}{\Omega^{3/2}} \tag{2.7}$$

$$Y_{010} = \times \int \exp\left\{-\frac{i}{2}(\mathbf{p}_d - 2\mathbf{p}_n, \mathbf{r})\right\} U(r)\varphi(r)\, d\mathbf{r}.$$

At this point the momentum transferred to the nucleus appears for the first time

$$\mathbf{q} = \mathbf{p}_p - \mathbf{p}_n - \mathbf{p}_p. \tag{2.8}$$

and its projections q_p and q_n on the plane are perpendicular to p_p and p_n, respectively.

The integral Y_{110} is somewhat more complicated but it belongs to the type of integrals obtained by Pomeranchuk[4]. First we notice that according to the law of conservation of energy,

$$\frac{p_d^2}{4M} - \varepsilon = \frac{p_n^2}{2M} + \frac{p_p^2}{2M},$$

Introducing the quantity $p = p_n - p_p$ and taking into account that $p \ll p_n, p_p, p_d$ as is verified by the last equation, and that it has in the important region a value of the order of $\sqrt{4M\epsilon}$, we obtain the following approximate relations:

$$p_d \approx 2p_n - p + (p^2 + 4M\varepsilon)/4p_n, \quad (2{:}9)$$

$$(p_d - p_n)^2 - p_p^2 = {}^1/_2\, p^2$$

$$+ 2M\varepsilon = (p_d - p_p)^2 - p_n^2.$$

Because of the small angles θ_p and θ_n (relative to the direction of the primary deuteron beam) at which the proton and neutron emerge, and also the smallness of the angle θ_{np} between the proton and the neutron (see below), we can also write:

$$(\mathbf{p}_d - \mathbf{p}_p)^2 - \mathbf{p}_n^2 \tag{2.10}$$

$$= {}^1/_2\,(p^2 + 4M\varepsilon + 2p_p p_d \vartheta_p^2),$$

$$(\mathbf{p}_d - \mathbf{p}_n)^2 - p_p^2 \tag{2.11}$$

$$= {}^1/_2\,(p^2 + 4M\varepsilon + 2p_n p_d \vartheta_n^2),$$

$$(\mathbf{p}_n + \mathbf{p}_p)^2 - p_d^2 \tag{2.12}$$

$$= -(p^2 + 4M\varepsilon + {}^1/_4\, p_d^2 \vartheta_{np}^2).$$

Expanding expressions of the type e^{ipt}/t in Fourier integrals, using the above formulae and the method of integration due to Pomeranchuk[4] we can reduce the integral Y_{110} to the form

$$Y_{110}=\frac{p_n p_p}{(2\pi i)^2\,\Omega^{3/2}}\int ds_n \int ds_p \int d\mathbf{r}\,U(r)\,\varphi(r)\exp\left\{-\frac{i}{2}\left(\mathbf{p}_d\frac{\mathbf{r}}{2}+p_n\sigma_d\right)\right\}$$

$$\times\frac{i}{p_d}\int_{-\infty}^{+\infty}\exp\{-b\sigma_\perp \operatorname{ch}\theta\}\,d\theta,$$

where σ_d and $\sigma_\perp$ are the projections of the vectors $\mathbf{s}_p-\mathbf{s}_n-\mathbf{r}$ along and perpendicular to the direction of $\mathbf{P}_d$. The variable r is limited by the value of the interaction of p and n, and s_p and s_n vary within the limits of 0 to R with the effective value $|s_p-s_n|\sim R$ much larger than r_{eff} according to our assumptions. Therefore it is possible to disregard r in the integral over θ in $\sigma_\perp$ and then the integrals over $\mathbf{s}_n$ and $\mathbf{s}_p$ separate from the integral over $\mathbf{r}$ and we obtain:

$$Y_{110}=\frac{4\pi i}{\Omega^{3/2}}\frac{p_d R}{(\mathbf{p}_n+\mathbf{p}_p)^2-p_d^2}\frac{J_1(q_d R)}{q_d} \tag{2.13}$$

$$\times\int\exp\left\{-i\left(\frac{1}{2}-\frac{p_n}{p_d}\right)\mathbf{p}_d\,\mathbf{r}\right\}U(r)\,\varphi(r)\,d\mathbf{r}$$

(q_d is the projection of q on a plane perpendicular to $\mathbf{p}_d$). Finally, we have in a similar way for Y_{001}

$$Y_{001}=\frac{4\pi i}{\Omega^{3/2}}\frac{p_d}{(\mathbf{p}_n+\mathbf{p}_p)^2-p_d^2} \tag{2.14}$$

$$\times\int\exp\left\{-\frac{i}{2}(\mathbf{p}_n-\mathbf{p}_p,\mathbf{r})\right\}$$

$$\times\,U(r)\,\varphi(r)\,d\mathbf{r}\int f\left(\frac{s_d-R}{a}\right)\exp\{-i\mathbf{q}\mathbf{s}_d\}\,d\mathbf{s}_d$$

We separate the integral over $\mathbf{s}_d$ into two parts: from 0 to R, where $f=1$, and from R to ∞ where, from Eq. (2.4), $f=e^{-(s_d-R)/a}$. The first integral is carried out in the same way as the previous one. In the second we note that those q are important that are close to $1/R_d$ and $R\gg R_d$, and consequently $qR\gg 1$. Therefore $qs_d\gg 1$.

Performing the angular part of the integration over s_d we obtain the function $J_0(qs_d)$ which we replace by its asymptotic value. In the expression preceeding the exponential in the integral over s_d instead of R. The result is

$$\int f\left(\frac{s_d-R}{a}\right)e^{-i\mathbf{q}\mathbf{s}_d}\,d\mathbf{s}_d=2\pi\frac{RJ_1(q_d R)}{q_d} \tag{2.14a}$$

$$+\sqrt{\frac{8\pi R}{q_d}}\frac{a}{1+a^2q_d^2}\left\{\cos\left(q_d R-\frac{\pi}{4}\right)\right.$$

$$\left.-\,q_d a\sin\left(q_d R-\frac{\pi}{4}\right)\right\}.$$

The integrals that remain in Eqs. (2.6), (2.7), (2.13) and (2.14) have the meaning of form factors. Their exact value depends on the form of the wave function. Indeed, if the deuteron equation

$$-(1/M)\,\nabla^2\varphi+U(r)\,\varphi=-\varepsilon\varphi$$

is multiplied by $e^{i\lambda\cdot r}$ and integrated over all space, we obtain, by integrating the first term by parts:

$$\int e^{i\vec{\lambda}\mathbf{r}}\;U(r)\,\varphi(r)\,d\mathbf{r} \tag{2.15}$$

$$=-(\varepsilon+\lambda^2/M)\int\exp\{i\vec{\lambda}\mathbf{r}\}\,\varphi(r)\,d\mathbf{r}.$$

If we take for φ the function of Eq. (1.3), then

$$\int\exp\{i\vec{\lambda}\mathbf{r}\}\,U(r)\,\varphi(r)\,d\mathbf{r}=-4\pi N/M. \tag{2.16}$$

Of course, the independence of $\overline{\lambda}$ is obtained only for this special choice of φ. Since the Eq. (1.3) is not correct at distances smaller than the range of the nuclear forces, the Eq. (2.16) is not correct for $\lambda\gg\mu$ (there should be present an additional decay with increasing λ). However, in all cases considered by us, λ has the magnitude $q<\mu$. One can convince himself of that fact by noticing that, according to the Eq. (2.8), $\overline{\lambda}$ is equal in Y_{100} Y_{010}, Y_{001} and Y_{110} respectively to $-1/2\,(\mathbf{p}_p-\mathbf{p}_n-\mathbf{q})$, $+{}^1\!/_2(\mathbf{p}_n-\mathbf{p}_p-\mathbf{q})$, $-{}^1\!/_2(\mathbf{p}_n-\mathbf{p}_p)$ and $\mathbf{p}_d(p_n-p_p)/2p_n$, and also the following relation is valid (see below):

---

[4] I. Ia. Pomeranchuk, Dokl. Akad. Nauk SSSR 96, 265 (1954).

$$p_n - p_p < 2\sqrt{M\varepsilon} \approx 0.6\ \mu.$$

Collecting the formulae of Eqs. (2.5)-(2.7), (2.13), (2.14) and (2.16), setting $q_n = q_p = q_d = q$ (because of the small scattering angles), and using the approximate relations (2.9)-(2.12), we obtain [in several cases we shall set $p_n \approx p_p \approx 1/2\, p_d$, forseeing the formula of Eq. (3.1)]:

$$
\begin{aligned}
<\chi_b^{(-)} \mid U \mid \psi_{0a} + \psi_d^{\text{пиф}}> &= \frac{4\pi i}{\Omega^{3/2}}\left(-\frac{4\pi N}{M}\right)\left\{\frac{RJ_1(qR)}{q}\left[\frac{p_n}{(\mathbf{p}_d - \mathbf{p}_p)^2 - p_n^2}\right.\right. \\
&\left.+\frac{p_p}{(\mathbf{p}_d - \mathbf{p}_n)^2 - p_p^2} + \frac{2p_d}{\mathbf{p}(_n + \mathbf{p}_p)^2 - p_d^2}\right] + \frac{p_d}{(\mathbf{p}_n + \mathbf{p}_p)^2 - p_d^2}\sqrt{\frac{2R}{\pi q}}\,\frac{a}{1+a^2q^2} \\
&\left.\times\left[\cos\left(qR - \frac{\pi}{4}\right) - qa\sin\left(qR - \frac{\pi}{4}\right)\right]\right\} \approx -\frac{16\pi^2 iN}{M\Omega^{3/2}}\,\frac{p_d}{(p_p - p_n)^2 + 4M\varepsilon} \\
&\times\left\{\frac{RJ_1(qR)}{q}\left[\frac{1}{1 + A^2\vartheta_n^2} + \frac{1}{1 + A^2\vartheta_p^2} - \frac{2}{1 + {}^1\!/_4\, A^2\vartheta_{np}^2}\right]\right. \\
&\left.-\frac{1}{1 + {}^1\!/_4\, A^2\vartheta_{np}^2}\sqrt{\frac{2R}{\pi q}}\,\frac{a}{1+a^2q^2}\left[\cos\left(qR - \frac{\pi}{4}\right) - qa\sin\left(qR - \frac{\pi}{4}\right)\right]\right\},
\end{aligned}
\tag{2.17}
$$

$$A^2 = \frac{p_d^2}{(p_p - p_n)^2 + 4M\varepsilon}, \qquad N^2 = \frac{3}{4\pi}\sqrt{M\varepsilon}.$$

It is understood that $J_1(qR)$ may be replaced everywhere by its asymptotic function.

3. THE LATERAL CROSS SECTION

According to Eqs. (1.1) and (2.17), squaring the matrix element, dividing by the current of the incident deuterons $p_d/2M\Omega$ and multiplying by the density of the final states

$$\frac{p_p^2\, dp_p\, d\omega_p\, p_n^2\, d\omega_n\, \Omega^2}{(2\pi)^6\,(dE/dp_n)}, \quad \frac{dE}{dp_n} = \frac{p_n}{M},$$

we obtain

$$d\sigma = \frac{12}{\pi^2}\sqrt{M\varepsilon}\,\frac{p_d}{[(p_p - p_n) + 4M\varepsilon]^2}\left\{\quad\right\}^2 p_n\, p_p^2\, dp_p\, d\omega_p\, d\omega_n, \tag{3.1}$$

where the quantity in parenthesis is the same as in Eq. (2.17). In squaring we, following Landau[3], shall replace $J_1(qR)$ by the average value of its asymptotic expression:

$$J_1^2(qR) \approx \frac{2}{\pi qR}\cos^2\left(qR - \frac{3\pi}{4}\right) \to \frac{1}{\pi qR};$$

and the product

$$\sin\left(qR - \frac{\pi}{4}\right)\cos\left(qR - \frac{\pi}{4}\right)$$

will also be replaced by its average value, i.e., zero, etc. Therefore

$$
\begin{aligned}
\left\{\quad\right\}^2 &= \frac{R}{\pi q^3}\left\{L^2 + \frac{a^2q^2}{1+a^2q^2}\left[\frac{1}{(1 + {}^1\!/_4\, A^2\vartheta_{np}^2)^2} + \frac{2L}{1 + {}^1\!/_4\, A^2\vartheta_{np}^2}\right]\right\}, \\
L &= (1 + A^2\vartheta_n^2)^{-1} + (1 + A^2\vartheta_p^2)^{-1} - 2\,(1 + {}^1\!/_4\, A^2\vartheta_{np}^2)^{-1}.
\end{aligned}
\tag{3.2}
$$

The denominator of the Eq. (3.1) shows that the neutron and proton produced by the splitting actually have very similar energies. The difference of the momenta is of the order

$$p = p_n - p_p \leqslant 2\sqrt{M\varepsilon}.$$

The difference of energies is

$$|E_p - E_n| \tag{3.3}$$

$$= \left|\frac{p_p^2}{2M} - \frac{p_n^2}{2M}\right| \approx \frac{2p_n}{2M}\left|p_p - p_n\right| \leqslant 2\sqrt{E_d\varepsilon},$$

where $E_d = p_d^2/4M$ is the kinetic energy of the incident deuteron. The scattering angles are of the order $(p^2 - 4M\epsilon)/p_d^2$, i.e.,

$$\vartheta_n \sim \vartheta_p \sim \vartheta_{np} \sim 8M\varepsilon / p_d^2 \sim \varepsilon / E_d. \tag{3.4}$$

Consequently, neutrons and protons emerge with practically the same energies (a few with somewhat greater difference in energy) and at the same angles as for the stripping process. However, the main difference rests in the fact that for each deuteron stripped by the nucleus, either a neutron or a proton emerges and the nucleus absorbs the remaining nucleon, undergoing a transmutation. In the diffraction splitting for each process both a neutron and a proton emerge from the interacting region. The nucleus meanwhile, experiences only a recoil by absorbing a small momentum $q \sim \sqrt{M\epsilon}$.

The total cross section is obtained by integration over p_p and the angles. We shall introduce two-dimensional vectors in place of the angles,

$$\vec{\alpha}_p = A\vec{\vartheta}_p,\ \vec{\alpha}_n = A\vec{\vartheta}_n,\ \vec{\alpha}_{np} = {}^1/_2\, A\vec{\vartheta}_{np}, \tag{3.5}$$

$$\vec{\vartheta}_{np} = \vec{\vartheta}_n - \vec{\vartheta}_p.$$

We also take into account that the component of q, the momentum transferred to the nucleus, relative $\mathbf{p}_d$ is equal [cf. Feinberg[1], Eq. (2.4a)]:

$$q_\parallel \sim 2M\varepsilon / p_d,$$

and the perpendicular component $q_\perp$ has the order of magnitude

$$p_n\vartheta_n \sim \sqrt{M\varepsilon},$$

i.e., much larger than the component along $\mathbf{p}_d$. Therefore, setting $q \approx q_\perp$, we have, according to Eq. (2.8), any one of the forms:

$$\mathbf{q} \approx (p_n\vec{\vartheta}_n + p_p\vec{\vartheta}_p) \approx (p_d/2)(\vec{\vartheta}_n + \vec{\vartheta}_p)$$

$$= ({}^1/_2\,\vec{\vartheta}_{np} + \vec{\vartheta}_p)\,p_d \tag{3.6}$$

$$= (\vec{\vartheta}_n - {}^1/_2\,\vec{\vartheta}_{np})\,p_d.$$

If we introduce new variables to facilitate integration,

$$\mathbf{q}_1 = {}^1/_2(\vec{\alpha}_n + \vec{\alpha}_p) = \mathbf{q}/c, \tag{3.7}$$

$$\mathbf{q}_2 = {}^1/_2(\vec{\alpha}_n - \vec{\alpha}_p) \equiv \vec{\alpha}_{np},$$

$$d\vec{\vartheta}_n\, d\vec{\vartheta}_p = 4A^{-4}\, d\mathbf{q}_1 d\mathbf{q}_2, \tag{3.8}$$

$$q = p_d\, q_1 A^{-1} = cq_1,\ c^2 = (p_p - p_n)^2 + 4M\varepsilon,$$

then the total cross section is:

$$\sigma = \frac{6\sqrt{M\varepsilon}R}{\pi^3} \tag{3.9}$$

$$\times \int \frac{dp_p}{[(p_p - p_n)^2 + 4M\varepsilon]^{3/2}} \frac{d\mathbf{q}_1 d\mathbf{q}_2}{q_1^3}\left\{L^2 + \frac{\beta^2 q_1^2}{1 + \beta^2 q_1^2}\right.$$

$$\left.\times\left[\frac{1}{(1 + q_2^2)^2} + \frac{2L}{1 + q_2^2}\right]\right\},$$

$$L = \frac{1}{1 + (\mathbf{q}_1 + \mathbf{q}_2)^2} + \frac{1}{1 + (\mathbf{q}_1 - \mathbf{q}_2)^2} - \frac{2}{1 + q_2^2},$$

$$\beta = ac = a\,[(p_p - p_n)^2 + 4M\varepsilon]^{1/2}.$$

carrying out the integration over $\mathbf{q}_2$ and the angles of the vector $\mathbf{q}_1$ we obtain

$$\sigma = \frac{24}{\pi}\sqrt{M\varepsilon}R \int \frac{dp_p}{[(p_p - p_n)^2 + 4M\varepsilon]^{3/2}} \int_0^{q_{1\max}} \frac{dq_1}{q_1^2}\left\{3 + \frac{1}{2q_1\sqrt{1 + q_1^2}} \ln \frac{\sqrt{1 + q_1^2} + q_1}{\sqrt{1 + q_1^2} - q_1}\right.$$

$$- \frac{4}{q_1\sqrt{4 + q_1^2}} \ln\left(1 + q_1\sqrt{4 + q_1^2}\,\frac{\sqrt{4 + q_1^2} + q_1}{\sqrt{4 + q_1^2} - q_1}\right) \tag{3.10}$$

$$\left. + \frac{1}{2}\,\frac{\beta^2 q_1^2}{1 + \beta^2 q_1^2}\left[\frac{4}{q_1\sqrt{4 + q_1^2}} \ln\left(1 + q_1\sqrt{4 + q_1^2}\,\frac{\sqrt{4 + q_1^2} + q_1}{\sqrt{4 + q_1^2} - q_1}\right) - 3\right]\right\}.$$

The integration over q_1 is carried out up to some maximum value where the momentum transferred to the nucleus $q = q_0$ (less than μ), the reciprocal of the magnitude of the smeared surface layer of the nucleus, i.e., up to

$$q_{1\,\max} = [(p_p - p_n)^2 + 4M\varepsilon]^{-1/2}\, q_0. \tag{3.11}$$

Since $\sqrt{4M\epsilon} \approx 0.6\ \mu$, it means that $q_{1\,\max} < 1$. Therefore the function inside the integral can be expanded in powers of q_1. In doing so an important problem becomes clear. We write the cross section in the form of a sum of a part independent of the deuteron dimensions, and a part, determined by the difference in the radii of the nucleus due to the interaction with the nucleon and the deuteron: $\sigma = \sigma' + \sigma''$ (so that, for example, for $\alpha = \beta = 0$ in Eq. (3.9) $d\sigma = d\sigma''$). Then the mentioned expansion yields (if the integral over $p_p - p_n$ is taken from $-\infty$ to $+\infty$):

$$\sigma' \approx \frac{24}{\pi}\sqrt{M\varepsilon}\, R \int\limits_{-\infty}^{+\infty} \frac{dp_p}{[(p_p - p_n)^2 + 4M\varepsilon]^{3/2}} \tag{3.12}$$

$$\int\limits_0^{q_{1\,\max}} dq_1 \frac{2}{5} q_1^2$$

$$= \frac{3}{80}\frac{Rq_0^3}{(M\varepsilon)^2} = \frac{3}{5} RR_d (R_d \mu)^3 \left(\frac{q_0}{\mu}\right)^3,$$

where q_0 is the maximum allowed value of the momentum absorbed by the nucleus, and $R_d = 1/2\sqrt{M\epsilon}$ is the average deuteron radius.

The second term dependent on β gives, after expansion in powers of q_1 ($aq_0 \ll 1$):

$$\sigma'' \approx \frac{12}{\pi}\sqrt{M\varepsilon}\, R \int \frac{dp_p\, a^2 q_0}{[(p_p - p_n)^2 + 4M\varepsilon]^3} = 6Ra^2 q_0. \tag{3.13}$$

Setting $a \approx 1/2R_d$ according to Eq. (2.4), we obtain

$$\sigma'' \approx {}^3/_2\, RR_d (q_0 R_d) = {}^3/_2\, RR_d R_d \mu (q_0/\mu). \tag{3.14}$$

and then

$$\sigma'/\sigma'' \approx {}^2/_5 (q_0 R_d)^2 = {}^2/_5 (R_d \mu)^2 (q_0/\mu)^2 \ll 1. \tag{3.15}$$

Consequently, the main part of the spectrum for small q is given by σ'', which is due to the difference in the effective cross sections of absorption of the nucleon and the deuteron by the nucleus.

The absolute magnitude of the cross section is not well determined. Because we have always neglected the smearing of the nuclear surface, q_0 should be much smaller than μ (as was already mentioned, it is clear from physical arguments that the differential cross-section becomes smaller at $q \gtrsim 0.6\ \mu$).

Furthermore, in computation of the main term σ'' the form of Eq. (2.4) was used for the transparency function. Because of the insufficient knowledge of the deuteron wave function this calculation cannot be trusted at $r \sim 1/\mu$. Therefore the result obtained for the integrated cross section can be good only within an order of magnitude. If we set $q_0/\mu \sim 1/3 / 1/2$, we obtain

$$\sigma \approx \sigma'' \sim RR_d. \tag{3.16}$$

If we attempt to extend the above calculations to all values of q, i.e., if we use the deuteron wave function of Eq. (1.3) for all separations, in which case we also have to change correspondingly the normalization constant N^2 by a factor of 2/3, then, integrating numerically Eq. (3.10) over q from 0 to ∞, we obtain an extremely large value for the cross section.

The energy distribution for the principal term is

$$d\sigma = \text{const}\, \frac{\sqrt{E_p}\, dE_p}{(E_p - E_n)^2 + 4\varepsilon E_d} \tag{3.17}$$

$$\sim \frac{\sqrt{E_p}\, dE_p}{(E_p - {}^1/_2 E_d)^2 + \varepsilon E_d}.$$

For stripping (transparent model) the formula has the same character (however, it should be remembered that Eq. (3.17) is strictly correct only for that part of the effect with $q \ll \mu$).

DISCUSSION OF RESULTS

The Eqs. (3.13)-(3.16) show that diffraction splitting is a real effect. Since the cross sections for production of neutrons and for production of protons by stripping are equal to $1/2\, \pi RR_d$ (for an opaque nucleus), the number of neutrons and protons emerging in correlated pairs due to diffraction splitting should be comparable with the number emerging singly due to stripping. The scattering angles and the energy distribution should be similar to those observed for stripping. Thanks to these circumstances these neutrons and protons can be separated from those produced by Coulomb stripping: the cross section of the Coulomb stripping is not only smaller than the cross section of the diffraction splitting, but it also has a different energy spectrum (two maxima).

We are not aware of any experiments in which correlated neutron-proton pairs were observed after bombardment of nuclei by deuterons with energies of the order of 100-150 mev. However, Gol'danskii L'ubimov and Medvedev[5] have pointed out that the neutron yield for these processes (at energy ~ 200 mev) is about $1\frac{1}{2} - 2$ times greater than the predictions of the stripping theory and that this discrepency can be only partially removed by the inclusion of the Coulomb stripping. Recent experiments[6] have determined the proton yield from deuterons of energy 190 mev bombarding both the light elements (Be, C) and the heavy ones (U). The results showed a considerably larger cross section than one computed for stripping by an opaque nucleus: for Be and C $\sigma_{exp} = 0.35 \pm 0.03$ barns, for U$\sigma_{exp} = 1.4 \pm 0.2$ barns[7], while the formula $\sigma^{opaque}_{strip} = 1/2\pi RR_d$ gives 0.12 and 0.43 barns, respectively. The cross section for the electric stripping is 0.1 barn for U.

Various authors bring up for consideration an additional stripping process which is due to the transparency of the U nucleus. In this process the deuteron is wholly absorbed by the nucleus — the cross section for this absorption is $\pi R^2 \sim 2.5$ barns - undergoes stripping inside the nucleus and the proton can escape from the nucleus due to the small but still present transparency of the U nucleus ~ 0.12. The exact theoretical calculation of this last effect is very difficult since small changes in the transparency factor and variations in the description of the details of the process cause sharp changes of its contribution to the total cross section.

It is not impossible that diffraction splitting takes place in this case. More definite results could be obtained only from experiments at somewhat smaller energies, at which the transparency of the nuclei does not come into effect, particularly because for a semitransparent nucleus the yield of correlated pairs may be due to stripping inside the nucleus (it is true that a simultaneous emergence of both particles is comparatively improbable.

An interesting facet of the discussed process is its independence of energy. That fact allows us to expect that it should have still a measurable magnitude even in the relativistic energy range.

Translated by M. J. Stevenson
15

---

[5] V. I. Gol'danskii, A. L. L'ubimov and B. V. Medvedev, Usp. Fiz. Nauk 48, 531 (1952).

[6] L. Schecter, W.E. Crandall, G. P. Millburn, D. A. Hicks and A. V. Shelton, Phys. Rev. 90, 633 (1953).

[7] L. Schecter and W. Heckrotte, Phys. Rev. 94, 1086 (1954).

SOVIET PHYSICS JETP VOLUME 3, NUMBER 1 AUGUST, 1956

The Theory of the Electron Field Mass in the Presence of an External Medium

A. A. SOKOLOV AND V. N. TSYTOVICH
Moscow State University

(Submitted to JETP editor October 29, 1954)
J. Exper. Theoret. Phys. USSR 30, 136-140, (January, 1956)

Examination is made of the field correction to electron mass caused by an external medium. Second-order perturbation theory is used in the calculations.

IT was shown in many works[1,2] that the interaction between a charged particle and a quantum electromagnetic field produces in the particle an additional field mass, due to the radiation field (real-photon field), with which this charged particle is in equilibrium. This change in mass, depending on the temperature of the equilibrium radiation, causes a shift in the levels of the atomic systems. Under normal conditions this shift is small relative to the Bethe shift which, in particular, is related to the peculiar process of virtual emission and absorption of photons.

We shall consider in this article field corrections to the mass of an electron (or in general of any charged particle having a spin 1/2), produced by a medium characterized by a dielectric constant $\epsilon(\omega)$ and a magnetic permeability $\mu(\epsilon)$. The electromagnetic self-energy of a Fermion is known to diverge logarithmically, but the difference between its value in an external medium and in a vacuum is convergent[3], as will be shown below. These field corrections to the electromagnetic mass of the Fermion depend naturally on the parameters that characterize the medium.

A macroscopic description of the medium in terms of the parameters ϵ and μ is made possible by so renormalizing the self-energy (subtracting the self-energy of the particle in vacuum) that the higher frequencies, i.e., the shorter wavelengths, are cut off. A substantial share of the field correction is due here only to frequencies below the resonant frequencies that cause dispersion. This corresponds to wavelengths considerably in excess of the interatomic distances.

2. The electromagnetic field in a medium obeys the known differential equations:

$$\nabla^2 A'_\nu - \frac{\varepsilon\mu}{c^2}\frac{\partial^2 A'_\nu}{\partial t^2} = 0, \quad \nu = 1,\ 2,\ 3,\ 4. \tag{1}$$

here: $A'_n = A_n/\mu\ (n = 1, 2, 3);\ A'_4 = \varepsilon A_4;$

A_n is the vector potential and $A_0 = -iA_4$ the scalar potential of the field. What matters now from here on is that ϵ and μ are frequency dependent as in the case of Cerenkov radiation. These quantities must therefore be considered as operators, the manipulation of which is defined, for example, by Eq. (27.5) of reference 4. One cannot therefore divide the first three equations of (1) by $1/\mu$ or the last of these equations by ϵ.

The quantization of the free transverse electromagnetic field in a medium has already been discussed[5-7] in connection with the quantum theory of the Cerenkov effect.

Let us consider the general quantization of the electromagnetic field in a medium with the aid of a Lagrangian that leads directly to (1) (see reference 8):

$$L = \frac{1}{8\pi}\varepsilon E^2 - \frac{1}{8\pi\mu}H^2 - \frac{1}{8\pi}\left(\operatorname{div}\mathbf{A} + \frac{\varepsilon\mu}{c}\frac{\partial A_0}{\partial t}\right)^2. \tag{2}$$

Assume the field to be contained in a large cube of side L, and expand the potentials in corresponding Fourier series, using standard methods; this results in an expression for the quantized potentials:

$$A_\nu = L^{-3/2}\sum_{\mathbf{q}}\sqrt{\frac{2\pi c'_\nu\hbar}{q}}\,[a_\nu(\mathbf{q}) \times \exp\{-ic'qt + i\mathbf{qr}\} + a_\nu^+(\mathbf{q})\exp\{ic'qt - i\,\mathbf{q}\cdot\mathbf{r}\}], \tag{3}$$

---

[1] S.V.Tiablikov, J. Exper. Theoret. Phys. USSR 21, 16 (1951).

[2] O. Kothary and F. Auluk, Nature 162, 143 (1948)

[3] V.N.Tsytovich, Dissertation, Moscow State University, 1954.

[4] D. Ivanenko and A. Sokolov. Classical Field Theory, Moscow-Leningrad, GITTL, 1951.

[5] A.A.Sokolov, Dokl. Akad. Nauk SSSR, 28, 415 (1940).

[6] V. L. Ginzburg, J. Exper. Theoret. Phys. USSR 10, 589 (1940).

[7] T. Taniuti, Progr. Theor. Phys. 6, 207 (1951).

[8] V. Fock and B. Podol'skii, Z. Phys. Sowjetunion 1, 801 (1932).

where $q = |\mathbf{q}|, \quad c'_n = c'\mu, \quad n = 1, 2, 3,$

$c'_4 = c'/\varepsilon, \quad c' = c/\sqrt{\varepsilon\mu}, \quad a_4 = ia_0, \quad a_4^+ = ia_0^+,$

and the amplitudes a_ν satisfy the commutation rules

$$[a_\nu(\mathbf{q}),\ a_{\nu'}^+(\mathbf{q}')] = a_\nu(\mathbf{q})\, a_{\nu'}^+(\mathbf{q}') - a_{\nu'}^+(\mathbf{q}')\, a_\nu(\mathbf{q}) = \delta_{\nu\nu'}\delta_{\mathbf{q}\mathbf{q}'}. \tag{4}$$

From this, it is also possible to find the commutation rules for the global fields:

$$[A_\nu(\mathbf{r}, t), A_\nu(\mathbf{r}', t')] = \frac{4\pi c'_\nu \hbar}{i}\, \frac{1}{8\pi^3} \int \exp\{i\mathbf{q}\cdot(\mathbf{r} - \mathbf{r}')\}\, d^3q\, \frac{\sin c'q\,(t - t')}{q}. \tag{5}$$

Comparing (5) with the commutation relations in vacuum we see that, owing to the frequency dependence of the velocity c' on the frequency, the function in the right half of Eq. (5) is spread out over the light cone. If $\epsilon = \mu = 1$, the functions (5) become the ordinary commutation relations in vacuum (Δ-functions).

The quantized wave functions of the free Dirac field are of the known form:

$$\psi_\nu(\mathbf{r}, t) = \sum_n c_n \psi_n(\mathbf{r}, t) = L^{-3/2} \sum_n c_n b_{n\nu} e^{-icKt + i\mathbf{k}\mathbf{r}}, \tag{6}$$

where

$K = \lambda\sqrt{k^2 + k_0^2}; \ k_0 = mc/\hbar; \ \lambda = \pm 1, \ b_{n\nu}$

are known matrices characterizing the spin states and

$$c_{n'}^+ c_n + c_n c_{n'}^+ = \delta_{nn'}. \tag{7}$$

Furthermore, the operators $\overline{\psi}$ and $\overline{A}_\nu$ of the interacting fields must satisfy the following equations:

$$\left(-\frac{\hbar}{i}\frac{\partial}{\partial t} - H\right)\overline{\psi} = -e\alpha_\nu \overline{A}_\nu \overline{\psi}, \tag{8}$$

$$\nabla^2 \overline{A}_\nu - \frac{\varepsilon\mu}{c^2}\frac{\partial^2 \overline{A}_\nu}{\partial t^2} = 4\pi e \overline{\psi}^+ \alpha_\nu \overline{\psi}, \tag{9}$$

where

$$\nu = 1, 2, 3, 4; \quad \overline{A}_n = \overline{A}_n/\mu, \quad n = 1, 2, 3,$$

$$\overline{A}_4 = \varepsilon \overline{A}_4; \quad e_- = -e$$

is the electron charge and $H = (c\hbar/i)\vec{\alpha}\cdot\vec{\nabla} + \beta mc^2$ is the Hamiltonian of the Dirac equation. Equations (8) and (9) are general equations for the semi-phenomenological quantum electrodynamics in media (in the Heisenberg representation).

The operators $\overline{\psi}$ and A_ν can be expressed in terms of the free-field operators ψ and A_ν using the known operator S;

$$\overline{\psi} = S\psi S^{-1}, \quad \overline{A}_\nu = SA_\nu S^{-1}, \tag{10}$$

where $S = e^{v} = 1 + v + v'v + v''v'v + \ldots, \ S^{-1} = e^{-v} = 1 - v + vv' + vv'v'' - \ldots,$

$$vv' = \int_{-\infty}^{t} u(t')\, dt' \int_{-\infty}^{t'} u(t'')\, dt''$$

etc., and

$$v = \int_{-\infty}^{t} u(t')\, dt' = \frac{ie}{\hbar}\sum_{nn'} C_{n'n} v_{n'n}, \tag{11}$$

$$u(t) = \frac{ie}{\hbar}\int \psi^+(\mathbf{r}, t)\,\alpha_\nu A_\nu(\mathbf{r}, t)\,\psi(\mathbf{r}, t)\, d^3x = \frac{ie}{\hbar}\sum_{n'n} C_{nn'} u_{n'n},$$

$$v_{n'n} = \int_{-\infty}^{t} u_{n'n}\, dt, \tag{12}$$

$$u_{n'n} = \int d^3x\, \psi_{n'}^+(\mathbf{r}, t)\,\alpha_\nu A_\nu(\mathbf{r}, t)\,\psi_n(\mathbf{r}, t), \tag{13}$$

whereby, since the theory is symmetrical with respect to the sign of the charge, we have

$$C_{n'n} = {}^1/_2\,(C_{n'}^+ C_n - C_n C_{n'}^+). \tag{14}$$

The validity of (10) is confirmed most simply by direct substitution into Eqs. (8) and (9), using the commutation relations (4), (5), and (7).

The fields $\overline{\psi}$ and $\overline{A}_\nu$ can be expanded in terms to the interaction constants as follows:

$$\overline{\psi} = \psi + [v\psi] + [v'[v\psi]] + \ldots \tag{15}$$

If second-order perturbation theory is used, the energy process of interest to us, that of emission and absorption of a virtual photon in the presence of a medium, is given by the third term of the right half of Eq. (15). To obtain the amplitude of the transition it is necessary to substitute Eqs. (11)-(13) and (3) into Eq. (15), and use the commutation relations corresponding to the absence of photons in the initial and final instant of time:

$$a_{\nu'}^+(\mathbf{q}')\, a_\nu(\mathbf{q}) = 0, \quad a_\nu(\mathbf{q})\, a_{\nu'}^+(\mathbf{q}') = \delta_{\nu\nu'}\delta_{\mathbf{q}\mathbf{q}'}, \tag{16}$$

and to the presence of one electron in state $n=0$ at the initial instant of time:

$$C^+_{n_+}C_{n_+} = \delta_{n_+0}, \quad C_{n_+}C^+_{n_+} = 1 - \delta_{n_+0}, \qquad (17)$$
$$C^+_{n_-}C_{n_-} = 1, \quad C_{n_-}C^+_{n_-} = 0,$$

where n_+ denotes states with positive energy and n_- those with negative energy. From this it is possible to find the average value of the perturbation energy, which in the approximation employed will have the following form:

$$V = \frac{e^2}{2i\hbar}\sum_{n_+n_-}(u_{0n_+}v_{n_+0} + v_{n_-0}u_{0n_-} - v_{0n_+}u_{n_+0} - u_{n_-0}v_{0n_-}). \qquad (18)$$

3. We shall restrict ourselves from now on to a discussion of transparent dielectrics, for which $\mu=1$, $n=\sqrt{\epsilon}$. In this case, substituting expressions (12), (13) and (3) into (18) and using (16) we obtain:

$$V = \frac{e^2}{4\pi^2}\int\frac{d^3q}{qn}\left\langle\psi_0^+\alpha_n\left[K_0 - H_{\mathbf{k}-\mathbf{q}} - \frac{q}{n}\frac{H_{\mathbf{k}-\mathbf{q}}}{|H_{\mathbf{k}-\mathbf{q}}|}\right]^{-1}\alpha_n\psi_0\right\rangle - \frac{e^2}{4\pi^2}\int\frac{d^3q}{qn^2}\left\langle\psi_0^+\left[K_0 - H_{\mathbf{k}-\mathbf{q}} - \frac{q}{n}\frac{H_{\mathbf{k}-\mathbf{q}}}{|H_{\mathbf{k}-\mathbf{q}}|}\right]^{-1}\psi_0\right\rangle. \qquad (19)$$

Here ψ_0 and K_0 refer to the initial state of the electron, $H_{k-q}=\alpha(k-q)+\beta k_0$. Further, squaring the denominator, averaging the entire expression over all angles of vector q, and assuming the momentum of the electron $k=0$, we obtain:

$$V = \langle\psi_0^+ U\psi_0\rangle = \int\psi_0^+ U\psi_0 d^3x;$$

where

$$U = \frac{e^2}{4\pi^2}k_0\int\frac{d^3q}{q}\frac{q(3+n^{-2})+2K'n^{-1}}{n^2K'q(q+qn^{-2}+2K'n^{-1})}, \qquad (20)$$

and $K' = \sqrt{q^2+k_0^2}$. Assuming $n=1$ in Eq. (20) we obtain a well-known result, namely the logarithmically divergent field energy

$$U_0 = \frac{\alpha}{\pi}\left(\frac{3}{2}\int_0^\infty\frac{dq}{K'} - \frac{1}{4}\right)mc^2, \qquad (21)$$

(see, for example, reference 9, page 399) where $\alpha=e^2/\hbar c$. The energy (21) must be subtracted from the energy (20) if we want to compute the effect of the dielectric on the field mass.

To obtain the dependence of the index of refraction on the field mass, we employ the following equation

$$n^2 = 1 + \frac{4\pi Ne_1^2}{m_1}\sum_k \mathrm{Re}\,\frac{f_k}{\omega_k^2-\omega^2-i\gamma\omega}, \qquad (22)$$

where N is the density of the medium, e_1 and m_1 the charge in the mass of the particles forming the medium, ω_K the resonant oscillation frequencies, and γ the damping coefficient.* Then for $n-1\ll 1$ the additional energy $U'=U-U_0$ will be

$$U' = \sum_k f_k U_k, \qquad (23)$$

where

$$U_k = -mc^2\frac{\alpha}{\pi}\frac{2\pi Ne_1^2}{m_1\omega_k^2} \qquad (24)$$
$$\left\{\mathrm{Re}\int_0^\infty\frac{xdx}{(1-x^2-i\eta_k x)(x+\sqrt{x^2+\zeta_k^2})\sqrt{x^2+\zeta_k^2}} + 2\,\mathrm{Re}\int_0^\infty\frac{dx}{\sqrt{x^2+\zeta_k^2}(1-x^2-i\eta_k x)}\right\},$$

and the parameter $\zeta_K=mc^2/\hbar w_K$ characterizes the ratio of the rest energy mc^2 of the particle under investigation to the binding energy of the electron (or other particles) forming the medium.

The integrals (24) can be evaluated in closed form. In this case we obtain:

$$U_k = -mc^2\frac{\alpha}{4\pi\sqrt{\zeta_k^2+1}}\frac{2\pi Ne_1^2}{m_1\omega_k^2} \qquad (25)$$
$$\left\{5\ln\frac{\sqrt{\zeta_k^2+1}+1}{\sqrt{\zeta_k^2+1}-1} - \frac{(\sqrt{\zeta_k^2+1}-1)^2}{\zeta_k^2}\ln\frac{2}{\sqrt{\zeta_k^2+1}-1} + \frac{(\sqrt{\zeta_k^2+1}+1)^2}{\zeta_k^2}\ln\frac{2}{\sqrt{\zeta_k^2+1}+1}\right\}.$$

4. Let us consider the limiting case, when the binding energy of the electrons in the medium is considerably less than the rest energy of the charged Fermion, $\hbar w_K \ll mc^2$, i.e., $\zeta\gg 1$. Then

---

* We introduced the damping term in (22) to establish the correct integration path around the singular points; in the final results we put $\gamma=0$ (transparent dielectric).

[9] A. Sokolov and D. Ivanenko, Quantum Field Theory, Moscow-Leningrad, 1952.

$$U_k \cong - mc^2 \frac{\alpha}{\pi} \left(\frac{2\pi N e_1^2}{m_1 \omega_k^2}\right) \frac{1}{\zeta_k^2}\left(2 - \ln\frac{\zeta_k}{2}\right), \tag{26}$$

$$U = \Delta mc^2, \Delta m = -\frac{\alpha}{\pi} m \sum_k f_k \frac{2\pi N e_1^2}{m_1\omega_k^2}\frac{\hbar^2\omega_k^2}{m^2c^2}\left(2-\ln\frac{mc^2}{2\hbar\omega_R}\right). \tag{27}$$

Using the fact that $\sum_k f_k=1$, we can write the last result in the following form:

$$\Delta m = -\frac{\alpha}{2\pi} m\,(\varepsilon(0)-1) \tag{28}$$
$$\times \left(\frac{\hbar\omega_0}{mc^2}\right)^2\left(2-\ln\frac{mc^2}{2\hbar\omega_f}\right),$$

where $\epsilon(0)$ is the value of the dielectric constant at zero frequency; $w_f = \prod_k w_k^{f_k}$, and w_0 is determined from the following equation

$$\omega_0^{-2} = \sum_k f_k\,\omega_k^{-2}. \tag{29}$$

If the dispersion of the dielectric constant is due to the bound electrons of the medium, then $\hbar w_0/mc^2$ is of the order of α^2, since $m_1=m$ and $e_1=e$. In this case Δm is 10^{-11} $[\epsilon(0)-1]$ times the mass of the electron.

For the hydrogen atom, for example, it is possible to obtain from (29) the following level shift, caused by the effect of the dielectric on the mass:

$$\Delta E = \frac{Rh}{n^2}\frac{\alpha}{2\pi}(\varepsilon(0)-1)\left(\frac{\hbar\omega_0}{mc^2}\right)^2 \tag{30}$$
$$\times\left(2-\ln\frac{mc^2}{2\hbar\omega_f}\right),$$

of the order of $(Rh/n^2)\alpha^5$. If $n=2$, the change in frequency is of the order

$$\Delta\nu \sim 0.01\,(\varepsilon(0)-1) \tag{31}$$

It must be noted that under normal conditions (under normal temperature and pressure) the incremental mass and the change in frequency caused by the presence of a medium are small compared with the corresponding Bethe quantities, but are nevertheless greater than the corrections required by the radiation field.[1]

Translated by J.G.Adashko
17

SOVIET PHYSICS JETP VOLUME 3, NUMBER 1 AUGUST, 1956

Excitation of the Collective Levels of Heavy Nuclei by Neutrons*

D. F. ZARETSKII AND A. V. SHUT'KO

(Submitted to JETP editor, April 9, 1955)
J. Exper. Theoret. Phys. USSR 30, 141-147 (January, 1956)

On the basis of the modal representation of A. Bohr and B. Mottelson[1,2], the inelastic scattering of neutrons by the collective levels of the target nucleus are calculated for the case in which there is no compound nucleus formation.

UNTIL recently, it has been assumed that reactions involving heavy nuclei (among which we include the inelastic scattering of neutrons) always pass through a compound nucleus phase. However, in the light of the recent researches of A. Bohr and B. Mottelson on a collective model of the nucleus[1,2], another mechanism for inelastic scattering can be considered: the neutron, in passing close to the target nucleus, produces a "tidal wave" in it, thus exciting surface vibrations (see reference 2, p. 158).

1. CALCULATION OF THE EFFECTIVE CROSS SECTION OF INELASTIC SCATTERING (GENERAL CASE)

We begin with the Hamiltonian of the total system: target nucleus and passing particle:

$$H_{\text{tot}}\,(\mathbf{r},\alpha,\mathbf{x}) = -\frac{\hbar^2}{2M}\nabla_r^2 + \hat{H}_{\text{n}}(\alpha,\mathbf{x}) + U(\mathbf{r},\alpha). \tag{1}$$

Here **r** represents the coordinates of the passing particle relative to the center of the target nucleus; α and **x** are, respectively, the set of collective coordinates and the coordinates of the individual particles of the target nucleus. The operator H_{n} defines the internal motion of the nucleus, $U(\mathbf{r},\alpha)$ is the energy of interaction between the scattered particle and the nucleus. Here we assume that the scattered particle interacts only with the collective degrees of freedom of the target nucleus. We can assume, approximately, that the incident neutron moves in an average field, changes in which are connected to the collective motions in the nucleus. In view of the small compressibility of nuclear matter, this collective motion can be associated only with the motion of the nuclear surface; for example, we can take as collective coordinates the expansion coefficients of the equation of the surface in spherical harmonics:

$$R(\vartheta,\varphi) = R_0\Big[1 + \sum_{\lambda,\mu}\alpha_{\lambda\mu}\,Y_{\lambda\mu}(\vartheta,\varphi)\Big], \tag{2}$$

where R_0 is the mean radius of the nucleus.

For a spherical nucleus, the mean field which acts on the nucleon is spherically symmetric:

$$U(\mathbf{r},\alpha) = V(r) \equiv f(r/R_0); \tag{3}$$

the equipotential surfaces, which include the surface of the nucleus, are concentric spheres. In adiabatic deformations of the nuclear surface, all equipotential surfaces will be deformed similarly; the potential in this case will no longer be spherically symmetric:

$$U(\mathbf{r},\alpha) = f(r/R(\vartheta,\varphi)) \equiv f(\xi), \tag{4}$$

where $R(\vartheta,\varphi)$ is the expression for the deformed surface (2); $\xi_0 = r/R$.

We expand the function (4) about the point $\xi_0 = r/R_0$:

$$f(\xi) = f(\xi_0) + \sum_{n=1}^{\infty}\frac{1}{n!}\frac{\partial^n f(\xi)}{\partial\xi^n}\bigg|_{\xi=\xi_0}(\xi-\xi_0)^n.$$

From Eq. (3) we obtain

$$\partial^n f(\xi)/\partial\xi^n\,|_{\xi=\xi_0} = R_0^n\,\partial^n V(r)/\partial r^n.$$

Taking Eq. (2) into account, we have

$$U(\mathbf{r},\alpha) = V(r) + \sum_{n=1}^{\infty}\frac{(-1)^n r^n}{n!}\frac{\partial^n V(r)}{\partial r^n}\cdot\left[\frac{\sum_{\lambda,\mu}\alpha_{\lambda\mu}Y_{\lambda\mu}(\vartheta,\varphi)}{1+\sum_{\lambda,\mu}\alpha_{\lambda\mu}Y_{\lambda\mu}(\vartheta,\varphi)}\right]^n. \tag{5}$$

In the study of processes involving excitation of the collective levels of the nuclei, we limit ourselves to the first two terms of the expansion (5), thus assuming the deformations to be small. We have for the total Hamiltonian in this case:

$$\hat{H}_{\text{tot}}\,(\mathbf{r},\alpha,\mathbf{x}) = -(\hbar^2/2M)\nabla_r^2 + V(r) + \hat{H}_{\text{n}}(\alpha,\mathbf{x}) + W(\mathbf{r},\alpha), \tag{6}$$

where the perturbation term is

---

* This work was completed in November, 1954.

[1] A. Bohr, Dan Mat. Fys. Medd. 26, 14 (1952).

[2] A. Bohr and B. R. Mottelson, Dan. Mat. Fys. Medd. 27, 16 (1953).

$$W(\mathbf{r}, \alpha) = -r\frac{\partial V(r)}{\partial r}\sum_{\lambda,\mu}\alpha_{\lambda\mu}Y_{\lambda\mu}(\vartheta, \varphi). \qquad (7)$$

In order to estimate the magnitude of the effective cross section of inelastic scattering, we make use of the general formula for the probability of transition between states of the continuous spectrum, under the action of a perturbation, which does not depend upon time:

$$dW_{\nu\nu'} = (2\pi/\hbar)\,|W_{\nu'\nu}|^2\,\delta(E_{\nu'} - E_\nu)\,d\nu', \qquad (8)$$

where ν represents the set of quantum numbers **k** and n (**k** is the propagation vector of the particle at infinity, n is the quantum number which characterizes the discrete levels of the target nucleus), $E_\nu = E_n + E_k$, where E_n is the energy level of the target nucleus and E_k is the kinetic energy of the particle at infinity.

The matrix element $W_{\nu'\nu} \equiv W_{nk}^{n'k'}$ is determined by means of the zeroth approximation wave functions:

$$\psi_{n,\mathbf{k}} = F_{\mathbf{k}}(\mathbf{r})\,\varphi_n(\alpha, \mathbf{x}), \qquad (9)$$

where the $\varphi_n(\alpha, x)$ are determined from the equation

$$H_{\mathbf{n}}(\alpha, \mathbf{x})\,\varphi_n(\alpha, \mathbf{x}) = E_n\varphi_n(\alpha, \mathbf{x}), \qquad (10)$$

and the functions $F_k(r)$ satisfy the equation

$$[-(\hbar^2/2M)\nabla_r^2 + V(r)]\,F_{\mathbf{k}}(\mathbf{r}) = E_{\mathbf{k}}F_{\mathbf{k}}(\mathbf{r}). \qquad (11)$$

We write the matrix element $W_{nk}^{n'k'}$ in the form:

$$\begin{aligned} W_{n\mathbf{k}}^{n'\mathbf{k}'} &= \int F_{\mathbf{k}'}(\mathbf{r}')\,\varphi_{n'}(\alpha, \mathbf{x})\,W(\mathbf{r}', \alpha)\,\varphi_n(\alpha, \mathbf{x})\,F_{\mathbf{k}}(\mathbf{r}')\,(d\mathbf{r}')\,(d\alpha)\,(d\mathbf{x}) \\ &= \int F_{\mathbf{k}'}(\mathbf{r}')\,W_{n'n}(\mathbf{r}')\,F_{\mathbf{k}}(\mathbf{r}')\,(d\mathbf{r}'), \end{aligned} \qquad (12)$$

where the matrix element $W_{n'n}$ is determined by means of the wave functions of the stationary state of the target nucleus: (13)

$$\begin{aligned} W_{n'n}(\mathbf{r}') &= \int \varphi_{n'}(\alpha, \mathbf{x})\,W(\mathbf{r}', \alpha)\,\varphi_n(\alpha, \mathbf{x})\,(d\alpha)\,(d\mathbf{x}) \\ &= -r'\frac{\partial V(\bar{r}')}{\partial r'}\sum_{\lambda,\mu}\langle\alpha_{\lambda\mu}\rangle\,Y_{\lambda\mu}(\vartheta', \varphi'). \end{aligned}$$

For the differential $d\nu'$ in Eq. (8) we use the element of volume in wave space: $dk'_x dk'_y dk'_z$. In spherical coordinates,

$$d\nu' = k'^2\,dk'\,d\Omega = {}^1/_2\,k'd(k'^2)\,d\Omega.$$

As wave functions for the incident and scattered neutrons we have the "distorted" waves $F_k(r)$ and $F_{k'}(r)$, where F_k is normalized to unit current density and $F_{k'}$ to the δ-function in the space of the propagation vector:

$$F_{\mathbf{k}} = (4\pi M/\hbar k)^{1/2} \qquad (14)$$

$$\times\sum_{l=0}^{\infty} i^l\sqrt{2l+1}\,R_{kl}(r')\,Y_{l0}(\vartheta', \varphi'),$$

$$F_{\mathbf{k}'} = (2\pi)^{-3/2}\,4\pi \qquad (15)$$

$$\times\sum_{l'=0}^{\infty}\sum_{m'=-l'}^{l'}(-i)^{l'}R_{k'l'}(r')\,Y_{l'm'}^{*}(\vartheta', \varphi')\,Y_{l'm'}(\vartheta, \varphi),$$

where ϑ, φ are the angles of scattering, R_{kl} are the radial wave functions.

For such normalized functions F_k and $F_{k'}$, the expression $dW_{\nu\nu'}$ is the differential inelastic scattering cross section

$$d\sigma_{\nu\nu'} = 4\pi M\hbar^{-3}k'\,|W_{\nu'\nu}|^2 d\Omega. \qquad (16)$$

We have already carried out integration over **k**′ in Eq. (16), which yields the value for k':

$$k' = [2M\hbar^{-2}(E_k - \Delta E_{n'n})]^{1/2},$$

$$\Delta E_{n'n} = E_{n'} - E_n.$$

The effective cross section of inelastic scattering of an unpolarized beam of neutrons is equal to

$$d\sigma_{AB} = (2I_A + 1)^{-1}\sum_{M_A}\sum_{M_B} d\sigma_{\nu\nu'}, \qquad (17)$$

where M_A and M_B are the projections of the spin of the target nucleus in the ground and excited states. Carrying out a series of calculations, we get

$$d\sigma_{AB} = d\Omega\sum_{J=0}^{\infty} B_J(k', k)\,P_J(\cos\vartheta), \qquad (18)$$

where $P_J(\cos\vartheta)$ are the Legendre polynomials, and the coefficients $B_J(k', k)$ are equal to

$$B_J(k', k) = \frac{1}{9(2I_A + 1)} \qquad (19)$$

$$\times\sum_{\lambda=|I_A - I_B|}^{I_A + I_B}(2\lambda + 1)\,(R_0^{\lambda})^{-2}\,|Q_{BA}^{(\lambda)}|^2 A_{J\lambda}(k', k),$$

$$A_{J\lambda}(k',k) = \frac{k'}{k}\sum_{L=0}^{\infty}\ \sum_{L'=|L-J|}^{L+J}\ \sum_{l=|L-\lambda|}^{L+\lambda}\ \sum_{l'=|L'-\lambda|}^{L'+\lambda} (-)^{J-\lambda}(2L+1)(2L'+1) \tag{20}$$

$$\times (2l+1)(2l'+1)(LL'00\,|\,LL'J0)(ll'00\,|\,ll'J0)\,W(LL'll';J\lambda)$$

$$\times (Ll00|Ll\lambda 0)(L'l'\lambda 0|L'l'\lambda 0)\,\mathrm{Re}\,[(-i)^{L+l'}\,i^{L'+l}\,P_{Ll}(k',k)\,P_{L'l'}(k',k)];$$

$$P_{Ll}(k',k) = 2M\hbar^{-2}\int_0^{\infty} R^{*}_{k'L}(r)\,\frac{\partial V(r)}{\partial r}\,R_{kl}(r)\,r^3 dr, \tag{21}$$

$W(LL'll';J\lambda)$ are the Racah coefficients[3,4], $(ab00|abc0)$ are the Klebsch-Gordon coefficients.

In Eq. (13) we have replaced the matrix element $W_{n'n}$ by the matrix element $<\alpha\lambda\mu>$ of the multipole moment of transition according to the equation (see Appendix)

$$\langle\alpha_{\lambda\mu}\rangle = (4\pi/3R_0^{\lambda})\left(\frac{2\lambda+1}{4\pi}\right)^{1/2} \tag{22}$$

$$\times (-)^{M_B}(I_B I_A - M_B M_A\,|\,I_B I_A \lambda\mu)\,Q^{(\lambda)}_{BA}.$$

It can be seen from Eq. (18) that the total cross section of inelastic scattering is equal to

$$\sigma_{AB} = 4\pi B_0(k',k), \tag{23}$$

with B_0 from Eq. (19), Eq. (20) reduces to

$$A_{0\lambda}(k',k) = \frac{k'}{k}\sum_{L=0}^{\infty}\ \sum_{l=|L-\lambda|}^{L+\lambda}(2L+1) \tag{24}$$

$$\times (2l+1)(Ll00\,|\,Ll\lambda 0)^2\,|P_{Ll}(k',k)|^2.$$

Knowing the quantities Q_{BA}, which characterize the collective levels of the target nucleus, we can calculate the differential and total cross sections of the inelastic scattering of neutrons by Eqs. (18)-(24).

2. EXCITATION OF THE ROTATIONAL LEVELS OF EVEN-EVEN NUCLEI

We now investigate the important case of the excitation of the rotational levels in heavy even-even nuclei. It is known from experiments that the lowest energy levels of even-even nuclei, far from closed shells, satisfy the relation:

$$E_I = (\hbar^2/2J)\,I(I+1), \quad I = 0, 2, 4\,\ldots, \tag{25}$$

where $J = 3B\beta$ is the effective moment of inertia, β characterizes the total deformation of the nucleus, B is a parameter associated with the mass.

In the energy region close to the ground state of the nucleus, the most important type of collective motion is the quadrupole vibration of the surface.

In the adiabatic approximation of the Bohr-Mottelson theory, the wave function describing even-even nucleus in the lower energy states (25) has the form

$$\psi_n = \sqrt{\frac{2I+1}{8\pi^2}}\,\varphi_{n_\beta n_\gamma}(\beta,\gamma)\,\chi_0\,D_{M0}(\theta_i), \tag{26}$$

where the functions $D^{I}_{M0}(\vartheta,\varphi\,\psi)$ describe the nuclear rotation; ϑ, φ ψ are the Euler angles which fix the principal axes of the deformed nucleus relative to the fixed system of coordinates; I and M are the spin of the nucleus and its projection on the fixed axis z.

We consider transitions between states which are characterized by the quantum numbers $I_A = 0$ and $I_N = I$. We seek the quantity $Q^{(\lambda)}_{BA} \equiv Q^{(I)}_{I0}$. It can be shown (see Appendix) that

$$Q^{(I)}_{I0} = \prod_{k=1}^{I/2}\left[\frac{10(4k-1)(4k-3)}{3\cdot 2k(2k-1)(4k+1)}\right]^{1/2} Q^{(2)}_{2k,2k-2} \tag{27}$$

We have for the wave functions (26)^2

$$Q^{(2)}_{2k,2k-2} = \left[\frac{3\cdot 2k(2k-1)}{10(4k-1)}\right]^{1/2}\frac{Q_0}{2Z}, \tag{28}$$

whence

$$Q^{(I)}_{I0} = (2I+1)^{-1/2}(Q_0/2Z)^{I/2}, \tag{29}$$

where Q_0 is the internal quadrupole moment of the target nucleus^2. The magnitude of Q_0 characterizes the degree of deformation of the nuclear material.

Substituting Eq. (29) into Eq. (23), we obtain the total effective cross section of inelastic scattering of neutrons on the rotational level of the heavy even-even nucleus:

$$\sigma_{0I} = (4\pi/9)(Q_0/2ZR_0^2)^I A_{0I}(k',k), \tag{30}$$

$$I = 2, 4, 6, \ldots$$

---

[3] L. C. Biedenharn, J. M. Blast and M. E. Rose, Rev. Mod. Phys. 24, 249 (1952).

[4] K. Alder, Helv. Phys. Acta 25, 235 (1952).

$$A_{0I}(k', k) = \frac{k'}{k} \sum_{L=0}^{\infty} \sum_{l=|L-I|}^{L+I} (2L+1)(2l+1)(L\,l\,00\,|\,L\,l\,I\,0)^2\,|P_{Ll}(k', k)|^2, \tag{31}$$

$$k'^2 = 2M\hbar^{-2}(E_k - \Delta E_{I0}), \quad \Delta E_{I0} = E_I - E_0,$$

where E_I is the energy of the rotational level (25).

If we assume $V(r)$ to be a potential well with sufficiently steep walls, we get from Eq. (21) (with a high degree of accuracy)

$$P_{Ll}(k', k) = 2M\hbar^{-2} R^{*}_{k'L}(R_0)\, V_0\, R_{kl}(R_0)\, R_0^3, \tag{32}$$

where V_0 is the effective depth of the potential well, R_0 is the radius of the nucleus. (For a square well of depth V_0, and radius R_0, the derivative $\partial V(r)/\partial r = V_0\delta(r-R_0)$; therefore Eq. (32) is satfied exactly).

The radial functions $R_{kl}(r)$ can be written in the form[5]

$$R_{kl}(r) = e^{i\delta_l}(kr)^{-1} G_{kl}(r).$$

The functions $G_{kl}(r)$ have the asymptotic form:

$$G_{kl}(r) \sim \sin(kr - {}^1\!/_2\, l\pi + \delta_l),$$

where $\delta_l = \delta_l(V(r), k)$ is the phase shift. We can now write

$$|P_{Ll}(k', k)|^2 \tag{33}$$

$$= (x')^{-2}\,|G_{k'L}(R_0)|^2\, x^{-2}\,|G_{kl}(R_0)|^2\, x_0^4\, R_0^2,$$

where $x = kR_0$, $x' = k'R_0$ and $x_0^2 = 2M\hbar^2 V_0 R_0^2$.

Let us consider the square well. In this case the functions $G(R_0)$ are represented by Bessel functions of half integer order. Chief interest lies in the case of such values of L and x_0 for which the relation

$$J_{L-1/2}(x_0) = 0, \tag{34}$$

is satisfied. This equation is the condition for the existences, in the case of the square well, of a one particle level with energy $E_{lev}=0$ and angular momentum L. In this case, for $x' \ll 1$,

$$G_{k'L}(R_0) = (-)^L (2/\pi x')^{1/2}\{J^2_{-(L-1/2)}(x') \tag{35}$$

$$+ J^2_{L-1/2}(x')\}^{-1/2}.$$

It is seen from Eqs. (30), (31), (33) and (35) that for $x' \to 0$ (at the threshold of inelastic scattering) $\sigma_{0I} \sim 1/x' \to \infty$ as a result of the terms in (31) with $L=0$ and $L=1$.

For $L=0$ or $L=1$, we get [from Eq. (34)] $\cos x_0=0$ and $\sin x_0=0$, i.e.,

$$x_0 = {}^1\!/_2\, n\pi \quad (n = 1, 2, 3, \ldots). \tag{36}$$

If we take as the depth of the well V_0=28 mev, then, for example for n=8, we get from Eq. (36) $R_0 \approx 8.2 \times 10^{-13}$ cm. Thus for nuclei with mass number $A \approx 180$ ($R_0 \approx$ 8.2 x 10^{-13} cm), the effect of excitation of the rotational levels can be very pronounced (elements Ta, W, etc.).

It can be assumed that, within the framework of the assumptions we have made, the general character of the behavior of the cross section of inelastic scattering ought not to depend essentially on the form of the potential well (for given effective depth and radius).

Calculations of the cross section of inelastic scattering on the first rotational level of W^{186}_{74} E_{lev}=123 kev, $|Q_0| \approx 18 \times 10^{-24}$ cm^2 *) give $\sigma_{02} \approx 10^{-24}$ to 10^{-23} cm^{-2}, in dependence on the depth V_0 of the square well and the energy E of the incident neutron:

---

[5] Mott and Massay, *Theory of Atomic Collisions*

* Such a value for Q_0 is obtained from the energy of the rotational levels of W^{186}. To use the value of Q_0 obtained from electromagnetic data (spectroscopic measurements, half life measurements, Coulomb excitation, etc) would be incorrect since the deformation of the nuclear material can be distinguished from deformation of the charge. Measurements of the cross section of inelastic scattering of neutrons with excitation of rotational levels can appear to be new (i.e., besides the energy of the rotational levels) precise data on the degree of deformation of the nuclear material.

$V_0 = 20$ mev

E (mev)	0.200	0.300	1.000
σ_{02} (barns)	0.39	0.59	0.68

$V_0 = 28$ mev

E (mev)	0.150	0.200	0.300	0.500
σ_{02} (barns)	2.97	11.42	11.02	8.78

It is evident from the table that in the case of one particle resonance the cross section of inelastic scattering without the formation of an intermediate nucleus can reach a considerable size. For comparison, the cross section of inelastic scattering with excitation of the first level of W^{186}_{74} passing through an intermediate nucleus, has been calculated according to the theory of Hauser and Feshbach[6]. For energies of the incident neutron of $E = 0.2$ mev, the cross section was equal to 0.6 barn. Thus in some cases the two mechanisms of excitation of the lowest level of the target nucleus can concur. The problem as to which of these mechanisms dominates can be solved only by experiment, on the basis of investigation of the path of the excitation curve of the first levels of the target nucleus in their dependence on the energy of the incident neutron. We note that, recently, Guernsey and Goodman[7,8] observed inelastic scattering of neutrons with $E = 1.1$ mev on the first rotational level of Ta ($E_{\text{lev}} = 136.5$ kev) which occurs, in their opinion, without formation of the intermediate state.

The authors consider it their duty to thank Professor A.S.Davydov for his valued advice and interest in the present work.

APPENDIX

1. CONNECTION BETWEEN DEFORMATIONS AND MULTIPOLE MOMENTS

1. We define the multipole moment of a system of nucleons as follows:

$$Q_{\lambda\mu} = \sum_{p=1}^{A} r_p^{\lambda} Y^*_{\lambda\mu}(\vartheta_p, \varphi_p), \tag{A.1}$$

If the number of particles is large, we can change to a continuous distribution of nucleons, i.e.,

$$Q_{\lambda\mu} = \int r^{\lambda} Y^*_{\lambda\mu}(\vartheta, \varphi)\, \rho\, dV, \tag{A.2}$$

where ρ is the density of nucleons in the nucleus. Taking ρ to be constant, we have $\rho = A/(4\pi/3)R_0^3$ and carrying out the integration over r in (A.2), we obtain

$$Q_{\lambda\mu} = \frac{A}{4\pi/3R_0^3(\lambda+3)} \int Y^*_{\lambda\mu}(\vartheta, \varphi) R^{\lambda+3}(\vartheta, \varphi)\, d\Omega.$$

For small deformations,

$$R^{\lambda+3} \approx R_0^{\lambda+3}\,[1 + (\lambda+3) \sum_{\lambda,\,\mu} \alpha_{\lambda\mu} Y_{\lambda\mu}(\vartheta, \varphi)],$$

therefore

$$\begin{gathered} Q_{\lambda\mu} = (3A/4\pi) R_0^{\lambda} \alpha_{\lambda\mu}, \\ \alpha_{\lambda\mu} = \frac{4\pi}{3AR_0^{\lambda}} \sum_{p=1}^{A} r_p^{\lambda} Y^*_{\lambda\mu}(\vartheta_p, \varphi_p). \end{gathered} \tag{A.3}$$

2. We have for the matrix elements of the operator $\alpha_{\lambda\mu}$

$$\langle \alpha_{\lambda\mu} \rangle = \frac{4\pi}{3AR_0^{\lambda}} \sum_{p=1}^{A} \int \psi_B^* r^{\lambda}_p Y^*_{\lambda\mu}(\vartheta_p, \varphi_p) \psi_A\, d\tau. \tag{A.4}$$

We make use of the well known expression:[9]

$$\begin{gathered} (-)^{M_B}(I_B I_A - M_B M_A | I_B I_A \lambda\mu) \\ \times Q^{(\lambda)}_{BA}\, [(2\lambda + 1)/4\pi]^{1/2} \\ = \int \psi_B^* r_p^{\lambda} Y^*_{\lambda\mu}(\vartheta_p, \varphi_p) \psi_A\, d\tau = \langle r_p^{\lambda}\; Y^*_{\lambda\mu}(\vartheta_p, \varphi_p) \rangle, \end{gathered} \tag{A.5}$$

Whence we obtain Eq. (22)

---

[6] W. Hauser and H. Feshbach, Phys. Rev. 87, 366 (1952).

[7] J. B. Guernsey and C. Goodman, Bull. Am. Phys. Soc. 29, 48 (1954).

[8] J. B. Guernsey and C.Goodman, Phys. Rev. 95, 636 (1954).

[9] K. A. Ter-Martirosian, J. Exper. Theoret. Phys.USSR 22, 284 (1952).

2. RELATION BETWEEN MULTIPOLE MOMENTS OF TRANSITION OF VARIOUS ORDERS

1. For the spherical harmonics $Y_{\lambda\mu}(\vartheta,\varphi)$ it is easy to obtain the relation

$$(l'l00\,|\,l'l\lambda 0)\left(\frac{4\pi}{2\lambda+1}\right)^{1/2} Y_{\lambda\mu}(\vartheta,\varphi) = \frac{4\pi}{[(2l'+1)(2l+1)]^{1/2}} \times \sum_{m,m'} (l'lm'm\,|\,l'l\lambda\mu)\, Y_{l'm'}(\vartheta,\varphi)\, Y_{lm}(\vartheta,\varphi).$$

From this we get

$$(l'l00\,|\,l'l\lambda 0)\left(\frac{4\pi}{2\lambda+1}\right)^{1/2} (r^{\lambda} Y^{*}_{\lambda\mu}) = \frac{4\pi}{[(2l'+1)(2l+1)]^{1/2}} \times \sum_{m,m'} (l'lm'm\,|\,l'l\lambda\mu)\,(r^{l'} Y^{*}_{l'm'})(r^{l} Y^{*}_{lm}),$$

where $\lambda = l' + l$.

2. For the matrix elements that are defined by means of the wave functions (26), we have

$$(l'l00\,|\,l'l\lambda 0)(4\pi/2\lambda+1)^{1/2}\langle r^{\lambda} Y^{*}_{\lambda\mu}\rangle \tag{A.6}$$

$$= \sum_{m,m'} (l'lm'm\,|\,l'l\lambda\mu) \sum_{I}\sum_{M} \langle r^{l'} Y^{*}_{l'm'}\rangle \langle r^{l} Y^{*}_{lm}\rangle,$$

where the summation is carried out over the intermediate states. Making use of (A.5) we get from (A.6)

$$\begin{aligned}(l'l00\,|\,l'l\lambda 0)&\left(\frac{4\pi}{2\lambda+1}\right)^{1/2}(-)^{M_B}(I_B I_A - M_B M_A\,|\,I_B I_A \lambda\mu)\,Q^{(\lambda)}_{I_B I_A}\sqrt{\frac{2\lambda+1}{4\pi}}\\ &= \frac{4\pi}{[(2l+1)(2l'+1)]^{1/2}}\sum_{I}\sum_{m,m',M}(-)^{M_B}\left(\frac{2l'+1}{4\pi}\right)^{1/2}(I_B I - M_B M\,|\,I_B I l' m')\\ &\times (l'lm'm\,|\,l'l\lambda\mu)(-)^{M}\sqrt{\frac{2l+1}{4\pi}}(I I_A - M M_A\,|\,I I_A l m)\,Q^{(l')}_{I_B I}\,Q^{(l)}_{I I_A}.\end{aligned} \tag{A.7}$$

In Eq. (A.7) we can carry out the summation over the magnetic quantum numbers:

$$\begin{aligned}&\sum_{m}\sum_{m'}\sum_{M}(-)^{M}(I_B I - M_B M\,|\,I_B I l' m')(l'lm'm\,|\,l'l\lambda\mu)(I I_A - M M_A\,|\,I I_A l m)\\ &= (-)^{I_A - I}[(2l+1)(2l'+1)]^{1/2}(I_B I_A - M_B M_A\,|\,I_B I_A \lambda\mu)\,W(I_B I \lambda I;\, l' I_A).\end{aligned} \tag{A.8}$$

Now

$$(l'l00\,|\,l'l\lambda 0)\,Q^{(\lambda)}_{I_B I_A} = (-)^{I_A - I}[(2l+1)(2l'+1)]^{1/2} \sum_{I} Q^{(l')}_{I_B I}\,Q^{(l)}_{I I_A}\; W(I_B \lambda I l;\, I_A l'), \tag{A.9}$$

where $\lambda = l' + l$.

3. Making use of the relation

$$W(I_B \lambda I l;\; 0\, l') = (-)^{I_B + l - l'}(2I_B + 1)^{-1/2}(2l+1)^{-1/2}\,\delta_{I_B \lambda}\,\delta_{Il},$$

we get

$$(l'l'00\,|\,l'l\lambda 0)\,Q_{\lambda 0}^{(\lambda)} = (-)^{\lambda - l'}\sqrt{\frac{2l'+1}{2\lambda+1}}\,Q_{\lambda l}^{(l')}\,Q_{l0}^{(l)}.$$

We set $l'=2$; then it follows that

$$Q_{\lambda 0}^{(\lambda)} = \left[\frac{10\,(2\lambda-3)\,(2\lambda-1)}{3\,(2\lambda+1)\,(\lambda-1)\,\lambda}\right]^{1/2} Q_{\lambda\lambda-2}^{(2)}\,Q_{\lambda-2,0}^{(\lambda-2)}\,(\lambda = 2, 4, 6\ldots) \qquad \text{(A.10)}$$

Eq. (27) follows readily from Eq. (A.10).

Translated by R. T. Beyer
18

SOVIET PHYSICS JETP VOLUME 3, NUMBER 1 AUGUST, 1956

The Problem of the Radiation of Ultra High Velocity Electrons Moving in a Constant Magnetic Field

A. A. SOKOLOV AND A. N. MATVEEV
Moscow State University

(Submitted to JETP editor, October 27, 1954)
J. Exper. Theoret. Phys. USSR 30, 126-135 (January, 1956)

As a further development of researches[1-4] on the quantum theory of the "luminous" electron, a formula has been obtained for the differential spectrum of radiation which is uniformly valid for any spectral range, for the comparitively small energies of the radiating electron, $E \ll E_{1/2} = mc^2(2Rmc/3h)^{1/2}$ as well as for energies $E \sim E_{1/2}$ and $E \gg E_{1/2}$. A closed formula for the total radiation energy (valid for arbitrary energies of the radiating electron) and a formula for the "critical" radiation frequency of the "luminous" electron have also been obtained.

1. INTRODUCTION

IN works on the quantum theory of the "luminous" electron[1,3], a formula has been found for the total radiation energy, taking into account the first quantum correction. This formula is valid for energy of the radiating electron $E \ll E_{1/2}$. A similar result has been obtained more recently by Schwinger.[4] A formula was obtained in reference 3 (see also reference 4) for the differential spectrum at these energies. Klepikov[5] has obtained formulas which characterize the angular distribution of the radiation. These formulas are also correct for energies $E \gtrsim E_{1/2}$. Formulas for the differential spectrum were not obtained in this research. The differential spectrum was calculated for a series of energy values, with the aid of numerical integration.

In the present research a formula is found for the differential spectrum of radiation of the "luminous" electron which is uniformly valid for any spectral range for arbitrary energies of the radiating electron. A closed formula for the total radiation energy (valid for arbitrary energies of the radiating electron) and a formula for the "critical" radiation frequency of the "luminous" electron have also been obtained. These formulas permit us to obtain a number of new physical results.

2. ANGULAR DISTRIBUTION OF THE RADIATION

The formula which characterizes the spectral composition and angular distribution of the radiation (see, for example, reference 3) can be written in the following form:

$$W_{n,n';s,s'} = \frac{ce^2}{4\pi}\int d\Omega\, \varkappa^2 d\varkappa\, \Phi_{n,n';s,s'}\,\delta(K - K' - \varkappa), \tag{2.1}$$

where

$$\Phi_{n,n;s,s'} = |\bar{\alpha}_x|^2 + \cos^2\vartheta\,|\bar{\alpha}_y|^2 + \sin^2\vartheta\,|\bar{\alpha}_z|^2 - (\bar{\alpha}_y^{+}\bar{\alpha}_z + \bar{\alpha}_z^{+}\bar{\alpha}_y)\sin\vartheta\cos\vartheta,$$

$$|\bar{\alpha}_x|^2 = I_{s,s'}^2\left\{\frac{KK' - k_0^2}{2KK'}(I_{n,n'-1}^2 + I_{n-1,n'}^2) - \frac{4\gamma\sqrt{nn'}}{KK'}I_{n,n'-1}I_{n-1,n'}\right\},$$

$$|\bar{\alpha}_y|^2 = I_{s,s'}^2\left\{\frac{KK' - k_0^2}{2KK'}(I_{n,n'-1}^2 + I_{n-1,n'}^2) + \frac{4\gamma\sqrt{nn'}}{KK'}I_{n,n'-1}I_{n-1,n'}\right\},$$

---

[1] A. A. Sokolov, N. P. Klepikov and I. M. Ternov, J. Exper. Theoret. Phys. USSR 23, 632 (1952).

[2] A. A. Sokolov, N. P. Klepikov and I. M. Ternov, J. Exper. Theoret. Phys. USSR 24, 249 (1953); Dokl. Akad. Nauk SSSR 89, 665 (1953).

[3] A. A. Sokolov and I. M. Ternov, J. Exper. Theoret. Phys. USSR 25, 698 (1953); Dokl. Akad. Nauk SSSR 92, 537 (1953).

[4] J. Schwinger, Proc. Nat. Acad. Sci. 40, 133 (1954).

[5] N. P. Klepikov, J. Exper. Theoret. Phys. USSR 26, 19 (1954).

$$|\bar{\alpha}_z|^2 = I^2_{s,s'}\left\{\frac{KK'-k_0^2}{2KK'}(I^2_{n,n'}+I^2_{n-1,n'-1}) - \frac{4\gamma\sqrt{nn'}}{KK'}I_{n,n'}I_{n-1,n'-1}\right\},$$

$$\bar{\alpha}_y^+\bar{\alpha}_z + \bar{\alpha}_z^+\bar{\alpha}_y = -I^2_{s,s'}\frac{\sqrt{4\gamma}\,\varkappa\cos\vartheta}{KK'}\{I_{n,n'-1}I_{n-1,n'-1}+I_{n-1,n'}I_{n,n'}\},$$

$$K=\sqrt{k_0^2+4\gamma n},\quad K'=\sqrt{k_0^2+4\gamma n'+\varkappa^2\cos^2\vartheta},\quad x=\frac{\varkappa^2\sin^2\vartheta}{4\gamma}\quad \gamma=\frac{eH}{2ch},$$

$$I_{n,n'}(x)=(n!n'!)^{-1/2}e^{-x/2}x^{(n-n')/2}Q_{n'}^{(n-n')}(x),$$

n is the principal quantum number, s the radial quantum number. The function $Q_n^{(n-n')}(x)$ is the associated Laguerre polynomial.

The expression for $\Phi_{n,n';s,s'}$ can be greatly simplified by means of relations among the functions $I_{n,n'}$. Using recurrence relations among the Laguerre polynomials, we get the following relations among the $I_{n,n'}$:

$$\begin{aligned}\sqrt{x}I_{n,n'-1} &= \sqrt{n}I_{n-1,n'-1}-\sqrt{n'}I_{n,n'};\\ \sqrt{x}I_{n-1,n'} &= \sqrt{n}I_{n,n'}-\sqrt{n'}I_{n-1,n'-1}.\end{aligned} \tag{2.2}$$

By differentiation of the $I_{n,n'}(x)$ with respect to x and use of the relations just written down, we can show that

$$\begin{aligned}\sqrt{n}I_{n-1,n'}-\sqrt{n'}I_{n,n'-1} &= \left(\frac{d}{d\sqrt{x}}+\sqrt{x}\right)I_{n,n'};\\ \sqrt{n'}I_{n-1,n'}-\sqrt{n}I_{n,n'-1} &= \left(\frac{d}{d\sqrt{x}}-\sqrt{x}\right)I_{n-1,n'-1}.\end{aligned} \tag{2.3}$$

Further, taking into account the equality

$$\tfrac{1}{2}(KK'-k_0^2)=\gamma(n+n'-x), \tag{2.4}$$

which arises from the conservation of energy ($K-K'=\varkappa$), the expression for $\Phi_{n,n';s,s'}$ can be reduced to the following form:

$$\begin{aligned}\Phi_{n,n';s,s'} = I^2_{s,s'}(x)\frac{4\gamma}{KK'}\Big\{&\frac{K^2}{4\gamma}\operatorname{ctg}^2\vartheta\,(I^2_{n,n'}+I^2_{n-1,n'-1})\\ &+x(I'^2_{n,n'}+I'^2_{n-1,n'-1})\\ &+x(I_{n,n'}I'_{n,n'}-I_{n-1,n'-1}I'_{n-1,n'-1})\Big\}.\end{aligned} \tag{2.5}$$

Problems involving a change in trajectory, where it is important to take radial quantum transitions into account, were considered in reference 3. Since we are presently interested only in the problem of the intensity of the radiation, we can carry out the summation over s' with the aid of the relation $\sum_s I^2_{s,s'}=1$. If we further change to the dimensionless variable $\vec{\xi}=\vec{\varkappa}/2\sqrt{\gamma}$ we can write the expression for the total radiation energy as

$$W=\sum_{m=0}^{n}W_m; \tag{2.6}$$

$$W_m=\frac{\gamma}{\pi}ce^2A\int\frac{\Phi_m(\vec{\xi})}{A-\xi}\delta[\varphi_m(\vec{\xi})]\,d^3\xi; \tag{2.6a}$$

$$A=K/2\sqrt{\gamma},$$

$$\varphi_m(\vec{\xi})=\xi-A+\sqrt{A^2-m^2+\xi^2\cos^2\vartheta},$$

$$\begin{aligned}\Phi_m(\vec{\xi}) = \operatorname{ctg}^2\vartheta\,&(I^2_{n,n-m}+I^2_{n-1,n-1-m})\\ &+\frac{\xi^2\sin^2\vartheta}{A^2}(I'^2_{n,n-m}+I'^2_{n-1,n-1-m})\\ &+\frac{\xi^2\sin^2\vartheta}{A^2}(I_{n,n-m}I'_{n,n-m}-I_{n-1,n-1-m}I'_{n-1,n-1-m}),\end{aligned}$$

where the argument of the function $I_{n,n'}$ is $\xi^2\sin^2\vartheta$, and the prime on the I indicates, the derivative with respect to this argument.

For further computation, in order to avoid the complicated argument which results from integration with δ-functions, it is appropriate to transform the integral in Eq. (2.6a) to a surface integral by means of the well-known formula

$$\int\ldots\delta(\varphi)\,d\tau=\int_{\varphi=0}\ldots d\sigma/|\nabla\varphi|, \tag{2.7}$$

where $d\sigma$ is an element of the surface $\varphi=0$. We then get, in place of Eq. (2.6a):

$$W_m=\frac{\gamma}{\pi}ce^2A\int_{S_m}\frac{\Phi_m(\vec{\xi})}{(\partial\varphi_m/\partial n)(A-\xi)}\,d\sigma, \tag{2.8}$$

Here S_m is the surface in the space of the dimensionless quantity $(\vec{\xi})$, determined by the equation

$\varphi_m(\vec{\xi})=0$; $d\sigma$ is an element of this surface; n is the outward drawn normal to this surface. There is axial symmetry relative to the z axis.

Each of the surfaces S_m gives a spatial picture of the distribution of the radiation frequencies for the quantum transition $n \to n'$ $(n-n'=m)$. The wave number of the radiation in a particular direction, in the dimensionless units employed here, is equal to the modulus of the radius vector drawn in this direction from the origin to the intersection with the surface S_m. It must be noted that, in the transition to very high frequencies, radiation will not be possible in all directions. The maximum possible angle between the direction of radiation of a given frequency and the plane of motion of the electrons (in the classical sense) decreases all the more strongly with increase in frequency. Such a decrease in the angle of possible radiation is a consequence of the law of conservation of energy--momentum.

In the entire region of frequencies of interest to us, the discrete spectrum is equivalent to the continuous, and we can therefore make the transition from summation over m to the integral

$$W=\int_0^n W_m\,dm. \tag{2.9}$$

in forming the total energy of radiation. In this transition, the family of surfaces S_m fills the entire space, the boundary of which is defined by the equation $\varphi_n=0$.

We take it into account that in the transition from one surface to another, the identity $\varphi_m\equiv 0$ exists. It follows from this identity that

$$dm=2(A-\xi)\frac{\partial\varphi_m}{\partial n}\,dn, \tag{2.10}$$

$$m=2A\xi-\xi^2\sin^2\vartheta,$$

where dn is the differential normal to the surface $\varphi_m=0$. Substituting (2.10) into (2.9), taking the value of W_m from (2.8) and considering that $d\sigma dn=d^3\vec{\xi}$ is an element of volume in the dimensionless space in which we are working, we finally obtain

$$W=\frac{2\gamma}{\pi}ce^2A\int\limits_{V_n}\Phi_{2A\xi-\xi^2\sin^2\vartheta}(\vec{\xi})\,d^3\vec{\xi}, \tag{2.11}$$

where V_n is the volume bounded by the surface S_n.

For what follows, it is appropriate to change to other units. In the units employed here, the wave number of the fundamental classical vibration (the "fundamental" in the sense of the classical theory of the "luminous" electron) is equal to $\xi_0=1/2A$. As the new independent variable, we select the ratio of ξ to ξ_0, i.e., what in the classical theory of the "luminous" electron in the discrete spectrum is known as the number of the harmonic. Setting $\vec{\nu}=2A\vec{\xi}$ we obtain

$$W=\frac{ce^2\beta^2}{4\pi R^2}\int\limits_{V_n}\Phi_{\nu'}\left(\frac{\vec{\nu}}{2A}\right)d^3\vec{\nu}, \tag{2.12}$$

where

$$\nu'=\nu\left(1-\frac{\nu}{4n}\beta^2\sin^2\vartheta\right),$$

$$\beta=\frac{\sqrt{n}}{A},\quad \sqrt{1-\beta^2}=\frac{mc^2}{E},$$

$R=\sqrt{n/\gamma}$ is the classical radius of the trajectory of the motion of the electron.

We further make use of approximations of the function $I_{n,n'}(x)$, correct over the entire spectrum[2,5]:

$$I_{n,n'}(x)=\frac{1}{\pi\sqrt{3}}\sqrt{1-\frac{x}{(\sqrt{n}-\sqrt{n'})^2}} \tag{2.13}$$

$$\times K_{1/3}\left\{\frac{2}{3}\sqrt[4]{nn'}(\sqrt{n}-\sqrt{n'})\left(1-\frac{x}{(\sqrt{n}-\sqrt{n'})^2}\right)^{3/2}\right\};$$

$$I'_{n,n'}(x)=\frac{1}{n\sqrt{3}}\frac{\sqrt[4]{nn'}}{(\sqrt{n}-\sqrt{n'})}\left(1-\frac{x}{(\sqrt{n}-\sqrt{n'})^2}\right) \tag{2.13a}$$

$$\times K_{2/3}\left\{\frac{2}{3}\sqrt[4]{nn'}(\sqrt{n}-\sqrt{n'})\left(1-\frac{x}{(\sqrt{n}-\sqrt{n'})^2}\right)^{3/2}\right\}$$

and neglect terms of order $\sqrt{1-\beta^2}$ in comparison with the fundamental terms, we get the following formula, which characterizes the angular distribution of the radiation:

$$W=\frac{ce^2}{R^2}\frac{1}{3\pi^2} \tag{2.14}$$

$$\times\int\frac{\nu^2d\nu}{1-\nu/2n}\sin\vartheta\,d\vartheta\left\{\varepsilon_\vartheta K^2_{1/3}\left(\frac{1}{3}\frac{\nu}{1-\nu/2n}\varepsilon_\vartheta^{3/2}\right)\cos^2\vartheta\right.$$

$$+\varepsilon_\vartheta^2K^2_{2/3}\left(\frac{1}{3}\frac{\nu}{1-\nu/2n}\varepsilon_\vartheta^{3/2}\right)$$

$$+\frac{1}{2}\left(\frac{\nu}{2n}\right)^2\left(1-\frac{\nu}{2n}\right)^{-1}\varepsilon_\vartheta^2\left[K^2_{1/3}\left(\frac{1}{3}\frac{\nu}{1-\nu/2n}\varepsilon_\vartheta^{3/2}\right)\right.$$

$$\left.\left.+K^2_{2/3}\left(\frac{1}{3}\frac{\nu}{1-\nu/2n}\varepsilon_\vartheta^{3/2}\right)\right]\right\},$$

where $\varepsilon_\vartheta = 1-\beta^2\sin^2\vartheta$, $d^3\nu^2 d\nu \sin\vartheta d\vartheta d\varphi$ is the element of volume in spherical coordinates. Integration over φ can easily be carried out in Eq. (2.14), since the integrand does not depend on φ.

3. DIFFERENTIAL SPECTRUM

In order to get the differential spectrum, we must integrate Eq. (2.14) with respect to ϑ. In this integration, taking into account the exponential fall off of the integrand as one departs from the angle $\vartheta = \pi/2$, we can make the change of variable $\cos\vartheta = x$ and extend the limits of integration to infinity.

The integrals appearing in Eq. (2.14) are computed by means of the theory of the Mellin transformation. For example, for calculation of the integral

$$I_1 = \int_0^\infty x^2 \varepsilon_x K^2_{1/3}(p\varepsilon_x^{3/2})\, dx; \quad (\varepsilon_x = 1-\beta^2+x^2) \tag{3.1}$$

we must take into consideration the Nicholson integral

$$K_\mu(z) K_\nu(z) = 2\int_0^\infty K_{\mu-\nu}(2z \operatorname{ch} t) \operatorname{ch}(\mu+\nu) t\, dt, \tag{3.2}$$

and also the value of the integrals

$$\int_0^\infty K_\nu(x)\, x^{\mu-1}\, dx = 2^{\mu-2}\Gamma\left(\frac{\mu-\nu}{2}\right)\mathrm{T}\left(\frac{\mu+\nu}{2}\right), \tag{3.3}$$

$$\int_0^\infty \frac{x^{2p-1}dx}{(a+x^2)^{p+q}} = \frac{1}{2a^q}\mathrm{B}(p,\ q), \quad (a>0), \tag{3.4}$$

$$\int_0^\infty \frac{\operatorname{ch} 2px}{\operatorname{ch}^{2q} x}\, dx = 2^{2(q-1)}\mathrm{B}(q+p,\ q-p), \tag{3.5}$$

$$(\operatorname{Re} q > |\operatorname{Re} p|).$$

We express the function $K^2_{1/3}$ in the integrand of Eq. (3.1) with the help of Eq. (3.2), and expressing the function K_0 (which enters into the result of this representation) by means of the equality following from Eq. (3.3) [by Mellin's theorem]. This lowers the order of integration and is possible because of the absolute convergence of the integrals Finally, making use of Eqs. (3.4) and (3.5), we get

$$I_1 = \frac{\varepsilon_0^{5/2}}{8\pi i}\int_{k-i\infty}^{k+i\infty} p_0^{-\mu} 2^{\mu-2}\varphi_1(\mu)\, d\mu, \tag{3.6}$$

where

$$\varphi_1(\mu) = \Gamma^2\left(\frac{\mu}{2}\right)\mathrm{B}\left(\frac{3}{2},\ \frac{3}{2}\mu-\frac{5}{2}\right)\mathrm{B}\left(\frac{\mu}{2}-\frac{1}{3},\ \frac{\mu}{2}+\frac{1}{3}\right),$$

$$\varepsilon_0 = 1-\beta^2, \quad p_0 = p\varepsilon_0^{3/2}.$$

If we transform the expression for $\varphi_1(\mu)$ by means of the product formula for the gamma function,

$$\Gamma(z)\Gamma\left(z+\frac{1}{n}\right)\ldots\Gamma\left(z+\frac{n-1}{n}\right) = (2\pi)^{1/2(n-1)} n^{1/2-nz}\Gamma(nz), \tag{3.7}$$

we get

$$I_1 = \frac{\pi}{4\sqrt{3}}\frac{\varepsilon_0}{p}\left[\int_{2p_0}^\infty K_{5/3}(x)\, dx - K_{2/3}(2p_0)\right]. \tag{3.8}$$

The other integrals are calculated in a similar way. As a result, we get the following formula for the differential spectrum of the "luminous" electron:

$$W = \int_{\nu=0}^{2\pi} dW_\nu, \tag{3.9}$$

$$dW_\nu = \frac{1}{\pi\sqrt{3}}\frac{ce^2}{R^2}\varepsilon_0 \nu\, d\nu \left\{\int_{\frac{2}{3}\frac{\nu}{1-\nu/2n}\varepsilon_0^{3/2}}^\infty K_{5/3}(x)\, dx + \left(\frac{\nu}{2n}\right)^2\left(1-\frac{\nu}{2n}\right)^{-1} K_{2/3}\left(\frac{2}{3}\frac{\nu}{1-\nu/2n}\varepsilon_0^{3/2}\right)\right\}.$$

This formula for the differential spectrum is applicable for the entire spectrum, both for energies $E \ll E_{1/2}$ as well as for $E \sim E_{1/2}$ and $E \gg E_{1/2}$. A formula for the differential spectrum which is valid for $E \ll E_{1/2}$ was obtained in reference 3:

$$dW = \frac{3\sqrt{3}}{4\pi}\frac{ce^2}{R^2}\left(\frac{E}{mc^2}\right)^4 y\, dy\left\{\int_y^\infty K_{5/3}(x)\, dx - \frac{3}{2}y^2\frac{h}{Rmc}\left(\frac{E}{mc^2}\right)^2 K_{5/3}(y)\right\}, \tag{3.10}$$

$$y = (2\omega/3\omega_0)(mc^2/E)^3, \quad \omega_0 = c/R.$$

This formula can be obtained from Eq. (3.9) if we limit ourselves to accuracy of first order in ν/n. We have

$$\int\limits_{\frac{2}{3}\frac{\nu}{1-\nu/2n}\varepsilon_0^{3/2}}^{\infty} K_{5/3}(x)\,dx \approx \int\limits_{\frac{2}{3}\nu\varepsilon_0^{3/2}}^{\infty} K_{5/3}(x)\,dx - \frac{\nu}{2n}\frac{2}{3}\nu\varepsilon_0^{3/2}K_{5/3}\left(\frac{2}{3}\nu\varepsilon_0^{3/2}\right) + \ldots \quad .$$

Since

$$\frac{2}{3}\nu\varepsilon_0^{3/2} = \frac{2}{3}\frac{\omega}{\omega_0}\left(\frac{mc^2}{E}\right)^3 = y \qquad (3.11)$$

and

$$1/2n = (h/Rmc)(mc^2/E), \qquad (3.12)$$

we can write Eq. (3.9) in the form of Eq. (3.10) with accuracy to first order in ν/n.

The functions which enter into Eq. (3.9) for the differential spectrum have been studied in the classical theory of the "luminous" electron. Therefore this expression makes it possible to study in full detail the entire spectrum of the "luminous" electron for arbitrary energies. In the study of the spectrum it is expedient to take the overall magnitude of the spectrum as unity. Then Eq. (3.9) takes the following form in the independent variable $\xi=\nu/2n=hw/E\,(0\leq\xi<1)$:

$$dW = \frac{ce^2}{\pi\sqrt{3}}\left(\frac{mc}{h}\right)^2 \xi d\xi \left\{ \int\limits_{\xi/(1-\xi)\zeta}^{\infty} K_{5/3}(x)\,dx + \frac{\xi^2}{1-\xi}K_{2/3}\left(\frac{\xi}{1-\xi}\frac{1}{\zeta}\right)\right\}, \qquad (3.13)$$

where

$$\zeta = (3h/2Rmc)(E/mc^2)^2 = (E/E_{1/2})^2.$$

In the case of extreme ultrarelativistic energy ($\zeta\gg1$) we have, for almost the entire spectrum (with the exception of the immediate vicinity of the far limit of the spectrum ($\zeta\to1$): $\zeta/(1-\xi)\zeta\ll1$, so that use can be made of the asymptotic formula

$$K_\nu(x) \approx 2^{\nu-1}\Gamma(\nu)x^{-\nu}, \quad x\ll1, \quad \nu>0. \qquad (3.14)$$

The asymptotic formula for the differential spectrum has the following form:

$$dW \approx \frac{ce^2}{R^2}\frac{3^{1/6}\Gamma(2/3)}{\pi}\left(\frac{Rmc}{h}\right)^{4/3} \times\left(\frac{E}{mc^2}\right)^{4/3} d\xi\xi^{1/3}(1-\xi)^{2/3}\left(1+\frac{\xi^2}{2(1-\xi)}\right). \qquad (3.15)$$

In what follows we verify the applicability of this formula for the description of almost the entire spectral range in the ultrarelativistic limit by the calculation of the total energy of radiation.

The form of the spectra for the values $E=E_{1/2}$ and $E=10E_{1/2}$ is shown in Figs. 1 and 2, where the spectra given by classical theory for the same conditions have been plotted for comparison.

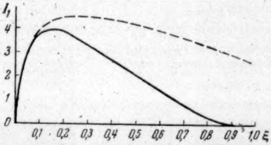

FIG. 1. Quantum and classical (dashed curve) spectra for $E=E_{1/2}$

$$I_1=\frac{\pi\sqrt{e}}{ce^2}\,\frac{h}{mc}^2\,\frac{dW}{d\xi};\quad \xi=\frac{h\omega}{E}$$

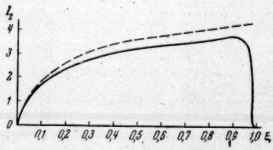

FIG. 2. Quantum and classical (dashed curve) spectra for $E=10E_{1/2}$

$$I_2=\frac{\pi\sqrt{3}}{ce^2}\,\frac{h}{mc}^2\,\frac{dW}{d};\quad \xi=\frac{hW}{E}$$

Analysis of the spectra for all energies shows that the criterion for the applicability of the classical theory of radiation of the "luminous" electron, which was established in the previous researches,

$$\zeta\ll1, \qquad (3.16)$$

has meaning only in relation to the calculation of the total radiation energy in the classical theory. So far as the applicability of the classical theory to the analysis of differential spectrum, the criterion mentioned tells us nothing. Relative to the applicability of the classical theory to the analysis of the differential spectrum, we must note that first, the classical theory is in general not applicable for the study of the far portions of the spectrum, independent of whether the criterion (3.16) is satisfied or not; second, the relative region of applicability of the classical theory for the analysis of the differential spectrum, i.e., the region of applicability for fixed relative error, taken in relation to the total magnitude of the spectrum, does not depend on the criterion (3.16) and is approximately constant. In particular, for example, if we set ourselves the goal of comparing the results of the quantum and classical theory relative to the density of radiation in a certain frequency interval (say in the visible light spectrum), then the agreement between the results of the classical and quantum theory will improve considerably with increase in energy.

It follows from the analysis of the spectra that the dependence of the form of the spectrum on the energy is weakened with increase of the energy of the radiating electron. In the limiting ultrarelativistic case, the form of the spectrum is practically independent of the energy.

4. THE "CRITICAL" FREQUENCY

First of all, it is evident directly from Eq. (3.9) that the number of the "critical" harmonic ν_c (in the continuous spectrum, this is the ratio of the "critical" frequency to the frequency of the fundamental $\omega_0=c/R$) at which the maximum energy radiation density is located, can be formally defined, just as in the classical theory, by the condition

$$\frac{2}{3}\frac{\nu_c}{1-\nu_c/2n}\varepsilon_0^{3/2}=1. \tag{4.1}$$

If we take Eq. (3.12) into account, we arrive at the following expression for the "critical" frequency:

$$\omega_c=(3c/2R)(E/mc^2)^3(1+\zeta)^{-1}. \tag{4.2}$$

This coincides with what was obtained by Klepikov[5] without development, on the basis of a consideration only of the density of energy radiation in the direction of the maximum angle of radiation $\vartheta=\pi/2$.

However, Eq. (4.2) is not sufficiently rigorous. Actually, as is known, it is assumed in classical theory that the "critical" frequency ω_c^{cl} is defined by the following expression

$$\omega_c^{Cl}=(3c/2R)(E/mc^2)^3. \tag{4.3}$$

As a direct construction of the classical spectrum of the radiation of the "luminous" electron shows, the critical frequency actually amounts to approximately one fourth this value. The quantum formula (4.2) reduces to the classical formula (4.3) at comparitively small energies of the radiating electron $\xi \ll 1$. The "critical" frequency is virtually the same as in the classical case, being about one fourth this value. Thus, in order to obtain the "critical" frequency, it is necessary to multiply the value obtained from Eq. (4.2) by the factor q, which is approximately 1/4 in the case $E \ll E_{1/2}$. If the value of this factor did not depend on the energy and was equal to the same constant value 1/4 even at energies $E \sim E_{1/2}$, and $E \gg E_{1/2}$, then Eq. (4.2) would have been rigorous, since the limitation on the constant factor is not essential, as is also the case in the classical theory. However, as direct construction of the spectrum shows, this factor is actually not a constant quantity, and increases somewhat with increase in energy, approaching unity in the extreme relativistic case $\zeta \gg 1$. Therefore, the more rigorous formula for the "critical" frequency has the following form:

$$\omega_c=q(\zeta)(3c/2R)(E/mc^2)^3(1+\zeta)^{-1}. \tag{4.4}$$

The function $q(\zeta)$ appearing in this formula can be found by graphical methods. The results of such a series of calculations are shown in Fig. 3.

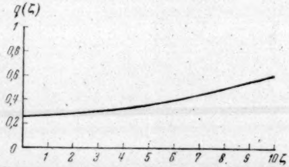

FIG. 3. Graph of the function $q(\zeta)$

5. TOTAL ENERGY OF RADIATION

To obtain the total energy of radiation, it is necessary to carry out integration in Eq. (3.9) over ν. Making the change of integration variable

$$x=\frac{2}{3}\frac{\nu}{1-\nu/2n}\varepsilon_0^{3/2}, \tag{5.1}$$

we can represent the total radiation energy in the form

$$W=\frac{2}{3}\frac{ce^2}{R^2}\left(\frac{E}{mc^2}\right)^4\varphi(\zeta);\quad \varphi(\zeta)=\varphi_1(\zeta)+\zeta^2\varphi_2(\zeta), \tag{5.2}$$

where

$$\varphi_1(\zeta) = \frac{9\sqrt{3}}{16\pi}\int_0^\infty \frac{x^2K_{5/3}(x)\,dx}{(1+\zeta x)^2}; \tag{5.2a}$$

$$\varphi_2(\zeta) = \frac{9\sqrt{3}}{8\pi}\int_0^\infty \frac{x^3K_{2/3}(x)\,dx}{(1+\zeta x)^4}.$$

We can express these integrals in the form of hypergeometric series for the cases $\zeta > 1$ and $\zeta < 1$. For $\zeta < 1$, the series are semi-convergent. For $\zeta > 1$, the series will converge. The latter series defines an analytic function of ζ on all planes of the complex variable ζ. However, the hypergeometric series, as well as the closed formula for the total radiation energy, are difficult to work with. Thus,it is difficult, starting from the latter hypogeometric series, to obtain an asymptotic expansion of the total radiation energy for $\zeta \ll 1$. Therefore, we calculate these integrals in such a form that that formula which is obtained can be used in practice as a closed formula for all values of ζ.

Writing the integral for $\varphi_1(z)$ in the form

$$\varphi_1(\zeta) = -\frac{9\sqrt{3}}{16\pi}\frac{\partial}{\partial\zeta}\int_0^\infty \frac{xK_{5/3}(x)\,dx}{1+\zeta x} \tag{5.3}$$

$$= -\frac{9\sqrt{3}}{16\pi}\frac{\partial}{\partial\zeta}Q(\zeta),$$

we can, with the aid of the Mellin transformation theory, represent the expansion for $Q(\zeta)$ in the form of an integral

$$Q = -\frac{\pi}{4}\frac{1}{\zeta^2}\frac{1}{2\pi i}\int_{k-i\infty}^{k+i\infty}\frac{\Gamma\left(\frac{s}{2}-\frac{5}{6}\right)\Gamma\left(\frac{s}{2}+\frac{5}{6}\right)}{\sin \pi s}(2\zeta)^s\,ds, \tag{5.4}$$

$$\frac{5}{3} < k < 2.$$

Introducing the notation

$$\Phi_\nu(z) = i^{-\nu}[J_\nu(z) - \mathbf{J}_\nu(z)] \tag{5.5}$$

$$+ i^\nu[J_{-\nu}(z) - \mathbf{J}_{-\nu}(z)],$$

where $J_\nu(z)$ is the Bessel function and $J_\nu(z)$ is an Anger function, and closing the contour of integration in Eq. (5.4) at infinity on the left, we get

$$Q(\zeta) = -\frac{2}{3}\pi^2\zeta^{-2}\left[\Phi_{5/3}\left(\frac{i}{\zeta}\right) + \frac{\sqrt{3}}{2\pi}\zeta\right]. \tag{5.6}$$

The integral $\varphi_2(\zeta)$ can be computed similarly. Carrying out the calculation, we obtain the following expression for $\varphi(\zeta)$:

$$\varphi(\zeta) = \frac{3\sqrt{3}}{8}\pi\left\{\frac{\partial}{\partial\zeta}\frac{\Phi_{5/3}(i/\zeta)}{\zeta^2}\right. \tag{5.7}$$

$$\left.-\frac{\zeta^2}{3}\frac{\partial^3}{\partial\zeta^4}\frac{\Phi_{2/3}(i/\zeta)}{\zeta} - \frac{\sqrt{3}}{2\pi}\frac{1}{\zeta^2}\right\}.$$

The functions on the right side of Eq. (5.7) are well known. In the calculation of Eq. (5.2) this expression gives a closed formula for the total radiation energy.

For $\zeta \gg 1$, use can be made of series expansions for the Bessel and Anger functions, keeping the desired number of terms. The principal term for the total radiation energy in this case has the form

$$W^{(\infty)} \approx \frac{32}{27}\frac{\Gamma(2/3)}{3^{4/3}}\frac{ce^2}{R^2}\left(\frac{Rmc}{h}\right)^{4/3}\left(\frac{E}{mc^2}\right)^{4/3}. \tag{5.8}$$

To find the asymptotic expression for the total energy of radiation for $\zeta \ll 1$, we can use the well-known asymptotic expansion (see reference 6)

$$\mathbf{J}_\nu(z) \approx J_\nu(z) - \frac{\sin\pi\nu}{\pi z}\left[\frac{\nu}{z} - \frac{\nu(2^2-\nu^2)}{z^3}\right. \tag{5.9}$$

$$\left.+\frac{\nu(2^2-\nu^2)(4^2-\nu^2)}{z^5} - \dots\right]$$

$$+\frac{\sin\pi\nu}{\pi z}\left[1 - \frac{1^2-\nu^2}{z^2} + \frac{(1^2-\nu^2)(3^2-\nu^2)}{z^4} - \dots\right],$$

from which it follows that in this case

$$\Phi_\nu(z) \approx 2\cos\frac{\nu}{2}\pi\,\frac{\sin\nu\pi}{\pi z}\left[\frac{\nu}{z} - \frac{\nu(2^2-\nu^2)}{z^3}\right. \tag{5.10}$$

$$\left.+\frac{\nu(2^2-\nu^2)(4^2-\nu^2)}{z^5} - \dots\right]$$

$$+2i\sin\frac{\nu}{2}\pi\,\frac{\sin\nu\pi}{\pi z}\left[1 - \frac{1^2-\nu^2}{z^2}\right.$$

$$\left.+\frac{(1^2-\nu^2)(3^2-\nu^2)}{z^4} - \dots\right].$$

Upon consideration of Eq. (5.10), it follows from Eq. (5.7) that for $\zeta \ll 1$ the asymptotic expression

---

[6] G.I. Watson, *Theory of Bessel Functions.*

$$W \approx W_{Cl}\left(1-\frac{55\sqrt{3}}{24}\zeta+\frac{64}{3}\zeta^2 - \frac{8855\sqrt{3}}{108}\zeta^3+\frac{89600}{81}\zeta^4-\dots\right), \tag{5.11}$$

holds. This coincides with the asymptotic expansion found in the direct calculation[5] of the total radiation energy in the asymptotic sense.

It was pointed out above that in the extreme relativistic case, one can, for the study of almost the whole spectrum, make use of the asymptotic formula (3.15). With the help of this formula, we can also compute the principal term of the total radiation energy. The result coincides with Eq. (5.8). In comparison with the total radiation energy given in the classical theory, a decrease of many orders of magnitude is observed in the extreme relativistic case. However, such a decrease comes about chiefly from the fact that in this case, classical theory takes into account mainly the frequencies which ought not to radiate. If, in the calculation of the total radiation energy by the formulas of classical theory, we restrict ourselves in the integration only to the region of frequencies which actually radiate, $\omega \leq E/h$ (it must be emphasized that it is impossible to incorporate such a limitation of the range of integration into the framework of the classical theory), we then get the following expression for the total energy:

$$W_{Cl}^{(\infty)} \approx 3^{1/6}(4\pi)^{-1}(ce^2/R^2)\,\Gamma(2/3)\,(Rmc/h)^{4/3}(E/mc^2)^{4/3}. \tag{5.12}$$

The constant h enters into the formula as a result of the upper limit of integration.

In this case the classical theory describes almost the entire spectrum sufficiently well (with a relative error not exceeding 10%).

Translated by R. T. Beyer
16

Letters to the Editor

Neutron Spectra in the Bombardment of Tritium and Deuterium by 14 mev Deuterons*

G. F. BOGDANOV, N. A. VLASOV, S. P. KALININ,
B. V. RYBAKOV AND V. A. SIDOROV

(Submitted to JETP editor June 21, 1955)
J. Exper. Theoret. Phys. USSR **30**, 185-7
(January, 1956)

In preceding articles by the authors[1] and by others[2], a maximum in the cross section for the reaction T(p,n)He^3 was observed at proton energies of 3 mev, indicating the existence of a broad excited level of He^4 at 22 mev. In the present work an attempt was made to verify the existence of this level by investigating the neutron spectrum from the reaction T(d,n)He^4. Because of the existence of the level, the energy of the reaction may have, as well as the well-known value $Q_0 = 17.6$ mev, a second value $Q_1 = -4.4$ mev, corresponding to formation of He^4 in the excited state. Although this state of He^4 is unstable with respect to decay into He$^3 + n$ or $T + p$, a more or less compact group should be observed in the neutron spectrum corresponding to the second value of Q. The present work is devoted to the search for this group.

This work was carried out in a cyclotron, the beam of which was extracted from the chamber and focussed by a magnetic prism at a distance of 12 m from the cyclotron.

The spectra were investigated by means of a time-of-flight apparatus. The natural modulations of the cyclotron were used. The acceleration of ions in the cyclotron occurs in a narrow interval of the phase of the accelerating voltage; therefore the ions fall on the target in short pulses. According to our observations, the length of a pulse on the target does not exceed 5 mμ sec (5×10^{-9} sec). The frequency of the accelerating voltage is 8.9 mc; consequently, the period of pulse repetition of particles is 112 mμ sec. Neutrons were registered by a fast scintillation counter consisting of a specimen of solid solution of terphenyl in polystyrene and a photomultiplier. Pulses from the photomultiplier were shaped by a shorted cable 30 cm long (after which they had a duration of ~ 3 mμ sec) and were fed to a germanium diode coincidence circuit. The second channel of the coincidence system received pulses of the same duration, synchronized with the accelerating voltage of the cyclotron. In this fashion the coincidence circuit registered the pulses of the counter, arising at some definite phase of the accelerating voltage. The value of this phase was changed by changing the length of cable in one of the lines of the coincidence system, as a result of which γ-rays or neutrons, having various times-of-flight from target to counter, were registered. The instant that the charged particles impinge on the target, that is, the instant of neutron production, was defined by the position of the peak of γ-rays, produced in the target as a result of various nuclear reactions; therefore there was no necessity for a special phasing of the system.

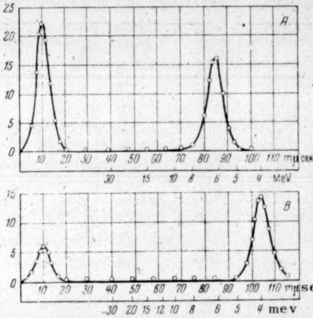

FIG. 1 Distribution with time of counter pulses in the bombardment of a tritium-zirconium target by protons. A corresponds to $E_p = 7.1$ mev, B to $E_p = 4.9$ mev.

In all measurements the neutron counter was placed in the direction of the beam of charged particles, that is, at an angle of 0°.

Figure 1 shows the distribution in time of the counters pulses, registering radiation from a tritium-zirconium target, bombarded by protons of energy 7.1 mev (curve A) and 4.9 mev (curve B). The curves were taken with the counter 2.9 m from the target. The first peak at $t = 10$ mμ sec came from γ-rays, accompanying the reaction in zirconium. They were observed both from the target (tritium + zirconium) and from the unmounted backing-container (zirconium only). The second peak was brought about by neutrons from the reaction T(p,n) He^3. Upon decreasing the proton energy from 7.1

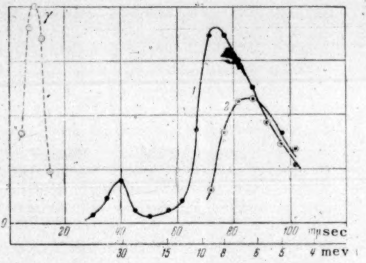

FIG. 2. Spectrum of neutrons in the bombardment of tritium by deuterons of energy: 1, 14.4 mev; 2, 12.4 mev. The γ-ray peak is displayed.

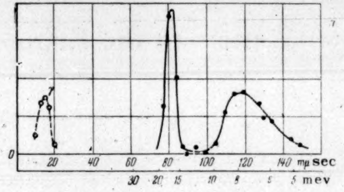

FIG. 3. Spectrum of neutrons in the bombardment of deuterium by deuterons of energy 13.0 mev. The γ-ray peak is displayed.

to 4.9 mev the energy of neutrons decreased from 6.3 to 4.1 mev and their time-of-flight increased; therefore, the peak was displaced to the right to a larger value of t. The width of the γ-peak is defined by the resolution of the system and is made up of the widths of pulses of the counter, of the master pulse and of the interval of working phase of the accelerating voltage of the cyclotron. The width of the neutron peak is somewhat larger; in the target 7 mev protons lose 0.5 mev and, consequently, the neutrons have approximately the same spread in energy.

The spectrum of neutrons from the bombardment of tritium by 14.4 mev deuterons is shown on Fig. 2. It is obtained at a distance of the counter from the target of 3 m, employing the same tritium-zirconium target. On the same figure is displayed the γ-peak, the magnitude of which is the same with the target and for the empty container is the same. The peak at $t = 40$ mμ sec is formed by neutrons of energy ~ 30 mev, corresponding to $Q_0 = 17.6$ mev in the reaction $T(d,n)He^4$, that is, to the formation of He^4 in the ground state. The wide peak with maximum at $t = 75$ mμ sec is formed by neutrons of mean energy ~ 8 mev. This neutron energy corresponds to the energy of the reaction $T(d,n)He^4$, $Q_1 = -5$mev. Reduction of the deuteron energy (by means of a platinum foil) to 12.4 mev leads to a displacement of the neutron group (see Fig. 2), agreeing with the value $Q_1 = -5$mev.

The curves (Figs 2 and 3) are corrected for the dependence of the efficiency of the detector on the neutron energy. It is assumed that this dependence has the form $\epsilon \sim \sigma(1 - B/E)$, where σ is the cross section of n-p scattering, E the energy of neutrons and B the threshold of the detector, which is defined by comparison of the observed intensities in the reaction $T(p,n)He^3$ of the neutron groups for two values of the energies of protons with intensities known from excitation curves[1]. In the region of energy studied, the efficiency was several per cent with thicknesses of the phosphor of 16 mm.

These results might be considered as a confirmation of the existence of a broad excited level of He^4 at ~ 22 mev. It should be noted, however, that the production of neutrons in the bombardment of tritium by deuterons is possible also in the reactions $T(d, pn)T$ and $T(d, 2n)He^3$. There is not enough basis to deny the possibility of production of the observed neutron groups in one of these reactions. To resolve this question, further experiments and calculations are necessary.

One such experiment has been carried out. It consisted in the investigation of the spectrum of neutrons produced in bombarding deuterium by deuterons of energy 13.0 mev. A gas target was used, in which the pressure of the deuterium was 3 atm, and the thickness (length along the deuteron beam) was 4 cm. The same target without gas was used as an 'empty target'. The results of the experiment are shown on Fig. 3. The distance from the target to the counter was 4.5 m. The peak at $t = 80$ mμ sec was formed by 16 mev neutrons, corresponding to $Q = 3.3$ mev in the reaction $D(d,n)He^3$. Besides this group, a second wide group of slower neutrons is visible. The maximum of intensity of this group corresponds to $t = 115$ mμ sec and, consequently, to an energy of 8.0 mev. These neutrons could be produced in the reaction $D(d,pn)D$, or by disintegration of both deuterons, or, finally, in the reaction $D(d,n)He^3$ with formation of He^3 in an excited state. In the last case $Q_1 = -3.5$ mev, which corresponds to an energy of ~ 7 mev of excited He^3.

The similarity of the spectra in the two reactions supports the fact that the second group of neutrons is produced rather by the breakup of the deuteron than by the ordinary reaction with formation of a final nucleus (He^4 or He^3) in an excited state.

Whatever the mechanism is, its large probability should be noted. Comparing the intensities of the neutron groups and taking into account the behavior of the detector efficiency with energy, it is possible to say that the cross section of production of a neutron of the second group at 0°, relative to the deuteron beam in the case T + $d(E_d = 14.4$ mev) is approximately 300 millibarn/sterad, and, in the case D + $d(E_d = 13.0$ mev), 100 millibarn/sterad.

The authors express their gratitude to colleagues in the Cyclotron Laboratory, headed by L. M. Nemenov, for providing the possibility of carrying out this work.

---

* The results of this work were communicated in the discussion at the Geneva conference in August, 1955.

[1] N. A. Vlasov, S. P. Kalinin, A. A. Oglublin L. N. Samoilov, V. A. Sidorov and V. I. Chuev, J. Exper. Theoret. Phys. USSR **28**, 639 (1955). Soviet Phys. JETP **1**, 500 (1956)

[2] H. B. Willard, T. K. Baira and J. D. Kington, Phys. Rev. **90**, 865 (1953).

Translated by G. Brown
23

Gamma and Photoluminescence Yields in Organic Crystals

Z. A. CHIZHIKOVA AND M. D. GALANIN
P. N. Lebedev Physical Institute
Academy of Sciences, USSR

(Submitted to JETP editor July 19, 1955)
J. Exper. Theoret. Phys. USSR **30**, 187-188
(January, 1956)

THE spectrum of luminescence due to gamma ray excitation coincides with the spectrum of photoluminescence[1]. This means that the last step in the process of the excitation of gamma luminescence is the transition from the same excited state that is involved in photoexcitation. Therefore, the energy yield for gamma luminescence can be represented as $B_\gamma = \rho B^q_\Phi$, where B^q_Φ is the absolute quantum yield of photoluminescence, depending on the correlation between the transitions with and without radiation; ρ can be called the effectiveness of the excitation. The magnitude of ρ shows what fraction of the energy absorbed in the substance is used for the excitation of the molecules which are effective in luminescence.

The aim of the present paper was to see if the magnitude of ρ is the same or differs appreciably for a number of substances. For this purpose the relative yields during gamma and photoexcitations were measured. Aromatic carbohydrates in the shape of monocrystals (dimensions $1.5 \times 1.2 \times 0.7$ cm^3) were investigated, and for comparison purposes the alkali-halide crystals NaI and KI, activated by Tl. Co^{60} was used as the source of gamma rays.

During the gamma excitation the amounts of energy absorbed in the crystals were determined from the relative absorption coefficients of gamma rays. As is known, during the passage of gamma rays through the substance the electrons are freed, and these electrons cause luminescence. The absorption of gamma rays with an energy of the order of 1 mev in organic substances takes place at the expense of the formation of Compton electrons; in NaI and KI crystals the probability for the Compton effect is 95% and the remaining 5% are due to the photoeffect. The probability of the Compton effect is proportional to the number of electrons; the number of electrons in P grams of the substance is $(PZ/M)N$, where Z is the number of electrons in a molecule, M – molecular weight, N – Avogadro's number.

Relative yields for gamma excitation were measured by two methods: a) by the observation of the average intensity of luminescence, b) by the observation of individual scintillations. For the measurement of the average intensity of luminescence, the crystal was placed in a photometric sphere which was covered on the inside with MgO. The light of the luminescence, excited in the crystal by gamma rays, went through an opening in the sphere and was incident on the window of the photomultiplier FEU-19. The values obtained for the photocurrent were divided by $(PZ/M)N$. A scintillation counter with an integral discriminator was used for the determination of the relative magnitude of the scintillations. For a comparison of the magnitude of the impulses it is necessary to reduce the distribution curves to such a scale that the total number of impulses contributing be the same; for this reason the ordinates of each curve were divided by $(PZ/M)N$. For the comparison of the relative magnitudes of the impulses the method of constant counting rates was used, i.e., the magnitudes of the displacements were compared, when the counting rate was the same for different crystals.

Measurements of the relative yields of photoluminescence were made during excitation by the 254 mμ line. This line was separated from the light emitted by the PRK-2 lamp by means of a monochromatic quartz and was focussed on the surface of the crystal which was placed in the photometric sphere. The sphere had two windows: one for the entrance of the excitation light, and one for the photomultiplier. The absorption of 254 mμ line in organic crystals is known to be complete,

Substance	$\overline{\lambda}$, mμ	k	B^q_ϕ, %	B_γ, %		ρ, %	
				1	2	1	2
Tolane	380	1.14	50	0.60	0.59	1.2	1.2
Stilbene	394	1.10	50	0.61	0.61	1.2	1,2
Naphthalene	350	1.23	17	0.21	0.23	1,2	1.4
Terphenyl	395	1.12	30	0,30	0,34	1.0	1.1
Dibenzyl	373	1.25	44	0.39	0,40	0.9	0.9
KI -Tl**	417	1.02	76	1,7	0,71	2.2	0,9
NaI - Tl**	411	1.0	66	1,25	1.21	1.9	1,8
Naphthalene with anthracene	—	—	—	—	0.7±0,2	—	—

the fraction of reflected light, according to the measurements by Morgenshtern made on the same samples[2], is 10-16%. Alkali-halide crystals were excited with the 291 mμ line in the first absorption band of Tl.

As a result of the measurement for gamma excitation as well as for photoexcitation, magnitudes proportional to $\int E_\lambda f_\lambda d\lambda$ were obtained, where E_λ is the energy distribution in the luminescence spectrum, and f_λ is the spectral sensitivity of the photomultiplier. In order to convert to magnitudes, proportional to the real yields, i.e., $\int E_\lambda d\lambda$, we measured f_λ and E_λ for all substances. From these data the magnitudes of $\int E_\lambda d\lambda$ were determined in relative units. Previously we measured the absolute quantum yields of photoluminescence for naphthalene and stilbene[3], and in reference 4 the absolute energy yield for gamma excitation of crystals of naphthalene with anthracene. This allowed us to give all magnitudes of yields in the absolute scale*.

In the above table $\overline{\lambda}$ – is the average wave length of the luminescence spectrum, K – relative sensitivity of the photomultiplier for the luminescence spectra, which is equal to $\int E_\lambda f_\lambda d\lambda / \int E_\lambda d\lambda$; B^q_ϕ, B_γ and ρ have the meaning given above. The magnitudes in columns 1 are from the measurements of the average intensity, those in columns 2 are from the scintillation measurements. For organic crystals ρ is the same with the precision ±15%; this precision is within the limits of accuracy of the experimental measurements. The variation of ρ for the organic alkali-halide crystals cannot be explained by the fact that the latter have a greater probability for the photoeffect, and thus points out the different processes of excitation in these two types of crystals. The difference in the magnitudes of the yield in KI - Tl, as determined by the average intensity and by the scintillations methods, is explained by the phosphorescence of KI - Tl, which is not taken into account in the method of scintillations.

We express our gratitude to L. M. Beliaev for submitting the crystals.

---

* The data obtained should be considered as the characteristics of the given samples, and not the substances, since it is possible that the samples contained small impurities which would influence the yield of luminescence.

** Crystals NaI and KI contained Tl in the concentration of the order of 10^{-3} gm/gm; this corresponds to a region where the intensity of gamma luminescence depends weakly on the concentration[5].

[1] J. C. D. Milton and R. Hofstadter, Phys. Rev. 75, 1289 (1949). W. S. Koski and C. O. Thomas, Phys. Rev. 79, 217 (1950). F. B. Harrison and G. T. Reynolds, Phys. Rev. 79, 732 (1950).

[2] Z. L. Morgenshtern, J. Exper. Theoret. Phys. USSR 29, 903 (1955). Soviet Phys. JETP 2, 773 (1956).

[3] M. D. Galanin and Z. A. Chizhikova, J. Exper. Theoret. Phys. USSR 26, 624 (1954).

[4] M. D. Galanin and A. P. Grishin, J. Exper. Theoret. Phys. USSR 30, 33 (1956); Soviet Phys. JETP 3, 32 (1956).

[5] L. M. Beliaev, M. D. Galanin, Z. L. Morgenshtern and Z. A. Chizhikova, Dokl. Akad. Nauk SSSR 99, 691 (1954); 105, 57 (1955).

Translated by M. Polonsky
24

Influence of Intermolecular Forces in Solutions on the Intensity of Raman Lines

IA. S. BOBOVICH AND T. P. TULUB

(Submitted to JETP editor December 6, 1954)
J. Exper. Theoret. Phys. USSR 30, 189-190
(January, 1956)

EARLIER[1,2] one of us observed anomalies in the thermal behavior of the intensities of the primary Raman series lines and explained these on the basis of the hypothesis of reciprocal deformation of the potential function of the excited electron states due to the collision of the molecules and expressible directly by the factor $\partial_{\nu_e}/\partial_q$ in derived polarizability (ν_e – frequency of virtual transition, q – the normal coordinate). It logically follows from such an explanation that, corresponding to these observed anomalies, there be spectral differences with solutions at constant temperature. Since there are only fragmentary and unreliable data of the effect of the solvent on the intensity of Raman lines in the literature[3-8], we made a systematic investigation of the pure substances carbon tetrachloride, benzene, hexane, chloroform, ethyl alcohol, acetone and of various 50% solutions of them. Spectra were recorded by photoelectric apparatus.[9] Integrated intensities of lines were measured. Each spectrum was recorded in this manner several times (from 3 to 22). Spectral reproducibility was within 1-6.5%. Account was taken of the possible influence of the refraction of the fluid. Based on these researches, the following were determined:

1. Due to intermolecular forces, the intensities of lines in the spectra investigated clearly showed more or less substantial alteration for proportional concentrations. Increased intensities in solutions were found with only infrequent exceptions.

2. All lines of the spectra of non polar compounds in solutions in polar liquids as a rule were weakened. This is very clearly shown in the solution of CCl_4 and benzene in ethyl alcohol (Fig. 1) and acetone, where the decrease (for instance, the lines of CCl_4) amounted to 20-40%.

3. All lines of spectra of polar compounds in solutions on non polar substances are intensified. Thus, for example, in the spectrum of a solution of alcohol in CCl_4 the intensity of the lines 1047 -1095 cm^{-1} increased more than 35% and the increase in intensity of other lines amounted on the average to about 20-25%.

4. In the case of an increase in intensities of lines of one component simultaneously there was, without exception, a decrease in intensity of the lines of the other component.

5. In certain non polar solutions and a few polar compounds for which additivity of the intensities might have been expected, lines of one component increased somewhat, but others were weakened (e.g. spectra of solutions of CCl_4 and chloroform in hexane). We are inclined to explain this on intricate spatial relations: The larger chlorine atoms of the molecules of CCl_4 and chloroform in a collision with hexane disturbs the reciprocal bonding interaction in such a close approach; which could easily occur to the hexane molecule in this mutual collision.

6. Elastic vibrations, as a rule, were more greatly modified by these intermolecular influences than valence vibrations. This rule is well illustrated by the data presented in Table I. The recordings of the spectra of solutions of acetone and ethyl alcohol in CCl_4 are exceptions where this difference between the elastic and valence vibrations does not appear. However, this result occured in only this one instance.

Thus, in the behavior of intensities of lines in

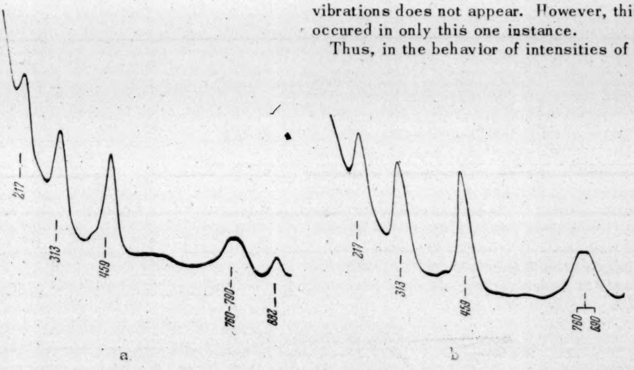

FIG. 1. Recordings of Raman Spectra
a) Solution 50% CCL_4 in ethyl alcohol
b) Solution 50% CCl_4 in Hexane

TABLE I

Variation in intensities of valence lines (v) and elastic oscillations (d) of the C-H coupling in certain solutions in comparison with pure substances.

Solution	frequency cm^{-1} type of vibration	$\frac{I_{\text{solution}} - I_{\text{pure substance}}}{I_{\text{pure substance}}}$ %
Hexane + CCl_4 Hexane lines	2852—2966, v	+ 8
	1440—1 460, d	+13
Hexane + chloroform Hexane lines	2852—2966, v	+ 6.5
	1440—1460, d	+13.3
Hexane + chloroform Chloroform lines	3019, v	—16.7
	1216, d	—23.5
Benzene + chloroform benzene lines	3047—3065, v	— 5
	1176, d	—14.3
Benzene + CCl_4 benzene lines	3047—3065, v	0
	1176, d	+10.0

solution and in the temperature variation of the intensities of spectra of pure liquids, many common features are developed. In these and in other cases, due to the influences of the polarity of bonding on the intensity of lines varying in the same direction, differences appear in the behavior between elastic and valence vibrations, showing the influence of spatial conditions. Consequently, in the explanation of these variation effects due to mutual distortion of potential functions of excited electron states it is probably possible to assume an operating hypothesis and to examine both phenomena from a unified point of view.

---

[1] Ia. S. Bobovich, Dokl. Akad. Nauk SSSR **48**, 39 (1954).

[2] Ia. S. Bobovich, Izv. Akad. Nauk SSSR Ser. Fiz. **19**, 219 (1955).

[3] W. Buchheim, Physik Z. **36**, 694 (1935).

[4] W. Hanle and F. Heidenreich, Physik Z. **37**, 594 (1936).

[5] F. Cennamoe and E. Vitale, Nuovo Cimento 13, 465 (1936).

[6] M. M. Sushchincki, Dokl. Akad. Nauk, SSSR 33, 21 (1941).

[7] G. Michel, Spectrochimica Acta 5, 218 (1952).

[8] I. Fedosow, Soc. Sci. Fennica, Comment. Phys. Math 14, 4 (1950).

[9] Ia. S. Bobovich and D. B. Gurevich, J. Exper. Theoret. Phys. USSR 27, 318 (1954).

Translated by E. S. Foster Jr.
25

An Attempt to Detect the Raman Effect in a Superconductor

M. S. Khaikin and V. P. Bykov
Institute for Physical Problems
Academy of Sciences, USSR

(Submitted to JETP editor July, 26, 1955)
J. Exper. Theoret. Phys. USSR **30**, 191-192
(January, 1956)

THEORETICAL considerations [1] indicate that it is possible that a gap of width $\Delta \sim kT_k$ appears in the electronic energy spectrum of a metal when it goes over into the superconducting state (T_k = transition temperature). Thus, when a light quantum ($h\nu > \Delta$) interacts with a metallic electron, Raman scattering of the light ought to take place, with a change of wavelength $\Delta\lambda = \lambda_0^2 \Delta/ch$; or, since $\Delta \sim kT_k$, $\Delta\lambda \simeq (k/ch)\lambda_0^2 T_k \simeq 0.7\,\lambda_0^2 T_k$ cm. For the *D* line of sodium this quantity amounts to ~ 2A for scattering from lead ($T_k = 7.2$°K). The intensity of the light scattered in this way should, apparently, be very small.[2,3,4,5]

The first attempt to observe the Raman effect in a superconductor was made by Verkin and Lazarev[6], but since their observations were carried out in reflected, rather than scattered light, they could observe only an extremely intense satellite . In the present work we undertook an investigation of the spectrum of scattered light, insuring the possibility of detecting extremely weak satellites.

When light of constant frequency is scattered by the inhomogeneities of a reflecting surface, a background is produced in the region of a satellite (because of the non-ideal monochromaticity of the light source) which limits the possibility of observing Raman scattering. A calculation shows that for our light source (see below) the radiation intensity in the region of the Raman satellite amounts to less than 10^{-3} - 10^{-4} of that at the center of the line. Since the surface of the sample scatters only a small fraction ($\sim 10^{-6}$)[7] of the light which would be scattered by a mat white surface, the background in the region of the Raman satellite amounts to 10^{-9} -10^{-10} of the intensity at the center of the line of the incident light. This consideration sets a theoretical lower limit to the intensity of the Raman-scattered light which we could detect.

We used an autocollimated spectrograph with an echelette-type diffraction grating, having the following characteristics: a resolving power of 10^5 in the region of the *D* doublet, linear dispersion of 4A/mm in the same range, a luminosity of 0.0015, and a focal length of 2 m. The grating was cut on aluminized glass and had 51,000 lines (600/mm). Approximately 50% of the light incident on the grating was concentrated into the first and second orders. The presence of weak ghosts, 4.5 A distant from the line, could not interfere with our observations.

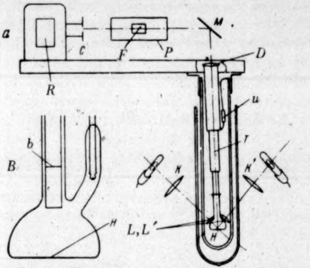

It was necessary to look in the spectrum for the hypothesized satellite at a distance of 0.2-0.5 mm from the center of the line. In order to prevent the formation of a corona, a resonant filter (see *F* in Fig. a) was placed along the path of the scattered light, which weakened the light of the original frequency by a factor of about 1000. The filter was made from pyrex in the form of a tray with plane-parallel top and bottom, and contained a small quantity of sodium and neon at a pressure of 1.7 mm (at 20° C). During an experiment the filter was heated to 255 ±5°C. The pressure of the neon and the temperature of the filter were selected so that there was no appreciable absorption at a distance of 0.5 A from the center of the line.

The samples were made from lead whose impurity content did not exceed 0.05%. Since the most important requirement for a sample was that it have a good reflecting surface, we used thin (10^{-5} cm) lead films, prepared by Shal'nikov's method[8]: the metal was evaporated in a vacuum onto a glass backing cooled to helium temperatures. The backing we employed was the smooth concave surface of a piece of glassware (Fig. b). Since at the temperature of liquid helium boiling under normal pressure (4.2°K) lead has already gone over into the superconducting state, the experiments were also carried out at this temperature.

Two spectral sodium lamps were used as light sources. With the aid of the condensing lenses *K, K', L, L'* (see figure), light from these lamps was directed onto the superconducting film *H*, applied on the inner surface of the small flask. A magnified image *B* (Fig. b) of the blackened inner surface of the deposited lead was formed in the concave lead mirror, so that the scattered light was observed as though it had an "absolutely black" body for its background. With the aid of the lens D and the pivoted mirror M, the image of the sample was projected on the slit of the spectrograph C, so that the scattered light passed through the resonant filter F, located in the furnace P. In order to prevent fogging of the flask from the freezing-out of air when the apparatus was cooled with liquid helium, the interior of the tube T was evacuated to a pressure of $\sim 10^{-3}$ mm Hg, and the remaining gas adsorbed by cold activated charcoal u. The spectrum of the light scattered by the sample was observed visually and also registered photographically on RF-3 X-ray film, which had been shown to be the most sensitive for the D-line.

Three experiments were carried out with exposures of 4, 11, and 12 hours. In visual examination of the scattered light, or in these photographs, no satellites were observed in the region of the D-doublet. Comparison of the exposures used in this experiment with those required in order to obtain noticeable blackening from light of intensity I_0 scattered by a mat white surface shows that a satellite of intensity $\sim 10^{-7}\, I_0$ could have been detected.

The authors express their profound gratitude to Professor A. I. Shal'nikov for his interest in this research.

---

[1] V. L. Ginsburg, Usp. Fiz. Nauk **48**, 25 (1952).

[2] E. Hirschlaff, Proc. Camb. Phil. Soc. **33**, 140 (1937).

[3] J. G. Daunt, T. C. Keely and K. Mendelssohn, Phil. Mag. **23**, 264 (1937).

[4] R. Hilsch, Phys. Z. **40**, 592 (1939).

[5] K. G. Ramanathan, Proc. Phys. Soc. (London) **A65**, 532 (1952).

[6] B. I. Verkin and B. G. Lazarev, Izv. Akad. Nauk SSSR Ser. Fiz. **12**, 598 (1948).

[7] C. V. Raman and L. A. Ramdas, Proc. Roy. Soc. (London) **A108**, 561 (1925).

[8] A. I. Shal'nikov, J. Exper. Theoret. Phys. USSR **10**, 636 (1940).

Translated by W. M. Whitney
26

Glow of Aluminum Alloys in an Electrolytic Bath

V. A. KRASNOKUTSKII
Khabarovsk

(Submitted to JETP editor July 24, 1955)
J. Exper. Theoret. Phys. USSR **30**, 192-193
(January, 1956)

IT is well known that aluminum and its alloys have protective oxide coatings on their surface, which prevent the penetration of oxygen into the interior of the metal. Much research[1-4] has been devoted to studies of the structure and properties of such oxide layers, in which the physical-chemical properties of the anticorrosive layers on aluminum have been studied rather thoroughly.

This paper presents a series of qualitative observations which reveal yet another feature, associated with the production of oxide films and their structure, namely the ability of aluminum and its alloys to glow under the action of an electric current in solutions of certain salts and bases.

The experimental arrangement for observation of the phenomenon of the glowing of electrodes in solutions of electrolytes during the passage of an electric current consisted of a bath containing the electrolyte and the electrodes. Alternating current was supplied from the line at 220v and direct current was supplied by a vacuum tube rectifier. Samples in the form of plates 50 mm × 30 mm × 1 mm and 60 mm × 70 mm × 1 mm were used as electrodes. The following materials were tested: copper, bronze, brass, lead, zinc, iron, silver, aluminum and its alloys AM, AMZ, D-1, D-16, "electron", "silumin" and others.

The following materials were used as electrolytes: 1-10% solutions of the salts: NaCl, NaBr, KCl, $NaHCO_3$, Na_2CO_3, NH_4Cl, $MgSO_4$, $(NH_4)_2SO_4$ Na_2SO_4, K_2SO_4, $KAl(SO_4)_2$, Na_2HPO_4, Na_3PO_4, $CaHPO_4$ and also 0.1-5% solutions of the bases NaOH, KOH and others.

During the observations, the potential drop between the terminals of the bath was read to an accuracy of 1v, while readings of the bath temperature were correct to 1°.

When the current flows through the bath in the dark, a uniform glow of the whole surface of the electrode can be observed by the unaided eye which in a way reminds one of the glow of luminescent material. In a 5% solution of $NaHCO_3$ the onset of the glow occurs at a voltage between 20 and 25v, and with increasing voltage, its intensity correspondingly increases.

By trying a number of different metals and alloys it was noticed that the glow occurs only on aluminum and its alloys. It was characteristic of these, that the color of the radiation of each aluminum alloy remains unchanged independent of the composition of the electrolyte, provided that, in the given electrolyte, the glowing does occur. Thus, for example, pure Al has a pale blue, nearly white radiation; the alloy AMZ has a rather intense orange colored radiation. It is difficult to distinguish visually the characteristics of the glow of the alloy D-1 from the glow of the alloy D-16, since both of them have nearly the same greenish blue radiation, but in contrast to other alloys, D-1 as well as D-16 exhibits an increase in intensity at the edge of the plates (a colored border).

The physical meaning of this phenomenon is not completely clear as yet. In every case it was evident that the glowing occurs only with the production of an oxide film and furthermore only with films of a specific structure, for oxide films on aluminum and its alloys, as is known, have a structure different from the films covering other metals like copper, lead, zinc, etc.

This hypothesis is confirmed by the fact that on first switching on the current the glowing does not begin instantaneously, but only after a certain time interval (0.25 to 0.5 sec); then the intensity of the glowing rises to a definite maximum which requires another time interval (2-4 sec). From this observation the glowing seems to accompany a process of formation of an oxide coating of a certain structure. At the conclusion of the formation of the oxide layer the brightness of the glowing remains constant and with subsequent switching of the current the growth described above is not observed. With the removal of the oxide film by boiling the electrode in alkali, the time for growth of the intensity of the glowing increases (4-5 sec), this being the time required for the appearance and growth of the oxide layer. When direct current is passed through a bath having two electrodes made from one and the same alloy it is observed that the glowing occurs only at the anode, i.e., only with motion of the current in the direction: metal, film, solution, and not in the reverse direction. This confirms again the connection between the glowing and the production of an oxide coating, which has control over this same valve action.

By trying a number of electrolytes, it was determined that the brightest glowing occurs in solutions of $NaHCO_3$, Na_2HPO_4, NaH_2PO_4, Na_3PO_4, NaOH, KOH. Somewhat weaker glowing occurs in solutions of Na_2CO_3, $(NH_4)_2CO_3$. Still weaker glowing occurs in $(NH_4)_2SO_4$, $MgSO_4$. The glowing does not occur in acids. The glowing is also absent in solutions of NaCl, KCl, NaBr and KBr. Furthermore, the addition of one of these salts to a solution in which glowing occurs brings about an attenuation and cessation of the glowing, a sharp increase of the voltage in the circuit and a growth of the temperature of the solution toward the boiling point. At the same time, one observes the onset of instantaneous spark discharges and afterwards unstable electric arcs between the electrodes and the solutions[5].

The concentration of the solutions required for convenient observation varies in its dependence on the degree of dissociation of a given substance. Thus, for $NaHCO_3$, NaH_2PO_4, 1-2% was sufficient, while for NaOH, KOH a smaller concentration was needed. As the concentration was increased, the intensity of the glowing increased correspondingly, up to a definite limit. With an applied voltage of 220v, upon increasing the concentration of the solution (e.g. $NaHCO_3$) with the addition of undissolved soda, one can observe a very beautiful phenomenon of instantaneously flashing and extinguishing tiny spark discharges, superficially resembling scintillation. This phenomenon starts up with the introduction of some more soda, but with the passage of time it grows weaker and stops until more soda is added. During the course of these experiments the temperature of the solution experienced an insignificant rise and only with high concentrations and greater current densities did the solution go as far as the boiling point. For moderate concentrations of the solution (e.g., 1-2% $NaHCO_3$), heating of the electrolyte was almost unobservable (cold glowing) and the temperature of the bath remained constant with the passage of time.

Further studies of this phenomenon will establish its physical meaning and will determine its practical applications; in particular, the ability of each alloy of aluminum to glow with a very specific color may make it possible to bring about the use of the phenomenon for the purpose of spectral-electrolytic analysis.

---

[1] N. D. Tomashov, *Theory of the Corrosion of Metals*, Metallurgizdat, 1952.

[2] N. D. Tomashov and A. V. Bialobzheskii, *Research on the Corrosion of Metals*, Tr. In-ta Fiz. Khim. Akad. Nauk SSSR 1, 1951, p. 136.

[3] N. D. Tomashov and M. N. Tiukina, loc. cit. p. 110.

[4] G. V. Akimov, *Theory and methods of observation of the corrosion of metals*, Acad. Sci. USSR, 1945.

[5] I. Z. Iasnogorodskii, *Heating of metals and alloys in electrolytes*, Mashgiz (1952).

Translated by J. J. Loferski
27

The Effect of Absorption of Luminescence on Its Intensity in the Powdered Luminophors

A. P. IVANOV

(Submitted to JETP editor June 8, 1954)
J. Exper. Theoret. Phys. USSR 30, 196-197
(January, 1956)

IN reference 1 the dependence was established of the intensity of luminescence of the powdered luminophors on the size of the grains, the relative index of refraction, the index of absorption for the exciting radiation, and the thickness of the layer. The absorption of the light of luminescence was not considered. In the present report we considered the influence of the latter factor.

Consider a horizontal infinite slab of thickness x_0. For the excitation of luminescence, let this slab be uniformly illuminated from above by diffuse monochromatic flux. Because of the heterogeneous nature of the slab, the light is scattered in all directions. Therefore, if we consider a horizontal plane inside the slab, this plane will be illuminated from above and below. Let us call E_1 the illumination from above, and E_2 the illumination from below. Gershun[2] showed that these illuminations are respectively equal to :

$$E_1(x) = \frac{R^{-1}e^{L(x_0-x)} - Re^{-L(x_0-x)}}{R^{-1}e^{Lx_0} - Re^{-Lx_0}}; \tag{1}$$

$$E_2(x) = \frac{e^{L(x_0-x)} - e^{-L(x_0-x)}}{R^{-1}e^{Lx_0} - Re^{-Lx_0}}$$

Here $L = \sqrt{k^2 + 2ks}$, and $R = 1 + k/s - \sqrt{(k/s)^2 + 2k/s}$ is the coefficient of reflection of an infinitely thick layer, s and k are the constants of scattering and absorption, respectively, calculated for unit thickness.

At the expense of the absorption of the scattered light, the object under consideration will luminesce. The spectral density of the light flux radiated above and below by the infinitely thin layer dx from the unit surface will be: $dI = {}^1/_2 CkB(E_1 + E_2)\,dx$. Adjacent to this layer on one side is a layer of thickness x, and on the other side – a layer of thickness $x_0 - x$. On these layers the light of luminescence suffers multiple reflections. When we sum all elementary fluxes from the infinitely thin layer and then integrate the resulting expressions over the entire thickness, we find for the intensity of the luminescence from the side opposite to the side of excitation:

$$I_1 = \frac{1}{2}CkB\frac{(1+R_l)e^{-L_l x_0}}{(1-R_l^2e^{-2L_l x_0})(R^{-1}e^{Lx_0} - Re^{-Lx_0})}\left\{\left(\frac{1}{R}+1\right)e^{Lx_0}\left[\frac{e^{(L_l-L)x_0}-1}{L_l-L} - R_l\frac{1-e^{-(L_l+L)x_0}}{L_l+L}\right] - (R+1)\,e^{-Lx_0}\left[\frac{e^{(L_l+L)x_0}-1}{L_l+L} - R_l\frac{1-e^{-(L_l-L)x_0}}{L_l-L}\right]\right\}; \tag{2}$$

and from the side of excitation*:

$$I_2 = \frac{1}{2}CkB\frac{1+R_l}{(1-R_l^2e^{-2L_l x_0})(R^{-1}e^{Lx_0} - Re^{-Lx_0})}\left\{\left(\frac{1}{R}+1\right)e^{Lx_0}\left[\frac{1-e^{-(L_l+L)x_0}}{L_l+L} - R_l\frac{e^{-(L_l+L)x_0}-e^{-2L_l x_0}}{L_l-L}\right] + (R+1)\,e^{-Lx_0}\left[\frac{e^{-(L_l-L)x_0}-1}{L_l-L} + R_l\frac{e^{-(L_l-L)x_0}-e^{-2L_l x_0}}{L_l+L}\right]\right\} \tag{3}$$

Here L_l and R_l are given in terms of the constant of scattering s_l and the constant of absorption k_l of the light of luminescence. As was shown in reference 1, s and k in many cases can be given in terms of the effective size of the grain d, the index of absorption k_b, the coefficient of reflection from the surface of the grain r, and the coefficient of packing c:

In case the layer is infinitely thick ($x_0 = \infty$)

$$I_2 = {}^1/_2 CB(1-R)(1+R_l)\,L/(L+L_l). \tag{4}$$

If the light of luminescence is not absorbed by the particles of the luminophors, then $L_l = 0$, $R_l = 1$ and $I_2 = I_0 = CB(1-R)$, i.e.,

$$I_2 = {}^1/_2 I_0(1+R_l)\,L/(L+L_l). \tag{5}$$

The expression obtained can be used for the conversion of the measured spectrum into the true radiation spectrum.

Let us consider some special cases of Eqs. (2) and (3).

1. The exciting radiation is weakly scattered and is attenuated according to the exponential law. X-rays approximately satisfy this condition. In this case $L = R$; $R \approx 0$ and formulae (2) and (3) are transformed respectively into

$$I_1 = \frac{1}{2} CkB \frac{1 + R_l}{1 - R_l^2 e^{-2L_l x_0}} \left[\frac{e^{-kx_0} - e^{-L_l x_0}}{L_l - k} + R_l \frac{e^{-(2L_l - k)x_0} - e^{-L_l x_0}}{L_l + k} \right], \tag{6}$$

$$I_2 = \frac{1}{2} CkB \frac{1 + R_l}{1 - R_l^2 e^{-2L_l x_0}} \left[\frac{1 - e^{-(L_l + k)x_0}}{L_l + k} - R_l \frac{e^{-(L_l + k)x_0} - e^{-2L_l x_0}}{L_l - k} \right] \tag{7}$$

2. The exciting radiation is weakly scattered and penetrates to a small depth (for instance, α-particles). Therefore, $L = k >> L_l$; $R \approx 0$ and we obtain:

$$I_1 = \frac{1}{2} CB \frac{(1 - R_l^2) e^{-L_l x_0}}{1 - R_l^2 e^{-2L_l x_0}}, \tag{8}$$

$$I_2 = \frac{1}{2} CB \frac{(1 + R_l)(1 - R_l e^{-2L_l x_0})}{1 - R_l^2 e^{-2L_l x_0}}.$$

When $x_0 = \infty$

$$I_2 = {}^1/_2 CB (1 + R_l), \tag{9}$$

i.e., with the increase of the size of the grain (d), the coefficient of reflection R_l decreases and, consequently, I_2 decreases.

3. The exciting radiation is weakly scattered and weakly absorbed (gamma rays). In this case the layer is found to be uniformly excited for sufficiently great thicknesses, and, therefore,

$$I_1 = I_2 = \frac{CkB}{2L_l} \frac{1 + R_l}{1 - R_l^2 e^{-2L_l x_0}} [1 - e^{-2L_l x_0} + R_l (e^{-2L_l x_0} - e^{-L_l x_0})].$$

For an infinitely thick layer, $I_1 = 0$ and $I_2 = {}^1/_2 CkB \times (1 - R_l)/k_l$, i.e., with the increase of d, the coefficient of reflection decreases and I_2 increases.

In such a way the different nature of the attenuation of the excitation flux leads to the result that an increase of the crushing of the powder of the luminophor increases the brightness of the luminescence in one case and decreases it in the second. Therefore we can imagine a case in which the brightness of the luminescence depends weakly on the degree of dispersion.

---

* The formulas obtained are indeterminate if the light of the luminescence is not absorbed. In this case it is necessary during the calculation to use the formulas $t(x) = 1/(1 + s_l x)$ and $r(x) = s_l x/(1 + s_l x)$ (see reference 3). As a result, expressions are obtained which coincide with the formulas for the intensity of luminescence, given in reference 1.

[1] A. P. Ivanov, J. Exper. Theoret. Phys. USSR 26, 275, (1954).

[2] A. A. Gershun, Trudy GOI 11, 99, 43 (1936).

[3] M. M. Gurevich, Trudy GOI 6, 57, 1, (1931)

Translated by M. Polonsky
29

Concerning Some Thermodynamic Inequalities

V. P. Silin
P. N. Lebedev Physical Institute,
Academy of Sciences, USSR

(Submitted to JETP editor July 24, 1954)
J. Exper. Theoret. Phys. USSR 30, 197-199
(January, 1956)

1. IN the thermodynamic investigation of the properties of materials which possess magnetic and dielectric properties that obey the general law set forth, for example, in reference 1, it is possible to obtain thermodynamic inequalities which are the necessary conditions for thermodynamic equilibrium . The present communication is devoted to a brief derivation of such inequalities, and to the obtaining, with the help of the latter, of certain conclusions as to the form of the equilibrium curve of the magnetization of a magnet.

Assuming that each element of the volume of a body is in a state of thermodynamic equilibrium, we can represent the first law of thermodynamics, for media of interest to us, in the following form

$$\Delta e = T\Delta s + (\mathbf{H}\Delta\mathbf{B} + \mathbf{E}\Delta\mathbf{D})/4\pi. \tag{1.1}$$

Following Landau and Lifshitz[1], it is easy to calculate the minimum work done on a body, located in some medium, by external, thermally isolated bodies. In such a case, the energy of the closed system (body + surroundings), when the body is not in equilibrium with the medium, differs from its own maximum value by an amount

$$\Delta S_p = -\frac{R_{\min}}{T_0} = -\frac{1}{T_0}\left[\Delta E - T_0\Delta S - \frac{1}{4\pi} \times \int dV\,(\mathbf{H}\cdot\Delta\mathbf{B} + \mathbf{E}\cdot\Delta\mathbf{D})\right], \tag{1.2}$$

where ΔE, etc., represent the differences between the equilibrium values of the appropriate quantities and their values in the state of total equilibrium.* It follows from Eq. (1.2) that for the element of volume of a body found in thermodynamic equilibrium with the remaining parts of the body (which can be considered as the medium) the following condition must hold

$$\Delta e - T\Delta s - (\mathbf{H}\cdot\Delta\mathbf{B} + \mathbf{E}\cdot\Delta\mathbf{D})/4\pi > 0. \tag{1.3}$$

For simplicity, we assume below that $\Delta\mathbf{D} \equiv 0$, and limit ourselves to taking only the magnetic field into account. It is evident that for an electric field, entirely analogous results will follow. Expanding Δe in a power series in Δs and ΔB, we get from Eq. (1.3):

$$\frac{\partial^2 e}{\partial s^2}(\Delta s)^2 + \sum_{i,j}\frac{\partial^2 e}{\partial B_i \partial B_j}\Delta B_i \Delta B_j > 0. \tag{1.4}$$

The condition of the positive nature of the principal minors of the quadratic form (1.4) gives the corresponding thermodynamic inequality. In this case, in particular, we get

$$(\partial H_i/\partial B_i)_T > 0. \tag{1.5}$$

We have neglected any change in the number of particles per unit volume. Account of such changes leads to the result that in differentiation in (1.5) must be carried out at constant chemical potential*.

The inequality (1.5) is the analogue of the thermodynamic inequality $(\partial p/\partial V)_T < 0$ and corresponds to the fact that, at constant temperature, an increase in the magnetic induction is always accompanied by an increase in the magnetic field. Thus, in the state of thermodynamic equilibrium, the magnetization curve of a magnet has neither maxima nor minima. For a linear medium $(\mathbf{B} = \mu\mathbf{H})$ it follows from Eq. (1.5) that μ must be greater than zero. We note that for thermodynamic stability of the equilibrium state, it is also necessary that the coefficients of the expansion of Δe in powers of Δs and ΔB_i should be bounded, since in the opposite case, small changes in the parameters would lead to arbitrarily large changes in the state. Then, from the condition of the finiteness of $(\partial H_i/\partial B_i)_T$, and from the condition (1.5), it follows that as $H \to 0$, the magnetic induction tends toward the value $B(H=0)$, as the first power of H.

Finally, we note that it follows from the condition (1.5) that for an isotropic magnet, the magnetic field, equal in this case to $\mathbf{H} = (4\pi\mathbf{B}/B)\,(\partial e/\partial B)_s$, and the induction must be parallel*. Actually, in this case the inequality (1.5) takes the following form

$$\frac{1}{4\pi}\frac{\partial H_z}{\partial B_z} = \frac{\partial}{\partial B_z}\left(\frac{B_z}{B}\frac{\partial e}{\partial B}\right) = \frac{\partial^2 e}{\partial B^2}\frac{B_z^2}{B^2} + \frac{1}{B}\frac{\partial e}{\partial B} - \frac{B_z^2}{B^3}\frac{\partial e}{\partial B} > 0 \tag{1.6}$$

and for $B_z = 0$ gives the result indicated.

2. We now consider the somewhat more complicated case of a system for whose phenomenological description it is generally not possible to introduce B or H. An example of such a system is a superconductor, considered from the point of view of the phenomenological theory of superconductivity developed by Ginzburg and Landau[2].

Let such a system be found in a constant and everywhere homogeneous magnetic field H_0. In other words, H_0 represents the magnetic field which existed before the introduction of the body. The first law of thermodynamics for processes which are carried out in an electromagnetic field has the form[3]

$$\Delta E = \Delta Q - \Delta t\,\frac{c}{4\pi}\int(\mathbf{E}\times\mathbf{H})\,d\mathbf{f} \tag{2.1}$$

Let the surface of integration extend to infinity; more accurately, we take the magnetic field on it to be equal to $\mathbf{H}_0$. Then we have

$$-\Delta t\int(\mathbf{E}\times\mathbf{H}_0)\,d\mathbf{f} = -\Delta t\int\mathbf{H}_0\,\nabla\times\mathbf{E}\,dV = 1/c\int\mathbf{H}_0\,\Delta\mathbf{H}\,dV$$

and consequently, Eq. (2.1) can be written in the following form $(\Delta Q = T\Delta S)$

$$\Delta E = T\Delta S + \frac{1}{4\pi}\int dV\,\Delta\mathbf{H}\cdot\mathbf{H}_0. \tag{2.2}$$

From this it follows that at constant temperature, and constant, everywhere homogeneous, magnetic field, the function has an extremum in the state of thermodynamic equilibrium.

$$\Phi(T, \mathbf{H}_0) = E - TS - \frac{1}{4\pi}\int\mathbf{H}_0\cdot\mathbf{H}\,dV \tag{2.3}$$

Actually, $\Delta\Phi = 0$ under these conditions, in agreement with Eq. (2.2). The relations (2.2) and (2.3) were used by the author[4] in the investigation of the destruction of the superconducting state in a magnetic field.

We can raise the question as to the determination of the minimum work done by an external source on a body placed in a medium where the magnetic field is constant and homogeneous. It is not difficult to find that

$$R_{\min} = \Delta(E - T_0 S) - \frac{1}{4\pi}\int \mathbf{H}_0 \Delta\mathbf{H}\, dV. \qquad (2.4)$$

Similar considerations permit us to obtain the following generalized form of (1.5):

$$(\partial H_0^i / \partial \overline{H}^i)_T > 0. \qquad (2.5)$$

Here $\overline{H}^i = V^{-1}\int H^i dV$ (V is the volume enclosed by the surface on which the magnetic field is taken to be equal to H_0). Conclusions can also be drawn from (2.5) as to the dependence of $\overline{H}$ on H_0, as was done above for the dependence of B on H.

---

* Equation (1.2) permits us to determine the probability of thermodynamic fluctuations in the following manner:

$$w \sim \exp\left\{-\frac{1}{2kT}\left[\Delta T \Delta S - \frac{1}{4\pi}\int dV\,(\Delta\mathbf{H}\Delta\mathbf{B} + \Delta\mathbf{E}\Delta\mathbf{D})\right]\right\}.$$

[1] L. D. Landau and E. M. Lifshitz, *Statistical Physics*, GITTL, 1951.

[2] V. L. Ginzburg and L. D. Landau, J. Exper. Theoret. Phys. USSR 20, 1064 (1950).

[3] I. E. Tamm, *Fundamentals of Electrical Theory*, Gostekhizdat, 1946.

[4] V. P. Silin, J. Exper. Theoret. Phys. USSR **21**, 1330 (1951).

Translated by R. T. Beyer
30

On the First Appearance of Atomic Electrons With l, n, n_r and $n + l$ Given

V. M. KLECHKOVSKII
Moscow

(Submitted to JETP editor August 3, 1954)
J. Exper. Theoret. Phys. USSR **30**, 199-201
(January, 1956)

EARLIER it was shown[1] that the expression for Z_l, the atomic number of an element [an expression obtained on the basis of the rule of systematic filling (Aufbau principle) of the $(n - l)$ groups[2]], in the electronic shell of neutral unexcited atoms of which the first electron appears with a given value for the orbital quantum number l, can be reduced to the form:

$$Z_l = {}^1\!/_6\,(2l + 1)^3 + {}^1\!/_6\,(5 - 2l). \qquad (1)$$

The second member of the right side of this equation represents a relatively small value and the dependence of Z_l on l is determined principally by the first member, which is proportional to $(2l + 1)^3$; this agrees well with the conclusions of statistical theory.[3] One can also reduce to a similar form a series of other equations[4] obtained on the basis of that same rule, equations for the first appearance of atomic electrons with a given value for the principal quantum numbers, for the radial quantum number and with a given value for the sum of the principal and orbital quantum numbers.

For the simplification of further exposition we shall introduce the following notation. Let

$$K(y) = {}^1\!/_6\, y^3 + \delta;\ \delta = \begin{cases} -{}^1\!/_6\, y, & \text{if } y \text{ is odd} \\ +1/3\, y, & \text{if } y \text{ is even.} \end{cases} \qquad (2)$$

From the condition $l \leq n - 1$ and from the integral value of l it follows that the maximum value of the orbital quantum number ($l_{\max}$) in the presence of the given value of $n + l$ is equal to $0.5\,(n + l - 1)$ if $n + l$ is odd and equal to $0.5\,(n + l - 2)$ if $n + l$ is even. Therefore, the number of different quantum positions in the limits of one $(n + l)$ group is equal to:[5]

$$\sum_{l=0}^{l_{\max}} 2(2l + 1) = 2(l_{\max} + 1)^2 = \begin{cases} 0.5(n + l + 1)^2, & \text{if } n + l \text{ is odd} \\ 0.5\,(n + l)^2, & \text{if } n + l \text{ is even} \end{cases} \qquad (3)$$

From this it follows that the number of different quantum positions in the limits of an aggregate, including the $(n + l)$ groups with all the values of $n + l$ less than a certain odd number $y = 2q + 1$ $(q = 0,1,2,3,..)$ is equal to

$$\sum_{q=0}^{0.5\,(y-1)} (2q)^2 = {}^1\!/_6\, y^3 - {}^1\!/_6\, y. \qquad (4)$$

For the aggregate itself, including the $(n + l)$ groups with the values of $n + l$ less than a certain even number $y = 2q + 2$, we have, consequently,

$$\sum_{q=0}^{0.5\,(y-2)} (2q)^2 + 1/2\, y^2 = 1/6\, y^3 + 1/3\, y. \qquad (5)$$

By such means, taking into consideration the determination of the operator K in accordance with Eq. (2), we can say that the total number of different quantum positions for which $n + l < y$ is equal to $K(y)$.

In conformity with the rule of systematic filling (Aufbau principle) of the $(n + l)$ groups, the electron adjoining the singly ionized atom occupies in the ground state the level with the minimum possible value of $n + l$[6] without violating the Pauli exclusion principle. Therefore, the transition to the filling of the levels with a new value of $n + l$ proceeds (with the increase of Z) after all levels with smaller values of $n + l$ are charged. From this it is possible to conclude that the value of Z_{n+l} equal to

$$Z_{n+l} = \mathrm{K}(n + l) + 1. \tag{6}$$

must correspond to the first appearance of the electron with given $n + l$.

In conformity with that same general rule, the filling of n of the l-subgroups in the limits of each $(n + l)$ group proceeds from the subgroups with large l's to the subgroups with smaller l's.[2] Therefore the first appearance of the electron with given l must have a place in the beginning of the filling of each $(n + l)$ group with an odd value for $(n + l)$ equal to $2l + 1$. Consequently,

$$Z_l = \mathrm{K}(2l + 1) + 1. \tag{7}$$

This expression is the same as Eq. (1).

The filling of the levels with a new value for the principal quantum number must begin in accordance with that same rule, in the midst of the filling of levels belonging to the $(n + l)$ group with a given value for $n + l$, the levels of the s-subgroup of this $(n + l)$ group remaining unfilled. From this it follows that:

$$Z_n = \mathrm{K}(n + 1) - 1. \tag{8}$$

The filling of the levels with a given value for the radial quantum number must begin likewise from the s-subgroup because, with n_r given, the levels with the least l are always more penetrating with regard to energy. Keeping in mind that $n = n_r + l + 1$ and that, consequently, in the case of the s-levels $n_r = n - 1$, we can write:

$$Z_r = \mathrm{K}(n_r + 2) - 1. \tag{9}$$

where Z_r is the atomic number of the element in the electronic shell of the neutral unexcited atoms, of which the first electron appears with a given value of the radial quantum number n_r.

Taking into consideration the fact that the change of the value of $K(y)$ with the increase of y is determined chiefly by the term $(1/6)y^3$ independent of the evenness of y, one can write the expression for Z_n, Z_r and $Z_n + l$ in the form:

$$Z_n = {}^1/_6\,(n + 1)^3 + \delta_n;\ \delta_n \tag{10}$$

$$= \begin{cases} +{}^1/_3\,(n - 2), & \text{if } n \text{ is odd} \\ -{}^1/_6\,(n + 7), & \text{if } n \text{ is even} \end{cases}$$

$$Z_r = {}^1/_6\,(n_r + 2)^3 + \delta_r;\ \delta_r \tag{11}$$

$$= \begin{cases} -{}^1/_6\,(n_r + 8), & \text{if } n_r \text{ is odd} \\ +{}^1/_3\,(n_r - 1), & \text{if } n_r \text{ is even} \end{cases}$$

$$Z_{n+l} = {}^1/_6\,(n + l)^3 + \delta_{n+l};\ \delta_{n+l} \tag{12}$$

$$= \begin{cases} -{}^1/_6\,(n + l - 6), & \text{if } n + l \text{ is odd} \\ +{}^1/_3\,(n + l + 3), & \text{if } n + l \text{ is even} \end{cases}$$

It is not difficult to be convinced that in the determination of the dependence of Z_l on l, Z_n on n, etc., the additional term (δ) plays a secondary role.

By such means it has been shown that the expressions for Z_l, Z_n, Z_r and Z_{n+l} can be reduced to a general binomial form for which it is found the principal dependence of Z_l, Z_n, Z_r and Z_{n+l} on one of the terms which is proportional, respectively, to $(2l + 1)^3$, $(2l + 1)^3$, $(n + 1)^3$, $(n_r + 2)^3$ and $(n + l)^3$.

Earlier it was noted[1] that Eq. (1) gives the values of Z_l for $l = 0$, 1 and 2 which correspond with the experiments and a value of Z_l, which is very close to the experimental value for $l = 3$. As concerns the equations (10)-(12) developed above, they then give the values of Z which correspond exactly with the experimentally obtained values without exceptions; Z_n and Z_r take the values 1, 3, 11, 19, 55 and 87 and Z_{n+l}, the values 1, 3, 5, 13, 21, 39, 57, and 89. The series of elements which correspond to the first appearance of the electron with given n and given n_r are identical because the filling of the levels with a new value for n_r, as also of the levels with a new value for n, always begins with the s-subgroup. In connection with this, the elements whose electron for the first time appears with a new value for n (and with a new value for n_r) are those elements of the first group of the system of Mendeleev, the elements lying at the beginning of each period. Since the chief quantum number of the s-subgroup of the levels with the filling of which (group) the period begins, is equal to the number of the period, one can consider that Eq. (10) as coming from the rule of systematic filling (Aufbau principle) of the $(n + l)^a$ groups, an expression of the relation between the number of the period in the system of Mendeleev and the charge of the nucleus of the atoms of the element beginning the period.

---

[1] V. M. Klechkovskii, J. Exper. Theoret. Phys. USSR 26, 760 (1954).

[2] V. M. Klechkovskii, Dokl. Akad. Nauk SSSR **80**, 603 (1951); J. Exper. Theoret. Phys. USSR **23**, 115 (1952); see also Yeou Ta, Ann. Physik 1, 88 (1946); L. Simmons, J. Chem Educ. **24**, 588 (1947); R. Hakala, J. Phys. Chem. **56**, 178 (1952).

[3] A.Sommerfeld, Wave Mechanics vol. II. D. Ivanenko and S. Larin, Dokl. Akad. Nauk SSSR **88**, 45, (1953).

[4] V. M. Klechovskii, Izv. Timiriaz s-kh. Akad. 2 (6), 205, 1954; Refer to Dokl. Timiriaz. s-kh. Akad. 20, 309 (1954).

[5] V. M. Klechkovskii, Zh. Fiz. Khim. **27**, 1251 (1953).; Dokl. Akad. Nauk SSSR **92**, 923 (1953).

[6] V. M. Klechkovskii, Dokl. Akad. Nauk SSSR **86**, 691 (1952); J. Exper. Theoret. Phys. USSR **25**, 179 (1953),

Translated by B. Abbott
31

Gamma Radiation Accompanying the Absorption of Fast Protons by Nuclei

A. I. AKHIEZER AND I. IA. POMERANCHUK

Physical Technical Institute
Academy of Sciences, Ukranian SSR

(Submitted to JETP editor April 29, 1955)
J. Exper. Theoret. Phys. USSR **30**, 201-203
(January, 1956)

THE absorption of fast protons by nuclei can be accompanied by the radiation of photons through two mechanisms. On the one hand, the absorption of a proton by the nucleus causes a diffraction perturbation of the proton wave, enabling it to radiate (diffraction radiation)[1]; on the other hand, radiation can be caused by the direct absorption of the proton (bremsstrahlung radiation)[2]. The second mechanism is more essential. In the present note we wish to estimate the role of the anomalous magnetic moment of the proton in bremsstrahlung radiation, our earlier calculation of which[2] was not exact.

We will assume that for an estimate of the bremsstrahlung the proton can be described by the Dirac equation with an anomalous magnetic moment μ':

$$(\gamma_\nu \partial/\partial x_\nu - ie\gamma_\nu A_\nu - i\mu'\gamma_\nu\gamma_\rho F_{\nu\rho} + m)\psi = 0, \qquad (1)$$

here $F_{\nu\rho} = \partial A_\rho/\partial x_\nu - \partial A_\nu/\partial x_\rho$ is the field tensor and A_ν is the vector potential, equal to $A_\nu = (2\omega)^{-1/2} e_\nu \exp\{-i(\mathbf{kr} - \omega t)\}$ (e_ν is the unit polarization vector, ω the frequency, $\mathbf{k}$ the wave vector of the photon; we employ the system of units in which $c = \hbar = 1$). Since $e \ll 1$, in terms containing the electromagnetic field, it is possible to replace ψ by $\psi_0 = ue^{i(\mathbf{pr} - Et)}$, where u is the spinor amplitude of the incident plane wave of the proton with momentum $\mathbf{p}$ and energy E. In this way we obtain an inhomogeneous equation for

$$(\vec{\gamma}\partial/\partial\mathbf{r} - \gamma_4 E' + m)\Phi = (2\omega)^{-1/2}(ie\hat{e} + 2\mu'\hat{k}\hat{e})\Phi_0(\mathbf{r})e^{-i\mathbf{kr}}, \qquad (2)$$

where

$$E' = E - \omega,\ \hat{a} = \gamma_\nu a_\nu \quad (\nu = 1, 2, 3, 4),\ \Phi_0(\mathbf{r}) = ue^{i\mathbf{pr}}.$$

Obtaining $\Phi(\mathbf{r})$ from this equation on the surface of the nucleus, which is assumed completely black with respect to the incident proton, it is possible to define the current of protons, absorbed by the nucleus, which has one photon at infinity. This current density is defined by the formula

$$j = \left(\bar{\Phi}\frac{\vec{\gamma}\mathbf{p}}{p}\Phi\right)_{r=R},\quad \bar{\Phi} = \Phi^*\gamma_4,$$

and the bremsstrahlung cross-section is equal to

$$d\sigma = (j\pi R^2/v)(2\pi)^{-3}\omega^2 d\omega d^2\theta \qquad (3)$$

where v is the proton velocity, $d^2\theta$ the solid angle in which the photon is emitted.

The solution of Eq. (2) has the form

$$\Phi(\mathbf{r}) = -(2\omega)^{-1/2}\int G_0(\mathbf{r}, \mathbf{r}') \times (ie\hat{e} + 2\mu'\hat{k}\hat{e})e^{-i\mathbf{kr}'}\Phi_0(\mathbf{r}')d\mathbf{r}', \qquad (4)$$

where G_0 is the Green's function for the Dirac equation[1]:

$$G_0(\mathbf{r}, \mathbf{r}') = \frac{1}{4\pi}\left(\vec{\gamma}\frac{\partial}{\partial\mathbf{r}} - \gamma_4 E' - m\right)\frac{e^{ip'|\mathbf{r}-\mathbf{r}'|}}{|\mathbf{r}-\mathbf{r}'|}, \qquad (5)$$

$$p' = \sqrt{E'^2 - m^2}.$$

Employing Eq. (5) it is possible to show that $\Phi(\mathbf{r})$ is given by the formula

$$\Phi(\mathbf{r}) = \frac{1}{2\sqrt{2\omega}}[i(\mathbf{p}-\mathbf{k})\vec{\gamma} - E'\gamma_4 - m]$$

$$\times [ie\hat{e} + 2\mu'\hat{k}\hat{e}]\, u\, \frac{e^{i(\mathbf{p}-\mathbf{k})\mathbf{r}}}{p'(p' - |\mathbf{p}-\mathbf{k}|)}$$

and that the current is equal to

$$j = \frac{i}{32\omega p E p'^2 (p' - |\mathbf{p}-\mathbf{k}|)^2} \operatorname{Sp}\{[-2\mu'\hat{e}\hat{k} - ie\hat{e}] \tag{6}$$

$$\times [i(\mathbf{p}-\mathbf{k})\vec{\gamma} - E'\gamma_4 - m]\vec{\gamma}\mathbf{p}$$

$$\times [i(\mathbf{p}-\mathbf{k})\vec{\gamma} - E'\gamma_4 - m]\, [ie\hat{e} + 2\mu'\hat{k}\hat{e}]$$

$$\times [i\mathbf{p}\vec{\gamma} - E\gamma_4 - m]\}.$$

Carrying out the summation over photon polarizations with the aid of the relation

$$\sum_e \mathbf{ea}\cdot\mathbf{eb} = \mathbf{ab} - k^{-2}(\mathbf{ak})(\mathbf{bk}),$$

where a and b are matrix vectors, we represent j in the form

$$j = \frac{1}{8\omega p E p'^2 (p' - |\mathbf{p}-\mathbf{k}|)^2} \operatorname{Sp} \tag{6'}$$

$$\times \{[i((\mathbf{pp}_1)\mathbf{p}_1 + \delta\mathbf{p})\vec{\gamma} - \mathbf{pp}_1(E'\gamma_4 + m)]$$

$$\times [2\mu'\hat{k} + ie][-i(\mathbf{pn})(\mathbf{n}\vec{\gamma}) + E\gamma_4 - m]\, [2\mu'\hat{k} + ie]\},$$

where

$$\mathbf{n} = \mathbf{k}/k,\ 2\delta = (E-k)^2 - m^2 - (\mathbf{p}-\mathbf{k})^2,$$

$$E' = E - k,\ \mathbf{p}_1 = \mathbf{p} - \mathbf{k}.$$

The differential cross-section for bremsstrahlung is equal to

$$d\sigma = \frac{R^2}{(2\pi)^2}\frac{d\omega}{\omega}\frac{p^2}{(m^2 + p^2\theta^2)^2} \tag{7}$$

$$\times \Big\{e^2\Big[p(p-\omega)\theta^2 + \frac{\omega^2}{2p^2}(m^2 + p^2\theta^2)\Big]$$

$$+ 2\mu'^2\frac{\omega^2}{p^2}(m^2 + p^2\theta^2)^2 - me\mu'\frac{\omega^2}{p^2}(m^2 + p^2\theta^2)\Big\}\, d^2\theta.$$

The first term in square brackets in Eq. (7) defines the bremsstrahlung for a particle without spin[3], and the second term comes from the spin of the proton. The last two terms define the radiation caused by the presence of the anomalous magnetic moment of the proton.

We see that the influence of spin and of the anomalous magnetic moment of the proton on bremsstrahlung are essential only in the region of high frequencies. One should bear in mind, however, that in the region of high frequencies, it is, strictly speaking, impossible to view the proton as a point charge, because here, due to the interaction of the proton with the meson vacuum, one should describe the 'smearing-out' of the proton, account of which can be taken in some circumstances by a form-factor F, depending on the invariant photon frequency*

$$F = F\left(\frac{E\omega - \mathbf{pk}}{mm_0}\right) = F\left[\frac{\omega}{2E}\left(1 + \frac{E^2}{m^2}\theta^2\right)\frac{m}{m_0}\right].$$

The cross section for radiation, taking into account the proton form-factor, is obtained by multiplying Eq. (7) by $|F|^2$.

We express our sincere gratitude to V. Bar'iakhtar and S. Peletminskii for help in carrying out a series of calculations.

---

* We consider the dimensions of the proton to be of the order $1/m_0$ (where m_0 is the meson mass).

[1] A. Akhiezer, Dokl. Akad. Nauk SSSR **94**, 651 (1954).

[2] A. Akhiezer and I. Ia. Pomeranchuk, Dokl. Akad. Nauk SSSR **94**, 821 (1954).

[3] L. D. Landau and I. Ia. Pomeranchuk, J. Exper. Theoret. Phys. USSR **24**, 505 (1953).

Translated by G. E. Brown
32

Multiple Meson Production in Particle Collisions

L. G. IAKOVLEV
Moscow State University

(Submitted to JETP editor April 6, 1955)
J. Exper. Theoret. Phys. USSR **30**, 203-205
(January, 1956)

THE results of experiments[1] on multiple meson production by nucleon collisions at 10^9-10^{12} ev are only unsatisfactorily explained by thermodynamical and statistical theories. Following reference 2 we shall consider the multiple production of mesons in light of the field theory of interaction of mesons with nucleons.

We shall use the pseudoscalar charge-symmetric theory with pseudoscalar (*PS*) and pseudovector (*PV*) coupling. Only the meson field is double-quantized; the virtual creation and annihilation of pairs is not taken into account. Canonical transformation of the total Hamiltonian creates nonlinear (in φ) terms. The perturbation theory is used in the first approximation; we assume that the term in the interaction Hamiltonian containing φ^n is the one mainly responsible for the production of n mesons.* From Lagrange Function**

$$L = \chi'^{+}\left[i\alpha_\nu \frac{\partial}{\partial x_\mu} - \rho_3 m - g\rho_2(\vec{\tau}, \vec{\varphi}) - f\sigma_\mu(\vec{\tau}, \vec{\varphi}_\mu)\right]\chi' + \nabla\varphi^+\nabla\varphi + \dot{\varphi}^+\dot{\varphi} - \varphi^+\varphi + {}^1/_2(\nabla\varphi_0)^2 + {}^1/_2\dot{\varphi}_0^2 + {}^1/_2\varphi_0^2 \tag{1}$$

With help of the variation principle we obtain the equation

$$[D_0 - U']\chi' = 0, \tag{2}$$

where

$$D_0 \equiv i\alpha_\mu \partial/\partial x_\mu - \rho_3 m, \quad U' \equiv g\rho_2(\vec{\tau}, \vec{\varphi}) + f\sigma_\mu(\vec{\tau}, \vec{\varphi}_\mu), \tag{3}$$

$$\varphi = \sum_{k=1}^{\infty}\left(\frac{2\pi}{\varepsilon_k L^3}\right)^{1/2}[a_{k_+}\exp\{i(p_k x)\} + a^+_{k_-}\exp\{-i(p_k x)\}], \quad \text{etc}$$

Performing the canonical transformation[3]

$$\chi = e^s\chi', e^{-s}[D_0 - U']e^s, \; s = -i\rho_1 f(\vec{\tau}, \vec{\varphi}) \tag{4}$$

and dropping contact terms, we have, instead of (2)

$$[D_0 - U]\chi = 0; \tag{5}$$

D_0 has the former meaning, and the interaction Hamiltonian density has the following form:

$$U = g\rho_2(\vec{\tau}, \vec{\varphi}) + (e^{-s} - 1)(m\rho_3 + g\rho_2(\vec{\tau}, \vec{\varphi})) \tag{6}$$

Expanding e^{-s} in series, we get U in the following form:

$$U = \sum_{n=1}^{\infty}\rho_i g_n(\vec{\tau}, \vec{\varphi})^n, \tag{7}$$

$$i = 2 \text{ for } n = 2k + 1, \; i = 3 \text{ for } n = 2k.$$

$$g_n = (-1)^k \frac{(2f)^{n-1}}{(n-1)!}\left(g + \frac{2}{n}mf\right).$$

According to the formula

$$W_n d\varepsilon_1 d\varepsilon_2 \ldots d\varepsilon_n = 2^{n-1}\pi^{1-2n}\left|H'_n\right|^2 \prod_{i=1}^{n}\varepsilon_i(\varepsilon_i - 1)^{1/2}d\varepsilon_i, \tag{8}$$

where $H'_n = \int\chi^+_m U_n\chi_l(d\mathbf{r})$ $[U_n = \rho_i g_n(\vec{\tau}, \vec{\varphi})^n]$ is the matrix element of the transition of the system from two nucleons to a system of two nucleons and n mesons, we find the probability of production, in unit time, n π-mesons in the energy interval

$$W_n d\varepsilon_1 \ldots d\varepsilon_n = 2^{1-n}\pi^{1-2n}g_n^2\left|\int\chi^+_m(\vec{\tau}, \vec{\varphi})^n\rho_i\chi_l(d\mathbf{r})\right|^2 \times \prod_{i=1}^{n}\varepsilon_i(\varepsilon_i - 1)^{1/2}d\varepsilon_i, \tag{9}$$

The integral in (9) depends on the nature of the colliding and produced particles. We shall assume that all the mesons and also all the nucleons are of the same type. Then the total probability of production of n mesons is:

$$W_n = \frac{(2f)^{2n-2}n!}{\pi^{n-1}(n-1)!(n-1)!}\left(g + \frac{1}{n}2mf\right)^2|N_n|^2 \times \int_1^{\Delta E}(\varepsilon_1^2 - 1)^{1/2}d\varepsilon_1 \ldots \int_1^{\Delta E - \sum_1^{n-1}\varepsilon_k}(\varepsilon_n^2 - 1)^{1/2}\delta\left(\Delta E - \sum_{k=1}^{n}\varepsilon_k\right)d\varepsilon_n. \tag{10}$$

$|N_n|$ is the part of the matrix element for the present not given explicitly. We assume only that it is of the same order for various transitions. ΔE = total energy (in the center of mass system) transferred from the nucleons to mesons.

Assuming $\epsilon_k > 1$, we have from (10):

$$W_n = \frac{n^3|N_n|^2 2^{2n-1}}{\pi^{n-1}n!(2n)!}f^{2n+2}\left(g + \frac{2mf}{n}\right)^2(\Delta E)^{2n-1}. \tag{11}$$

The relative probability, for large n, is

$$W_n/W_{n-1} = \pi^{-1}f^2 n^{-3}\Delta E^2.$$

The most probable number of mesons is proportional to $\Delta E^{2/3}$ in the center of mass system; that is, $n_p \sim (\Delta E_{\mathrm{lab}})^{1/3}$ in the lab system. The experiments show that $\Delta E = \eta E$; η changes little between 0.2 - 0.4. One can put therefore*** $np \sim E^{1/3}_{\mathrm{lab}}$. In recent experiments[1] the production of mesons by bombardment of protons with neutrons at 2×10^9 ev was investigated. The following reactions were studied: $n + p \to p + p + \pi^-$ and $n + p \to n + p + \pi^+ + \pi^-$. It was found that $W(\pi + \pi^-)/W(\pi^-) \sim 4$. No cases of three meson production were discovered. From (9) one can find:

$$\frac{W(\pi^+, \pi^-)}{W(\pi^-)} = \frac{64}{3\pi} f^2 \left(\frac{g + mf}{g + 2mf}\right)^2 \frac{\Delta E_2^3}{\Delta E_1} \tag{12}$$

Assuming that in the mean 30% of the total energy in center of mass system was transferred to the mesons[4] (which does not contradict data of reference 1), we find that $\Delta E \approx 9(1.27 \times 10^9$ ev). The values of g and f we take as usual, namely $g \sim 8$ - 10 and $f \sim 0.2 - 0.6$. All these values for f and g (g does not possess a great influence) give values of W_2/W_1 in good agreement in order of magnitude. Taking into account that here $W_3/W_2 \sim 0$, one should put $0.2 \leq f < 0.3$. If we had only PV coupling ($g = 0$), it would be $f \sim 0.5$.

In an analogous way the probability of meson production in meson-nucleon collisions is calculated:

$$W_n = \frac{2^{n+2} |N_n|^2}{\pi^{n-2} (2n)!\,(n-1)!} \left(g + \frac{1}{n+1} 2mf\right)^2 f^{2n} \varepsilon_0^{2n-2} \tag{13}$$

(ϵ_0 – energy of the incident meson in center of mass system).

The author wishes to express his deep gratitude to Prof. D. D. Ivanenko, M. M. Mirianashvili and V. V. Lebedev.

---

* The use of perturbation theory would be more acceptable if we had only PV coupling, as the constant of this type of coupling is $f < 1$. However, even in the presence of the two types of coupling, the results are reasonable, as obviously the PV coupling has a greater influence on the variation in probability for different numbers of mesons [see (11) and (12)]. A fast nucleon in a collision with another one at rest loses in the mean only 30% of its energy in the center of mass system, which makes the use of perturbation theory somewhat more plausible.

** We make use of dimensionless units: $c = \hbar = \mu_\pi = 1$. The mass of the nucleon $m = 6.7$; the energy unit, 1.4×10^8 ev;

$$x_\mu = x,\ y,\ z,\ it; \quad \varphi_\mu \equiv \partial\varphi/\partial x_\mu, \quad \dot{\varphi} = \partial\varphi/\partial t.$$

*** The used method is approximate only and does not pretend to be rigorous. The part of the matrix element containing the nucleonic functions is not given explicitly. Equation (11) gives only the energy dependence. One can assume, however, that the relative probabilities depend only in a small degree on $|N_n|$ and a more exact calculation has little influence on n_p.

[1] W. B. Fowler, R. P. Shutt et al. Phys. Rev. **95**, 1026 (1954).

[2] D. Ivanenko and V. Lebedev, Dokl. Akad. Nauk SSSR **86**, 357, (1951); V. Lebedev, Dissertation, Moscow

[3] E. C. Nelson, Phys. Rev. **60**, 830 (1941). F. J. Dyson, Phys. Rev. **73**, 929 (1948).

[4] N. L. Grigorov and V. S. Murzin, Izv. Akad. Nauk SSSR, Ser Fiz. **17**, 21 (1953) V. S. Murzin, Dissertation. Moscow State Univ. 1954. J. H. Noon et al. Phys. Rev. **95**, 1103 (1954).

Translated by H. Kasha
33

Influence of Quantum Radiation Fluctuations on the Trajectory of an Electron in a Magnetic Field

A. A. KOLOMENSKII AND A. N. LEBEDEV

P. N. Lebedev Physical Institute,
Academy of Sciences, USSR

(Submitted to JETP editor August 1, 1955)
J. Exper. Theoret. Phys. USSR **30**, 205-207
(January, 1956)

THE influence of radiation should be, in general, taken into account in investigating the motion of a relativistic electron in a magnetic field. The quantum mechanical treatment of this problem, based on the Dirac equation, has been given by Sokolov and Ternov.[1] The motion of an electron is described by two quantum numbers. The interaction with the field of virtual photons gives the probability of the change of these numbers, and consequently the change of trajectory in time. In reference 1 a formula was found giving the increase of the mean-square fluctuation of the radius with time, an effect not possessing a classical analogue. At the same time simple physical considerations[2] show, that the quantum (wave) character of the electronic motion should reveal itself only at energies $E \gtrsim E_{1/2} = mc^2(Rmc/\hbar)^{1/2}$ (R = radius of the orbit.), which, for usual values of magnetic field intensity, amounts to the extremely great value of $E_{1/2} \sim 10^{15}$ ev. It is therefore not necessary, in studying electron orbits at $E \ll E_{1/2}$, to use the solution of the

Dirac equation, a procedure connected with tedious approximation by Laguerre polynomials.

We would like here to draw attention to the fact, that the above-mentioned effect of "widening" of the trajectory can be very easily obtained and explained on the basis of the usual classical theory of betratron oscillations, in which we need only to take into account, additionally, the statistical character of radiation. This approach permits us not only to obtain all the results of reference 1, but also to correct certain omissions there from.

From the point of view of the theory of betatron oscillations, the emission of a quantum of the energy $\epsilon = \hbar\omega$ is accompanied by a discrete shortening of the radius of the so-called instantaneous orbit, about which the oscillations occur, by the amount

$$\Delta\rho_{\text{M}} \doteq (\varepsilon / E)\, R / (1 - n), \tag{1}$$

where $n = -(R/H)\, \partial H / \partial R$ is the magnetic field factor. The amplitude of the oscillations changes as well by a given value ΔA. The random changes $\Delta\rho_M$ and ΔA, added statistically, bring about the "widening" of the trajectory. The situation here is analogous to pendulum oscillations (betatron oscillations), the point of suspension of which (instantaneous orbit) is subjected to random impulses, governed by a given distribution law.

We shall consider an electron, having a constant energy (in the mean), moving in an axially-symmetric magnetic field. The equation of the radial motion of such an electron can be written;

$$\rho'' + \rho = \frac{1}{eH\,(1-n)} \left[\int\limits_{\tau_0}^{\tau} \left(\sum_{i=1}^{k} \varepsilon_i\, \delta\,(\tau - \tau_i) \right) d\tau - D\tau \right], \tag{2}$$

where $\tau = (c/R)\sqrt{1-n}\, t$, $\varepsilon_i = \hbar\omega_i$ is the energy of the ith emitted photon, δ = delta function, ρ = deviation of the particle from the basic orbit of radius R, which is determined by the condition, that the mean (in time) energy $\widetilde{E} \doteq eH(R)R$. The ϵi and τi in Eq. (2) should be regarded as independent random variables. The right side of Eq. (2) describes the influence of radiation fluctuations, the constant D, describing the compensation of losses, being selected so that $\widetilde{\rho} = 0$. Finding the oscillatory part of the solution of Eq. (2), $\rho^2{}_{\text{bet}}$, and taking its mean value in time, we obtain

$$\widetilde{\rho}^2_{\text{бет}} = \frac{1}{2e^2 H^2 (1-n)^2} \sum_{j=1}^{\infty} \varepsilon_j^2 \widetilde{n}_j, \tag{3}$$

where $\widetilde{n}_j$ is the mean number of photons of jth frequency emitted during the phase τ. Passing, with the help of well-known formulas (see e.g. reference 3) to the continuous spectrum, and taking the mean we obtain

$$\overline{\overline{\rho}}{}^2_{\text{бет}} = \frac{55}{48\sqrt{3}} \frac{1}{(1-n)^2} \frac{e^2}{mc} \frac{\hbar}{Rmc} \left(\frac{E}{mc^2}\right)^5 t. \tag{4}$$

This result is easily generalized for the case of a slowly (adiabatically) varying field. Since the betatron oscillations are damped as $H^{-1/2} \sim E^{-1/2}$, it follows immediately from Eq. (4)

$$\overline{\overline{\rho}}{}^2_{\text{бет}} = \frac{55}{48\sqrt{3}} \frac{1}{(1-n)^2} \frac{e^2}{mc} \frac{\hbar}{Rmc} \frac{mc^2}{E} \int\limits_{t_0}^{t} \left(\frac{E}{mc^2}\right)^6 dt, \tag{5}$$

which, as well as (4), exactly coincides with the results of reference 1.

Apart from the excitation of the betatron orbits, still another effect, not mentioned in reference 1 and consisting in statistical "widening" of the instantaneous orbit r_M itself should be taken into account. We have then only $\widetilde{r}_{\text{M}} = R$, and not $r_{\text{M}} = R$, , as it has been assumed in reference 1. The expression for $\overline{\overline{\rho}}{}^2$ can be written therefore

$$\overline{\overline{\rho}}{}^2 = \overline{\overline{\rho}}{}^2_{\text{M}} + \overline{\overline{\rho}}{}^2_{\text{бет}}. \tag{6}$$

We shall note, that one can, of course, deduce the expression for $\overline{\overline{\rho}}{}^2_M$ directly from (1).

For the explanation of the behavior of fluctuations of the instantaneous orbit we shall consider the acceleration of an electron in a hypothetical betatron, in which radiative losses are compensated in the mean by the vortex field. Writing down the energy change of particle on an instantaneous orbit, ρ_M, we obtain the equation

$$\frac{d\rho_{\text{M}}}{dt} = \frac{\bar{\varepsilon}\,[\widetilde{a}_1 - \sum_i \delta\,(t - t_i)]}{eH\,(1-n)} - \frac{\dot{H}}{H}(1+g)\,\rho_{\text{M}}, \tag{7}$$

where $\bar{\epsilon}$ – is the mean value of the energy of quanta emitted at a given energy E, $\widetilde{a}_1$, is the mean number of such quanta, emitted in unit time, and

$$g = \frac{2}{3} \frac{3-4n}{1-n} \frac{e^2 c}{R^2} \left(\frac{E}{mc^2}\right)^4 \frac{1}{\dot{E}}. \tag{8}$$

Solving (7), we obtain, for $g \gg 1$ and linear increase of energy with time,

$$\widetilde{\rho}^2_{\text{M}} = \frac{55\sqrt{3}}{96} \frac{\hbar R}{mc} \frac{1}{(1-n)(3-4n)} \left(\frac{E}{mc^2}\right)^2. \tag{9}$$

It is interesting to note, that (9), obtained for the betatron in question, coincides with the expression for the mean square amplitude of small radial phase oscillations in a synchrotron, caused by radiation fluctuations,[4] while the condition $g \gg 1$ is equivalent to the condition $E \gg E_c \doteq 10^8$ ev assumed in reference 4. The slow dependence of (9) on time (or energy) is explained by the strong influence of the damping due to radiation.

Remark received during proof: Further investigations by the authors show, that if Eq.(2) is complemented by a term accounting for the law of conservation of momentum in radiation processes, one obtains, instead of Eqs. (4) and (5), the following formula:

$$\bar{\bar{\rho}}^2_{\text{bet}} \leqslant \frac{55\sqrt{3}}{96}\,\frac{\hbar R}{mc}\,\frac{1}{(1-n)^2}\left(\frac{E}{mc^2}\right)^2,$$

which materially differs from the formula of Sokolov and Ternov[1].

This problem is studied in detail in another article by the authors[5].

[1] A. A. Sokolov and I. M. Ternov, J. Exper. Theoret. Phys. **24**, 249 (1953); **28**, 431 (1955); Soviet Phys. JETP **1**, 227 (1955);Doklady Akad. Nauk **97**, 823 (1954).

[2] V. V. Vladimirskii, **18**, 392 (1948).

[3] D. D. Ivanenko and A. A. Solokov, *The classical Theory of Fields*, GITTL, 1949, p. 275.

[4] M. Sands, Phys. Rev. **97**, 470 (1955).

[5] A. A Kolomonskii and A. N. Lebedev, Dokl. Akad. Nauk SSSR **106**, 5 (1956).

Translated by H. Kasha
34

Excitation of Synchrotron due to Electron Radiation Fluctuation in Strong Focusing Accelerators

A. A. KOLOMENSKII
P. N. Lebedev Physical Institute,
Academy of Sciences, USSR

(Submitted to JETP editor September 10, 1955)
J. Exper. Theoret. Phys. USSR **30**, 207-209
(January, 1956)

IT is well known that the quantum fluctuations of the radiation of a relativistic electron moving in a magnetic field leads to the particular effect of "broadening" of the trajectory. This was noticed first by Sokolov and Ternov[1]. The effect of radiation fluctuation on the excitations of synchrotron oscillations in accelerators with weak focussing has been studied by Sands[2] (see also a paper by Lebedev and the author[3]). The aim of this note is the investigation of this effect in strong focussing accelerators[4] whose designing is now under consideration.

Consider a system composed of sectors with magnetic field (with an angular spread ν each) and sectors free of field (of length L each), forming identical elements of periodicity. The magnetic field gradients (large in absolute magnitude) have opposite signs in neighboring sectors. If the electron energy deviates by ΔE from its equilibrium value, the instantaneous orbit near which the betatron oscillations take place are deformed and deviate from the main equilibrium orbit by a length $\rho_M(\theta)$, which can be written in the form:

$$\rho_M(\theta) = (R\,\psi(\theta)/|n|)\,\Delta E/E, \qquad (1)$$

where R is the radius of the main orbit, n =the index of the magnetic field $(|n| \gg 1)$, θ = the generalized azimuth, $\psi(\theta)$ = a function determined by the parameters of the system and having a period equal to the period of the system $\theta_0 = 2\pi/N$. For the behavior of the function $\psi(\theta)$ in the simplest case, see reference 4. In the case of weak focussing, the expression $\psi(\theta)/|n|$ in (1) is replaced by $1/(1-n)$ where $0 < n < 1$. The mode of the synchrotron is characterized by ΔE, $\rho_M(\theta)$, and also by $\eta = \varphi - \varphi_0$, i e., the difference between the phase φ of the particle (with respect to the accelerating field) and the equilibrium phase l_0. Using (1) we get the relationship:

$$\frac{\bar{\psi}_H}{\sigma|n|}\,\frac{\Delta E}{E} = -\frac{\Delta\omega}{\omega} = \frac{1}{q\omega}\,\frac{d\eta}{dt}, \quad \sigma = 1 + \frac{L}{R\nu}, \qquad (2)$$

where ω is the rotation frequency, q = the acceleration, and $\bar{\psi}_H$=the average of $\psi(\theta)$ over the regions with magnetic field.

Using the well-known expression for the instantaneous power of radiation loss[5]

$$dW/dt = (2e^2c/3R^2_{\text{кр}})(E/mc^2)^4 \qquad (3)$$

One has to take in consideration that, in the given case, the radius of curvature R_c of the trajectory at the point of the instantaneous orbit does not coincide with the radius-vector of the point:

$$R_{\text{кр}} = R\left[1 + \frac{|n| + n(\theta)\,\psi(\theta)}{\psi(\theta)}\,\frac{\rho_M(\theta)}{R}\right]. \qquad (4)$$

Writing the balance between the energy received by the particle from the accelerating field and the energy used up by radiation in one period (taking into account fluctuations), and using equations (2)-(4), we obtain the linearized phase relation in the form

$$\frac{d^2\eta}{dt^2} + \frac{1}{E}\left(\frac{Q}{\sigma}\,\frac{dW}{dt} + \dot{E}\right)\frac{d\eta}{dt} \qquad (5)$$

$$+ \frac{q\omega^2\bar{\psi}_H eV_0 \sin\varphi_0}{\sigma|n|E}\,\eta = \frac{q\omega\bar{\psi}_H}{\sigma^2|n|E}(a_1 - \bar{a}_1)\bar{\varepsilon},$$

where $V_0 \cos\varphi$ is the accelerating potential; $\bar{\varepsilon}$ — the mean value of the quanta emitted by the electron at the given energy E; $a_1 - \bar{a}_1$ — the deviation (fluctuation) of the number of quanta emitted per unit time, from its mean value; the coefficient Q is determined by the accommodation parameters

$$Q = 2 + \bar{\psi}_{\Phi} - \bar{\psi}_{\text{Д}} + \bar{\psi}_H / |n|, \tag{6}$$

where $\bar{\psi}_F$ and $\bar{\psi}_D$ are the averages of $\psi(\theta)$ over focussing $(n < 0)$ and defocussing $(n > 0)$ sectors. The calculations show that $Q \simeq 4$. Note that the coefficient E of $d\eta/dt$ in (5) can be neglected in that range of energy where radiation (and its fluctuation) is important. Assuming a linear time dependence, we can solve Eq. (5). For the mean square of η, we find:

$$\overline{\eta^2} = \frac{55\sqrt{3}}{64} \frac{\hbar c}{e^2} \frac{q}{\sigma} \frac{\bar{\psi}_H}{Q|n|} \operatorname{ctg} \varphi_0 \frac{mc^2}{E}, \tag{7}$$

where the factor $\bar{\psi}_H / Q|n|$ is approximately equal to $1/|n|$. Equation (7) can be used to find the azimuthal dimensions of the electron concentration, which are of some interest for evaluation of loss by coherent radiation.

The largest radial deviation $\rho_{\max}$ of the instantaneous orbit is determined by (1), when $\psi(\theta)$ is given its maximum value $\psi_{\max}(\theta)$. Using (1), (2), (5), and (7) we obtain the mean square value:

$$\overline{\rho^2_{\max}} = (55\sqrt{3}/96)(\hbar R/mc)(\psi^2_{\max}/Q|n|^2)(E/mc^2)^2. \tag{8}$$

Note that exactly the same correction characterizes the instantaneous orbit in a strong focussing betatron, in which the radiation losses compensate on the average. The evaluations show that, near the center of steadiness $(\sqrt{|n|}\,\nu \simeq \pi/2)$ the factor $\psi^2_{\max}/Q|n|^2 \simeq 10/|n|^2$, while in the case of weak focussing[2,3] it is replaced by the expression $1/(1-n)(3-4n)$, which, for $n \sim 0.6$-0.7 is $\simeq 10$. The small dependence of θ^2_{max} on E or t is explained by the influence of powerful extinction linked to the large magnitude of the mean radiation losses. This extinction has a simple physical meaning. It can be shown that it corresponds to the fact that when the orbit is displaced along the radius, the particle radiates in such a way that the change of its energy tends to restore the instantaneous orbit in its equilibrium position.

If, for instance, we let $H_{\max} \approx 10^4$ oersteds, then, according to Eq. (8), we get the evaluation $\left(\overline{\rho^2_{\max}}\right)^{1/2}_{\text{cm}} \leqslant E^{3/2}_{\text{BeV}}/|n|$, which shows that even for $E \simeq 5 \div 10$ BeV is only of the order of a centimeter. The considered effect has thus, by itself, no appreciable effect on acceleration.

---

[1] A. A. Sokolov and I. M. Ternov, J. Exper. Theoret. Phys. USSR **24**, 249 (1953); **28**, 431 (1955); Dokl. Akad. Nauk SSSR **97**, 823 (1954). Soviet Phys. JETP **1**, 227 (1955)

[2] M. Sands, Phys. Rev. **97**, 470 (1955).

[3] A. A. Kolomenskii and A. N. Lebedev, J. Exper. Theoret. Phys. USSR **30**, 205 (1956). (English Translation: Soviet Phys. JETP **2**, 130 (1956).

[4] E. Courant, M. Livingston and H. Snyder, Phys. Rev. **88**, 1190 (1952).

[5] D. D. Landau and E. M. Lifshitz, *The Classical Theory of Fields*, 1953.

Translated by E. S. Troubetzkoy
35.

Auger Effect in Heavy Atoms

V. N. Mokhov and M. G. Urin
Moscow Physico-engineering Institute

(Submitted to JETP editor September 15, 1955)
J. Exper. Theoret. Phys. USSR **30**, 209-210
(January, 1956)

EXCITED atoms, in which one of the interior electrons (say a K-electron) is missing, undergo transitions to a lower energy state by means of radiation of a quantum or by a nonradiative transition with the emission of an electron (Auger Effect). The total number of transitions per unit time $(1/c)_\epsilon$ has been obtained for the nonrelativistic case for arbitrary Z with the aid of the Coulomb function.[1] Only in the case of the interaction of L-electrons (for $Z = 47$) has the screening of the atomic nucleus been taken into account.[2]

In first order perturbation theory,

$$\frac{1}{\tau} = \frac{2\pi}{k} \left| V(n_1 l_1 m_1,\ n_2 l_2 m_2 \,|\, 100,\ kl'm') - V(n_2 l_2 m_2,\ n_1 l_1 m_1 \,|\, 100,\ kl'm') \right|^2$$

and

$$\frac{1}{\tau} = \frac{2\pi}{k} \left| V(n_1 l_1 m_1,\ n_2 l_2 m_2 \,|\, 100,\ kl'm') \right|^2$$

for the interaction of electrons with parallel and antiparallel spins, respectively. Here we have the matrix elements of the operator $V = 1/|\mathbf{r}_1 - \mathbf{r}_2|$, which corresponds to a transition from a state with quantum numbers n_1, l_1, M_1; m_2, l_2, m_2 to a state with quantum numbers 1, 0, 0; l', m' and with momentum k of the emerging electron (atomic units are used here). In the radial integral which enters into the matrix element, the important region is evidently $r_1, r_2 \lesssim 1/Z$. In this region the wave function of the initial state coincides with the Coulomb function with accuracy to a normalization factor A_{nl}. To find A_{nl}, we make use of the fact that the initial and Coulomb functions are quasi-classical for $r \gg 1/Z$. If we write out the quantization rule and the normalization condition for them, we get, after some simple transformations,

$$A_{nl} = B_{nl} \sqrt{(n^3/Z^2)(\partial E_{nl}/\partial n)},$$

where B_{nl} is the normalization coefficient of the Coulomb function, E_{nl} is the energy of the corresponding level. In this case, it is assumed in the calculations that for $n = 1, 2$, $A_{nl} = B_{nl}$.

For large n_2 and for $n_1 = 2$,

$$1/\tau = A_{l_1 l_2}\, \partial E_{n_2 l_2} / \partial n_2 ,$$

where $A_{l_1 l_2}$ is almost independent of n_2. Therefore, replacing the sum over n_2, beginning with $n_2 = 3$, by an integral, we can write the total number of Auger-transitions per unit time in the form:

$$(1/\tau)_\Sigma = (1/\tau)_{L-L} + \sum_{l_1=0}^{1} \sum_{l_2=0}^{2} A_{l_1 l_2} \int_{n_2=3}^{\infty} (\partial E_{n_2 l_2}/\partial n_2)\, dn_2$$

$$+ \sum_{l_1=0}^{1} A_{l_1 3} \int_{n_2=4}^{\infty} (\partial E_{n_2 3}/\partial n_2)\, dn_2 + \ldots$$

$$= (1/\tau)_{L-L} - \sum_{l_1=0}^{1} \sum_{l_2=0}^{2} A_{l_1 l_2} E_{3 l_2} - \sum_{l_1=0}^{1} A_{l_1 3} E_{43} - \ldots,$$

where small terms of the type

$$A_{l_1 l_2} (\partial E_{n_2 l_2}/\partial n_2)(\partial E_{n_1 l_1}/\partial n_1) \qquad (n_1 > 2).$$

are discarded.

In the first approximation,

$$(1/\tau)_\Sigma = (1/\tau)_{L-L} - \sum_{l_1=0}^{1} \sum_{l_2=0}^{2} A_{l_1 l_2} E_{3 l_2}.$$

We can put $E_{3 l_2}$ in the form:[3]

$E_{3l} = -(Z - s_l)^2/18$, where s_l is the screening constant

For $(1/\tau)_{L-L}$, making use of the well-known results of reference 2, we obtain for $Z = 47$, after some computation,

$$(1/\tau)_\Sigma = 45{,}9 \text{ atomic units} \qquad (1)$$

A quantity defined from experiment is the coefficient

$$\alpha_K = Z^4 (1/\tau)_\Sigma / (1/\tau)_{\mathrm{rad}},$$

where $(1/\tau)_{\mathrm{rad}}$ is the number of radiative transitions per unit time. For $Z = 47$: $(1/\tau)_{\mathrm{rad}} = 0.197$ atomic units.[4] Making use of Eq. (1), we obtain $\alpha_K = 1.14 \mathrm{X} 10.^6$ The experimental value is[4] $\alpha_K = 1.14 \times 10.^6$ Calculation with the help of the Coulomb functions gives $\alpha_K = 1.65 \cdot 10^6$.

The authors express their deep gratitude to Prof. A. B. Migdal, who directed the present research.

---

[1] M. Pincherle, Nuovo cimento 12, 91 (1935).

[2] E. H. S. Burhop, Proc. Roy. Soc. (London) 148A, 272 (1935).

[3] P. Gombas, *Ths statistical theory of the atom and its applications.* Russian translation, Moscow, 1951.

[4] E. H S. Burhop, *The Auger effect and other radiationless transitions*, Cambridge, 1952.

Translated by R. T. Beyer
36

Scattering of Fast Neutrons by Semi-transparent Nonspherical Nuclei

E. V. INOPIN
Physico-technical Institute, Academy of Sciences, Ukrainian SSR

(Submitted to JETP editor September 27, 1955)
J. Exper. Theoret. Phys. USSR 30, 210-212
(January, 1956)

THE scattering of fast neutrons by an opaque nonspherical nucleus with spin zero has been studied by Drozdov[1,2]. The scattering of fast neutrons by an even-even semitransparent nonspherical nucleus is considered in the present work.

According to Bohr and Mottelson[3,4], the even-even nuclei in their rotational states have the form of an ellipsoid of revolution and the wave function of such a state is a spherical harmonic $Y_{lm}(\omega)^*$, where l, m are the spin of the nucleus and the projection of that spin, ω represents the angles ϑ, φ which characterize the direction of the axes of symmetry of the ellipsoid. The rotational levels are determined by the formula $E_l = (\hbar^2/2I)\, l(l+1)$, $l = 0, 2, 4, \ldots$, where I is the effective moment of inertia of the nucleus. If we introduce the eccentricity of the nucleus $\epsilon = 1 - (a/b)^2$ (b is the radius of the largest circular cross section of the ellipsoid), then $I = 1/4 I_0\epsilon^2$, where I_0 is the ordinary moment of inertia of a spherical nucleus of equal volume. For most nuclei, $|\epsilon| \approx 0.2$-0.3. For fast neutrons, we can use the adiabatic approximation and consider the scattering of the neutron on a fixed nucleus. We can then write the wave function of the system in the form $\Psi(\mathbf{r}, \omega) \approx u_{\mathbf{k}}(\mathbf{r}, \omega) \times Y_{l_0 m_0}(\omega)$, where $u_{\mathbf{k}}$ is the wave function of the neutron scattered by a fixed nucleus whose orientation is given by the angles ω. In what follows we shall consider that the nucleus is in the ground state before scattering, i.e., $l_0 = 0$.

To calculate the amplitude of the scattering, we make use of the formula of Francis and Watson[5]:

$$f(\Omega, \omega) = -\frac{\mu U}{2\pi h^2}\int \exp\{i(\mathbf{k}-\mathbf{k}')\mathbf{x} + i(n-1)kD(\mathbf{x})\}\, d\mathbf{x}, \tag{2}$$

Here $\mathbf{k}$, $\mathbf{k}'$ are the propagation vectors of the incident and scattered neutron, respectively, Ω represents the angles which define the direction of $\mathbf{k}'$; $D(\mathbf{x})$ is the distance traversed by the incident neutron (in the nucleus) which is found at the point $\mathbf{x}$; integration is carried out over the volume of the ellipsoid, whose orientation is defined by the angles ω; the complex potential U is connected with the complex index of refraction n by the relation $U = -(h^2k^2/2\mu)(n^2-1)$. The region of applicability of Eq. (2) is evidently limited by the condition $|U|/E \ll 1$, where E is the energy of the neutron. The cross section for scattering in the direction Ω with excitation of the rotational level l, m is determined by the formula

$$\sigma_{lm}(\Omega) = \frac{1}{4\pi}\left|\int d\omega\, Y_{lm}(\omega) f(\omega, \Omega)\right|^2. \tag{3}$$

The total cross section of all processes and the cross section of capture are given by the relations

$$\sigma_t = \frac{1}{k}\,\mathrm{Im}\int d\omega f(\Omega, \omega)\Big|_{\theta=0},$$

$$\sigma_c = \frac{1}{4\pi\lambda}\int d\omega\, d\mathbf{x}\, e^{-D(\mathbf{x})/\lambda},$$

where $\lambda = 1/(2klmn)$, θ is the scattering angle. If we take the direction of the vector $\mathbf{k}$ as the axis of quantization, then the symmetry properties of Eq. (2) lead to the relations $\sigma_{l,m}(\Omega) = 0$ if l is odd, $\sigma_{l,m}(\Omega) = \sigma_{l,-m}(\Omega)$; $\sigma_{l,m}(\Omega) = 0$ for $\theta = 0$ if $m \neq 0$.

With the help of a coordinate transformation which transforms the ellipsoid into a sphere, with a change to a cylindrical system of coordinates, the integral (2) becomes

$$f(\Omega, \omega) = ab^2k^2\,\frac{n^2-1}{q} \times \int_0^1 J_0(\rho\varkappa)\sin\left(q\sqrt{1-\rho^2}\right)\exp\left\{ip\sqrt{1-\rho^2}\right\}\rho\, d\rho, \tag{4}$$

where

$$\varkappa = 2kb\sin\frac{\theta}{2}\left[1-\varepsilon\cos^2\gamma - \left(a\sin\frac{\theta}{2}\Big/ b\xi(\vartheta)\right)^2\right]^{1/2},$$

$$p = ka\,\frac{n-1}{\xi(\vartheta)},$$

$$q = p\left(1+\frac{2\sin^2(\theta/2)}{n-1}\right), \quad \xi(\vartheta) = \sqrt{1-\varepsilon\sin^2\vartheta},$$

γ is the angle between the vector $\mathbf{k}' - \mathbf{k}$ and the axis of symmetry of the ellipsoid. With the use of Eqs. (3) and (4), it can be shown that the excitation cross section of the lth level is proportional to ϵ^l; i.e., excitation is practicable only with $l = 2$.

The integral (4) is computed for small angles $kb\theta < 1$. For angles which satisfy the condition $2kb\sin\theta/2 \gg 1$ for (4), we get the asymptotic expression

$$f(\Omega, \omega) \approx ab^2k^2\,\frac{1-n^2}{4q}\left[\frac{(q+p)\exp\left(i\sqrt{\varkappa^2+(q-p)^2}\right)}{\varkappa^2+(q+p)^2} + \frac{(q-p)\exp\left(i\sqrt{\varkappa^2+(q+p)^2}\right)}{\varkappa^2+(q-p)^2}\right]. \tag{5}$$

Calculation of the cross section (3) is carried out by means of a decomposition of the integral (4) (or its asymptotic expression) in a series in the small parameter ϵ.

If we start out in the calculation of the amplitude of the scattering, not from Eq. (2), but from the optical diffraction formula:[6]

$$f(\Omega, \omega) = \frac{ik}{2\pi}\int_S \left[1-e^{2i(n-1)ks}\right] e^{i(\mathbf{k}-\mathbf{k}')\mathbf{x}}\, df_n, \tag{6}$$

(here $2s$ is the penetration of the neutron in the nucleus; integration is carried out over the area of the projection of the ellipsoid on a plane perpendicular to the vector $\mathbf{k}$) then the following expression is obtained:

$$f(\Omega, \omega) = ikb^2\xi(\vartheta)\int_0^1 \left[1-\exp\left(2ip\sqrt{1-\rho^2}\right)\right] J_0(\varkappa_0\rho)\,\rho\, d\rho, \tag{7}$$

where

$$\varkappa_0 = kb \sin\theta [\cos^2\varphi + \xi^2(\vartheta)\sin^2\varphi]^{1/2},$$

φ is the azimuthal angle of the axis of symmetry, measured from the plane determined by the vectors **k**, **k**′. It is easy to see that Eq. (4) transforms into Eq. (7) for small angles of scattering θ, with accuracy to $(n+1)/2 \approx 1$. Evidently the optical approach of Eq. (6) is valid only for very small scattering angles.

In the Born approximation, which is valid for $kR|U|/E \ll 1$ (R is the radius of the nucleus), we can set $n - 1 = 0$ everywhere in Eq. (4) except in the multiplicative factor $n^2 - 1$. We then obtain

$$f(\Omega, \omega) = \sqrt{2\pi}\hbar^{-2}\mu a b^2 U y^{-3/2} J_{3/2}(y), \qquad (8)$$

where $y = 2kb\sin(\theta/2)\sqrt{1-\varepsilon\cos^2\gamma}$. Here the dependence of the amplitude on the angles ω is determined only by the angle γ. Therefore, if we choose as the angle of quantization the direction of the vector **k**′ − **k** only such states will be excited for which the projection of the momentum is equal to zero. The cross section of excitation of the lth level can be calculated, not by Eq. (3), but by the simpler formula

$$\sigma_l(\Omega) = (2l+1)\left|\int_0^\pi P_l(\cos\gamma) f(\gamma, \Omega)\, d\cos\gamma\right|^2; \qquad (9)$$

the cross sections of excitation of a level with momentum l and projection m in the direction of the vector **k**, are calculated with the help of the addition theorem for spherical functions. There also follow from Eq. (8) certain conclusions on the angular correlation between the scattered neutron and the photon produced in the transition $l \to 0$. Thus, for example, for $l = 2$, the photon has an angular momentum equal to two and a projection of this momentum in the direction of the vector **k**′ − **k** equal to zero; therefore, we get for the angular distribution of photons[7]:

$$I(\alpha) = (15/8\pi)(\cos^2\alpha - \cos^4\alpha), \qquad (10)$$

where α is the angle between the direction of the photon and the vector **k**′ − **k**.

Starting out with Eq. (8) and the expression for the total cross section of elastic scattering and of the excitation of all rotational levels $\sigma_s(\Omega) = (4\pi)^{-1}\int d\omega\, |f(\omega, \Omega)|^2$, one can show that the angular distributions just obtained are the mean of the angular distributions, taken with a weighting factor for elastic scattering on spherical nuclei having radii from $R_1 = a$ to $R_2 = b$.

For small eccentricity ($|\epsilon| \ll 1$) we get from Eqs. (8) and (9):

$$\sigma_l(\Omega) = \varepsilon^l A_l \left|\left(2kb\sin\frac{\theta}{2}\right)^{(l-3)/2} J_{(l+3)/2}\left(2kb\sin\frac{\theta}{2}\right)\right|^2, \qquad (11)$$

$$A_l = 2^{l+1}(2l+1)\pi\left|\frac{\mu a b^2 U^l (l!)^2}{\hbar^2 (l/2)!\,(2l+1)!}\right|^2.$$

In conclusion, the author expresses his deep gratitude to I. M. Lifshitz, A. V. Pogorelov, L. N. Rozentsveig, D. V. Volkov and A. G. Sitenko for their valued advice and criticism.

---

[1] S. I. Drozdov, J. Exper. Theoret. Phys. USSR **28**, 734 (1955); Soviet Phys. 1, 591 (1955).

[2] S. I. Drozdov, J. Exper. Theoret. Phys. USSR **28**, 736 (1955); Soviet Phys. 1, 588 (1955).

[3] A. Bohr, Dan. Mat. Fys. Medd. **26**, 14 (1952).

[4] A. Bohr and B. R. Mottelson, Dan. Mat. Fys. Medd. 27, 16 (1954).

[5] N. C. Francis and K. M. Watson, Am. J. Phys. **21**, 659 (1953).

[6] A. I. Akhiezer and I. Ia. Pomeranchuk, *Some Problems of Nuclear Theory*, GITTL, Moscow, 1950.

[7] A. I. Akhiezer and V. V. Berestetskii, *Quantum Electrodynamics*, GITTL, Moscow, 1953.

Translated by R. T. Beyer
37

Possibility of Using Artificial Earth Satellites for the Experimental Verification of the Theory of General Relativity

V. L. GINZBURG
P. N. Lebedev Physical Institute,
Academy of Sciences, USSR

(Submitted to JETP editor October 2, 1955)
J. Exper. Theoret. Phys. USSR **30**, 213-214
(January, 1956)

AT the present time it is possible to assert that experimental tests have brought about a convincing verification of the general theory of relativity.[1] However, an even further verification of the theory does not appear superfluous. Therefore it is appropriate at this time to point out the possibility of an experimental verification of the general theory of relativity by utilizing artificial earth satellites.

The reception of the radio signals on earth from the satellite can be used to determine the gravitational shift of frequency in the earth's field[2]. The relativistic gravitational change of frequency ν is

$$\frac{\Delta\nu}{\nu}=\frac{\varkappa M_{\text{♁}}}{c^2}\left(\frac{1}{r_{\text{♁}}}-\frac{1}{r_{\text{♁}}+h}\right)\simeq\frac{gh}{c^2}\left(1-\frac{h}{r_{\text{♁}}}\right) \qquad (1)$$

$$=1{,}09\cdot 10^{-18}h\left(1-\frac{h}{r_{\text{♁}}}\right),$$

where $\varkappa = 6.670 \times 10^{-8}$ is the gravitational constant, $M = 5.98 \times 10^{27}$ is the mass of the earth, $r = 6.38 \times 10^8$ is the earth's radius, $g = 981$ the gravitational acceleration, h is the height of the satellite above the earth's surface. For $h \approx 800$ km, $\Delta\gamma/\gamma = 7.6 \times 10^{-11}$; if $h >> r$, then $\Delta\nu/\nu = 7 \times 10^{-10}$. (the observed shift in the earth's field is of course, violet and not red). Furthermore, in the radio band it is in principle possible to achieve an accuracy of one part in 10^{12} using atomic clocks[3], and an accuracy of greater than a part in 10^{10} has already been achieved[4]. Equation (1) does not give the total change in frequency of the radiation emitted from the satellite since it is necessary to include the Doppler shift as well. It may be easily shown from the general expression for the Doppler effect in the gravitational field (cf. reference 5, sec. 116) that to the pertinent accuracy of the order of $\sim \nu^2/c^2$ the gravitational and the Doppler shifts of frequency simply add. It is then possible to use for the Doppler shift the usual formula

$$\left(\frac{\Delta\nu}{\nu}\right)_\partial=\frac{\sqrt{1-(v^2/c^2)}}{1-(v/c)\cos\theta}$$

$$\approx 1+\frac{v}{c}\cos\theta-\frac{v^2}{2c^2}(1-2\cos^2\theta),$$

where v is the velocity of the satellite relative to the earth's surface and θ is the angle between the velocity and the line of sight. For v and θ it is possible to use their instantaneous values and the acceleration of the source does not enter anywhere into the result. For satellites close to the earth, the corrections connected with the rotation of the earth (one is considering the system in which measurements are performed as fixed on the earth) are small and may be neglected (these corrections are $\lesssim \nu_0^{\,2}/c^2 \sim 2 \times 10^{-12}$ where $v_0 = 4.6 \times 10^4$ is the velocity of the earth's surface at the equator). In observations of the satellite at the angle $\theta = \pi/2$, the linear Doppler effect disappears, but the quadratic effect remains, and is equal to $(\Delta\nu/\nu)_\partial = -v^2/2c^2$

$$=-\varkappa M_{\text{♁}}\,2c^2(r_{\text{♁}}+h)\cong-3.5\cdot10^{-10}\ [1-(l/r_{\text{♁}})],$$

where the orbit is considered circular for the sake of simplicity. For $h = 800$ km $(\Delta\nu/\nu)\partial = -3 \times 10^{-10}$ i.e., the quadratic Doppler effect is already 4 times greater than the gravitational frequency shift. For that and other reasons the difficulties standing in the way of the discussed experiment should certainly not be underestimated. More distant satellites are more favorable for such an experiment.

The second effect of the general theory of relativity that may be verified with the help of a satellite is the precession of the perihelion of the orbit. For the earth's satellites this precession (in angular seconds per century) is, according to the formula of Einstein, equal to

$$\Psi=\frac{5\pi^2a^2Y}{24c^2T^{\cdot}(1-e^2)}=8.35\cdot10^{-19}\frac{a^2}{T^3(1-e^2)} \qquad (2)$$

$$=\frac{1.74\cdot10^{25}}{a^{5/2}(1-e^2)},$$

where $Y = 365.25$ is the number of days in a year, a is the major semi-axis of the orbit in centimeters, e is the eccentricity of the orbit and T is the period of rotation of the satellite in days (for the earth in particular only the last expression applies, of course).

Equation (2) does not include the effect of the sun on the motion of the perihelion of the satellite which is 7.6″ per century. The effect of Eq. (2) may be very large for the earth's satellites, as was already emphasized[6]. For satellites close to earth it reaches approximately 1500″ per century, while for Mercury $\Psi = 43''$ per century. More detailed considerations show that, from the point of view of feasibility of measuring the effect, the observations of the satellite over one year may be more favorable than observations of Mercury over one hundred years. It is not impossible that employment of the radio method for the measurement of the perihelion precession will result in even more favorable results. Still, as is shown below, there is a tempting possibility of discovering the influence of the earth's rotation on the precession of the satellite's perihelion and also on the rotation of the modes of its orbit.

In the Galilean system of coordinates the field of a rotating body has non-zero components of the type $g_{0\alpha}\ (\alpha = 1, 2, 3)$. Then we have for the case of a weak field at a large distance from the body (cf. reference 7, Sec. 100):

$$\mathbf{g}\approx-\frac{2\varkappa}{c^3r^3}[\mathbf{Ir}],\quad \mathbf{I}=\int[\mathbf{r}',\ \mu\mathbf{v}]\,\partial V, \qquad (3)$$

Where $g_\alpha = -g_{0a}/g_{00} \cong g_{0\alpha}$, μ is the mass density at the point $\mathbf{r}'$ moving with velocity V and r is the distance from the center of the body to the point of observation. For a sphere the Eq. (3) is applicable everywhere outside the sphere and for μ const., $I = 2/5Mr_0^2\,\omega$, where M is the mass of the sphere, r_0 its radius and ω the angular velocity of rotation. Lense and Thirring[8] have shown that the field of Eq. (3) results in an additional precession of the perihelion of the satellite(planet) by the angle (in angular seconds per century)

$$\Psi_R = -\frac{\pi^2 r_0^2 Y}{9c^2 \tau T^2 (1-e^2)^{3/2}}, \qquad (4)$$

$$\Delta = \frac{|\Psi_R|}{\Psi} = \frac{8}{15}\left(\frac{r_0}{a}\right)^2 \frac{T}{\tau (1-e^2)^{1/2}},$$

where τ(in days) is the period of rotation of the central sphere producing the field. In Eq. (4) it is assumed, for simplicity, that the plane of the orbit coincides with the equator of the rotating sphere and that the rotation of both the satellite and the sphere take place in the same direction. In a general case[8] a multiplicative factor $(1-3\sin^2(i/2))$, appears in Eq. (4), where i is the angle between the equatorial plane and the plane of the orbit. The angle of rotation of the nodes is smaller by a factor of 2 than the angle of Eq. (4) and has an opposite sign. To obtain the total effect it is only necessary to add algebraically the precession of the perihelion of Eq. (4) with the precession of Eq. (2).

In the case of Mercury ($a = 5.8 \times 10^{12}$, $T = 88$ days, $r_0 = r_\odot = 6{,}96 \cdot 10^{10}$ and $\tau = \tau_\odot \simeq 28$ days) $\Delta \approx 2.5 \times 10^{-4}$ and $\Psi_r = 0.01''$. At the present time the accuracy of measurement of the precession of the perihelion has reached the order of $1''$. For a nearby satellite of earth the picture is quite different. For h=400 km, $T \approx 1.54$ hours: $\Delta \approx 3 \times 10^{-2}$ and $\Psi_r \approx -43''$ per century. Thus the relativistic effect connected with the rotation of the earth is of the same magnitude as the total relativistic effect for Mercury. Thus it appears desirable to give attention to the possibility of a measurement of this relativistic "rotation effect".

---

[1] V. L. Ginzburg, Usp. Fiz. Nauk 58, 4 (1956).

[2] V. L. Ginzburg, Dokl. Akad. Nauk SSSR 97, 617 (1954).

[3] C. H. Townes, J. Appl. Phys. 22, 1365 (1951); N. G. Basov and A. M. Prokhorov, Usp. Fiz. Nauk 57, 485 (1955).

[4] J. P. Gordon, H. J. Zeiger and C. H. Townes, Phys. Rev. 99, 1264 (1955).

[5] R. C. Tolman, *Relativity Thermodynamics and Cosmology*, Oxford, 1934.

[6] L. La Paz, Publ. Astron. Soc. Pacific 66, 13 (1954).

[7] L. Landau and E. Lifshitz, *Classical Theory of Fields*

Translated by M. J. Stevenson

Regularized Theory of Field System

E. M. Lipmanov
Novosibirsk State Teachers' Institute

(Submitted to JETP editor October 15, 1955)
J. Exper. Theoret. Phys. USSR **30**, 214-216
(January, 1956)

IN the papers[1,2], it is shown that the meaning of the relativistically invariant regularization removing the divergences in the current field theory consists in replacing the usual field equations by equations with higher order derivatives. However, because of the known difficulties related to negative energies[3], the problem of interpretation of the field theory with higher order derivatives is not solved.

For sake of simplicity let us consider a neutral scalar field, subject to the equation:

$$\prod_{i=0}^{n} (\Box - \varkappa_i^2)\, \Phi(x) = -e'\rho(x), \qquad (1)$$

where $\varkappa_0 < \varkappa_1 < \ldots \varkappa_n$, and $\rho(x)$ is the density of the field sources. Equation (1) is equivalent to the system of equations

$$(\Box - \varkappa_i^2)\, \Phi_i(x) = -e' C_i \rho(x), \quad i = 0, 1, 2, \ldots, n, \qquad (2)$$

where the constants C_i are

$$C_i = \left[\prod_{i \neq j = 0}^{n} (\varkappa_j^2 - \varkappa_i^2)\right]^{-1} \qquad (3)$$

and satisfy the Pauli-Villars regularization conditions. In this case the solution of Eq. (1) has the form

$$\Phi(x) = \sum_{i=0}^{n} \Phi_i(x). \qquad (4)$$

In the absence of sources, the solution of (2) can be written in the form of a Fourier expansion:

$$\Phi_i(x) \qquad (5)$$

$$= \left(\frac{\hbar c^2 |C_i|}{2L^3}\right)^{1/2} \sum_k \omega_i^{-1/2} \{a_i(k) \exp(-i\omega_i t + i\mathbf{kr})$$

$$+ a_i^{+}(k) \exp(i\omega_i t - i\mathbf{kr}),$$

where $\omega_i = (k^2 + \varkappa_i^2)^{1/2}$. The expression for the entire energy of a free field takes the form:

$$H=\sum_{l=0}^{n} H_i = {}^1\!/_2 \sum_{l=0}^{n} \sum_{k} \hbar\omega_l (a_i^+ a_l + a_l a_i^+)(-1)^l. \qquad (6)$$

The canonical quantization gives the following relations for the operators a_i, a_i^+.

$$[a_l(k), a_j^+(k')] = (-1)^l \delta_{lj}\delta_{kk'}. \qquad (7)$$

It follows from Eq. (6) that to the "usual" fields there correspond even i's, and to the "unusual" fields, odd i's. From Eq. (7) it follows that, for usual fields, the particle number operator is $N_i = a_i^+ a_i$, and, for unusual fields, it is $N_i = a_i a_i^+$. Expression (6) takes then the form

$$H=\sum_{l=0}^{n} H_i = \sum_{l=0}^{n} \sum_{k} \hbar\omega_l (N_i + {}^1\!/_2)(-1)^l. \qquad (8)$$

An attempt to interpret this theory in the sense that it describes a system of fields with rest masses $m_i = \hbar\varkappa_i/C$, and coupling constants $e_i = e'C_i$ encounters some difficulties in what concerns negative energies of the free unusual field [as it can be seen from Eq. (8)]. To eliminate these difficulties and to conserve the advantages of the theory (convergence), let us do the following: let us write the Heisenberg S– matrix corresponding to the interaction of the considered field (described by equations with derivatives of order $2(2n + 1)$ of the type (1) with the field of the sources, and let us average this S– matrix over the vacuum of the n unusual fields

$$S=\Big\langle \sum_{r=0}^{\infty} \left(-\frac{i}{\hbar c}\right)^r \frac{1}{r!} \qquad (9)$$

$$\times \int_{-\infty}^{\infty} dx_1 \ldots dx_r P[H(x_1), \ldots H(x_r)] \Big\rangle_{\text{vac. unusual Fields}}$$

$$H(x) = -e'\rho(x)\Phi(x) = -e' \sum_{l=0}^{n} \Phi_i(x)\rho(x). \qquad (10)$$

The S-matrix (9) does not depend on the changes of the unusual fields: we take it as the fundamental law describing the interaction between the field of the sources and the $(n + 1)$ usual fields, characterized by rest-masses m_i $(i = 0, 2, \ldots 2n)$ and by coupling constants e_i which are expressed in terms of rest-masses of the usual and unusual fields. It is clear that, inversly, to any given system of $(n + 1)$ fields with identical spin, characterized by rest-masses and coupling constants, we can associate a relativistically invariant, finite S-matrix (9); the unknown constants e' and the rest-masses m_i (i odd) of unusual fields are determined in terms of rest masses m_i $(i = 0, 2, \ldots 2n)$ of the usual (real) fields, and of their constants e_i of coupling with the sources, by the equation

$$e'C_i = e_i, \; i = 0, 2, 4 \ldots, 2n. \qquad (11)$$

It is easy to see that the S-matrix (9) corresponds to a quantum system of fields described with higher derivatives (1) in the Heisenberg representation, and obeying a particular conservation law: for any real transition of the system the vacuum of the unusual fields has to be conserved. Quanta of the unusual fields may appear only in intermediate states. One has to point out, however, that this theory is not unique. The system of $(n+1)$ fields can be described by equations with derivatives of order either $2(2n + 1)$ or $2(2n + 2)$ – which correspond to the existence of n or $n + 1$ unusual fields.

A complete uniqueness of the formalism is obtained by the restriction to equations containing derivatives of the lowest order. According to Eqs. (11) and (3) this restriction corresponds to the physical requirement that no other experimental constants occur in the theory except the rest masses and the constants of coupling of these fields with the sources; this is the same requirement as in ordinary electrodynamics. However, in this case, the theory with a single field is not regularized. To regularize the S-matrix it is necessary and sufficient that the sources interact with at least two fields of identical spins.

If one removes the restriction of lowest order derivatives, the S-matrix is always regularized – but in addition to the rest masses and the coupling constants of the usual field, an additional arbitrary constant e' enters the theory*. It can be determined by comparing the theory with experimental data.

The system of equations (11) does not depend on the tensor dimensionality of the field operator $\phi(x)$. The theory can be thus applied to any system of integral spin fields, for example to a system of mesons interacting with nucleons.

---

* Equation (11) is then a system of $n + 1$ equations for $(n + 2)$ unknowns.

Translated by E. S. Troubetzkey
39

[1] D. Ivanenko and V. Grigor'ev, J. Exper. Theoret. Phys. USSR **21**, 563 (1951); A. Sokolov and D. Ivanenko, *Quantum Field Theory*, GITTL, pages 571, 589, Moscow, 1952.

[2] R. Thirring, Phys. Rev. **79**, 703 (1950).

[3] A. Pais and G. E. Uhlenbeck, Phys. Rev. **79**, 145 (1950).

Electron Plasma Oscillations in an External Electric Field

A. I. Akhiezer and A. G. Sitenko
Physico-Technical Institute, Ukrainian Academy of Sciences,
Kharkov State University

(Submitted to JETP editor January 3, 1955)
J. Exper. Theoret. Phys. USSR **30**, 216-218
(January, 1956)

THIS letter is concerned with the determination of the frequency of oscillations of electron plasma placed in a constant and uniform electric field E_0*.

We shall denote by $F(\mathbf{r}, \mathbf{v}, t)$ a distribution function of the plasma electrons. This function satisfies the kinetic equation

$$\frac{\partial F}{\partial t}+\mathbf{v}\,\mathrm{grad}\,F+\frac{e}{m}(\mathbf{E}_0+\mathbf{E})\frac{\partial F}{\partial \mathbf{v}}+J[F]=0,$$

where $J(F)$ is the collision integral and $\mathbf{E}$ is the electric field specified by the plasma oscillations and satisfying the relation

$$\mathrm{div}\,\mathbf{E}=4\pi e\int F d\mathbf{v}-4\pi e n_0$$

where n_0 is the equilibrium density of the ions. The equilibrium distribution function F_0 of the electrons in the absence of oscillations has the form[2]

$$F_0=f_0(v^2)+\mathbf{E}_0\mathbf{v}f_1(v^2),$$

$$f_0(v^2)=C\exp\left\{-w+\int_0^w\left[1+\frac{w}{\xi}\right]^{-1}dw\right\},$$

$$f_1(v^2)=-\frac{el}{m}\frac{\partial f_0}{\partial v},$$

where $w=mv^2/2T$, $\xi=(M/6m)(eE_0l/T)^2$, m and M are the masses of electrons and ions respectively, l is the mean free path of electrons and T the temperature. If we assume that the distribution function F differs only slightly from F_0, we obtain the following equations for $f=F-F_0$ and the field $\mathbf{E}$:

$$\frac{\partial f}{\partial t}+\mathbf{v}\,\mathrm{grad}\,f+\frac{e\mathbf{E}_0}{m}\frac{\partial f}{\partial \mathbf{v}}+\frac{e\mathbf{E}}{m}\frac{\partial F_0}{\partial \mathbf{v}}+\frac{1}{\tau}f=0, \tag{1}$$

$$\mathrm{div}\,\mathbf{E}=4\pi e\int f d\mathbf{v},$$

where the term f/τ phenomenologically takes into account the presence of collisions (τ is the average time between collisions).

We seek a solution for the set of equations (1) according to Landau[3] in the form

$$f(\mathbf{r},\mathbf{v},t)=\int f_{\mathbf{k}}(\mathbf{v},t)\,e^{i\mathbf{k}\mathbf{r}}\,d\mathbf{k},\ f_{\mathbf{k}}(\mathbf{v},t) \tag{2}$$

$$=\frac{1}{2\pi i}\int_{-i\infty+\sigma}^{i\infty+\sigma} f_p(\mathbf{v})\,e^{pt}\,dp,$$

$$\mathbf{E}(\mathbf{r},t)=-\mathrm{grad}\,\varphi=-i\int\mathbf{k}\varphi_{\mathbf{k}}(t)\,e^{i\mathbf{k}\mathbf{r}}\,d\mathbf{k},$$

$$\varphi_{\mathbf{k}}(t)=\frac{1}{2\pi i}\int_{-i\infty+\sigma}^{i\infty+\sigma}\varphi_p e^{pt}\,dp,\ \sigma>0,$$

and we obtain

$$\varphi_p=\frac{\dfrac{4\pi m}{E_0}\displaystyle\int\exp\left\{-\frac{m}{eE_0}\int_0^{v_x}\left(p+i\mathbf{k}\mathbf{v}+\frac{1}{\tau}\right)dv_x\right\}\left\{\int_{-\infty}^{v_x}g(\mathbf{v})\exp\left\{\frac{m}{eE_0}\int_0^{v_x}\left(p+i\mathbf{k}\mathbf{v}+\frac{1}{\tau}\right)dv_x\right\}dv_x\right\}d\mathbf{v}}{k^2-\dfrac{4\pi e}{E_0}\displaystyle\int\exp\left\{\frac{-m}{eE_0}\int_0^{v_x}\left(p+i\mathbf{k}\mathbf{v}+\frac{1}{\tau}\right)dv_x\right\}\left\{\int_{-\infty}^{v_x}i\mathbf{k}\frac{\partial F_0}{\partial \mathbf{v}}\exp\left[\frac{m}{eE_0}\int_0^{v_x}\left(p+i\mathbf{k}\mathbf{v}+\frac{1}{\tau}\right)dv_x\right]dv_x\right\}d\mathbf{v}}. \tag{3}$$

where $g(\mathbf{v}) = f_k(\mathbf{v}, 0)$ and the field $\mathbf{E}_0$ is assumed to be along the x axis.

In the following we shall be interested only in the plasma oscillatory properties which are determined by the so-called dispersion relation. The latter is obtained by setting the denominator of Eq. (3) equal to zero.

It is easy to establish that even in the case of strong fields when $\xi \gg 1$, the inequality $m\Omega\bar{v}/eE_0 \gg 1$ holds, where $\Omega = \sqrt{4\pi n_0 e^2/m}$ is the Langmuir frequency and $\mathbf{v}$ the average velocity of the electrons. Therefore we shall assume that $mp\bar{v}/eE_0 \gg 1$. Neglecting orders of E_0 higher than the first, and carrying out the integration in the dispersion relation over the velocity components perpendicular to the direction of the wave vector $\mathbf{k}$ we have

$$k^2 - \frac{8\pi^2 e^2}{m}\left\{\int_{-\infty}^{\infty} \frac{u f_0(u^2)}{\omega'/k - u}\,du - \frac{1}{2}\mathbf{E}_0\mathbf{n}\int_{-\infty}^{\infty} \frac{\Phi_1(u^2)}{\omega'/k - u}\,du + \mathbf{E}_0\mathbf{n}\int_{-\infty}^{\infty} \frac{u^2 f_1(u^2)}{\omega'/k - u}\,du + i\frac{e\mathbf{E}_0\mathbf{n}}{mk}\int_{-\infty}^{\infty} \frac{u f_0(u^2)}{(\omega'/k - u)^3}\,du\right\} = 0, \tag{4}$$

where $\omega' = i(p + \tau^{-1})$, $\mathbf{n} = \mathbf{k}/k$; u is the component of velocity along the wave vector $\mathbf{k}$ and

$$\Phi_1(u^2) = \int_{|u|}^{\infty} f_1(u^2)\,2u\,du.$$

Expanding Eq. (4) into a series of powers of ku/ω', and retaining only the terms up to the fourth order of ku/ω' we finally obtain the dispersion relation in the form

$$k^2 - k^2\frac{\Omega^2}{\omega'^2} - k^4\overline{v^2}\frac{\Omega^2}{\omega'^4} - 2\Omega^2\frac{k^3}{\omega'^3}(\mathbf{nv}) - 3i\Omega^2\frac{e\mathbf{E}_0\mathbf{n}}{mk}\frac{k^4}{\omega'^4} = 0, \tag{5}$$

where $\overline{v}^2$ and $\mathbf{v}$ are the average values of the square of the velocity and of the velocity vector of the electron.

$$\overline{v^2} = \frac{1}{n_0}\int v^2 f_0(v^2)\,dv, \quad \mathbf{v} = \frac{\mathbf{E}_0}{3n_0}\int v^2 f_1(v^2)\,dv. \tag{6}$$

Solving Eq. (5) for ω' we obtain

$$\omega' = \Omega + k^2\overline{v^2}/2\Omega + (\mathbf{kv}) + i3e\mathbf{E}_0\mathbf{k}/2m\Omega. \tag{7}$$

From Eq. (2) the Fourier components of the electric field vary according to the relation $E = \text{const}.\exp(i\mathbf{kr} + pt)$. Since $\omega' \doteq i(p + \tau^{-1})$, then $E_k \doteq \text{const}\exp\{-\gamma t + i\mathbf{kr} - i\omega t\}$, where

$$\omega = \Omega + \frac{1}{2}\frac{k^2\overline{v^2}}{\Omega} + (\mathbf{kv}),\ \gamma = \frac{1}{\tau} - \frac{3e\mathbf{E}_0\mathbf{k}}{2m\Omega}. \tag{8}$$

Equation (8) determines the frequency and the damping of the plasma oscillations in the presence of the electric field. These are correct if $k^2\overline{v^2} \ll \Omega^2$, $\mathbf{kv} \ll \Omega$. It is evident that the electric field decreases damping if the angle between the wave vector $\mathbf{k}$ and the electric field $\mathbf{E}_0$ is less than $\pi/2$. However, even in the case of strong fields, when $\xi \gg 1$ the inequality $3e\mathbf{E}_0\mathbf{k}/2m\Omega < 1/\tau$ is true. Indeed $\tau \simeq l/\bar{v}$, where, in the case of strong fields, $\bar{v} \simeq (M/m)^{1/4}(e\mathbf{E}_0 l/m)^{1/2}$, and since $\mathbf{k} \simeq \Omega/\bar{v}$, then $(3e\mathbf{E}_0\mathbf{k}/2m\Omega)\tau \simeq \sqrt{m/M} < 1$.

We shall give the expressions for the frequency of the plasma oscillations in the limiting cases of weak and strong fields, assuming that the mean free path does not depend on the velocity of the electrons. In the case of weak fields ($\xi \ll 1$):

$$\omega = \Omega + \frac{k^2 s^2}{2\Omega} + \sqrt{\frac{8}{3\pi}}\frac{e\mathbf{E}_0\mathbf{k}l}{ms-},\quad s = \sqrt{\frac{3T}{m}}.$$

For the case of strong fields ($\xi \gg 1$):

$$\omega = \Omega + \frac{1}{2}\frac{\Gamma(5/4)}{\Gamma(3/4)}\frac{k^2\sigma^2}{\Omega} + \frac{4}{3}\frac{\Gamma(3/2)}{\Gamma(3/4)}\frac{e\mathbf{E}_0\mathbf{k}l}{m\sigma},$$

$$\sigma = \left(\frac{4M}{3m}\right)^{1/4}\left(\frac{e\mathbf{E}_0 l}{m}\right)^{1/2}.$$

The authors express their gratitude to Academician L. L. Landau for his interest in this work and to R. A. Demirkhanov and G. Ia. Liubarskii for discussions.

---

[*] Gordeev[1] has devoted an article to this problem. However, he uses an equilibrium function which does not satisfy the kinetic equation.

[1] G. V. Gordeev, J. Exper. Theoret. Phys. USSR 27, 19 (1954).

[2] B. I. Davydov, J. Exper. Theoret. Phys. USSR 7, 1069 (1937).

[3] L. L. Landau, J. Exper .Theoret. Phys. USSR **16**, 574 (1946).

Translated by M. J. Stevenson
40

K-Meson Charge Exchange in Hydrogen and Deuterium

L. B. OKUN'

(Submitted to JETP editor October 20, 1955)
J. Exper. Theoret. Phys. USSR **30**, 218-219
(January, 1956)

COMPARISON of cross sections for charge exchange of *K*-mesons in hydrogen and deuterium can give valuable information about their spins and parities. Theoretical investigation can be carried out similarly to the charge exchange of π-mesons in hydrogen and deuterium[1]. At the present time, apparently, the existence of at most two different *K*-mesons has been established: θ and τ. θ-meson decays into two π-mesons and consequently should have even parity with even spin and odd parity with odd spin. Analysis carried out by Dali[2] indicates that τ-meson apparently has odd parity and even spin. We shall consider the charge exchange of mesons with spins 0 and 1.

In a general case the amplitude of charge exchange of a meson with a proton is equal to $u_p = a + \mathbf{b}\vec{\sigma}$. Here a and $\mathbf{b}$ are functions of momenta and spins of meson before and after the charge exchange; $\vec{\sigma}$ is the spin operator. The amplitude of charge exchange with deuteron is expressed by u_p:

$$u_d = \sqrt{2}\int \psi^*(\mathbf{r})\, e^{i\vec{\varkappa}\mathbf{r}}\, u_p \psi_d(\mathbf{r})\, d\mathbf{r}.$$

Here ψ_d is the wave function of the deuteron, $\psi(\mathbf{r})$ is the wave function of two neutrons appearing as a result of the collision, $\vec{\varkappa} = (\mathbf{k} - \mathbf{k}')/2$ and $\mathbf{k}$ and $\mathbf{k}'$ are the momenta of the meson before and after the collision ($\hbar = c = 1$).

The cross section for the charge exchange with a proton in terms of the amplitude is $\sigma_p = \sigma_a + \sigma_b$; $\sigma_a = \overline{a^2}$, $\sigma_b = \overline{b^2}$. The cross section of charge exchange with deuteron, summed over states of the two neutrons after collisions*

$$\sigma_d = (\sigma_a + {}^2/_3\,\sigma_b)\, F_- + {}^1/_3\,\sigma_b F_+,$$
$$F_\pm = 1 \pm (\alpha / \varkappa) \operatorname{arc\,tg} (\varkappa / \alpha).$$

For $\varkappa = 0$: $F_+ = 2$, $F_- = 0$. Here $\epsilon = \alpha^2/M$ is the binding energy of the deuteron and the bars denote averaging and summations over the spin states of the meson (if it has spin).

We shall consider charge exchange with scattering at small angles. In this case $\varkappa \ll k$ and it may be assumed that $\mathbf{k}$ and $\mathbf{k}'$ have the same direction. We shall now consider several cases in more detail:

1. Charge exchange of *K*-meson with spin 0 without a change in parity. In this case a is a scalar, $\mathbf{b}$ is a pseudovector. However, since there is only one vector in the problem, $\mathbf{k}$, and for the construction of a pseudovector at least two vectors are necessary, then $\mathbf{b} = 0$. We obtain $\sigma_p = \sigma_a$, $\sigma_d = \sigma_a F_-$.

For $\varkappa = 0$: $\sigma_d / \sigma_p = 0$.

2. Charge exchange of *K*-meson with spin 1 without a change in parity. Beside the vector $\mathbf{k}$ there are two other vectors (pseudovectors): $\mathbf{j}$ and $\mathbf{j}'$, determining the direction of the meson spin before and after the charge exchange. In this case $\mathbf{b} \sim [\mathbf{j}\mathbf{j}']$

$$\sigma_p = \sigma_a + \sigma_b; \qquad \sigma_d = (\sigma_a + {}^2/_3\,\sigma_b)\, F_- + {}^1/_3\,\sigma_b F_+.$$

For $\varkappa = 0$: $\sigma_d / \sigma_p = 2\sigma_b / 3\,(\sigma_a + \sigma_b)$.

3. Charge exchange of *K*-meson with spin 1 into *K*-meson with spin 0 without a change in parity. In this case $a = 0$, $\mathbf{b} \sim \mathbf{j}$.

$$\sigma_p = \sigma_b, \qquad \sigma_d = {}^2/_3\,\sigma_b F_- + {}^1/_3\,\sigma_b F_+.$$

For $\varkappa = 0$: $\sigma_d / \sigma_p = {}^2/_3$.

4. Charge exchange of *K*-meson with spin 0 with a change in parity. In this case $a = 0$, $\mathbf{b}$ is a vector ($\mathbf{b} \sim \mathbf{k}$) and

$$\sigma_p = \sigma_b, \quad \sigma_d = {}^2/_3\,\sigma_b F_- + {}^1/_3\,\sigma_b F_+.$$

For $\varkappa = 0$: $\sigma_d / \sigma_p = {}^2/_3$.

5. Charge exchange of *K*-mesons with spin 1 with a change in parity. In this case $\mathbf{b} \sim \mathbf{k} \times [\mathbf{j}\mathbf{j}']$,

$$\sigma_p = \sigma_a + \sigma_b, \quad \sigma_d = (\sigma_a + {}^2/_3\,\sigma_b)\, F_- + {}^1/_3\,\sigma_b F_+.$$

For $\varkappa = 0$: $\sigma_d / \sigma_p = 2\sigma_b / 3\,(\sigma_a + \sigma_b)$.

6. Charge exchange of *K*-meson with spin 1 into *K*-meson with spin 0 with a change in parity. In this case $\mathbf{b} \sim [\mathbf{j}\mathbf{k}]$,

$$\sigma_p = \sigma_a + \sigma_b, \quad \sigma_d = (\sigma_a + {}^2/_3\,\sigma_b)\, F_- + {}^1/_3\,\sigma_b F_+.$$

For $\varkappa = 0$: $\sigma_d / \sigma_p = 2\sigma_b / 3(\sigma_a + \sigma_b)$.

The authors express their gratitude to Professor I. Ia. Pomeranchuk for the suggestion of this problem and V. V. Sudakov for his valuable advice.

---

* The corresponding expression for σ_d in the article of Berestetskii[1] contains several misprints.

[1] V. B. Berestetskii and I. Ia. Pomeranchuk, Dokl. Akad. Nauk SSSR **81**, 1019 (1951).

[2] Rochester conference, 1955.

Translated by M. J. Stevenson
41

On the Theory of Galvanomagnetic Effects in Metals

I. M. LIFSHITZ, M. IA. AZBEL' AND M. I. KAGANOV
Physiko-Technical Institute, Academy of Sciences, Ukrainian SSR

(Submitted to JETP editor October 25, 1955)
J. Exper. Theoret. Phys. USSR **30**, 220-222 (January, 1955)

IN this communication we develop the theory of galvanomagnetic effects in metals, without making any special assumptions on the law of dispersion of conduction electrons or on the form of the collision integral.

1. An electron in a metal is here taken to be a quasiparticle carrying a charge e, with energy ϵ and a quasi-momentum **p**; ϵ is a periodic function of **p**, with the period of the reciprocal lattice. With an electron moving in a constant magnetic field $\mathbf{H}\,(H_x = H_y = 0;\ H_z = H)$, ϵ and p_z remain unaltered. Thus, in the momentum zone an electron moves along the curve

$$\varepsilon(\mathbf{p}) = \text{const};\quad p_z = \text{const}. \tag{1}$$

From the equations of motion, $d\mathbf{p}/dt = (e/c)[\mathbf{v}, \mathbf{H}]$ $(\mathbf{v} = \nabla_p \epsilon)$ we obtain:

$$t = -(c/eH)\int dl / v_\perp. \tag{2}$$

Here dl represents an element of arc of curve (1), taken in the direction of motion, while $v_\perp$ represents a projection of velocity vector upon the plane (x, y). The character of an electron's motion along a trajectory within the momentum zone actually depends on whether curve (1) is closed (i.e., whether it consists of a series of closed curves each of which is disposed within the limits of a single space in the reciprocal lattice)*, or whether it is open (i.e., whether it passes uninterruptedly through the entire reciprocal lattice). If curve (1) is closed, then the transition along this curve is

$$T = -\frac{c}{eH}\oint\frac{dl}{v_\perp} = -\frac{2\pi m^* c}{eH};\quad m^* = \frac{1}{2\pi}\frac{\partial S}{\partial \varepsilon}; \tag{3}$$

where $S = S(\varepsilon, p_z)$ corresponds to the area of intersection of surface $\epsilon(p) = \text{const}$ with plane $p_z = \text{const}$.

The quantity m^* can actually be called the effective mass of an electron in a magnetic field. The sign of this effective mass (and of the period as well) depends on whether the energy within the surface $\epsilon(p) = \epsilon$ is smaller than $\epsilon\,(m^* > 0)$ or larger than $\epsilon\,(m^* < 0)$; this criterion does not hold true for the intersecting curves. It should be noted here that the concept of effective mass cannot be introduced for open trajectories.

2. While describing the state of an electron in a magnetic field it is proper to use variables ϵ, p_z and a dimensionless variable $\tau = t/T_0$, indicating the location of an electron in the trajectory (1) within the momentum zone ($T_0 = 2\pi c m_0/eH$, with m_0 representing the mass of a free electron). T_0 was introduced for the sake of convenience, so as to free τ from its dependence on H. The kinetic equation for the distribution function of f in the variable chosen by us is

$$\frac{\partial f}{\partial \tau}\dot{\tau} + \frac{\partial f}{\partial p_z}\dot{p}_z + \frac{\partial f}{\partial \varepsilon}\dot{\varepsilon} + \left(\frac{\partial f}{\partial t}\right)_{\text{CT}} = 0. \tag{4}$$

(In studying a stationary case, the values of $\dot{\tau}$, $\dot{p}_z$, $\dot{\varepsilon}$ are obtained from the equations of motion). Assuming that $f = f_0 - e t_0 \psi_i E_i$, we align (4) along the electric field E. Noting that $\dot{\varepsilon} = e\mathbf{v}\mathbf{E}$; $\dot{p}_z = eE_z$, $\dot{\tau} = 1/T_0$, we obtain

$$\begin{gathered}\partial\psi_i / \partial\tau + \gamma\hat{W}\psi_i = \gamma f_0'(\varepsilon)\, v_i;\\ \hat{W}\psi_i = t_0\,(\partial\psi_i / \partial t)_{\text{CT}};\ \gamma = H_0 / H;\end{gathered} \tag{5}$$

where f_0 represents the equilibrium Fermi function, t_0 represents the characteristic time of relaxation, and $T_0(H_0) = t_0$. The limiting condition for Eq. (5) is represented, for closed curves, by the condition of periodicty (with a period of T/T_0) of the function ψ_i and, for open trajectories, by the boundedness of the function ψ_i.

As the mean value of Eq. (5) we obtain

$$\overline{\hat{W}\psi_i} = f_0'(\varepsilon)\,\bar{v}_i. \tag{6}$$

The prime in the above equation indicates that the mean value was obtained with respect to τ. For the closed curves, assuming that $2\pi m_0 v_x = -\partial p_y / \partial\tau$, $2\pi m_0 v_y = \partial p_x / \partial\tau$, we obtain $\bar{v}_\alpha = 0$ $(\alpha = x, y)$.

3. We will find the solution for Eq. (5) under conditions (6) for large fields $(\gamma \ll 1)$, in the form of a series* with interval γ. Computations show that for closed curves (1)

$$\psi_x = \gamma[-(f_0'/2\pi m_0)p_y + C_x] + \gamma^2\psi_x^{(2)} + \dots,$$
$$\psi_y = \gamma[(f_0'/2\pi m_0)p_x + C_y] + \gamma^2\psi_y^{(2)} + \dots, \qquad (7)$$
$$\psi_z = C_z + \gamma\psi_z^{(1)} + \dots,$$

C_i represents solely the functions of ϵ, p_z. For the open curves (1): $\psi_i = C_i^{(0)} + \gamma\psi_i^{(1)} + \dots$. The functions $\psi_i^{(k)}$, C_i are determined by means of Eqs. (5) and (6), and are dependent on the collision integral. The fact that the zero member is absent in the expansion of ψ_α for the case of closed curves is related to the condition $v_\alpha = 0$. Here we assume that the interval $\delta\varepsilon \sim \Theta$ of the smearing out of the Fermian function f_0 (near ϵ_0) does not contain open trajectories (ϵ_0 = energy limit at absolute zero; θ = temperature).

4. Making use of Eq. (7), it is possible to represent the conductivity tensor σ_{ik}, in the case when interval $\delta\varepsilon \sim \Theta$ of the spreading out of the Fermi function f_0 contains only closed trajectories, in the form

$$\sigma_{ik}(H) = \begin{pmatrix} \gamma^2 a_{xx} & \gamma a_{xy} & \gamma a_{xz} \\ \gamma a_{yx} & \gamma^2 a_{yy} & \gamma a_{yz} \\ \gamma a_{zx} & \gamma a_{zy} & a_{zz} \end{pmatrix}, \qquad (8)$$

in which the subdivision of the factors of matrix a_{ik} begins with the zero value of member γ.

The factor a_{xy} is not dependent on the collision integral when γ approaches zero. Making use of expression (7), we obtain:

$$a_{xy}^{(0)} \sim \int f_0' d\varepsilon \int dp_z \int p_y \partial p_x/\partial\tau \cdot d\tau \qquad (9)$$
$$= \int f_0' d\varepsilon \int dp_z \oint p_y dp_x.$$

Assuming that $f_0'(\varepsilon) = -\delta(\varepsilon - \varepsilon_0)$, we find $a_{xy}^{(0)} \sim V_1 - V_2 \sim n_1 - n_2$. Here $V_1 - V_2$ are the volumes bounded by the closed surfaces $\varepsilon(\mathbf{p}) = \varepsilon_0$, within which $\epsilon < \epsilon_0 (m^* > 0)$ and conversely, $\varepsilon > \varepsilon_0 (m^* < 0)$; here n_1 represents the number of bound electronic states with a positive mass m^*, and n_2 represents the number of free electronic states with a negative effective mass. In this way the magnitudes of n_1 and n_2 in the following theory may be properly considered as the number of electrons and "holes". It must be emphasized here that the introduction of these concepts is possible only in the case where the energy interval $\delta\epsilon$ contains only closed nonintersecting surfaces of constant energy. In this case we obtain asymptotically (for large fields) $\sigma_{xy} = ec\,(n_1 - n_2)/H$; at $n_1 = n_2$ $a_{xy} \sim \gamma$, that is, $\sigma_{xy} \sim H^{-2}$. In the case of closed trajectories on open surfaces, the integral (9) has no such simple meaning and cannot be expressed in terms of a number of particles.

In the case when integral $\delta\varepsilon \sim \Theta$ contains a layer of open trajectories, the quantities σ_{ik} approach a finite limit as $H \to \infty$. This is related to the fact that the expansion of all the ψ_1, in this case begins with the zero term in γ. Consequently, experimental determination of the asymptoticity of $\sigma_{ik}(H)$ in strong magnetic fields allows us, in principle, to explain the topology of isoenergetic surfaces near the limiting value of Fermia energy.

5. The specific resistance of a metal in a magnetic field is usually measured by making use of the Hall effect. Assuming that magnetic field is perpendicular to the direction of current (an assumption commonly made for this experiment), and choosing the direction of current for the x-axis, we obtain $\rho(H) = (\sigma^{-1})_{xx}$. If there are no open surfaces within the interval ϵ, then, making use of expression (2) we find that

$$\rho = [a_{yy}^{(0)} a_{zz}^{(0)} + (a_{yz}^{(0)})^2] / (a_{xy}^{(0)})^2 a_{zz}^{(0)}$$

approaches saturation when the number of "holes" is not equal to the number of electrons $(n_1 \neq n_2)$. When the number of "holes" is equal to the number of electrons $(n_1 \neq n_2)$ and $a_{xy}^{(0)}$ becomes zero, it becomes necessary to consider the subsequent terms in the expansion of σ_{ik} in respect to γ. This introduces a quadratic increase of resistance with a magnetic field. Consequently, the existence of a group of metals with an indefinitely increasing resistance in a magnetic field, which is known from experiment[1], can be explained by the most general assumptions of the electronic theory of metals. A similar result has been previously arrived at in the simplest common cases[2].

Apparently the law of Kapitza[3] (linear increase of resistance with magnetic field) represents a transition zone between the quadratic relation of resistance in small fields[4] and quadratic relation with a different coefficient in strong fields.

Consideration of the departure of the temperature from zero leads to the saturation of resistance even in the case when $n_1 = n_2$. However, this saturation is reached in very strong fields $H \sim H_0 e^{\Delta\varepsilon/\Theta}$, where $\Delta\epsilon$ represents the distance between the final Fermi surface and the nearest open surface.

In the case when energy interval $\delta\epsilon$ contains open surfaces (or when the Fermi surface itself is open) then, as can be seen from the above, the absolute resistance ρ approaches saturation at $H >> H_0$. The entire matter actually depends on the temperature. The point of greatest interest here lies in measuring of asymptoticity of the Hall coefficient $R = \rho_{xy} H$ in large fields. For the closed surfaces, R does not depend on the direction and is equal to $R = 1^{0}ec\,(n_1 - n_2)\,(n_1 \mp n_2)$. In the case of open surfaces, the magnitude and even the sign of R depends on the field.

The authors are indebted to L. D. Landau and E. C. Borovik for their valuable discussions.

---

* It should be noted that if plane (x, y) does not coincide with any of the crystallographic planes, then the curves are not identical.

* If we assume, as is commonly done, that $W \equiv 1$, then Eqs. (5) and (6) can be easily solved for any values of γ. In this way we obtain

$$\psi_i = \gamma \int_0^\infty e^{-\gamma\tau'} v_i(\tau - \tau')\,d\tau' \cdot f_0'(\varepsilon),$$

and for conductivity σ_{ik} we obtain the expression

$$\sigma_{ik} = \frac{2e^2 f_0}{h^3} \int \varphi_{ik}(\varepsilon, p_z)\, f_0'(\varepsilon)\,(d\mathrm{p});$$

$$\varphi_{ik} = \gamma \int_0^\infty e^{-\gamma\xi}\,\overline{v_i(\tau)\,v_k(\tau + \xi)}\,d\xi.$$

[1] E. Justi, Leitfahigkeit und Leitungsmechanismus fester Stoffe, Gottingen, 1948; E. S. Borovik, J. Exper. Theoret. Phys. USSR **23**, 83, 91 (1952).

[2] D. I. Blokhintsev and L. Nordheim, Z. Physik **84**, 168 (1933). T. Kontorova and Ia. I. Frenkel, J. Exper. Theoret. Phys. USSR **5**, 405 (1935); B. I. Davidov and I. Ia. Pomeranchuk, J. Exper. Theoret. Phys. USSR **9**, 1295 (1939); E. Sondheimer and A. Wilson Proc. Roy. Soc. (London) **A 190** 435 (1947); M. Kohler, Ann Physik **6**, 18 (1949); G. E. Zilberman, J. Exper. Theoret. Phys. USSR **29**, 762 (1955). Soviet Phys. **1**, 611 (1956).

[3] P. L. Kapitza, Proc. Roy. Soc. London, **A123**, 292 (1929).

[4] H. Jones and C. Zener, Proc. Roy Soc. (London) **A 145** 268 (1934).

Translated by R. G. Huzarski
42

ANNOUNCEMENT

Beginning with the present (August, 1956), Soviet Physics JETP will appear monthly. Volume 3 (August, 1956-January, 1957) will contain translations of all articles appearing in Volume 30 of the Journal of Experimental and Theoretical Physics of the USSR (January-June, 1956). Volume 4 (February-July, 1957) will be a translation of Volume 31 (July-December, 1956) of the Soviet Journal.

Subscribers to Soviet Physics JETP for the calender year 1956 will receive Volume 3 as the completion of their subscription. For new subscribers (beginning with Volume 3) the subscription price will be $60.00 per year (two volumes, twelve issues) in the United States and Canada, $64.00 per year elsewhere. The single issue price will remain at $6.00.

Beginning in the very near future, 1956, the American Institute of Physics will commence translations of the Journal of Technical Physics of the USSR, the Acoustics Journal of the USSR and the physical sciences portions of Doklady. Price schedules for these journals are given below. Subscriptions should be addressed to the American Institute of Physics, 57 East 55 Street, New York 22, N. Y.

Soviet Physics—Technical Physics

A translation of the "Journal of Technical Physics" of the Academy of Sciences of the U.S.S.R. Eighteen issues per year, approximately 4,000 Russian pages. Annually, $90.00 domestic, $95.00 foreign.

Soviet Physics—Acoustics

A translation of the "Journal of Acoustics" of the Academy of Sciences of the U.S.S.R. Four issues per year, approximately 500 Russian pages. Annually, $20.00 domestic, $22.00 foreign. The 1955 issues of "Journal of Acoustics" U.S.S.R. will also be published. Will consist of two volumes, approximately 500 pages, and the subscription price will be $20.00 for the set.

Soviet Physics—Dokaldy

A translation of the "Physics Section" of the Proceedings of the Academy of Sciences of the U.S.S.R. Six issues per year, approximately 900 Russian pages. Annually $25.00 domestic, $27.50 foreign.

CONTENTS – *continued*

Russian Reference

Letters to the Editor:

Neutron Spectra in the Bombardment of Tritium and Deuterium by 14 mev Deuterons* . . . G. F. Bogdanov, N. A. Vlasov, S. P. Kalinin, B. Y. Rybakov and V. A. Sidorov 113 30, 185
Gamma and Photoluminescence Yields in Organic Crystals . . . Z. A. Chizhikova and M. A. Galanin 115 30, 187
Influence of Intermolecular Forces in Solutions on the Intensity of Raman lines . . . Ia. S. Bobovich and T. P. Tulub 116 30, 189
An Attempt to Detect the Raman Effect in a Superconductor . . . M. S. Khaikin and V. P. Bykov 119 30, 191
Glow of Aluminum Alloys in an Electrolytic Bath . . . V. A. Krasnokutskii 120 30, 192
The Effect of Absorption of Luminescence on Its Intensity in the Powdered Luminophors . . . A. P. Ivanov 121 30, 196
Concerning Some Thermodynamic Inequalities . . . V. P. Silin 123 30, 197
On the First Appearance of Atomic Electrons With l, n, n_r and $n + l$ Given . . . V. M. Klechkovskii 125 30, 199
Gamma Radiation Accompanying the Absorption of Fast Protons by Nuclei . . . A. I. Akhiezer and I. Ia. Pomeranchuk 127 30, 201
Multiple Meson Production in Particle Collisions . . . L. G. Iakovlev 128 30, 203
Influence of Quantum Radiation Fluctuations on the Trajectory of an Electron in a Magnetic Field . . . A. A. Kolomenskii and A. N. Lebedev 130 30, 205
Excitation of Synchrotron due to Electron Radiation Fluctuations in Strong Focussing Accelerators . . . A. A. Kolomenskii 132 30, 207
Auger Effect in Heavy Atoms . . . V. N. Mokhov and M. G. Urin 133 30, 209
Scattering of Fast Neutrons by Semitransparent Nuclei . . . E. V. Inopin 134 30, 210
Possibility of Using Artificial Earth Sattelites for the Experimental Verification of the Theory of General Relativity . . . V. L. Ginzburg 136 30, 213
Regularized Theory of Field System . . . E. M. Lipmanov 138 30, 214
Electron Plasma Oscillations in an External Electric Field . . . A. I. Akhiezer and A. G. Sitenko 140 30, 216
K-Meson Charge Exchange in Hydrogen and Deuterium . . . L. B. Okun' 142 30, 218
On the Theory of Galvanomagnetic Effects in Metals . . . I. M. Lifshitz, M. Ia. Azbel' and M. I. Klaganov 143 30, 220
Announcement . . . 145

SOVIET PHYSICS JETP VOLUME 3, NUMBER 1 AUGUST, 1956

CONTENTS

Russian Reference

Abram Fedorovich Ioffe 1 30, 3

Photoelectric Quantum Yield in Silver Bromide Crystals . . . . M. S. Egorova and P. V. Meikliar 4 30, 60

Total Cross Sections of Positive π-Mesons on Hydrogen . . . . A. E. Ignatenko, A. I. Mukhin, E. B. Ozerov and B. M. Pontecorvo 10 30, 7

An Investigation of High Frequency Discharge . . . . G. M. Pateiuk 14 30, 12

An Investigation of Magnetic Spectra of Solid Solutions of Some NiZn-ferrites in the Radio Frequency Range . . . . L. A. Fomenko 19 30, 18

The Change of the Absorption Spectrum of Copper Chloride Containing an Excess of Copper Under the Action of Water Vapor . . . . P. N. Kokharenko 29 30, 30

The Absolute Luminescence Yield for γ-Scintillations in a Naphthalene Crystal with Anthracene . . . . M. D. Galanin and A. P. Grishin 32 30, 33

Electrical Explosion of Metal Wires . . . . I. F. Kvarkhtsava, A. A. Pliutto, A. A. Chernov and V. V. Bondarenko 40 30, 42

The Investigation of Cathode Sputtering in the Near Threshold Region. I . . . . N. D. Morgulis and V. D. Tischenko 52 30, 54

The Multiplicative Renormalization Group in the Quantum Theory of Fields . . . . N. N. Bogoliubov and D. V. Shirkov 57 30, 77

Vertex Parts at Very High Energies in Quantum Electrodynamics . . . . V. V. Sudakov 65 30, 87

The Infrared Catastrophe in Quantum Electrodynamics . . . . A. A. Abrikosov 71 30, 96

A Theoretical Property of Relaxation Curves in Luminescence and Photoconductivity . . . . N. A. Tolstoi and A. V. Shatilov 81 30, 109

Diffraction Splitting of Fast Nonrelativistic Deuterons . . . . A. I. Aliev and E. L. Feinberg 85 30, 115

The Theory of the Electron Field Mass in the Presence of an External Medium . . . . A. A. Sokolov and V. N. Tsytovich 94 30, 136

Excitation of the Collective Levels of Heavy Nuclei by Neutrons* . . . . D. F. Zaretskii and A. V. Shut'ko 98 30, 141

The Problem of the Radiation of Ultra High Velocity Electrons Moving in a Constant Magnetic Field . . . . A. A. Sokolov and A. N. Mateev 105 30, 126

(*Contents Continued on inside back cover*)